Interplay between gut bacteria and Parkinson's disease medication

van Kessel, Sebastiaan P.

DOI:
10.33612/diss.182831964

Interplay between gut bacteria and Parkinson's disease medication

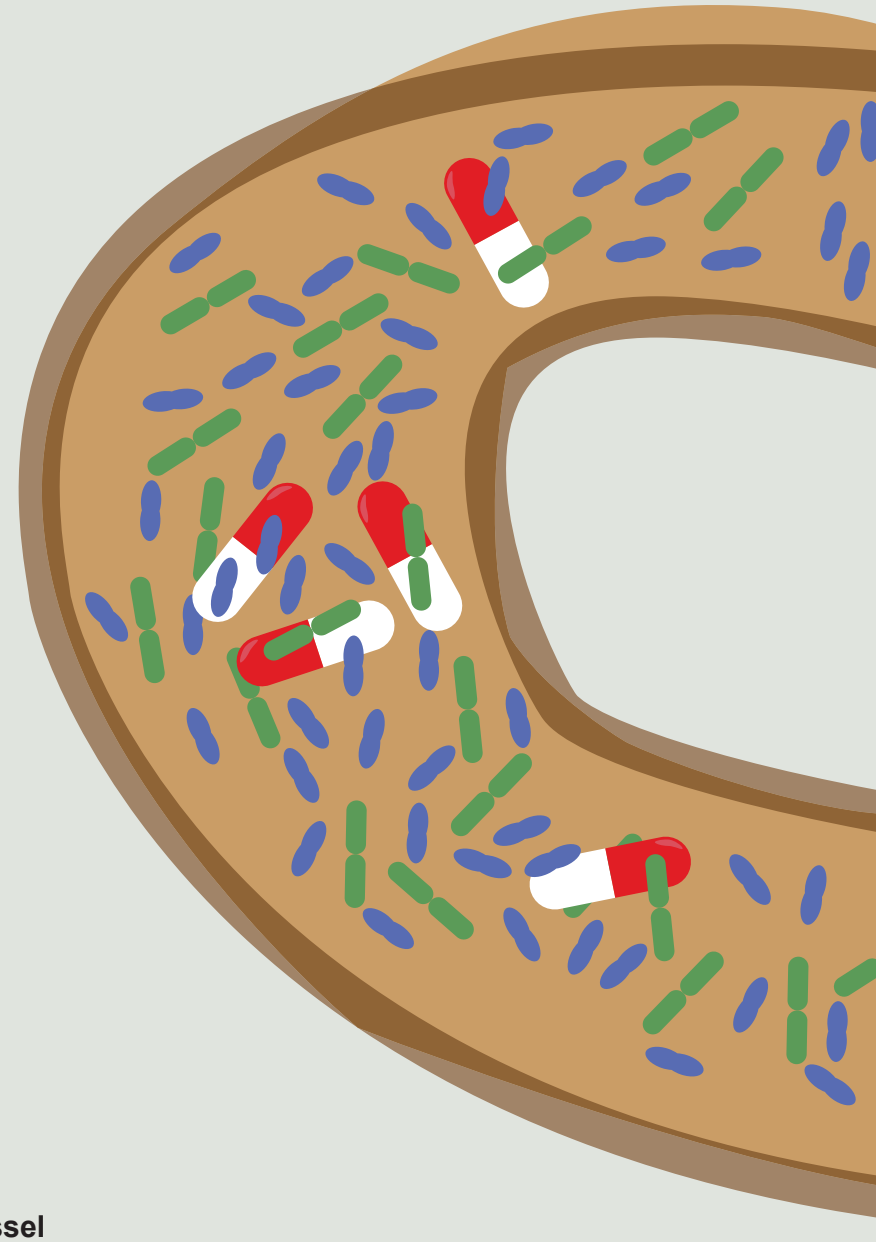

Sebastiaan P. van Kessel

van Kessel, S.P.
Interplay between gut bacteria and Parkinson's disease medication (2021)

Cover & Lay-Out: van Kessel, S.P.
Printing: Ridderprint, The Netherlands

The research described in this thesis was carried out in the department of Host-Microbe Interactions which is part of the Groningen Biomolecular Sciences and Biotechnology Institute (GBB) at the University of Groningen, The Netherlands.
The research described in this thesis was supported by a Rosalind Franklin Fellowship awarded to Sahar El Aidy, co-funded by the European Union and University of Groningen, The Netherlands.

rijksuniversiteit
groningen

Interplay between gut bacteria and Parkinson's disease medication

Proefschrift

ter verkrijging van de graad van doctor aan de
Rijksuniversiteit Groningen
op gezag van de
rector magnificus prof. dr. C. Wijmenga
en volgens besluit van het College voor Promoties.

De openbare verdediging zal plaatsvinden op

vrijdag 5 november 2021 om 14.30 uur

door

Sebastiaan Pieter van Kessel

geboren op 9 december 1990
te Groningen

Promotores

Prof. dr. S. El Aidy
Prof. dr. L. Dijkhuizen

Beoordelingscommissie

Prof. dr. A. Kortholt
Prof. dr. B.R. Bloem
Prof. dr. L. Verhagen Metman

Beknopte Samenvatting

De ziekte van Parkinson (ZvP) is een neurodegeneratieve aandoening die wereldwijd ongeveer 6 miljoen mensen treft. Het belangrijkste pathologische kenmerk dat wordt waargenomen bij ZvP-patiënten is de abnormale aggregatie van eiwitten en verlies van dopaminerge neuronen in de middenhersenen, wat resulteert in motorische stoornissen.

Levodopa blijft de "gouden" standaardbehandeling om de afwezigheid van dopamine in de hersenen te herstellen. Hoewel de start van de behandeling met levodopa een optimale werkzaamheid heeft, veroorzaakt de progressie van de ziekte een grote variabiliteit in de werkzaamheid van de behandeling met levodopa bij patiënten, wat resulteert in een onstabiel en onvoorspelbaar klinische respons; motorische schommelingen. Naast motorische stoornissen ervaren ZvP-patiënten ook verschillende niet-motorische symptomen, zoals gastro-intestinale disfunctie.

In dit proefschrift hebben we aangetoond dat darmbacteriën kunnen bijdragen aan de vermindering van de beschikbaarheid van levodopa in de bloedcirculatie en dat ze de niet-geabsorbeerde residuen van levodopa kunnen metaboliseren tot verschillende producten die de darmmotiliteit veranderen. Verder toonden we aan dat de meest gebruikte ZvP-medicatie ook zelf de motiliteit van de dunne darm, de belangrijkste plaats van medicijnabsorptie, kan beïnvloeden, waardoor de samenstelling van de microbiota verandert. Dergelijke gebeurtenissen kunnen mogelijk een vicieuze cirkel creëren tussen de microbiota, ZvP-medicatie en gastro-intestinale functie, en dringt er op aan om ZvP-medicatie en gastro-intestinale functie in overweging te nemen bij het beoordelen van veranderingen in de ZvP-geassocieerde microbiota. Ten slotte zal het bepalen van de klinische impact van darmbacteriën op ZvP-medicatie helpen de factoren te reduceren die bijdragen aan een verminderede biologische beschikbaarheid van levodopa en de ongewenste bijwerkingen die mogelijk resulteren in en van een verhoogd behandelingsregime.

Brief Summary

Parkinson's disease (PD) is a neurodegenerative disorder, which affects approximately 6 million individuals worldwide. The main pathologic feature observed in PD patients is the abnormal aggregation of protein and loss of dopaminergic neurons in the midbrain, resulting in motor deficits.

Levodopa remains the "golden" standard treatment to restore the absence of dopamine in the brain. Although the start of levodopa treatment has an optimal efficacy, the progression of the disease causes a high variability in the efficacy of levodopa treatment among patients resulting in an unstable and unpredictable clinical response; motor-fluctuations. Besides motor deficits, PD patients also experience various non-motor symptoms such as gastrointestinal dysfunction.

In this thesis, we showed that gut bacteria can contribute to the reduction of levodopa availability in the blood-circulation and that they can metabolize the unabsorbed residues of levodopa to various products that alter the gut motility. Furthermore, we showed that the most commonly used PD medications *per se* may affect the small intestinal motility, the main site of drug absorption, thereby altering the microbiota composition. Such events will potentially create a vicious cycle among the microbiota, PD medication, and gastrointestinal function, and urges for consideration of PD medication and gastrointestinal function when assessing alterations in the PD-associated microbiota. Finally, determining the clinical impact of gut bacteria on PD medication will help reduce the factors contributing to compromised levodopa bioavailability and the unwarranted side effects that result potentially in and from increased treatment regimen.

Table of Contents

CHAPTER 1

Introduction

This chapter is merged and adapted from,

REVIEW

Contributions of Gut Bacteria and Diet to Drug Pharmacokinetics in the Treatment of Parkinson's Disease

Sebastiaan P. van Kessel and Sahar El Aidy*
Frontiers in Neurology, 2019, 10, 1087
DOI: 10.3389/fneur.2019.01087

REVIEW

Bacterial Metabolites Mirror Altered Gut Microbiota Composition in Patients with Parkinson's Disease

Sebastiaan P. van Kessel and Sahar El Aidy*
Journal of Parkinson's Disease, 2019, 9, S359–S370
DOI: 10.3233/JPD-191780

Host-Microbe Interactions, Groningen Biomolecular Sciences and Biotechnology Institute (GBB), University of Groningen, Nijenborgh 7, 9747 AG Groningen, The Netherlands.

*Correspondance: Sahar El Aidy, sahar.elaidy@rug.nl

BACKGROUND

Parkinson's disease (PD) is the second-most common neurodegenerative disorder worldwide [1]. The prevalence of PD increases with age and peaks at 1.5 % between 85 years and 89 years of age and 6.1-6.2 million individuals were diagnosed with PD globally in 2015-2016 [1,2]. During the progression of PD, patients encounter increasing severity of symptoms, which is associated with rising costs for medical treatment, hospitalizations and nursing home care [3], besides a significant decrease in the quality of life [3–6].

The main pathologic feature observed in PD patients is the aggregation of α-synuclein in Lewy bodies and loss of dopaminergic neurons in the substantia nigra pars compacta [7]. It has been postulated that α-synuclein pathology spreads out from the enteric nervous system of the gastrointestinal tract (GI) to the central nervous system in the brain [8]. Which is in agreement with the detection of α-synuclein aggregates in colonic tissue and appendix prior to the onset of PD [9,10]. Recently, it has been shown that pathogenic α-synuclein aggregates spread from the gut to the brain in a mouse model, supporting Braak's hypothesis of the etiology of idiopathic PD [11]. Although the exact factors contributing to the etiology of PD are not well understood, the gut microbiota is likely to be a key contributor.

Indeed, PD patients have an altered microbiota composition compared to healthy control (HC) subjects [12–24]. The main metabolic products produced by the large intestinal bacteria, short chain fatty acids (SCFA), reduced in PD patients [16], have been implicated in α-synuclein pathology and microglia activation in a mouse model of PD [25], supporting the hypothesis that α-synuclein pathology starts in the enteric nervous system [26]. Additionally an altered microbial composition could lead to a shift in circulating bacterial derived metabolites [27], and could be involved in low-grade inflammation, an important trigger for the onset of PD [28]. Increasing evidence supports the involvement of the peripheral immune system in PD. Inflammation via the GI tract, potentially through infections, may contribute to disease pathogenesis, and to the risk of PD development, which was recently reviewed in [28,29]. Houser and Tansey proposed a model of PD pathogenesis originating from the gut where an initial inflammatory trigger could lead to a low-grade inflammation, driving shifts in the microbiota composition, and increasing gut permeability, thus allowing leakage of bacteria and their potential inflammatory metabolites [28]. This leakage in gut barrier would increase the blood brain barrier permeability and α-synuclein pathology, which would ultimately lead to neuroinflammation followed by neurodegeneration [28].

Equally important to elucidating the mechanisms involved in the cause of PD is to uncover the microbial and dietary interference with the pharmacological treatment of the disease. Previous studies have shown that *Helicobacter pylori* (HP) can interfere with levodopa treatment and can bind to levodopa (3,4-dihydroxyphenylalanine; L-DOPA) [30,31]. Bacterial mediated reduction in

levodopa absorbed from the GI tract would lead to reduction in striatal dopamine levels and an "off"-episode, especially in patients with advanced stage PD, who have a reduced capacity to store dopamine in the brain [32,33]. Besides, fluctuating levodopa plasma levels could result in increased pulsatile stimulation which is associated with dyskinesia [34].

ADMINISTRATION ROUTES AND TRANSPORT PROCESS OF LEVODOPA

The most common route for levodopa administration is orally via immediate-release or extended-release formulations of levodopa, where the latter might have potential benefits over other levodopa formulations, reviewed in [35]. Parenteral administration via subcutaneous injections are impossible due to the low solubility of levodopa [36] and continuous intravenous administration, although effective [37], is impractical, as it requires large volumes of daily injections. A promising alternative option to conventional levodopa therapy for advanced PD patients with motor fluctuations and dyskinesia is intestinal infusion of a levodopa/carbidopa gel via a nasoduodenal tube [38] or via gastrojejunostomy [34].

When levodopa is administered orally, it is absorbed in the proximal small intestine [39], where it has to be actively transported from the lumen over the intestinal epithelial barrier into the blood stream [40]. To prevent peripheral and intestinal levodopa metabolism by DOPA decarboxylase (DDC), peripheral DDC inhibitors, such as carbidopa, are co-administered with levodopa. Levodopa (**Figure 1**) is a non-proteinogenic large neutral amino acid (LNAA), and is therefore transported by amino acid transporters in the GI-tract and at the blood brain barrier (BBB) (**Figure 2**). The human body contains at least 11 different epithelial amino acid transport systems expressed in the intestine, 10 of which are also expressed in the renal epithelia, which was thoroughly reviewed before [41]. Only two amino acid transporters are expressed on the blood brain barrier (BBB), LAT1 (SLC7A5) and SNAT5/11 (SLC38A5/11) [42]. The amino acid transporters, which are most likely responsible for the transport of levodopa from the GI-tract to the blood and over the BBB, based on *in vitro/ex vivo* studies, are discussed below and summarized in **Figure 2**.

As a model for the BBB, a mouse brain endothelial cell line (MBEC4), was tested for the expression of 4F2hc/LAT1 (SLC3A2/SLC7A5) and [^{3}H]-levodopa transport was evaluated in the presence of other amino acids (1:100 levodopa/amino acids). The study showed that tryptophan, tyrosine, phenylalanine, isoleucine, leucine, histidine, and 2-amino-2-norbornane-carboxylic acid (BCH), which is used as the defining synthetic amino acid for the L-system (consisting of LAT1 to 4) [43], inhibited at least 80% of the [^{3}H]-levodopa uptake independent of Na^+ [44]. However, the potential contribution of 4F2hc/LAT2 (SLC3A2/SLC7A8) or other transporters were not addressed. Similar results were obtained in Caco2 cells [45–48], renal proximal tubular epithelial cells [49], and opossum kidney cells with either a high (HC) or a low (LC) Na^+ influx. Comparing the HC and LC cell lines indicated that there was a minor contribution of Na^+ dependent transport. The authors concluded that 4F2hc/LAT2 (apparent from BCH transport)

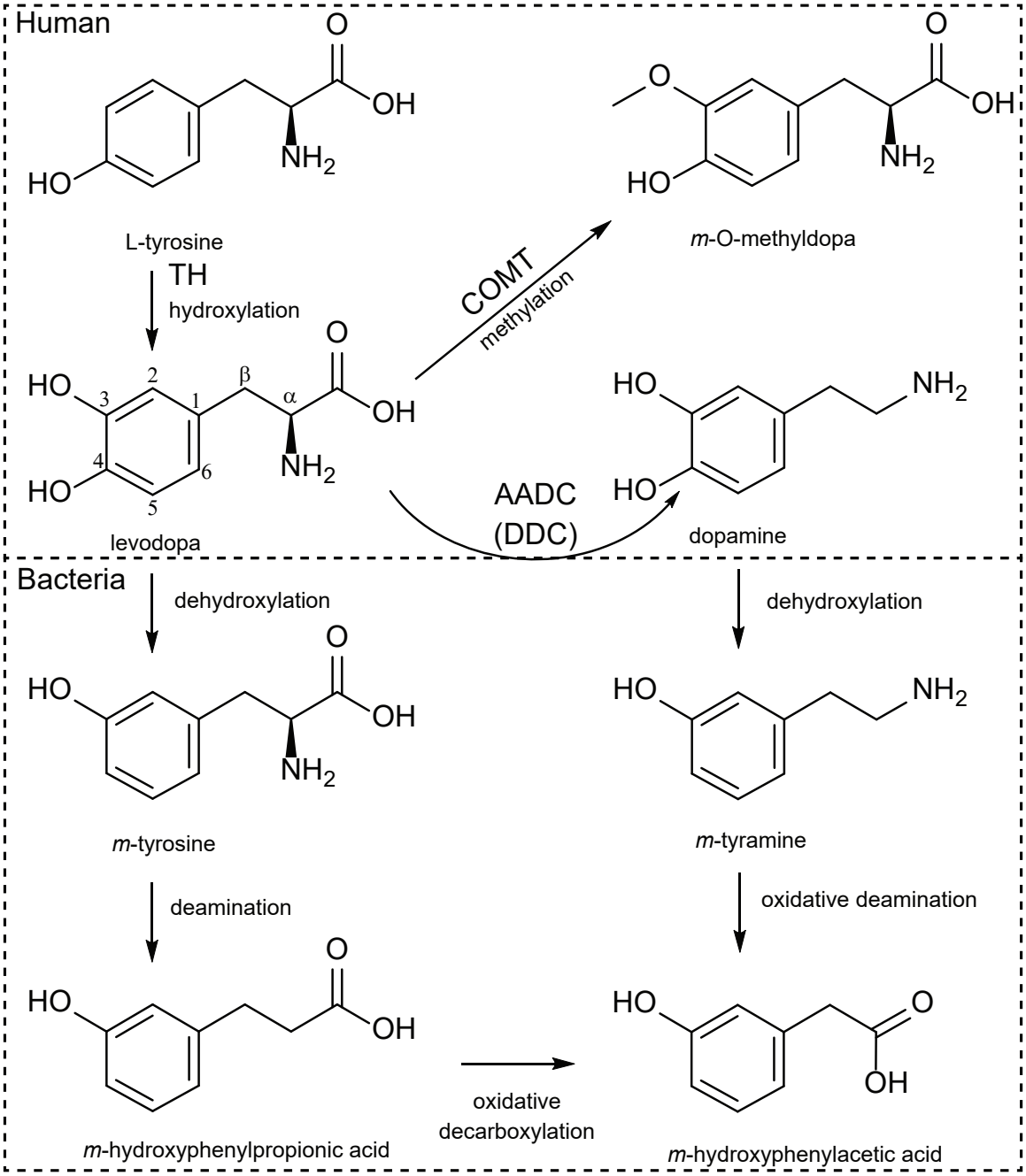

Figure 1 | Human and bacterial levodopa metabolism. Levodopa is produced by hydroxylation of the meta-position of the phenyl-ring from tyrosine by TH (tyrosine hydroxylase) using molecular oxygen. Sequentially levodopa can be decarboxylated to the active neurotransmitter dopamine by the AADC (aromatic amino acid decarboxylase, also known as DDC (DOPA decarboxylase)), or can be methylated by COMT (catechol-O-methyltransferase). Bacteria can dehydroxylate the para-hydroxyl group of either levodopa or dopamine and can sequentially deaminate the dehydroxylated products.

and rBAT/$b^{0,+}$ (SLC3A1/SLC7A9; apparent from the uptake of the rBAT defining amino acid dimer, cystine) were involved in levodopa transport [50]. Although these studies indicate which transporters are involved in levodopa transport in the GI-tract, renal epithelia and the BBB, it remains unclear which specific transporter is involved.

Studies using *Xenopus laevis* oocytes, an ideal single-cell expression system for transporters

due to its relatively large size and low background activity [51], showed that 4F2hc/LAT1 (from rat C6 glioma cells) [52], 4Fhc/LAT2 [53], rBAT/$b^{0,+}$ (from rabbit intestine and human) [53,54], and TAT1 (SLC16A10) (from rat intestine) [55] are independently responsible for levodopa transport. Only substrates with both positive and negative charges at the α-carbon (the relative positive and negative charges are from the amine-group and carboxyl-group from levodopa, respectively; **Figure 1**) are being able to be transported via 4F2hc/LAT1 [52]. Importantly levodopa analogs (*m*-O-methylDOPA, α-methylphenylalanine, α-methyltyrosine, α-methylDOPA), gabapentin (γ-aminobutyric acid (GABA) analog), melphalan (a chemotherapeutic agent), and thyroid hormones (T3, triiodothyronine and T4, thyroxine) were able to inhibit transport of L-[^{14}C]-phenylalanine, and thus levodopa [52], showing the broad range of potential levodopa transport inhibitors. In fact, anti-thyroid treatment in a 70-year-old male subject with PD on levodopa treatment had a beneficial effect on the exaggerated parkinsonian tremor [56]. The authors could not explain why the parkinsonian tremor was aggravated by the presence of hyperthyroidism. However, a plausible explanation, which was not discussed, is the interference of exaggerated thyroid hormone levels with levodopa uptake in the brain. Thus, hyperthyroidism, which is prevalent at higher age, should be considered in PD patients [56].

In *X. laevis* oocytes expressing TAT1, around 80 % of L-[^{14}C]-tryptophan uptake was inhibited by tyrosine and tryptophan and about 40% was inhibited by phenylalanine, levodopa, and *m*-O-methylDOPA, indicating that TAT1 is an aromatic amino acid transporter partly responsible for levodopa uptake. Using N-acetylated amino acids, the authors concluded that the α-carboxyl group (**Figure 1**) is essential for substrate recognition by TAT1. Furthermore, it was shown that TAT1 is mainly expressed throughout in the rat GI-tract and in the liver, in particular, on the basolateral side of rat small intestine [55] (**Figure 2**). Using trans-well culturing and everted murine jejunal sacs, the authors concluded that 4F2hc/LAT2 (LAT1 was not tested) and TAT1 are responsible for the basolateral transport of levodopa [40]. In contrast to 4F2hc/LAT1, 4F2hc/LAT2, and TAT1, which are expressed basolaterally, rBAT/$b^{0,+}$AT is expressed apically and thus is mainly responsible for levodopa absorption from the intestinal lumen. Further characterization of rBAT/$b^{0,+}$AT showed that the common co-administered inhibiters of peripheral levodopa degradation, carbidopa, benserazide (decarboxylase inhibitors) and entacapone (catechol-O-methyltransferase (COMT) inhibitor) were unable to compete with rBAT/$b^{0,+}$AT mediated levodopa transport, indicating that other transporters/mechanisms are involved in the uptake of peripheral levodopa metabolism inhibitors [40]. The transport of levodopa via other apical transporters, PAT1, SIT1/ACE2, ASCT2, and B^0AT1/ACE2 (the main other natural amino acid transporter), expressed in *X. laevis* oocytes was investigated and showed that none of them was able to transport levodopa, indicating that rBAT/$b^{0,+}$AT is the main apical levodopa transporter [40] (**Figure 2**).

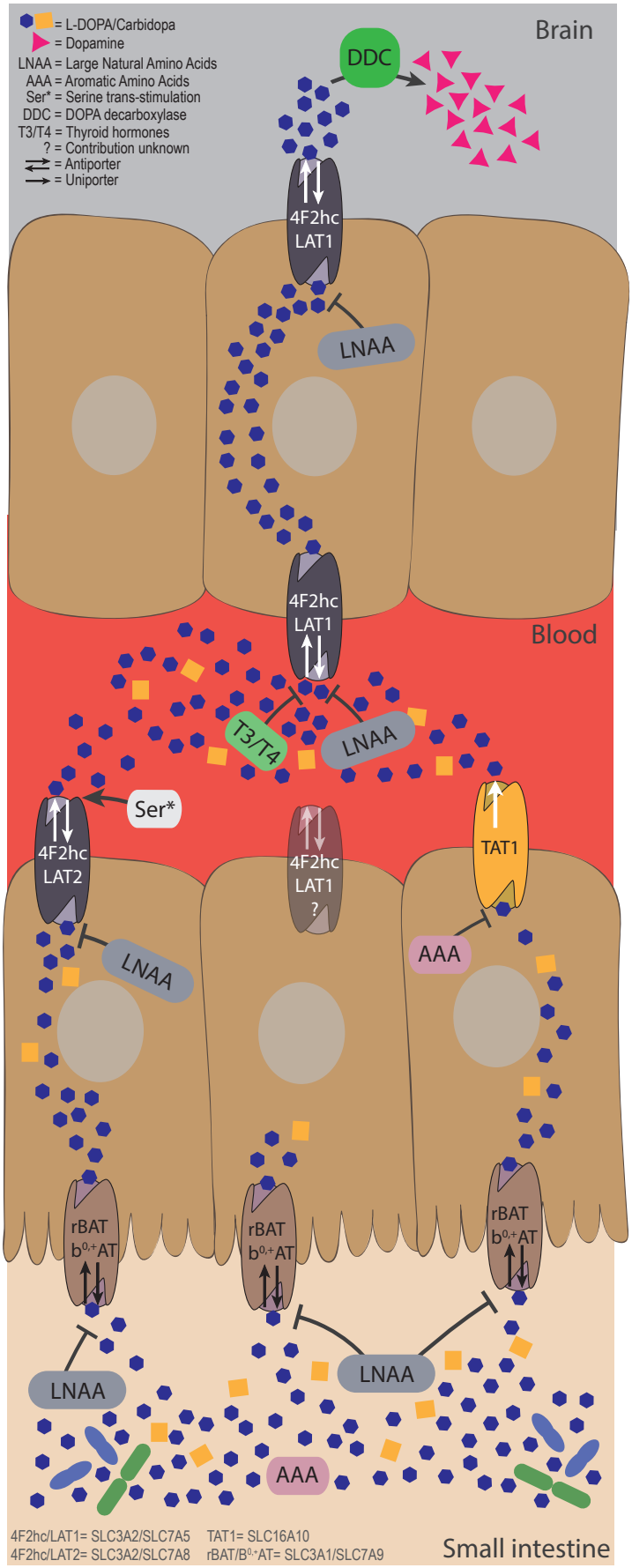

Figure 2 | Dietary components restrict levodopa transport.
(See legend on next page).

(See figure on previous page.)

Figure 2 | Dietary components restrict levodopa transport . Levodopa is taken up in the small intestine by the apical transporter rBAT/$b^{0,+}$AT, and is sequentially transported over the basolateral membrane by 4F2hc/LAT2 and TAT1. The uptake from the lumen can be compromised by LNAAs apically and by LNAAs and AAAs basolaterally. The fraction of levodopa that ends up in the blood has to be transported over the BBB via 4F2hc/LAT1, which can be compromised by high levels of thyroid hormones (T3/T4), or LNAA. Serine left over from a late proteic meal, can trans-stimulate 4F2hc/LAT2 inducing higher efflux of levodopa in the circulation. Finally, the remaining levodopa will be converted to dopamine in the brain by DDC, to compensate the loss of striatal dopamine levels in PD patients.

EFFECT OF DIET AND AGE ON THE BIOAVAILABILITY OF LEVODOPA

Early studies *in vivo*, using radiolabeled levodopa ([^{14}C]-levodopa) showed that ~90% of the total radioactivity is transported into the circulatory system as measured in urine samples after 48 hours [57–59]. Notably, only ~13% of the total radioactivity in blood plasma after the first hour was from intact levodopa, and decreased further overtime. When carbidopa was used in combination with levodopa the intact levodopa after the first hour increased to ~43% [57]. These studies indicate that less than half of the administered levodopa would reach the brain and that approximately 10% of the total levodopa radioactivity is not absorbed and could end up in fecal samples. Moreover, levels of unabsorbed levodopa increase over age. For example, a 10-fold increase (24.6-35.4% vs 2.7-3.5% recovered radioactivity) in levels of levodopa (including its metabolites) were detected in fecal samples of old rats (0.5-2 years old) when compared with their younger counterparts (5-15 weeks old) after oral administration of [^{14}C]-levodopa [60]. This was not related to an increased fecal excretion or decreased jejunal blood flow, suggesting that there is impaired uptake at older age [60]. When levels of levodopa were measured over time in plasma (AUC), older animals (1-2 years) had a higher AUC and a longer half-life ($T_{1/2}$) of systemic levodopa compared to younger animals (9-26 weeks), suggesting an age-dependent slower total body clearance of levodopa [60]. Furthermore the study showed that the intestinal metabolism (mainly by DDC), which prevents levodopa to reach the brain and decreases over age, contributes the most to the increased systemic availability of levodopa at older age [60]. The decreased clearance of levodopa at higher age in rats is in agreement with a study performed in healthy human subjects, who were administered levodopa without DDC inhibitors [61]. Coherently, a higher AUC and systemic levodopa bioavailability ($AUC_{oral}/AUC_{intravenous}$) for levodopa was observed in elderly (71.0 years n=9) compared to young subjects (21.8 years n=8). Administration of carbidopa diminished the differences in systemic levodopa bioavailability between the two groups, while a higher AUC was still observed in the elderly group. This suggests a lower systemic clearance at higher age because carbidopa abolished the age differences in systemic levodopa bioavailability [61]. In PD patients, age correlated significantly with higher levodopa (supplied with DDC inhibitor) AUC and decrease in clearance [62,63]. However, the high scatter in the correlation (r^2= 0.15-0.24) from that study implies that other factors besides age contribute to the variation among PD patients in the pharmacokinetics of levodopa [62].

Indeed, impaired uptake of [^{14}C]-levodopa into the brain was observed when rats were supplied intravenously with the amino acids, phenylalanine, tryptophan, and to a lesser extent histidine [64]. The same effects were reported in humans, for example, a clinical study showed that PD patients (n=9), who received levodopa/carbidopa intravenously directly after a protein rich meal (containing LNAAs) or administration of LNAAs, had increased parkinsonian symptoms. Similarly, when levodopa/carbidopa was taken orally, levodopa absorption from the intestine was delayed after a protein-rich meal [65]. When levodopa/benzerazide (another DDC inhibitor) was infused intraduodenally, motor functions decreased after protein ingestion [66], indicating fluctuation in levodopa uptake in the brain. Nonetheless no decrease in levodopa absorption was observed [66] suggesting that the variability in plasma LNAAs, absorbed from the intestine, could be responsible for the fluctuating levodopa uptake in the brain [67]. The authors concluded that during ingestion of regular (hospital) diets, 10% of the levodopa brain uptake variability is explained by LNAAs in plasma and the other 90% by levodopa plasma levels [67]. These hospital diets contained 2-3.7 fold less LNAAs compared to other human studies (615±105 µM [67] compared to 1235-1973 µM [65], 1615-2012 µM [68], 1624-2292 µM [66]) indicating that high LNAA levels do interfere with levodopa absorption in PD patients but are not solely responsible for the "on"-"off" fluctuations observed in PD patients. Notably, cationic (lysine) or small (glycine) amino acids had no effect on the "on"-"off" fluctuations [65]. Using regional jejunal perfusion of levodopa in healthy human subjects it was shown that the LNAA L-leucine interfered with the levodopa absorption from small intestine [69], at least at high concentrations. This finding supports the involvement of the L-transport system for levodopa transport (as described above) from the intestine to the blood circulation, and, ultimately, to the brain (**Figure 2**).

In vitro data and clinical investigations on the effect of amino acids on the transport and bioavailability of levodopa clearly indicate that amino acids can interfere with the uptake of levodopa from the lumen or the systemic circulation. Therefore, low protein diets (LPD) or protein redistribution diets (PDR), where all dietary protein is ingested only during the evening meal, are proposed for PD patients with motor fluctuations [70]. Refined physiologically based pharmacokinetic (PBPK) modeling for GI absorption (WB-ACAT, Whole Body – Advanced Compartmental Absorption and Transit Model) combined with dynamic flux balance analysis (which measures the flow of metabolites through a metabolic network) on an epithelial cell (sIEC) model for small intestine segmented into 7 parts, (WB-ACAT-sIEC), was used to investigate the spatiotemporal relationship between amino acids and levodopa uptake kinetics [71]. Simulation of levodopa absorption during an aproteic or proteic meal showed that that dietary intervention would be beneficial for PD patients with Hoehn and Yahr scale 3/4 (HY3/4; HY describes the disease progression from (mild=1) to severe=5) [71]. These findings are in agreement with the guidelines for PD treatment, where dietary interventions are proposed for advanced PD patients [32,33]. Comparing a LPD (*in silico* administration of 0.8 g/kg amino acids together with 200 mg levodopa) versus a PRD (assuming a high fraction of amino acids present in the systemic circulation before the morning levodopa dose) in the WB-ACAT-sIEC model showed

a cumulative increase in AUC of levodopa during PRD. Furthermore, the AUC after a morning levodopa dose was higher (11.23 %) during PRD than during a fasting state, which was attributed to a higher influx of residual systemic LNAA from the last protein meal taken the evening before levodopa administration. This higher influx through the basolateral antiporter induced a higher efflux of levodopa (trans-stimulation) into the circulation [71] (**Figure 2**). Although PRD could provide short-term benefits as evident by the reported response rates of >80 % [70], it might not provide a long-term solution as it is undesired by patients and is an imbalanced diet [32,33] that results in weight loss among patients [70]. Extending the WB-ACAT-sIEC model with kidney and brain compartments and setting the objective function (a desired outcome) for optimizing levodopa transport across the BBB revealed that threonine, serine and asparagine resulted in the highest brain bioavailability of levodopa. This led the authors to propose that a serine-rich meal taken after the last levodopa treatment could be beneficial for the levodopa bioavailability [71]. Nonetheless, sensitivity analyses (i.e., the variable that contributes most to the dependent outcome) showed that intestinal loss of levodopa was the most influential factor on levodopa bioavailability [71].

GUT BACTERIAL INTERFERENCE WITH LEVODOPA BIOAVAILABILITY

Levodopa is a non-proteinogenic amino acid produced by the hydroxylation at the meta-position of the phenyl ring of tyrosine. Subsequently, levodopa can be converted to dopamine by DDC or to *m*-O-methylDOPA by COMT methylating of the *m*-hydroxyl group in the human body (**Figure 1**). The microbiota also poses enzymes able to perform similar or additional reactions, which metabolize levodopa. In the early 70s, a study, comparing the metabolic profile of germ-free and conventional rats, showed production of *m*-hydroxyphenylacetic acid and *m*-hydroxyphenylpropionic acid (**Figure 1**) only in conventional rats when fed with levodopa, suggesting that a bacterial dehydroxylation reaction was involved [72]. When rat caecal content was incubated with levodopa or dopamine for six days also *m*-tyramine was found, confirming earlier findings in humans [73]. Metabolites were detected over periods of three days in the urine indicating that the detected metabolites could originate from in the large intestine, which is supported by the caecal incubations [72]. Since the main site of levodopa absorption is the proximal small intestine, it is unlikely that bacterial metabolism of levodopa in the large intestine would affect the drug bioavailability. Therefore, it is crucial to investigate potential bacterial interference with levodopa treatment in the proximal small intestine.

In healthy conditions, small intestinal bacterial overgrowth (SIBO) is prevented by the ileocecal valve, pancreatic enzyme activity, gut motility and gastric acid [74]. Importantly in PD patients, the prevalence of gut motility dysfunction (constipation) and proton pump inhibitor (PPI) usage is relatively high (77.1% and 39.6% respectively, n=39) [75] and is associated with SIBO [76]. In patients (n=200) with gastroesophageal reflux disease using PPIs, varying from 2 months to 7 years, SIBO was detected in 50 % of the cases and was significantly higher than in healthy controls (n=50) [76]. Studies looking at the alteration of the microbiota in subjects using PPIs showed

increased levels of Bacilli (including *Lactobacillus*, *Staphylococcus* and *Enterococcus*) in fecal samples [77,78]. In duodenal samples, SIBO was also observed in 56% of patients on PPIs (n=25) and included mainly genera from the Bacilli class [79]. When SIBO is eradicated in PD patients with *Helicobacter pylori* infection using rifaximin, a common non-absorbable antibiotic used to treat SIBO [80], motor fluctuations were improved as apparent from the significant decreased delayed "on" episodes/day and daily "off" time, although no significant increase in levodopa pharmacokinetics was observed [81]. The underlying explanation of improved motor fluctuations following SIBO eradication remains to be elucidated. However, a plausible explanation is small intestinal inflammation caused by SIBO [81].

In 2001, investigators observed a clinical improvement in PD patients after treatment with antibiotics used to eradicate *Helicobacter pylori* (HP) in two almost identical reports. When HP-infections were treated, the mean AUC of levodopa in the blood significantly increased by ~1.2 fold. A UPDRS-III motor examination showed indeed a significant decrease in motor score [82,83]. A follow-up study confirmed these findings in a larger cohort (n=17) and showed that either 2 weeks or 3 months after HP eradication, PD patients had higher levodopa blood levels (AUC) and lower UPDRS-III motor scores compared to before the eradication [31]. Other studies did not find a significant difference in pharmacokinetics [84] or LEDD (levodopa equivalent daily dose) [85,86] of levodopa between PD patients tested positive or negative for HP infection. In addition, no motor improvement (UPDSR-III) was found after HP eradication in 34 patients [85]. Despite the discrepancy among studies, HP might still play a significant role in drug absorption. The mechanism of HP affecting the levodopa absorption is unclear, one possible explanation for altered drug absorption might be the gastric acidity, which is altered by HP infection and therefore interferes with drug pharmacokinetics of levodopa, delavirdine, and thyroxine [87]. Interestingly, an *in vitro* study showed that adhesins exposed on the outer membrane of HP might bind to levodopa and therefore might contribute to the lower pharmacokinetics in HP infected PD patients [30]. No follow-up studies were published and it remains to be elucidated which adhesin(s) are responsible for binding levodopa. Besides, whether the antibiotic cocktail used to treat HP infections (1000/500 mg amoxicillin/clarithromycin) could also eradicate other bacterial species in the small intestine, which might interfere with the availability of levodopa, was not investigated.

ALTERED BACTERIAL-DERIVED METABOLITES IN PATIENTS WITH PARKINSON'S DISEASE

Although it is clear that PD patients have an altered microbiota composition [12–24], which was reviewed recently [88,89] and updated and merged in **Table 1**, there is a large variation among studies and there is no clear consensus about which bacteria might be involved, which might be due to several factors including sample storage, technical differences of sampling, sequencing methods, statistical approach, demographics, clinical details, and sample size [12]. Nevertheless, the altered microbiota composition could result in metabolic changes in PD patients which

could play an important role in disease onset and progression of PD [27]. Therefore, many studies focused on metabolic biomarker screening (comparing healthy subjects with either familial PD or idiopathic PD), for an early detection of potential development of PD. The metabolic profiles of PD patients (in cerebrospinal fluid (CSF), blood or urine) usually reflect oxidative stress [27,90–94] or mitochondrial dysfunction [27,94–98]. However, many studies also observed differences in metabolites from bacterial origin, which are summarized in **Table 2.**

Comparing the 13 different studies in **Table 1**, 62% (8/13) report a decrease in species from the *Lachnospiraceae* family (including *Blautia sp.*, *Dorea sp.*, *Coprococcus sp.*, *Rosburia sp.*, and *Clostridium XIVa sp.*), 38% (5/13) report a decrease of *Faecalibacterium sp.,* and 15% (2/13) report a decrease in *Bacteroides sp*. (one study reported an increase), all of which are known to be SCFAs producers [99].

In mouse models, it was shown that the gut microbiota is involved in α-synuclein aggregation pathology through their production of SCFAs [25]. Using murine models overexpressing α-synuclein, germ-free (GF) or antibiotic treated mice had reduced PD pathology compared to conventional mice. In addition, when those GF or antibiotic treated mice were administered a mixture of SCFAs, the PD pathology was restored as observed in their conventional counterparts [25]. GF mice (WT or overexpressing α-synuclein) colonized with human stool from PD patients had increased relative levels of butyrate and propionate but decreased levels of acetate compared to mice colonized with human stool from HCs [25]. These findings are in contrast with the finding that PD patients have decreased levels of absolute SCFAs and reduced relative levels of butyrate but not acetate and propionate in their stool samples compared to age matched HCs [16], which is in agreement with reduced levels of acetate found in the blood of PD patients [100]. This discrepancy is most likely because of the differences between humans and mice, specifically those born germ-free. In addition, in Sampson *et al.* 2016 mice were recolonized with human faecal transplant, representing more acute effects as well as shifts in the microbiome based on species effects.

Table 1 | Bacterial composition alterations in PD patients compared to healthy controls

Decreased	Increased	Method	PD	HC	Sample	Reference
Prevotellaceae, Lachnospiraceae, Puniceicoccaceae, Roseburia, Prevotella, Blautia, Clostridium XIVa*	*Bifidobacteriaceae*, Bifidobacterium*, Rikenellaceae, Lactobacillaceae, Lactobacillus*	16S rRNA	64	64	Feces	Aho et al. [12]
Lachnospiraceae	*Akkermansia muciniphila, Enterobacteriaceae, Lactobacillaceae*	16S rRNA	193	113	Feces	Barichella et al. [13]
Prevotella copri, Eubacterium bioforme	*Akkermansia muciniphila, unclassified Firmicutes*	Shotgun metagenomics	31	28	Feces	Bedarf et al. [17]
Clostridium coccoides, Clostridium leptum, Bacteroides fragilis, Prevotella (ns)	*Lactobacillus sp.*	Targeted qPCR for 19 species	45	32	Feces	Hasegawa et al. [18]
Lachnospiraceae, Faecalibacterium prausnitzii.	*Akkermansia muciniphila, Bifidobacterium sp., Lactobacillus sp.*	16S rRNA	212	136	Feces	Hill-Burns et al. [19]
none	*Lactobacillaceae, Barnesiellaceae, Enterococcaceae*	16S rRNA	29	29	Feces	Hopfner et al. [20]
Corpobacillaceae, Lachnospiraceae (Blautia sp., Dorea sp., Roseburia sp., Coprococcus sp.)	*Bacteroides sp.*	16S rRNA	38	34	Feces	Keshavarzian et al. [21]
Coprobacillaceae, Lachnospiraceae (Dorea sp.), Faecalibacterium sp.	*Oxalobacteraceae, Ralstonia*	16S rRNA	38	34	Sigmoid mucosa	Keshavarzian et al. [21]
Blautia sp., Faecalibacterium sp., Ruminococcus sp.	*Escherichia sp., Streptococcus sp., Proteus sp., Enterococcus sp.*	16S rRNA	24	14	Feces	Li et al. [22]
Lachnospiraceae	*Eubacteraceae, Bifidobacteraceae*	16S rRNA	75	45	Feces	Lin et al. [23]
Dorea sp., Bacteroides sp., Prevotella sp., Faecalibacterium sp.	*Lactobacillus sp., Christensenella sp., Catabacter sp., Oscillospira sp., Bifidobacterium sp.*	16S rRNA	89	66	Feces	Petrov et al. [24]

(Continued)

Table 1 | Continued

Decreased	Increased	Method	PD	HC	Sample	Reference
Prevotellaceae, Clostridales incertae sedis IV	*Lactobacillaceae, Verrucomicrobiaceae (Akkermansia), Bradyrhizobiaceae, Ruminococcaceae, Enterobacteriaceae*	16S rRNA	72	72	Feces	Scheperjans et al. [14]
Lactobacillus, Sediminibacterium	*Clostridium IV, Aquabacterium, Holdemania, Sphingomonas, Clostridium XVIII, Butyricicoccus, Anaerotruncus*	16S rRNA	45	45	Feces	Qian et al. [15]
Bacteroidetes, Lactobacilli, Faecalibacterium sp., Enterococcaceae, Prevotellaceae (ns)	*Enterobacteriaceae, Bifidobacterium sp.*	Targeted qPCR for 9 taxa	34	34	Feces	Unger et al. [16]

Updated table adapted and merged from Sampson [91] and Sun and Shen [92]; *Also significant after the two-year follow up; ns = not significant.

Table 2 | Bacterial metabolites significantly altered in PD patients compared to healthy controls

Study	Sample	PD	Healthy	Method	Decreased (FC, PD vs HC)	Increased (FC, PD vs HC)	Description
Trezzi et al. [95]	CSF	34	35	GC-MS	none	none	Lumbar puncture after fasting.
Willkommen et al.[97]	CSF	31	95	FT-ICR-MS	none	*p*-cresol sulfate (9.29); quinic acid (1.7)	Lumbar puncture; 18 patients without PD medications and 11 with PD medication.
Lewitt et al. [170]	CSF	48	57	GC/LC-MS	none	none	Postmortem (within 4 hours) collection of lateral ventricular CSF.
Öhman and Forsgren [171]	CSF	10	10	1D 1H-NMR	none	none	Six patients started dopaminergic treatment at the time of CSF collection.
Trupp et al. [121]	CSF, Plasma	20	20	GC-TOF-MS	none	none	PD baseline; Samples were collected without overnight fasting, between 8-9 AM.
Lewitt et al. [114]	CSF, Plasma	49*	NA	LC-GC-MS	Correlation with the progression of PD: Benzoic acid (CSF: r=-0.42, plasma: ns)	Correlation with the progression of PD: indoleacetic acid (CSF:0.29, plasma: ns)	*Placebo treated PD patients from study from 1989. Lumbar puncture for CSF samples and blood samples were collected after overnight bed rest (between 6 and 10 AM before breakfast).
Wuolikainen et al. [172]	CSF, Plasma	22	28	GC/LC-MS	3-(4-hydroxyphenyl) acetic acid (NA)	indole (NA)	Lumbar puncture and plasma samples from non-fasting patients; Samples were age, sex, and sampling-date matched.
Havelund et al. [173]	CSF, Plasma	26	14	LC-MS	none	none	Lumbar punctures were performed between 09.30 and 10.00 am after overnight fasting; Blood was drawn from the cubital fossa immediately after the lumbar puncture.
Ahmed et al. [103]	Plasma	43	37	2D 1H-NMR	trimethylamine (NA), acetate (NA), threonate (NA)	none	Samples were obtained from drug-naïve PD patients with age and gender-matched healthy controls.

(Continued)

Table 2 | Continued

Study	Sample	PD	Healthy	Method	Decreased (FC, PD vs HC)	Increased (FC, PD vs HC)	Description
Johansen et al. [174]	Plasma	53	46	LC-ECA	none	none	53 PD patients (41 iPD, 12 LRRK2G2019S) were compared to 31 healthy family members (21 positive and 10 negative for LRRK2 mutation) and 15 non-related controls.
Hatano et al. [94]	Serum	35	7	GC/LC-MS	indoleacetic acid (0.67)	phenyllactate (1.84); 3-(4-hydroxyphenyl) lactate (1.23)	Blood was withdrawn after 4 hours of fasting.
Burté et al. [99]	Serum	41	40	Discovery HD4TM Metabolon Platform	catechol sulfate (0.62)	none	Mass spectrometry-based; Blood was withdrawn after fasting from 41 idiopathic early-stage Parkinson's patients (disease duration<1 year).
Han et al. [96]	Serum	43	42	CIT-LC-MS	none	vanillic acid (3.48) (mainly dietary source)	Determined of PD patients not developing dementia (n=27) and PD patients that did develop dementia (n=16). Blood was withdrawn at baseline.
Zhao et al. [98]	Serum	28	18	LC-MS	none	none	Blood was withdrawn in the morning before any food or drink.

(Continued)

Table 2 | Continued

Study	Sample	PD	Healthy	Method	Decreased (FC, PD vs HC)	Increased (FC, PD vs HC)	Description
Okuzumi et al. [27]	Serum	6	19	LC-MS	indoleacetic acid (0.82); hippuric acid (0.52); 3-hydroxyhippuric acid (0.39); catechol sulfate (0.62); 3-(3-hydroxyphenyl) propionic acid (0.49); indole-3-methyl acetate (0.70); 2-furoylglycine (0.37)	none	PARK2 PD patients; Blood was withdrawn after overnight fasting.
D'Andrea et al. [134]	Serum	48[#]	10	LC-MS	phenylethylamine (0.34[d], 0.16[e])	tyramine (1.70[d], 2.44[e])	[#]21 de novo PD patients, [d]de novo PD patients, [e]treated PD patients; Blood was withdrawn in the morning after fasting.
Roede et al. [175]	Serum	80	20	LC-FT-ICR-MS	none	none	39 rapid progressing PD Patients and 41 slowly progressing PD patients. No fasting was required. No medication was alowed in the morning. Samples were taken at the morning exam between 8 AM and 12 PM
Luan et al. [101]	Urine	106	104	LC-MS	none	3-(4-hydroxyphenyl) acetic acid (1.96-2.16); tryptamine (2.22-3.31); indoleacetic acid (1.66-3.23); phenylacetic acid (2.36-2.71)	After overnight fasting morning midstream urine samples were collected at week 0, 16 and 32.

(Continued)

Table 2 | Continued

Study	Sample	PD	Healthy	Method	Decreased (FC, PD vs HC)	Increased (FC, PD vs HC)	Description
Luan et al. [100]	Urine	92	65	GC/LC-MS	none	3-(4-hydroxyphenyl) acetic acid (1.66[a], 2.78[b], 5.85[c]); indoleacetic acid (2.64[a], 3.49[b], 1.88[c]); aminobenzoic acid (6.63[a], 25.43[b], 16.74[c]); hydroxybenzoic acid (4.30[a], 4.26[b], 6.68[c])	After overnight fasting morning midstream urine samples were collected at week 0, 16 and 32; [a]Early-stage (HY 1-1.5), [b]Mid-stage (HY 2-2.5), [c]Advanced-stage (HY 3-4).
Unger et al. [16]	Feces	34	44[$]	GC-MS	acetate (0.43[f], 0.71[g]), butyrate (0.38[f], 0.57[g]), propionate (0.48[f], 0.61[g])	none	[$]34 age matched controls and 10 young healthy controls. Fold changes derived from figure compared to young controls[g] and age matched controls[f]. All subjects were on an omnivorous diet without special dietary habits or restrictions. During the last 3 months no intake of antibiotics, probiotics, or prebiotics was reported.

*Parkinson Study Group. Effect of deprenyl on the progression of disability in early Parkinson's disease. N Engl J Med 1989;321:1364–1371.

GC, Gas Chromatography; LC, Liquid Chromatography, MS, Mass Spectrometry; CIT, Chemical Isotope Labeling; FT-ICR, Fourier-transform ion cyclotron resonance; NMR, Nuclear Magnetic Resonance; LC-ECA, LC Electochemical Array

A decrease in *Prevotellaceae* or *Prevotella sp*. was observed in 31% (4/13) of the studies listed in **Table 1**. *Prevotella* produces (among others) hydrogen sulfide (H_2S), a gasotransmitter (for review see [101]), which has been linked to PD and neuroprotection [102]. Free H_2S levels in plasma, cecum, and colon of germ-free mice were significantly reduced compared to their conventional counterparts, indicating that the microbiota contributes to free H_2S levels [103]. H_2S breathing (40 ppm) restored the movement disorder, protected dopaminergic neurons, prevented microglia and astrocyte activation and upregulated the expression of antioxidant genes from the Nrf2 pathway in a 1-methyl-4-phenyl-1,2,3,6-tetrahydropyridine (MPTP) induced PD mouse model [104]. Similar results were found in a 6-hydroxydopamine (6-OHDA) and rotenone induced PD rat model receiving 30 or 100 μmol/kg NaHS (an H_2S donor) [105]. Similarly, H_2 another and potentially overlooked gasotransmitter, which can be produced by gut microbiota, such as *Blautia sp.* and *Clostridium spp.*, might have an important link to PD as it has been described to neutralize toxic hydroxyl radicals, downregulate the expression of proinflammatory factors, and preserve cerebrovascular reactivity [106]. Intriguingly, 0.08 ppm of H_2 in drinking water reduced the loss dopaminergic neurons by 16% compared to the control in the substantia nigra and slightly improved the mobility in an open-field test using a MPTP induced PD mouse model [107]. Similarly, the protection of dopaminergic neurons, by drinking hydrogenated water, was also observed in a 6-OHDA rat model [108]. Bacterial species representing the genera of bacteria altered in PD have been tested for their production of H_2 [109]. *Blautia coccoides* and *Clostridium leptum,* which are reported to be underrepresented in PD patients (**Table 1**) produced the highest levels of H_2 (~1.6 and 0.62 μmol/10^8 cells) [109], and therefore might contribute to the availability of molecular H_2 which potentially plays a role in neuroprotection.

Other organic metabolites produced by *Clostridium* species [110] were found to be differentially present in serum, urine, and CSF samples of PD patients (**Table 2**). For example, an increase in 3-phenyllactate, and 3-(4-hydroxyphenyl)lactic acid and a decrease of indoleacetic acid (IAA) was observed in serum of patients with idiopathic PD and familial PD (PARK2 mutations) [27,91], although in urine, an increase of 3-(4-hydroxyphenyl)acetic acid and IAA was observed [97,98]. In addition, a minor but significant correlation was observed between IAA and the progression of PD in CSF but not in plasma, however these samples were stored for 25 years before analysis on LC/GC-MS, which could influence the accuracy of sample analysis [111]. IAA is produced via oxidative decarboxylation or deamination of indolepyruvate or tryptamine, respectively. Levels of IAA and tryptamine, produced by *Ruminococcus gnavus* and *Clostridium sporogenes* [112], are strongly dependent on the microbiota as GF mice showed ~30 fold decrease in IAA cecal or fecal levels and a corresponding ~10 fold decrease in tryptamine levels when compared to their conventional raised counterparts [113,114]. Congruously to the increased IAA levels in urine, an increase in tryptamine was detected in urine of PD patients in one of the studies [98]. Importantly, IAA was shown to modulate inflammatory responses reducing pro-inflammatory cytokine production by macrophages stimulated with LPS and palmitate or attenuating the cytokine mediated lipogenesis through the aryl hydrogen receptor (AHR) in hepatocytes [114]. Furthermore,

IAA has an anti-neuroinflammatory activity in LPS-stimulated BV2 microglial cells [115]. Taken together, data available suggest that altered levels of IAA, which are caused by changes in microbial composition, might play a role in attenuating inflammation in PD patients.

p-Cresol sulfate (sulfonated by the liver), which is exclusively produced by gut bacteria [116], mainly by species belonging to *Clostridiaceae* (*Clostridium clusters I, IV, IX, XI, XIII, XIVa, XVI*) and *Bacteroidaceae* families [117] (**Table 1**), is also observed to be ~10 fold increased in in the CSF of PD patients [94] but not in blood samples [27,91]. However, differential metabolite levels in blood do not necessarily reflect CSF levels [118]. *p*-Cresol has a profound effect on the inflammatory response of macrophages and T-cells [119–121]. In murine peritoneal exudate cells (the adherent fraction, mainly macrophages) and in a J774.1 macrophage cell line, pre-treatment with *p*-cresol at non-cytotoxic levels was able to inhibit Il-12 production after stimulation with heat-killed *Lactobacillis casei* [119]. The same effect was observed later in murine peritoneal exudate cells and RAW276.3 macrophage cell-line stimulated with LPS or LPS and IFNγ [121]. In addition, *p*-cresol sulfate increased Il-10 levels but did not alter levels of TNFa [121]. In a hypersensitive mouse model, *p*-cresol and *p*-cresol sulfate correlated negatively with ear swelling, suggesting that *p*-cresol (sulfate) attenuates T cell mediated immune response [120]. When *in vitro* $CD3^+$ splenocytes were stimulated with *p*-cresol or *p*-cresol sulfate a decrease in IFNγ and an increase IL-4 levels were observed, which was confirmed by a decreased Th1/Th2 ratio ($CD3^+/CD4^+$ splenocytes, intracellular stained for IFNγ (Th1) or IL-4 (Th2) production), but no difference between untreated and *p*-cresol treated cytotoxic T-cells or regulatory T-cells were found [120].

In contrast to *p*-cresol sulfate, catechol sulfate, a product of bacterial and human co-metabolism, was found to be decreased in PD patients [27,96]. Catechol is an intermediate bacterial product from the benzoate degradation pathway [122,123]. Notably, higher bacterial metabolism of catechol seems to be associated with inflammation as concluded from the higher relative abundance of bacteria representing the benzoate pathway are higher in a murine colitis model during the active disease compared to remission [123]. For example, *Ralstonia pickettii*, which is known to produce and degrade catechol [124,125] was reported to be increased in the sigmoid mucosa of PD patients (**Table 1**) potentially reflecting inflammation [21], which is in agreement with the reported higher abundance of bacteria representing the benzoate degradation pathway [123].

Molecular mimicry by extracellular amyloid proteins produced by bacteria have been proposed as one potential trigger inducing misfolding of neuronal proteins via cross-seeding [126]. Recently the amyloid protein produced by *Escherichia coli* (curli) has been implicated in α-synuclein pathology in rats and *Caenorhabditis elegans* [127]. Rats orally administered with wild type *E. coli* or *E. coli* lacking the curli-gene revealed increased α-synuclein aggregates in the brain and gut of rats (hippocampus, striatum, and enteric nervous system) when treated with wild type *E. coli*. Furthermore, increased expression of IL-6, TLR2 and TNF were observed in the striatum or rats treated with wild type *E. coli* [127]. Various species from the *Enterobacteriaceae* family (*E. coli*, *Salmonella typhimurium Citrobacter sp*., *Citrobacter freundii*, *Cronobacter sakazakii*, and *Proteus mirabilis*) produce curli [128]. Importantly, 31% (4/13) of the studies

reported increased abundance of *Enterobacteriaceae spp.* [13,14,16,22] (**Table 1**). Intriguingly, oral administration of *P. mirabilis* in a MPTP induced PD mouse model induced neuronal damage, motor deficits, neuroinflammation and α-synuclein aggregation [129]. The authors suggested that higher levels of LPS by *P. mirabilis* induced the observed neuronal damage. However, the fact that *P. mirabilis* produces curli could be another factor involved in the observed PD pathology.

BACTERIAL-MEDIATED SIDE EFFECTS OF PARKINSON'S TREATMENT

Orally administered PD medication could have an effect on gastrointestinal (GI) function and therefore on the microbial composition alterations in PD patients. For example, the COMT-inhibitors, anticholinergics and levodopa/carbidiopa (borderline significant) were associated with microbiota alterations within PD patients [19]. Furthermore, COMT-inhibitors were significantly associated with an increase of *Lactobacillaceae* and a decrease of *Clostridiales Family IV (Incertae Sedis)* [14]. In 54% (7/13) of the studies *Lactobacillaceae* or *Lactobacillus* were reported to be increased in PD patients (**Table 1**). Some *Lactobacillus* species are known to produce tyramine [130] and tyramine has been proposed as a biomarker for PD patients because of the significantly higher levels of tyramine compared to HC observed in the blood circulation (2.4 and 1.7 fold, respectively) [131], **Table 2**. Although other studies did not find an increase in tyramine, an increase in the downstream metabolite of tyramine, 3-(4-hydroxyphenyl) acetic acid, was observed in PD patients [97,98], potentially supporting increased levels of tyramine. The authors associated the human aromatic amino acid decarboxylase (AADC, also known as DOPA decarboxylase (DDC)) with the observed levels, without speculating about possible contribution of gut bacteria. Tyramine is abundant in fermented foods particularly produced by lactic acid bacteria (*Lactobacillus sp.*, *Enterococcus sp.*) harboring tyrosine decarboxylases (TDC), which are also commensals in the human GI-tract [130,132,133], supporting the increased abundance of *Lactobacillaceae* or *Lactobacillus* found in PD patients.

Because of levodopa treatment, PD patients are exposed to higher circulating levels of dopamine compared to matched HCs. Indeed, serum dopamine levels (sulfonated by the liver) are found to be 30-40 times higher compared to HC [27] and serum dopamine levels correlated with the dosage of levodopa [134]. Comparing healthy and PD subjects on either a low dose (400 mg/day) or a on a high dose (700 mg/day) of levodopa showed that PD patients on a high dosage of levodopa have significantly more dopamine in their peripheral blood lymphocytes (PBLs), however, (nor)epinephrine or DOPAC levels were not altered [135]. In contrast, non-treated PD patients have low dopamine levels in their PBLs, even ~3 fold lower than in healthy subjects, but after treatment showed an ~30 fold increase in the PBL dopamine content [136]. Likewise, higher levels of dopamine were detected in plasma of levodopa treated PD patients (~2.5 fold increase) compared to HC or *de novo* PD patients and no significant differences were observed between HC and *de novo* PD patients [137].

The high levels of dopamine exposure in PD patients, resulting from human levodopa metabolism, could affect immune homeostasis, as dopaminergic systems are involved in

either the adaptive and innate immune system, recently reviewed [138,139]. Dopamine receptors are widely expressed on human leukocytes and dopamine, through its receptors, can modulate T-cell response, and might act as auto- or paracrine signaling molecule in the cells of the immune system [139]. Importantly, the percentage of Dopamine Receptor D5 (DRD5) positive $CD4^+$ T-cells correlated negatively with the UPDRS-III (Unified Parkinson's Disease Rating Scale, Part III, motor examination) score [137], indicating that the severity (progression) of the disease, and thus the disease duration [140] and drug treatment might be associated with reduced $DRD5^+$ $CD4^+$ T-cells. A follow up study investigating $CD4^+$ T cell subsets (T helper cells, T_{H1}, T_{H2}, T_{H17}; and T regulatory cells, T_{reg}) showed an overall decrease of $CD4^+$ T cells in *de novo* PD patients and treated PD patients attributed by a decrease in most T-cell subsets except for T_{H1}. Remarkably, there were little differences observed between the *de novo* PD and treated PD patients except for T_{reg} mediated inhibition of T effector cell (T_{eff}, mixture of T helper cells) proliferation by dopamine. T_{reg} subsets from healthy subjects, *de novo* PD patients, and treated PD patients showed similar T_{reg} mediated inhibition of T_{eff} proliferation, which is almost abolished by dopamine except for T_{reg} cells isolated from treated PD patients, those cells appeared to be insensitive to dopamine [141]. This finding is consistent with an earlier report showing that dopamine prevents inhibition of murine T_{eff} proliferation by T_{reg} cells [142]. Furthermore, it was shown that the effect of dopamine was mediated through DRD1-like receptors (DRD1 or DRD5) [142], which is in agreement with the negative correlation observed between disease severity (and thus indirectly disease and treatment duration) and $DRD5^+$ $CD4^+$ T-cells in PD patients [137]. This T_{reg} insensitivity might potentially be originated from the of long-term levodopa treatment of PD patients. In addition, DRD2-like receptors (D2, D3, D4) seem to be involved in the dopaminergic immune pathway in PD. DRD3 knock out (KO) mice or RAG1 KO mice (which are devoid of T and B cells) reconstituted with DRD3-deficient splenocytes or DRD3-deficient $CD4^+$ T cells resulted in a strong neuroprotection in MPTP-induced PD, showing a fundamental role of DRD3 expressed on $CD4^+$ T cells in the degeneration of dopaminergic neurons. Furthermore it was shown that DRD3 deficient $CD4^+$ T cells are unable to acquire the T_{h1} effector phenotype, indicating that dopaminergic signaling (by dopamine or agonists) through DRD3 would produce T_{h1} cells which are key in neurodegeneration observed [143]. Which is in agreement with the higher Th1/Th2 ratio observed in progressing PD patients but not in *de novo* PD patients, potentially through dopamine mediated T_{h1} differentiation in combination with the inability of T_{reg} cells to inhibit T_{eff} cells [141].

Besides levodopa, which results in higher exposer to peripheral dopamine, blocking DDC to avoid peripheral conversion of levodopa to dopamine, might have a profound influence on the immune system. Recently, it has been reported that carbidopa, a DDC inhibitor, has immunosuppressive properties as it prevents T-cell proliferation and T-cell autoimmunity in a mouse model [144]. Furthermore, it has been demonstrated that carbidopa is an AHR-ligand [145], and therefore might play a role in the immune system, as AHR is an important contributor to the adaptive immune system by modulating T-cell differentiation, reviewed recently [146].

Importantly, proliferation of murine B-cell enriched lymphocyte cultures isolated from spleen, lymph nodes and Peyer's patches are inhibited by dopamine in a concentration dependent manner (1-100 μM), which coincided with immunoglobulin production (IgA, IgM, IgG) [147]. IgA is known to shape the microbiota composition, reviewed here [148], and thus a decrease in IgA production due to the exposure to dopamine could potentially lead to alteration in the microbiota composition. In a recent study, inflammatory markers in fecal samples of PD patients were compared to their HCs counterparts. The mean levels of the angiogenesis factor (Flt1), the pro-inflammatory cytokines IL-1α, and CXCL8 were significantly higher in PD patients. Importantly, consumption of probiotics was associated with significantly higher levels of the chemokines CCL4 (MIP-1ß), and CCL17 (TARC), and the pro-inflammatory cytokine IL-7 [149]. Unfortunately, the potential effect of anti-Parkinson medication on the fecal immune profiles was not included in the analysis, which could have a profound effect on the outcome (discussed above).

EFFECT OF DOPAMINE AND DOPAMINE AGONISTS ON GUT MOTILITY

Gut motility is an important factor contributing to the variation observed in human microbiota profiles [150]. Importantly, dopamine and their agonists have been shown to affect the gut motility (discussed below). In addition, the dopamine agonists used in the treatment of PD, which are usually used in combination with levodopa treatment, could have a similar effect on influencing gut motility. Therefore, studies investigating the effects of dopamine on gut motility of rodents, dogs, and humans are discussed, with a complete overview in **Table 3**.

Using electrical field stimulation (EFS) on longitudinal muscle strips of guinea pig ileum in organ baths, dopamine (1-100 μM) and bromocriptine (0.15-15 μM), a dopamine agonist used in PD treatment, inhibited the cholinergic twitch up to ~46% and ~82%, respectively. Neither dopamine antagonists, metoclopramide nor pimozide prevented the observed inhibition by dopamine or bromocriptine. When using the α-adrenoceptor antagonist, phentolamine, only the observed inhibition of dopamine but not of bromocriptine was rescued, indicating that dopamine acts through the α-adrenoceptors [151]. The same conclusions on the inhibitory effect of dopamine were shown in an almost identical study using ileum of guinea pig [152]. Notably, tyramine, a product of bacterial TDC, resulted in similar inhibitions of cholinergic twitch [152]. Dopamine, bromocriptine, and to a lesser extent tyramine, were also able to relax methacholine-contracted jejunal tissues from guinea pig [153]. In rats, dopamine initiated directly a short longitudinal contraction followed by relaxation within 5 minutes in the duodenum and jejunum. However, in the ileum, only relaxations were observed [154]. In addition, dopamine had also an inhibitory effect on the spontaneous contractions of longitudinal muscle strips from rat distal colon [155]. The motility of mouse longitudinal fixed ileum [156], circular muscle strips of colon [157] and longitudinal fixed colon [158] were all inhibited by dopamine and in the latter study also by bromocriptine, attributed to dopaminergic and/or adrenergic receptors. In dogs, the gut motility of the small intestine [159] and the colon [160] was monitored *in vivo* using implanted electrodes.

Injection of dopamine (10 μg/kg) intracerebroventricularly 1 hour before a meal decreased the duration of the migrating motor complex (MMC; intestinal motility pattern of the interdigestive state) episodes in the small intestine compared to controls, although this effect was not observed when dopamine was injected intravenously (100 μg/kg) [159]. In the colon, a similar inhibition was observed, although with a 10 times higher concentration of dopamine (1 mg/kg/h) injected intravenously [160]. Importantly, bromocriptine had an opposite effect, where it induced the colon motility instead [160]. In fasted human subjects, intravenous administration of dopamine (75 μg/kg in 15 min) induced phase-III like MMCs (last phase in the MMC cycle which consists of strong contractions to completely occlude the lumen) in the duodenum [161], which is in contrast to the previous studies in rodents (organ bath experiments) and dogs. The MMCs were similar to spontaneous phase-III MMCs, although with a slight longer period of complete inhibition after phase-III MMCs [161]. Similar results were found in terminally ill patients [162]. A follow up study in humans during fed state showed that dopamine disrupted the fed state MMCs and induced phase-III like MMCs, followed by a short period of complete quiescence (phase-I like MMCs), which was inhibited by the dopamine receptor D2 blocker (DRD2) domperidone, suggesting the involvement of peripheral D2 receptors [163]. Lastly, when the gut motility was investigated using orocaecal transit time (OCT) and paracetamol pharmacokinetics as gastric emptying marker during intravenous injection of dopamine [164], a reduction in the $AUC_{t=60\ min}$ of paracetamol was observed. This suggests that dopamine causes delayed OCT time, which could be due to delayed gastric emptying and a decrease in gut motility [164]. Functional studies investigating the dopamine receptors in the GI-tract of mouse showed that the dopamine receptor D2 (Drd2) is important for gut motility. Mice lacking Drd2, but not Drd3, receptor showed an increased gut transit time compared to the controls [165] suggesting that endogenous dopamine has an inhibitory effect on intestinal motility [165]. The findings confirm the earlier organ bath experiments with rodent tissue. In summary, these studies (**Table 1**) show that in rodents and dogs the GI motility is inhibited by dopamine through dopaminergic and adrenergic receptors. In contrast, in humans, dopamine seems to inhibit stomach motility and induce phase-III like MMCs followed by a short time of quiescence through dopaminergic receptors. A potential explanation of the discrepancy among the human and the animal studies might be the experimental setup. In rodents, dissected intestinal parts were placed in an organ bath *ex vivo* and in dogs electrodes were implanted on the basal side of segments of the GI-tract [159,160]. In contrast, in human studies, nasojejunal luminal-tubes consisting of catheters with side openings were fluoroscopically placed in the GI-tract and perfused with 0.2-1.59 mL/min water [161–163]. The latter might induce an altered gut motility *per se* in a non-physiological manner. More studies should be conducted to test the effects of dopamine on the gut motility in humans, and especially in PD patients, who might already have an altered gut motility [4].

Table 3 | Studies investigating the effects of dopamine and dopamine agonists on gut motility in rodents, dogs and humans.

Study	Organism	Method	Tissue	Effect on motility	Tested agonists (μM)	Dopamine receptor antagonist (μM)	Adrenergic receptor antagonist (μM)	Other inhibitors	Effect inhibited by	Conclusion
Zar et al. [154]	Guinea pig	Organ bath	Ileum; longitudinal muscle; electrical field stimulation	Relaxation	Dopamine (1-100), Bromocriptine (0.15-15)	Pimozide (1)	Phentolamine (5), Metoclopramide (90)	none	Phentolamine (only DA)	Inhibition of longitudinal muscle motility through α-adrenergic receptors
Görich et al. [155]	Guinea pig	Organ bath	Ileum; longitudinal fixation (reserpine pretreatment)	Inhibitory	Dopamine, Noradrenaline, Clonidine, (and tyramine) (1-100)	Metoctopromide (1-30), sulpiride (1-300), domperidone (0.01-1), pimozide (0.01-0.1) cis-flupentixol (0.1-1)	Tolazoline (0.3-3)	Reserpine (VMAT2 inhibitor)	Metoclopramide, sulpiride, tolazoline	Inhibition of motility by all compounds tested. Potentially through α-adrenergic receptors. The potency (pA2*) of metoclopramide and sulpiride was not different between dopamine or norepinephrine, indicating an α-adrenergic inhibition, confirmed by tolazoline.

(Continued)

Table 3 | Continued

Study	Organism	Method	Tissue	Effect on motility	Tested agonists (μM)	Dopamine receptor antagonist (μM)	Adrenergic receptor antagonist (μM)	Other inhibitors	Effect inhibited by	Conclusion
Lucchelli et al. [156]	Guinea pig	Organ bath	Jejunum; longitudinal fixation; methacholine induced contraction	Relaxation	Dopamine (1-3000), Apomorphine (3-100), Bromocriptine(1-56), Fenoldopam(1-1000), (and tyramine 1-3000 [data not shown])	Haloperidol (1,3), cis-flupenhixol (1), SCH-23390 (1, 3)	Phentolamine (1,3), propranolol (0.3, 1,3,10)	Reserpine (I.P. 5 mg/kg), TTX (0.3)	Phentolamine (only ~7%) and propranolol (up to ~45%)	Relaxation of tissue of all tested compounds (Reserpine, had no effect on DA induced relaxation, and a minor effect on the others). Slight inhibition of phentolamine (α-adrenoceptor antagonist) and propanolol (ß-adrenoceptor antagonist). Inconclusive which receptor is involved
Kirschstein et al. [157]	Rat	Organ bath	Duodenum, jejunum, ileum; longitudinal fixation	Relaxation and Constriction	Dopamine (100)	SCH-23390 (1), raclopride (1)	Propranolol (3), Prazosin (30)	none	All tested	Contraction and relaxation observed in duodenum and jejunum, relaxation only observed in Ileum. Contraction inhibition by SCH-23390 and raclopride, relaxation inhibition by propranolol and prazosin
Zha-ng et al. [158]	Rat	Organ bath	Distal colon; longitudinal strips	Inhibitory	Dopamine (3-30)	SCH-23390 (10), Supiride (10)	Not tested	TTX (1)	SCH-23390	Dopamine inhibited the spontaneous contractions with EC50=8.3μM and was not affected by TTX. The inhibotry affect was affected only by D1R antagonist SCH-23390

(Continued)

Table 3 | Continued

Study	Organism	Method	Tissue	Effect on motility	Tested agonists (μM)	Dopamine receptor antagonist (μM)	Adrenergic receptor antagonist (μM)	Other inhibitors	Effect inhibited by	Conclusion
Zizzo et al. [159]	Mouse	Organ bath	Ileum; longitudinal fixation	Inhibitory	Dopamine (1-300), SKF-38393 (0.003-100)	SCH-23390 (3,10), Sulpiride (10), Domperidone (5)	Propanolol (10) SR-59230A (0.1), Phentolamine, (10) Yohimbine (10)	DDA (10), Apamin (0.1), Charybdotoxin (0.1), Iberiotoxin (0,1), TTX (1), L-NAME (100), Atropine(1), DPCPX (10), DMPX (10), MRS-1220 (0.1), Methysergide (1)	SR-59230, Phentolamine, Yohimbine (at high concentration of DA), SCH-23390 and SCH-23390 in combination with Sulpiride or Domperidone	Contractibility was inhibited by dopamine and SKF-38933 (D1R agonist), at high concentrations adrenoceptor antagonists (SR-59230, phentolamine, yohimbine) slightly prevented the inhibitory effect of dopamine. D2 antagonists sulpiride and domperidone had little effect on the inhibitory effect of dopamine, except when combined with SCH-23390 (D1R antagonist) which induced a stronger effect then SCH-23390 alone. Suggesting a synerigic contribution of D1 and D2 receptors.

(Continued)

Table 3 | Continued

Study	Organism	Method	Tissue	Effect on motility	Tested agonists (μM)	Dopamine receptor antagonist (μM)	Adrenergic receptor antagonist (μM)	Other inhibitors	Effect inhibited by	Conclusion
Auteri et al. [160]	Mouse	Organ bath	Colon; cicrular muscle strips; Carbachol precontracted or electrical field stimulation	Relaxation/ Inhibitory	Dopamine (1-300), SKF-38393 (up to 100), bromocriptine (0.3-100), isoproterenol	SCH-23390 (3), domperidone (5)	Prazosin (1), Yohimbine (1), propanolol (1), SR-59230A (0.1)	TTX (1), ω-conotoxin (0.1), SNX-482 (0.1), ω-agatoxin TK (0.1), L-NAME (100) MRS-2179 (1),	Domperidone (during carbochol conctraction); SCH-23390 (during electrical field stimulation)	Relaxation induced by DA via a D2-like receptors; Not dependent on NO or P2Y1 receptors; Not affected by adrenergic antagonists; not dependent on enteric neuronal action potential or on modulation of neurotransmitter release; SCH-23390 increased basal tone and the amplitude of the spontaneous contractions; Relaxation of bromocriptine is inhibited by domperidone
Walker et al. [161]	Mouse	Organ bath	Distal colon (WT and DAT-/-); Longitudinal fixation; Electrical field stimulation	Inhibitory	Dopamine (0.01-300)	SCH-23390 (10), sulpiride (10)	Not tested	None	SCH-23390/ sulpiride	Dopamine was only tested on WT distal colon and showed a inhibitory effect (EC50=4.5 μM), which was slightly abolished by SCH-23390/sulpiride mixture (EC50=12.9 μM, single applications of antagonist were not performed).

(Continued)

Table 3 | Continued

Study	Organism	Method	Tissue	Effect on motility	Tested agonists (μM)	Dopamine receptor antagonist (μM)	Adrenergic receptor antagonist (μM)	Other inhibitors	Effect inhibited by	Conclusion
Fioramonti et al. [162]	Dog	Implanted Ni/Cr electrodes	Duodenum and jejunum	Inhibitory	Intracerebroventricularly dopamine (10 ug/kg); Intravenous dopamine (100 μg/kg)	None	None	None	NA	Decreased the duration of the migrating motor complex episodes in the small intestine 1 hour before a meal compared to controls (from 9.4 to 3.4 hour and 7.8 to 2.4 h in duodenum and jejunum), although intravenously (100 μg/kg) this effect was not observed
Bueno et al. [163]	Dog	Implanted strain gauge transducers	Ascending, traverse, descending colon	Inhibitory and Inducing	iv injections of dopamine at 1 mg/kg/h or bromocriptine 40ug/kg/h	Haloperidol (0.2mg/kg)	Phentolamine (0.1 mg/kg), Tolazoline (2mg/kg), Prazosin (0.2 mg/kg), propranolol (0.5 mg/kg)	None	Phentolamine, prazosin and haloperidol for dopamine inhibitory effect,	Dopamine had a inhibitory effect on the ascending and transverse colon and a inducing effect on the descending colon MMCs. Bromocriptine had a inducing effect in the whole colon MMCs; Potentially through adrenergic and dopaminergic action

(Continued)

Table 3 | Continued

Study	Organ-ism	Method	Tissue	Effect on motility	Tested ago-nists (μM)	Dopamine receptor antagonist (μM)	Adrenergic receptor antagonist (μM)	Other inhibi-tors	Effect inhibited by	Conclusion
Marzio et al. [164]	Human, heal-thy	(A)	Duode-num, proximal jejunum	Induc-ing	intravenously dopamine 5 μg/kg/min for 15 min	Domperi-don (10 mg) and sulpiride (100 mg)	None	None	Domperi-don and sulpiride	Dopamine induced phase-III like MMCs in the duodenum, similar to spontaneous phase-III MMCs, although a slight longer period of complete inhibition after phase-III MMCs; Domperidon and sulpiride pre-vented the inducing phase-III MMCs effect.
Marzio et al. [166]	Human, heal-thy	(B)	Stomach, Duode-num, Proximal Jejunum	Induc-ing/In-hibitory	Intravenously dopamine 5 μg/kg/min for 15 min	Domperi-don (20 mg)	None	None	Domperi-don	Dopamine induced phase-III like MMCs during fed state in the small intestine, which was inhibited by domperidone, and decreased the motility of the stomach. After the phase-III MMCs a short period of complete quiescence was observed.
Levein et al. [167]	Human, heal-thy	Par-aceta-mol AUC; oro-caecal transit time	Mouth -> Ileum	Inhibi-tory	Intravenously dopamine 5 μg/kg/min	None	None	None	NA	Dopamine reduced the AUC(60 min) of paracetamol significant-ly, associated with a delayed gastric emptying; OCT time was significantly longer then controls indicating a delayed gastric emptying and gut motility.

(Continued)

Table 3 | Continued

Study	Organism	Method	Tissue	Effect on motility	Tested agonists (μM)	Dopamine receptor antagonist (μM)	Adrenergic receptor antagonist (μM)	Other inhibitors	Effect inhibited by	Conclusion
Dive et al. [165]	Human, critically ill [(C)]	[(D)]	Stomach, duodenum	Inhibitory/Inducing	Intravenously dopamine 4 μg/kg/min	None	None	None	NA	Decreased number of contractions in the gastric antrum (only significant during fasting) and induced phase III motor activity in the duodenum (only significant during feeding).

*pA2, the concentration that produces a 2-fold shift in the agonist concentration-response curve; **Dopaminergic antagonists:** SCH-23390, D1 receptor antagonist; Domperidone, Haloperidol, Metoclopramide, Pimozide, Raclopride, Sulpiride, D2 receptor antagonist; cis-flupentixol, D1 and D2 receptor antagonist; **Adrenergic antagonists:** Tolazoline, Phentolamine, Prazosin, α1 adrenergic receptor antagonist; Yohimbine, α2 adrenergic receptor antagonist; Propanolol, ß adrenergic receptor antagonist; SR-59230A, β3-adrenoceptor antagonist; **Other antagonists and inhibitors:** Apamin, SKCa channel blocker; Atropine, Muscarinic receptor blocker; Carbachol, Cholinergic agonist; Charybdotoxin, IKCa-BkCa channel blocker; DDA, Adenylyl cyclase inhibitor; DMPX, Adenosine A2 receptor antagonist; DPCPX, Adenosine A1 receptor antagonist; Iberiotoxin, BKCa channel blocker; L-NAME, NO synthase inhibitor; Methysergide, 5-HT receptor antagonist; MRS-1220, Adenosine A3 receptor antagonist; MRS-2179, Purinergic P2Y1 receptor antagonist; Reserpine, VMAT inhibitor; SNX-482, P/Q-type Ca2+ channel blocker; TTX, Na+voltage-gated neural channel blocker; ω-agatoxin TK, R-type Ca2+ channel blocker; ω-conotoxin, N-type Ca2+ channel blocker;

[(A)] Intestinal radiopaque tube consisting of four polyvinyl catheters with 4 side openings equally spread perfused with 1,59 ml/min with distilled water. Closure of the openings gives rise 100 mm hg/sec

[(B)] Nasoduodenal probe consisting of 5 polyethylene catheters with evenly spaced openings 20 cm apart continuously perfused with 0.5 ml/min distilled water

[(C)] Human, critically ill adults under mechanical ventilation without suffering from active gastrointestinal diseaes

[(D)] Multilumen tube consisting of polyvinyl catheters with side openings, 1,5 cm apart for stomach and 10 cm apart for duodenum continuously perfused with 0.2 ml/min distilled water

SCOPE AND OUTLINE OF THIS THESIS

The "on"/"off" motor fluctuations in PD patients are highly dependent on the pharmacological treatment and factors contributing to its efficacy. Dietary amino acids and possibly gut bacterial interference with levodopa treatment can contribute to the reduction of levodopa dosage absorbed in the small intestine. Although the start of levodopa treatment is often referred to as the "honeymoon"-period because of its optimal efficacy for approximately the first 2 years, the progression of the disease will reduce the efficacy of the levodopa resulting in a unstable and unpredictable clinical response (**Figure 3**). This results in increasing the amounts and frequencies of levodopa dosage prescribed [166]. A reduction in levodopa absorption leads to reduction in striatal dopamine levels resulting in an "off"-episode. Over the progression of the disease, the therapeutic window becomes increasingly smaller resulting in increased motor fluctuations.

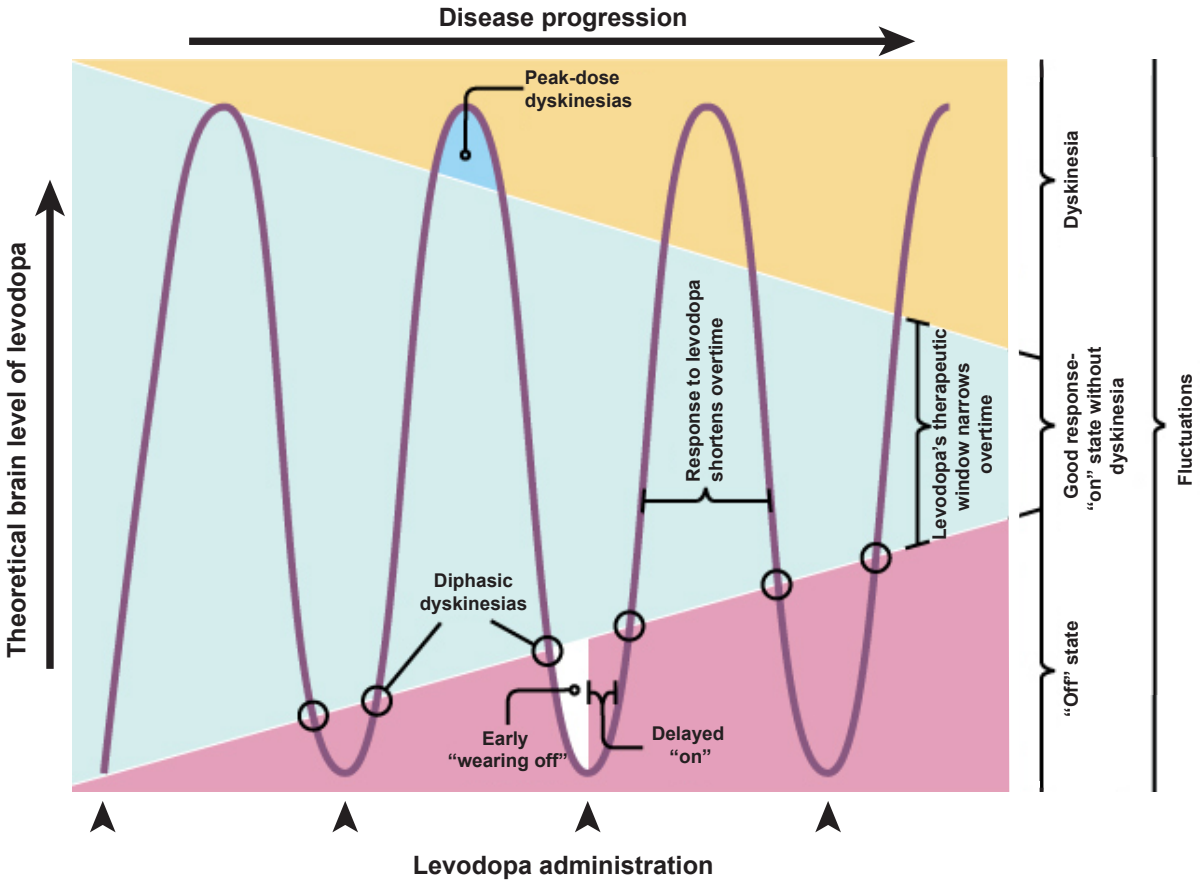

Figure 3 | Therapeutic window of levodopa. Figure adapted from [167]. On the vertical axis the theoretical brain levels of levodopa are depicted, with at every arrow a new dose of levodopa. On the top horizontal axis the disease progression is depicted. Overtime, after the ~2 year "honeymoon" period dyskinesia, involuntary and uncontrollable movements induced by long-term levodopa treatment, start to occur. Some patients start to experience early "wearing off" signs (the PD symptoms return) before the next levodopa dose is due. Additionally some patients experience delayed "on" signs where, although a new dose of levodopa is administered, the medications require more time to reduce the PD symptoms. During the progression of the disease the therapeutic window of levodopa, where there is a good response to levodopa without dyskinesias, is getting smaller and minor dose-fluctuations can result in inconsistent and unpredictable responses to levodopa; motor fluctuations.

Because the intestinal loss of levodopa has been described as the most influential factor on levodopa bioavailability [71], with a great variability among PD patients, and there are a substantial number of bacteria residing in the small intestine, it is likely that the small intestinal gut microbiota may affect levodopa bioavailability. Besides, anti-PD medications side-effects could alter the GI-function through unbalancing the immune homeostasis and affect the gut motility, thereby shifting the microbial composition as often reported to be different in PD patients.

This thesis investigates the effect of members of the gut bacteria on the metabolization of levodopa (**Chapter 2**) and their potential side effects of the drug's unabsorbed residues (**Chapter 3**). In **Chapter 2,** we show how small-intestinal bacteria harboring tyrosine decarboxylase (TDC) enzymes could metabolize levodopa to dopamine, and describe their impact on PD treatment. In **Chapter 3,** we uncovered another gut bacterial metabolic-pathway of levodopa in *Clostridium sporogenes*. This metabolic pathway results in a bioactive molecule, produced from levodopa, which ultimately affects the ileal contractility *ex vivo*. Next, we asked whether anti-PD medications could alter the small-intestinal motility, potentially leading to bacterial overgrowth and affect the overall microbial composition, which was investigated in a rat model (**Chapter 4**). Finally, **Chapter 5** describes the association of different anti-PD medications with the *tdc*-gene abundance levels in a human longitudinal cohort consisting of PD and age and sex-matched healthy controls.

REFERENCES

1. Feigin, V. L. *et al.* Global, regional, and national burden of neurological disorders during 1990–2015: a systematic analysis for the Global Burden of Disease Study 2015. *Lancet Neurol.* **16**, 877–897 (2017).
2. Dorsey, E. R. *et al.* Global, regional, and national burden of Parkinson's disease, 1990–2016: a systematic analysis for the Global Burden of Disease Study 2016. *Lancet Neurol.* **17**, 939–953 (2018).
3. Kowal, S. L., Dall, T. M., Chakrabarti, R., Storm, M. V. & Jain, A. The current and projected economic burden of Parkinson's disease in the United States. *Mov. Disord.* **28**, 311–318 (2013).
4. Barone, P. *et al.* The PRIAMO study: A multicenter assessment of nonmotor symptoms and their impact on quality of life in Parkinson's disease. *Mov. Disord.* **24**, 1641–1649 (2009).
5. Chapuis, S., Ouchchane, L., Metz, O., Gerbaud, L. & Durif, F. Impact of the motor complications of Parkinson's disease on the quality of life. *Mov. Disord.* **20**, 224–30 (2005).
6. Martinez-Martin, P., Rodriguez-Blazquez, C., Kurtis, M. M. & Chaudhuri, K. R. The impact of non-motor symptoms on health-related quality of life of patients with Parkinson's disease. *Mov. Disord.* **26**, 399–406 (2011).

7. Braak, H. *et al.* Staging of brain pathology related to sporadic Parkinson's disease. *Neurobiol. Aging* **24**, 197–211 (2003).
8. Braak, H., Rüb, U., Gai, W. P. & Del Tredici, K. Idiopathic Parkinson's disease: Possible routes by which vulnerable neuronal types may be subject to neuroinvasion by an unknown pathogen. *J. Neural Transm.* **110**, 517–536 (2003).
9. Killinger, B. A. *et al.* The vermiform appendix impacts the risk of developing Parkinson's disease. *Sci. Transl. Med.* **10**, eaar5280 (2018).
10. Shannon, K. M., Keshavarzian, A., Dodiya, H. B., Jakate, S. & Kordower, J. H. Is alpha-synuclein in the colon a biomarker for premotor Parkinson's Disease? Evidence from 3 cases. *Mov. Disord.* **27**, 716–719 (2012).
11. Kim, S. *et al.* Transneuronal Propagation of Pathologic α-Synuclein from the Gut to the Brain Models Parkinson's Disease. *Neuron* **103**, 627-641.e7 (2019).
12. Aho, V. T. E. *et al.* Gut microbiota in Parkinson's disease: Temporal stability and relations to disease progression. *EBioMedicine* **44**, 691–707 (2019).
13. Barichella, M. *et al.* Unraveling gut microbiota in Parkinson's disease and atypical parkinsonism. *Mov. Disord.* **34**, 396–405 (2019).
14. Scheperjans, F. *et al.* Gut microbiota are related to Parkinson's disease and clinical phenotype. *Mov. Disord.* **30**, 350–358 (2015).
15. Qian, Y. *et al.* Alteration of the fecal microbiota in Chinese patients with Parkinson's disease. *Brain. Behav. Immun.* **70**, 194–202 (2018).
16. Unger, M. M. *et al.* Short chain fatty acids and gut microbiota differ between patients with Parkinson's disease and age-matched controls. *Parkinsonism Relat. Disord.* **32**, 66–72 (2016).
17. Bedarf, J. R. *et al.* Functional implications of microbial and viral gut metagenome changes in early stage L-DOPA-naïve Parkinson's disease patients. *Genome Med.* **9**, 1–13 (2017).
18. Hasegawa, S. *et al.* Intestinal dysbiosis and lowered serum lipopolysaccharide-binding protein in Parkinson's disease. *PLoS One* **10**, 1–15 (2015).
19. Hill-Burns, E. M. *et al.* Parkinson's disease and Parkinson's disease medications have distinct signatures of the gut microbiome. *Mov. Disord.* **32**, 739–749 (2017).
20. Hopfner, F. *et al.* Gut microbiota in Parkinson disease in a northern German cohort. *Brain Res.* **1667**, 41–45 (2017).
21. Keshavarzian, A. *et al.* Colonic bacterial composition in Parkinson's disease. *Mov. Disord.* **30**, 1351–1360 (2015).
22. Li, W. *et al.* Structural changes of gut microbiota in Parkinson's disease and its correlation with clinical features. *Sci. China Life Sci.* **60**, 1223–1233 (2017).
23. Lin, A. *et al.* Gut microbiota in patients with Parkinson's disease in southern China. *Park. Relat. Disord.* **53**, 82–88 (2018).

24. Petrov, V. A. *et al.* Analysis of gut microbiota in patients with parkinson's disease. *Bull. Exp. Biol. Med.* **162**, 734–737 (2017).
25. Sampson, T. R. *et al.* Gut Microbiota Regulate Motor Deficits and Neuroinflammation in a Model of Parkinson's Disease. *Cell* **167**, 1469-1480.e12 (2016).
26. Hawkes, C. H., Del Tredici, K. & Braak, H. Parkinson's disease: A dual-hit hypothesis. *Neuropathol. Appl. Neurobiol.* **33**, 599–614 (2007).
27. Okuzumi, A. *et al.* Metabolomics-based identification of metabolic alterations in PARK2. *Ann. Clin. Transl. Neurol.* **6**, 525–536 (2019).
28. Houser, M. C. & Tansey, M. G. The gut-brain axis: is intestinal inflammation a silent driver of Parkinson's disease pathogenesis? *NPJ Park. Dis.* **3**, 3 (2017).
29. Tansey, M. G. & Romero-Ramos, M. Immune system responses in Parkinson's disease: Early and dynamic. *Eur. J. Neurosci.* **49**, 364–383 (2019).
30. Niehues, M. & Hensel, A. In-vitro interaction of L-dopa with bacterial adhesins of *Helicobacter pylori*: an explanation for clinicial differences in bioavailability? *J. Pharm. Pharmacol.* **61**, 1303–7 (2009).
31. Pierantozzi, M. *et al. Helicobacter pylori* eradication and L-dopa absorption in patients with PD and motor fluctuations. *Neurology* **66**, 1824–1829 (2006).
32. Olanow, C. W. & Koller, W. C. An algorithm (decision tree) for the management of Parkinson's disease: treatment guidelines. American Academy of Neurology. *Neurology* **50**, S1-57 (1998).
33. Olanow, C. W., Watts, R. L. & Koller, W. C. An algorithm (decision tree) for the management of Parkinson's disease (2001): treatment guidelines. *Neurology* **56**, S1–S88 (2001).
34. Olanow, C. W. *et al.* Continuous intrajejunal infusion of levodopa-carbidopa intestinal gel for patients with advanced Parkinson's disease: a randomised, controlled, double-blind, double-dummy study. *Lancet. Neurol.* **13**, 141–9 (2014).
35. Mittur, A., Gupta, S. & Modi, N. B. Pharmacokinetics of Rytary®, An Extended-Release Capsule Formulation of Carbidopa–Levodopa. *Clin. Pharmacokinet.* **56**, 999–1014 (2017).
36. Lundqvist, C. Continuous levodopa for advanced Parkinson's disease. *Neuropsychiatr. Dis. Treat.* **3**, 335–348 (2007).
37. Hardie, R. J., Lees, A. J. & Stern, G. M. On-off fluctuations in Parkinson's disease. A clinical and neuropharmacological study. *Brain* **107 (Pt 2**, 487–506 (1984).
38. Nyholm, D. *et al.* Duodenal levodopa infusion monotherapy vs oral polypharmacy in advanced Parkinson disease. *Neurology* **64**, 216–223 (2005).
39. Gundert-Remy, U. *et al.* Intestinal absorption of levodopa in man. *Eur. J. Clin. Pharmacol.* **25**, 69–72 (1983).

40. Camargo, S. M. R. *et al.* The Molecular Mechanism of Intestinal Levodopa Absorption and Its Possible Implications for the Treatment of Parkinson's Disease. *J. Pharmacol. Exp. Ther.* **351**, 114–123 (2014).
41. Bröer, S. Amino Acid Transport Across Mammalian Intestinal and Renal Epithelia. *Physiol. Rev.* **88**, 249–286 (2008).
42. Geier, E. G. *et al.* Structure-based ligand discovery for the Large-neutral Amino Acid Transporter 1, LAT-1. *Proc. Natl. Acad. Sci.* **110**, 5480–5485 (2013).
43. Wade, L. A. & Katzman, R. Synthetic amino acids and the nature of L-DOPA transport at the blood-brain barrier. *J. Neurochem.* **25**, 837–42 (1975).
44. Kageyama, T. *et al.* The 4F2hc/LAT1 complex transports L-DOPA across the blood-brain barrier. *Brain Res.* **879**, 115–121 (2000).
45. Fraga, S., Serrão, M. P. & Soares-da-Silva, P. L-Type Amino Acid Transporters in Two Intestinal Epithelial Cell Lines Function as Exchangers with Neutral Amino Acids. *J. Nutr.* **132**, 733–738 (2002).
46. Fraga, S., Sampaio-Maia, B., Serrão, M. P. & Soares-da-Silva, P. Regulation of apical transporter of L-DOPA in human intestinal Caco-2 cells. *Acta Physiol. Scand.* **175**, 103–11 (2002).
47. Fraga, S., Serrão, M. P. & Soares-da-Silva, P. The L-3,4-dihydroxyphenylalanine transporter in human and rat epithelial intestinal cells is a type 2 hetero amino acid exchanger. *Eur. J. Pharmacol.* **441**, 127–135 (2002).
48. Fraga, S., Pinho, M. J. & Soares-da-Silva, P. Expression of LAT1 and LAT2 amino acid transporters in human and rat intestinal epithelial cells. *Amino Acids* **29**, 229–233 (2005).
49. Pinho, M. J. *et al.* Over-expression of renal LAT1 and LAT2 and enhanced L-DOPA uptake in SHR immortalized renal proximal tubular cells. *Kidney Int.* **66**, 216–226 (2004).
50. Gomes, P. & Soares-da-Silva, P. Na+-independent transporters, LAT-2 and b0,+, exchange L-DOPA with neutral and basic amino acids in two clonal renal cell lines. *J. Membr. Biol.* **186**, 63–80 (2002).
51. Bröer, S. Xenopus laevis Oocytes. *Methods Mol. Biol.* **637**, 295–310 (2010).
52. Uchino, H. Transport of Amino Acid-Related Compounds Mediated by L-Type Amino Acid Transporter 1 (LAT1): Insights Into the Mechanisms of Substrate Recognition. *Mol. Pharmacol.* **61**, 729–737 (2002).
53. Quiñones, H., Collazo, R. & Moe, O. W. The dopamine precursor L-dihydroxyphenylalanine is transported by the amino acid transporters rBAT and LAT2 in renal cortex . *Am. J. Physiol. Physiol.* **287**, F74–F80 (2004).
54. Ishii, H. *et al.* Involvement of rBAT in Na+-dependent and -independent transport of the neurotransmitter candidate L-DOPA in Xenopus laevis oocytes injected with rabbit small intestinal epithelium poly A+ RNA. *Biochim. Biophys. Acta - Biomembr.* **1466**, 61–70 (2000).

55. Kim, D. K. *et al.* Expression Cloning of a Na + -independent Aromatic Amino Acid Transporter with Structural Similarity to H + /Monocarboxylate Transporters. *J. Biol. Chem.* **276**, 17221–17228 (2001).
56. Kim, H. T., Edwards, M. J., Lakshmi Narsimhan, R. & Bhatia, K. P. Hyperthyroidism exaggerating parkinsonian tremor: A clinical lesson. *Parkinsonism Relat. Disord.* **11**, 331–332 (2005).
57. Bianchine, J. R., Messiha, F. S. & Hsu, T. H. Peripheral aromatic L-amino acids decarboxylase inhibitor in parkinsonism. II. Effect on metabolism of L-2- 14 C-dopa. *Clin. Pharmacol. Ther.* **13**, 584–94 (1972).
58. Morgan, J. P. Metabolism of Levodopa in Patients With Parkinson's Disease. *Arch. Neurol.* **25**, 39 (1971).
59. Sasahara, K. *et al.* Dosage form design for improvement of bioavailability of levodopa IV: Possible causes of low bioavailability of oral levodopa in dogs. *J. Pharm. Sci.* **70**, 730–733 (1981).
60. Iwamoto, K., Watanabe, J., Yamada, M., Atsumi, F. & Matsushita, T. Effect of age on gastrointestinal and hepatic first-pass effects of levodopa in rats. *J. Pharm. Pharmacol.* **39**, 421–425 (1987).
61. Robertson, D. *et al.* The effect of age on the pharmacokinetics of levodopa administered alone and in the presence of carbidopa. *Br. J. Clin. Pharmacol.* **28**, 61–69 (1989).
62. Contin, M., Riva, R., Martinelli, P., Albani, F. & Baruzzi, A. Effect of age on the pharmacokinetics of oral levodopa in patients with Parkinson's disease. *Eur. J. Clin. Pharmacol.* **41**, 463–466 (1991).
63. Nagayama, H. *et al.* Influence of ageing on the pharmacokinetics of levodopa in elderly patients with Parkinson's disease. *Park. Relat. Disord.* **17**, 150–152 (2011).
64. Daniel, P. M., Moorhouse, R. S. & Pratt, O. E. Letter: Do changes in blood levels of other aromatic aminoacids influence levodopa therapy? *Lancet (London, England)* **1**, 95 (1976).
65. Nutt, J. G., Woodward, W. R., Hammerstad, J. P., Carter, J. H. & Anderson, J. L. The On–Off Phenomenon in Parkinson's Disease. *N. Engl. J. Med.* **310**, 483–488 (1984).
66. Frankel, J. P. *et al.* The effects of oral protein on the absorption of intraduodenal levodopa and motor performance. *J. Neurol. Neurosurg. Psychiatry* **52**, 1063–7 (1989).
67. Nutt, J. G., Woodward, W. R., Carter, J. H. & Trotman, T. L. Influence of fluctuations of plasma large neutral amino acids with normal diets on the clinical response to levodopa. *J. Neurol. Neurosurg. Psychiatry* **52**, 481–487 (1989).
68. Leenders, K. L., Poewe, W. H., Palmer, A. J., Brenton, D. P. & Frackowiak, R. S. Inhibition of L-[18F]fluorodopa uptake into human brain by amino acids demonstrated by positron emission tomography. *Ann. Neurol.* **20**, 258–62 (1986).
69. Lennernas, H. *et al.* The effect of L-leucine on the absorption of levodopa, studied by regional jejunal perfusion in man. *Br. J. Clin. Pharmacol.* **35**, 243–250 (1993).

70. Cereda, E., Barichella, M., Pedrolli, C. & Pezzoli, G. Low-protein and protein-redistribution diets for Parkinson's disease patients with motor fluctuations: A systematic review. *Mov. Disord.* **25**, 2021–2034 (2010).
71. Guebila, M. Ben & Thiele, I. Model-based dietary optimization for late-stage, levodopa-treated, Parkinson's disease patients. *npj Syst. Biol. Appl.* **2**, 16013 (2016).
72. Goldin, B. R., Peppercorn, M. A. & Goldman, P. Contributions of host and intestinal microflora in the metabolism of L-dopa by the rat. *J. Pharmacol. Exp. Ther.* **186**, 160–6 (1973).
73. Sandler, M., Goodwin, B. L., Ruthven, C. R. J. & Calne, D. B. Therapeutic implications in Parkinsonism of m-tyramine formation from L-dopa in man. *Nature* **229**, 414–416 (1971).
74. Quigley, E. M. M. & Quera, R. Small Intestinal Bacterial Overgrowth: Roles of Antibiotics, Prebiotics, and Probiotics. *Gastroenterology* **130**, S78–S90 (2006).
75. Gabrielli, M. *et al.* Prevalence of Small Intestinal Bacterial Overgrowth in Parkinson's Disease. *Mov. Disord.* **26**, 889–892 (2011).
76. Lombardo, L., Foti, M., Ruggia, O. & Chiecchio, A. Increased Incidence of Small Intestinal Bacterial Overgrowth During Proton Pump Inhibitor Therapy. *Clin. Gastroenterol. Hepatol.* **8**, 504–508 (2010).
77. Freedberg, D. E. *et al.* Proton Pump Inhibitors Alter Specific Taxa in the Human Gastrointestinal Microbiome: A Crossover Trial. *Gastroenterology* **149**, 883-885.e9 (2015).
78. Imhann, F. *et al.* Proton pump inhibitors affect the gut microbiome. *Gut* **65**, 740–748 (2016).
79. Fried, M. *et al.* Duodenal bacterial overgrowth during treatment in outpatients with omeprazole. *Gut* **35**, 23–26 (1994).
80. Steffen, R. Rifaximin: a nonabsorbed antimicrobial as a new tool for treatment of travelers' diarrhea. *J. Travel Med.* **8**, S34-9 (2001).
81. Fasano, A. *et al.* The role of small intestinal bacterial overgrowth in Parkinson's disease. *Mov. Disord.* **28**, 1241–1249 (2013).
82. Pierantozzi, M. *et al. Helicobacter pylori*-induced reduction of acute levodopa absorption in Parkinson's disease patients. *Ann. Neurol.* **50**, 686–7 (2001).
83. Pierantozzi, M. *et al.* Reduced L-dopa absorption and increased clinical fluctuations in *Helicobacter pylori*-infected Parkinson's disease patients. *Neurol. Sci.* **22**, 89–91 (2001).
84. Narozańska, E. *et al.* Pharmacokinetics of levodopa in patients with parkinson disease and motor fluctuations depending on the presence of *Helicobacter pylori* infection. *Clin. Neuropharmacol.* **37**, 96–99 (2014).
85. Lee, W. Y., Yoon, W. T., Shin, H. Y., Jeon, S. H. & Rhee, P. L. *Helicobacter pylori* infection and motor fluctuations in patients with Parkinson's disease. *Mov. Disord.* **23**, 1696–1700 (2008).

86. Rahne, K. E., Tagesson, C. & Nyholm, D. Motor fluctuations and *Helicobacter pylori* in Parkinson's disease. *J. Neurol.* **260**, 2974–2980 (2013).
87. Lahner, E., Annibale, B. & Delle Fave, G. Systematic review: Heliocobacter pylori infection and impaired drug absorption. *Aliment. Pharmacol. Ther.* **29**, 379–386 (2009).
88. Sampson, T. The impact of indigenous microbes on Parkinson's disease. *Neurobiol. Dis.* 104426 (2019)
89. Sun, M. F. & Shen, Y. Q. Dysbiosis of gut microbiota and microbial metabolites in Parkinson's Disease. *Ageing Res. Rev.* **45**, 53–61 (2018).
90. de Farias, C. C. *et al.* Highly specific changes in antioxidant levels and lipid peroxidation in Parkinson's disease and its progression: Disease and staging biomarkers and new drug targets. *Neurosci. Lett.* **617**, 66–71 (2016).
91. Hatano, T., Saiki, S., Okuzumi, A., Mohney, R. P. & Hattori, N. Identification of novel biomarkers for Parkinson's disease by Metabolomic technologies. *J. Neurol. Neurosurg. Psychiatry* **87**, 295–301 (2016).
92. Trezzi, J. P. *et al.* Distinct metabolomic signature in cerebrospinal fluid in early parkinson's disease. *Mov. Disord.* **32**, 1401–1408 (2017).
93. Han, W., Sapkota, S., Camicioli, R., Dixon, R. A. & Li, L. Profiling novel metabolic biomarkers for Parkinson's disease using in-depth metabolomic analysis. *Mov. Disord.* **32**, 1720–1728 (2017).
94. Willkommen, D. *et al.* Metabolomic investigations in cerebrospinal fluid of Parkinson's disease. *PLoS One* **13**, 1–16 (2018).
95. Zhao, H. *et al.* Potential biomarkers of Parkinson's disease revealed by plasma metabolic profiling. *J. Chromatogr. B Anal. Technol. Biomed. Life Sci.* **1081**–**1082**, 101–108 (2018).
96. Burté, F. *et al.* metabolic profiling of Parkinson's disease and mild cognitive impairment. *Mov. Disord.* **32**, 927–932 (2017).
97. Luan, H. *et al.* Comprehensive urinary metabolomic profiling and identification of potential noninvasive marker for idiopathic Parkinson s disease. *Sci. Rep.* **5**, 1–11 (2015).
98. Luan, H. *et al.* LC-MS-based urinary metabolite signatures in idiopathic Parkinson's disease. *J. Proteome Res.* **14**, 467–78 (2015).
99. Flint, H. J., Duncan, S. H., Scott, K. P. & Louis, P. Links between diet, gut microbiota composition and gut metabolism. *Proc. Nutr. Soc.* **760**, 13–22 (2014).
100. Ahmed, S. S., Santosh, W., Kumar, S. & Christlet, H. Metabolic profiling of Parkinson's disease: evidence of biomarker from gene expression analysis and rapid neural network detection. *J. Biomed. Sci.* **16**, 63 (2009).
101. Li, L., Rose, P. & Moore, P. K. Hydrogen Sulfide and Cell Signaling. *Annu. Rev. Pharmacol. Toxicol.* **51**, 169–187 (2011).
102. Cakmak, Y. O. *Provotella*-derived hydrogen sulfide, constipation, and neuroprotection in Parkinson's disease. *Mov. Disord.* **30**, 1151–1151 (2015).

103. Shen, X. *et al.* Microbial regulation of host hydrogen sulfide bioavailability and metabolism. *Free Radic. Biol. Med.* **60**, 195–200 (2013).
104. Kida, K. *et al.* Inhaled Hydrogen Sulfide Prevents Neurodegeneration and Movement Disorder in a Mouse Model of Parkinson's Disease. *Antioxid. Redox Signal.* **15**, 343–352 (2010).
105. Hu, L. F. *et al.* Neuroprotective effects of hydrogen sulfide on Parkinson's disease rat models. *Aging Cell* **9**, 135–146 (2010).
106. Ostojic, S. M. Inadequate Production of H_2 by Gut Microbiota and Parkinson Disease. *Trends Endocrinol. Metab.* **29**, 286–288 (2018).
107. Fujita, K. *et al.* Hydrogen in drinking water reduces dopaminergic neuronal loss in the 1-methyl-4-phenyl-1,2,3,6-tetrahydropyridine mouse model of Parkinson's disease. *PLoS One* **4**, 2–11 (2009).
108. Fu, Y. *et al.* Molecular hydrogen is protective against 6-hydroxydopamine-induced nigrostriatal degeneration in a rat model of Parkinson's disease. *Neurosci. Lett.* **453**, 81–85 (2009).
109. Suzuki, A. *et al.* Quantification of hydrogen production by intestinal bacteria that are specifically dysregulated in Parkinson's disease. *PLoS One* **13**, e0208313 (2018).
110. Elsden, S. R., Hilton, M. G. & Waller, J. M. The end products of the metabolism of aromatic amino acids by clostridia. *Arch. Microbiol.* **107**, 283–288 (1976).
111. Lewitt, P. A., Li, J., Lu, M., Guo, L. & Auinger, P. Metabolomic biomarkers as strong correlates of Parkinson disease progression. *Neurology* **88**, 862–869 (2017).
112. Williams, B. B. *et al.* Discovery and Characterization of Gut Microbiota Decarboxylases that Can Produce the Neurotransmitter Tryptamine. *Cell Host Microbe* **16**, 495–503 (2014).
113. Sridharan, G. V *et al.* Prediction and quantification of bioactive microbiota metabolites in the mouse gut. *Nat. Commun.* **5**, 5492 (2014).
114. Krishnan, S. *et al.* Gut Microbiota-Derived Tryptophan Metabolites Modulate Inflammatory Response in Hepatocytes and Macrophages. *Cell Rep.* **23**, 1099–1111 (2018).
115. Kim, D. C. *et al.* Anti-neuroinflammatory activities of indole alkaloids from kanjang (Korean fermented soy source) in lipopolysaccharide-induced BV2 microglial cells. *Food Chem.* **213**, 69–75 (2016).
116. Wikoff, W. R. *et al.* Metabolomics analysis reveals large effects of gut microflora on mammalian blood metabolites. *Proc. Natl. Acad. Sci. U. S. A.* **106**, 3698–3703 (2009).
117. Saito, Y., Sato, T., Nomoto, K. & Tsuji, H. Identification of phenol- and *p*-cresol-producing intestinal bacteria by using media supplemented with tyrosine and its metabolites. *FEMS Microbiol. Ecol.* **94**, 1–11 (2018).

118. Trupp, M. *et al.* Metabolite and peptide levels in plasma and CSF differentiating healthy controls from patients with newly diagnosed Parkinson's disease. *J. Parkinsons. Dis.* **4**, 549–560 (2014).
119. Kawakami, K., Makino, I., Kato, I., Uchida, K. & Onoue, M. *p*-Cresol inhibits IL-12 production by murine macrophages stimulated with bacterial immunostimulant. *Immunopharmacol. Immunotoxicol.* **31**, 304–309 (2009).
120. Shiba, T. *et al.* Effects of intestinal bacteria-derived *p*-cresyl sulfate on Th1-type immune response in vivo and in vitro. *Toxicol. Appl. Pharmacol.* **274**, 191–199 (2014).
121. Shiba, T. *et al. p*-Cresyl sulfate suppresses lipopolysaccharide-induced anti-bacterial immune responses in murine macrophages in vitro. *Toxicol. Lett.* **245**, 24–30 (2016).
122. Neidle, E. *et al.* cis-diol dehydrogenases encoded by the TOL pWW0 plasmid *xylL* gene and the Acinetobacter calcoaceticus chromosomal *benD* gene are members of the short-chain alcohol dehydrogenase superfamily. *Eur. J. Biochem.* **204**, 113–20 (1992).
123. Rooks, M. G. *et al.* Gut microbiome composition and function in experimental colitis during active disease and treatment-induced remission. *ISME J.* **8**, 1403–17 (2014).
124. Olsen, R. H., Kukor, J. J. & Kaphammer, B. A novel toluene-3-monooxygenase pathway cloned from Pseudomonas pickettii PKO1. *J. Bacteriol.* **176**, 3749–3756 (1994).
125. Bruins, M. R., Kapil, S. & Oehme, F. W. *Pseudomonas pickettii*: A common soil and groundwater aerobic bacteria with pathogenic and biodegradation properties. *Ecotoxicol. Environ. Saf.* **47**, 105–111 (2000).
126. Friedland, R. P. Mechanisms of Molecular Mimicry Involving the Microbiota in Neurodegeneration. *J. Alzheimer's Dis.* **45**, 349–362 (2015).
127. Chen, S. G. *et al.* Exposure to the Functional Bacterial Amyloid Protein Curli Enhances Alpha-Synuclein Aggregation in Aged Fischer 344 Rats and Caenorhabditis elegans. *Sci. Rep.* **6**, 1–10 (2016).
128. Zogaj, X., Bokranz, W., Nimtz, M. & Römling, U. Production of Cellulose and Curli Fimbriae by Members of the Family. *Infect. Immun.* **71**, 4151–4158 (2003).
129. Choi, J. G. *et al.* Oral administration of *Proteus mirabilis* damages dopaminergic neurons and motor functions in mice. *Sci. Rep.* **8**, 1–13 (2018).
130. Marcobal, A., de las Rivas, B., Landete, J. M., Tabera, L. & Muñoz, R. Tyramine and Phenylethylamine Biosynthesis by Food Bacteria. *Crit. Rev. Food Sci. Nutr.* **52**, 448–467 (2012).
131. D'Andrea, G. *et al.* Different Circulating Trace Amine Profiles in De Novo and Treated Parkinson's Disease Patients. *Sci. Rep.* **9**, 1–11 (2019).
132. Perez, M. *et al.* Tyramine biosynthesis is transcriptionally induced at low pH and improves the fitness *of Enterococcus faecalis* in acidic environments. 3547–3558 (2015)
133. Torriani, S. *et al.* Rapid detection and quantification of tyrosine decarboxylase gene (tdc) and its expression in gram-positive bacteria associated with fermented foods using PCR-based methods. *J. Food Prot.* **71**, 93–101 (2008).

134. Nagai, Y. *et al.* Decrease of the D3 dopamine receptor mRNA expression in lymphocytes from patients with Parkinson's disease. *Neurology* **46**, 791–5 (1996).
135. Rajda, C., Dibó, G., Vécsei, L. & Bergquist, J. Increased dopamine content in lymphocytes from high-dose L-Dopa-treated Parkinson's disease patients. *Neuroimmunomodulation* **12**, 81–84 (2005).
136. Caronti, B. *et al.* Reduced dopamine in peripheral blood lymphocytes in Parkinson's disease. *Neuroreport* **10**, 2907–2910 (1999).
137. Kustrimovic, N. *et al.* Dopaminergic Receptors on CD4+ T Naive and Memory Lymphocytes Correlate with Motor Impairment in Patients with Parkinson's Disease. *Sci. Rep.* **6**, 1–17 (2016).
138. Pinoli, M., Marino, F. & Cosentino, M. Dopaminergic Regulation of Innate Immunity: a Review. *J. Neuroimmune Pharmacol.* **12**, 602–623 (2017).
139. Sarkar, C., Basu, B., Chakroborty, D., Dasgupta, P. S. & Basu, S. The immunoregulatory role of dopamine: An update. *Brain. Behav. Immun.* **24**, 525–528 (2010).
140. Alves, G., Wentzel-Larsen, T., Aarsland, D. & Larsen, J. P. Progression of motor impairment and disability in Parkinson disease. *Neurology* **65**, 1436–1441 (2006).
141. Kustrimovic, N. *et al.* Parkinson's disease patients have a complex phenotypic and functional Th1 bias: Cross-sectional studies of CD4+ Th1/Th2/T17 and Treg in drug-naïve and drug-treated patients. *J. Neuroinflammation* **15**, 1–17 (2018).
142. Kipnis, J. Dopamine, through the Extracellular Signal-Regulated Kinase Pathway, Downregulates CD4+CD25+ Regulatory T-Cell Activity: Implications for Neurodegeneration. *J. Neurosci.* **24**, 6133–6143 (2004).
143. Gonzalez, H. *et al.* Dopamine Receptor D3 Expressed on CD4+ T Cells Favors Neurodegeneration of Dopaminergic Neurons during Parkinson's Disease. *J. Immunol.* **190**, 5048–5056 (2013).
144. Zhu, H. *et al.* Carbidopa, a drug in use for management of Parkinson disease inhibits T cell activation and autoimmunity. *PLoS One* **12**, 1–15 (2017).
145. Ogura, J. *et al.* Carbidopa is an activator of aryl hydrocarbon receptor with potential for cancer therapy. *Biochem. J.* **474**, 3391–3402 (2017).
146. Gutiérrez-Vázquez, C. & Quintana, F. J. Regulation of the Immune Response by the Aryl Hydrocarbon Receptor. *Immunity* **48**, 19–33 (2018).
147. Kouassi, E., Yue Sheng Li, Boukhris, W., Millet, I. & Revillard, J. P. Opposite effects of the catecholamines dopamine and norepinephrine on murine polyclonal B-cell activation. *Immunopharmacology* **16**, 125–137 (1988).
148. Macpherson, A. J., Köller, Y. & McCoy, K. D. The bilateral responsiveness between intestinal microbes and IgA. *Trends Immunol.* **36**, 460–470 (2015).
149. Houser, M. C. *et al.* Stool Immune Profiles Evince Gastrointestinal Inflammation in Parkinson's Disease. *Mov. Disord.* **33**, 793–804 (2018).

150. Falony, G. *et al.* Population-level analysis of gut microbiome variation. *Science* **352**, 560–564 (2016).
151. Zar, M. A., Ebong, O. & Bateman, D. N. Effect of metoclopramide in guinea-pig ileum longitudinal muscle: evidence against dopamine-mediation. *Gut* **23**, 66–70 (1982).
152. Görich, R., Weihrauch, T. R. & Kilbinger, H. The inhibition by dopamine of cholinergic transmission in the isolated guinea-pig ileum. Mediation through alpha-adrenoceptors. *Naunyn. Schmiedebergs. Arch. Pharmacol.* **318**, 308–12 (1982).
153. Lucchelli, A., Boselli, C. & Grana, E. Dopamine-induced relaxation of the guinea-pig isolated jejunum is not mediated through dopamine receptors. *Pharmacol. Res.* **22**, 433–44 (1990).
154. Kirschstein, T. *et al.* Dopamine induces contraction in the proximal, but relaxation in the distal rat isolated small intestine. *Neurosci. Lett.* **465**, 21–26 (2009).
155. Zhang, X. *et al.* Dopamine receptor D1 mediates the inhibition of dopamine on the distal colonic motility. *Transl. Res.* **159**, 407–414 (2012).
156. Zizzo, M. G., Mulè, F., Mastropaolo, M. & Serio, R. D1 receptors play a major role in the dopamine modulation of mouse ileum contractility. *Pharmacol. Res.* **61**, 371–378 (2010).
157. Auteri, M., Zizzo, M. G., Amato, A. & Serio, R. Dopamine induces inhibitory effects on the circular muscle contractility of mouse distal colon via D1- and D2-like receptors. *J. Physiol. Biochem.* **73**, 395–404 (2016).
158. Walker, J. K., Gainetdinov, R. R., Mangel, A. W., Caron, M. G. & Shetzline, M. A. Mice lacking the dopamine transporter display altered regulation of distal colonic motility. *Am. J. Physiol. Gastrointest. Liver Physiol.* **279**, G311-8 (2000).
159. Fioramonti, J., Fargeas, M. J., Honde, C. & Bueno, L. Effects of central and peripheral administration of dopamine on pattern of intestinal motility in dogs. *Dig. Dis. Sci.* **29**, 1023–1027 (1984).
160. Bueno, L., Fargeas, M. J., Fioramonti, J. & Honde, C. Effects of dopamine and bromocriptine on colonic motility in dog. *Br. J. Pharmacol.* **82**, 35–42 (1984).
161. Marzio, L., Neri, M., Di Giammarco, A. M., Cuccurullo, F. & Lanfranchi, G. A. Dopamine-induced migrating myoelectrical complex-like activity in human duodenum. *Dig. Dis. Sci.* **31**, 349–354 (1986).
162. Dive, A., Foret, F., Jamart, J., Bulpa, P. & Installé, E. Effect of dopamine on gastrointestinal motility during critical illness. *Intensive Care Med.* **26**, 901–907 (2000).
163. Marzio, L. *et al.* Dopamine interrupts gastrointestinal fed motility pattern in humans. *Dig. Dis. Sci.* **35**, 327–332 (1990).
164. Levein, N. G., Thörn, S. E. & Wattwil, M. Dopamine delays gastric emptying and prolongs orocaecal transit time in volunteers. *Eur. J. Anaesthesiol.* **16**, 246–50 (1999).

165. Li, Z. S., Schmauss, C., Cuenca, A., Ratcliffe, E. & Gershon, M. D. Physiological modulation of intestinal motility by enteric dopaminergic neurons and the D2 receptor: analysis of dopamine receptor expression, location, development, and function in wild-type and knock-out mice. *J. Neurosci.* **26**, 2798–807 (2006).
166. Mercuri, N. B. & Bernardi, G. The 'magic' of L-dopa: Why is it the gold standard Parkinson's disease therapy? *Trends Pharmacol. Sci.* **26**, 341–344 (2005).
167. Parkinson's Dyskinesia: A Bookmarkable Guide. https://www.invigoratept.com/blog/parkinsons-dyskinesia-a-bookmarkable-guide (2017).
168. Lewitt, P. A. *et al.* 3-hydroxykynurenine and other Parkinson's disease biomarkers discovered by metabolomic analysis. *Mov. Disord.* **28**, 1653–1660 (2013).
169. Öhman, A. & Forsgren, L. NMR metabonomics of cerebrospinal fluid distinguishes between Parkinson's disease and controls. *Neurosci. Lett.* **594**, 36–39 (2015).
170. Wuolikainen, A. *et al.* Multi-platform mass spectrometry analysis of the CSF and plasma metabolomes of rigorously matched amyotrophic lateral sclerosis, Parkinson's disease and control subjects. *Mol. Biosyst.* **12**, 1287–1298 (2016).
171. Havelund, J. F. *et al.* Changes in kynurenine pathway metabolism in Parkinson patients with L-DOPA-induced dyskinesia. *J. Neurochem.* **142**, 756–766 (2017).
172. Johansen, K. K. *et al.* Metabolomic profiling in LRRK2-related Parkinson's disease. *PLoS One* **4**, 1–9 (2009).
173. Roede, J. R. *et al.* Serum Metabolomics of Slow vs. Rapid Motor Progression Parkinson's Disease: A Pilot Study. *PLoS One* **8**, 1–11 (2013).

Back to table of contents

CHAPTER 2

ARTICLE

Gut Bacterial Tyrosine Decarboxylases Restrict Levels of Levodopa in the Treatment of Parkinson's Disease

Sebastiaan P. van Kessel[1], Alexandra K. Frye[1], Ahmed O. El-Gendy[1†], Maria Castejon[1], Ali Keshavarzian[2], Gertjan van Dijk[3], and Sahar El Aidy[1*]

Nature Communications, 2019, 10, 310
DOI: 10.1038/s41467-019-08294-y

[1]Host-Microbe Interactions, Groningen Biomolecular Sciences and Biotechnology Institute (GBB), University of Groningen, Nijenborgh 7, 9747 AG Groningen, The Netherlands.
[2]Division of Digestive Disease and Nutrition, Section of Gastroenterology, Department of Internal Medicine, Rush University Medical Center, 1725 W. Harrison, Suite 206, Chicago, Illinois 60612, USA.
[3]Department of Behavioral Neuroscience, Groningen Institute for Evolutionary Life Sciences (GELIFES), University of Groningen, Nijenborgh 7, 9747 AG Groningen, The Netherlands.
[†]Present address: Faculty of Pharmacy, Department of Microbiology and Immunology, Beni-Suef University, Beni-Suef 62514, Egypt.

*Correspondence: Sahar El Aidy, sahar.elaidy@rug.nl

Gut Bacterial Tyrosine Decarboxylases Restrict Levels of Levodopa in the Treatment of Parkinson's Disease

Sebastiaan P. van Kessel, Alexandra K. Frye, Ahmed O. El- Gendy, Maria Castejon, Ali Keshavarzian, Gertjan van Dijk, and Sahar El Aidy

ABSTRACT Human gut microbiota senses its environment and responds by releasing metabolites, some of which are key regulators of human health and disease. In this study, we characterize gutassociated bacteria in their ability to decarboxylate levodopa to dopamine via tyrosine decarboxylases. Bacterial tyrosine decarboxylases efficiently convert levodopa to dopamine, even in the presence of tyrosine, a competitive substrate, or inhibitors of human decarboxylase. In situ levels of levodopa are compromised by high abundance of gut bacterial tyrosine decarboxylase in patients with Parkinson's disease. Finally, the higher relative abundance of bacterial tyrosine decarboxylases at the site of levodopa absorption, proximal small intestine, had a significant impact on levels of levodopa in the plasma of rats. Our results highlight the role of microbial metabolism in drug availability, and specifically, that abundance of bacterial tyrosine decarboxylase in the proximal small intestine can explain the increased dosage regimen of levodopa treatment in Parkinson's disease patients.

Nature Communications, 2019, 10, 310
DOI: 10.1038/s41467-019-08294-y

INTRODUCTION

The complex bacterial communities inhabiting the mammalian gut have a significant impact on the health of their host [1]. Numerous reports indicate that intestinal microbiota, and in particular its metabolic products, have a crucial effect on various health and diseased states. Host immune system and brain development, metabolism, behavior, stress and pain response all have been reported to be associated with microbiota disturbances [2-6]. In addition, it is becoming increasingly clear that gut microbiota can interfere with the modulation of drug efficacy [7,8].

Parkinson's disease (PD), the second most common neurodegenerative disorder, affecting 1% of the global population over the age of 60, and has recently been correlated with alterations in microbial gut composition [9-11]. The primary treatment of PD is levodopa (L-3,4-dihydroxyphenylalanine or L-DOPA) in combination of an aromatic amino acid decarboxylase inhibitor (primarily carbidopa) [12]. However, the bioavailability of levodopa/ decarboxylase inhibitor, required to ensure sufficient amounts of dopamine will reach the brain [13], varies significantly among PD patients. Because of this, levodopa/ decarboxylase inhibitor is ineffective in a subset of patients, and its efficacy decreases over time of treatment, necessitating more frequent drug doses, ranging from 3 to 8-10 tablets/day with higher risk of dyskinesia and other side effects [14]. A major challenge in the clinic is an early diagnosis of motor response fluctuation (timing of movement-related potentials) and decreased levodopa/ decarboxylase inhibitor efficacy to determine optimal dosage for individual patients and during disease progression. What remains to be clarified is whether inter-individual variations in gut microbiota composition and functionality play a causative role in motor response fluctuation in PD patients requiring higher daily levodopa/decarboxylase inhibitor treatment dosage regimen.

In fact, it had been shown that large intestinal microbiota could mainly dehydroxylate levodopa as detected in urine and cecal content of conventional rats [15]. However, these results do not explain a possible role of gut microbiota in the increased dosage regimen of levodopa/ decarboxylase inhibitor treatment in PD patients because the primary site of levodopa absorption is the proximal small intestine (jejunum) [16].

Several amino acid decarboxylases have been identified in bacteria. Tyrosine decarboxylase genes (*tdc*) have especially been encoded in the genome of several bacterial species in the genera *Lactobacillus* and *Enterococcus* [17,18]. Though tyrosine decarboxylase (TDC) is named for its capacity to decarboxylate L-tyrosine into tyramine, it might also have the ability to decarboxylate levodopa to produce dopamine due to the high similarity of the chemical structures of these substrates. This implies that TDC activity of the gut microbiota might interfere with levodopa/ decarboxylase inhibitor availability, thus the treatment of PD patients.

The aim of the present study is to parse out the effect of levodopa metabolizing bacteria, particularly in the jejunum, where levodopa is absorbed. Initially, we established TDC present in small intestinal bacteria efficiently converted levodopa to dopamine, confirming their capacity to influence the *in situ* levels of the primary treatment of PD patients. We show that higher relative abundance of bacterial *tdc* gene in stool samples of PD patients positively correlates

with higher daily levodopa/carbidopa dosage requirement and duration of disease. We further confirm our findings in rats orally administered levodopa/carbidopa, illustrating that levodopa levels in plasma negatively correlate with the abundance of bacterial *tdc* gene in the jejunum.

RESULTS

Upper small intestinal bacteria convert levodopa to dopamine

To determine whether jejunal microbiota maintain the ability to metabolize levodopa, luminal samples from the entire jejunum of wild-type Groningen rats housed in different cages were incubated *in vitro* with levodopa and analyzed by High-Performance Liquid Chromatography with Electrochemical Detection (HPLC-ED). Chromatograms revealed that levodopa decarboxylation to dopamine coincides with the conversion of tyrosine to tyramine (**Figure 1A**). Ranking the chromatograms from high to low decarboxylation of levodopa and tyrosine, shows that only when tyrosine is decarboxylated, dopamine is produced (**Figure 1b**). No other metabolites were detected in the treated samples, except of few unknown peaks, which were also present in the control samples, thus are not products of bacterial metabolism of levodopa. In addition, no dopamine production was observed in control samples (**Supplementary Figure 1**). Of note, no basal levels of levodopa were detected in the measured samples by HPLC. Taken together, the results suggest that bacterial TDC is involved in levodopa conversion into dopamine, which may, in turn, interfere with levodopa uptake in the proximal small intestine.

Levodopa decarboxylation by bacterial tyrosine decarboxylase

The coinciding tyrosine and levodopa decarboxylation observed in the luminal content of jejunum was the basis of our hypothesis that TDC is the enzyme involved in both conversions. Species of the genera *Lactobacillus* and *Enterococcus* have been reported to harbor this enzyme [17,19]. To identify whether the genome of other (small intestinal) gut bacteria also encode *tdc*, the TDC protein sequence (EOT87933) from *Enterococcus faecalis* v583 was used as a query to search the US National Institutes of Health Human Microbiome Project (HMP) protein database. This analysis exclusively identified TDC proteins in species belonging to the bacilli class, including more than 50 *Enterococcus* strains (mainly *E. faecium* and *E. faecalis*) and several *Lactobacillus* and *Staphylococcus* species (**Supplementary Figure 2A**). Next, we aligned the genome of *E. faecalis* v583 with two gut bacterial isolates, *E. faecium* W54, and *L. brevis* W63, illustrating the conservation of the *tdc*-operon among these species (**Figure 2A**). Intriguingly, analysis of *E. faecium* genomes revealed that this species encodes a second, paralogous *tdc* gene ($^{P}TDC_{EFM}$) that did not align with the conserved *tdc*-operon and was absent from the other species (**Figure 2A, Supplementary Figure 2A and 6**).

To support our *in silico* data, a comprehensive screening of *E. faecalis* v583, *E. faecium* W54, and *L. brevis* W63 and 77 additional clinical and human isolates of *Enterococcus*, including clinical isolates and strains from healthy subjects, was performed. All enterococcal isolates and

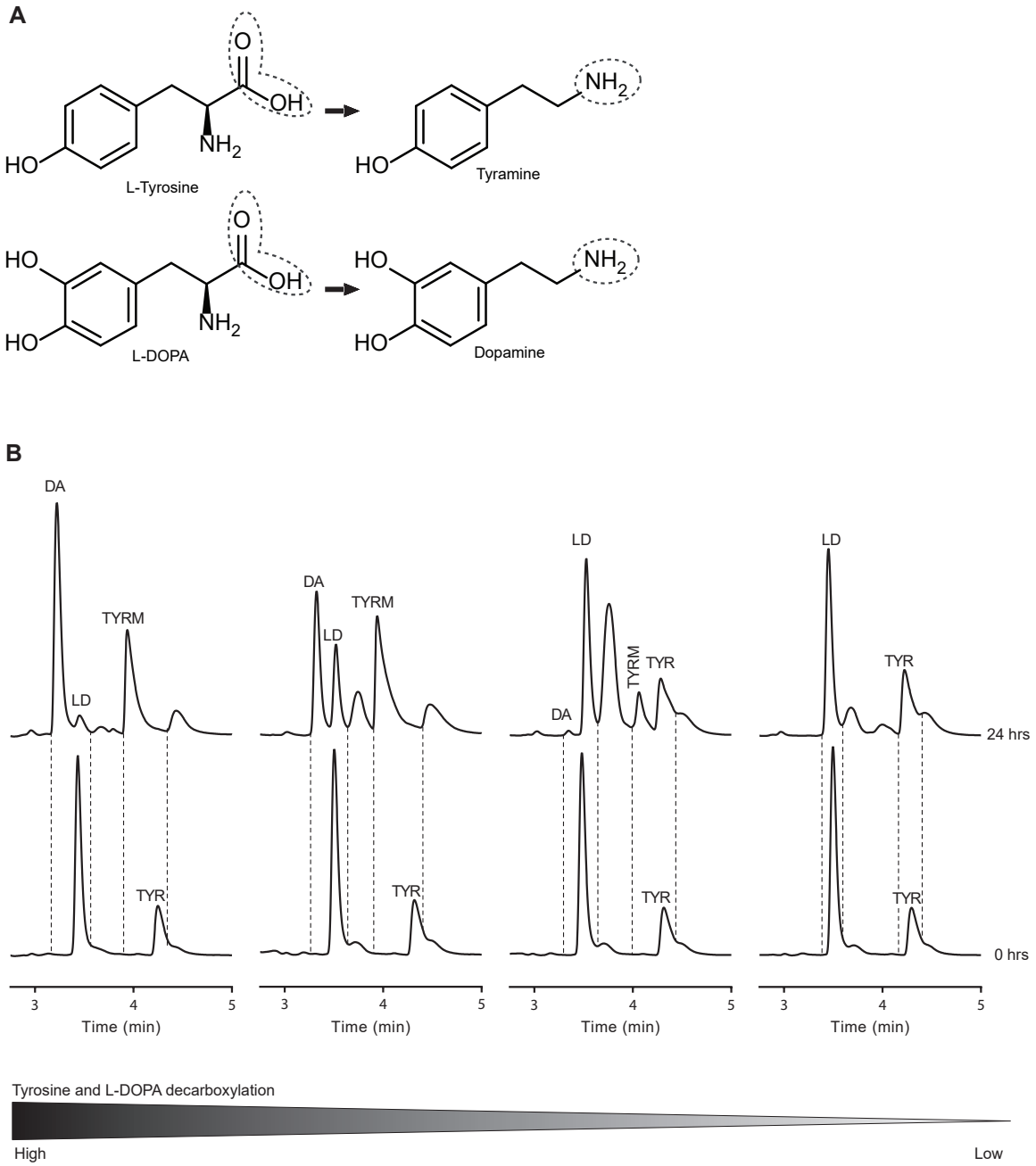

Figure 1 | Bacteria in jejunal content decarboxylate levodopa to dopamine coinciding with their production of tyramine *ex vivo*. (**A**) Decarboxylation reaction for tyrosine and levodopa. (**B**) From left to right coinciding bacterial conversion of tyrosine (TYR) to tyramine (TYRM) and 1 mM of supplemented levodopa (LD) to dopamine (DA) during 24 h of incubation of jejunal content. The jejunal contents are from four different rats ranked form left to right based on the decarboxylation levels of tyrosine and levodopa, showing that tyrosine decarboxylation is coinciding with levodopa decarboxylation.

L. brevis were able to convert tyrosine and levodopa into tyramine and dopamine, respectively (**Figure 2B-D, Supplementary Table 1**). Notably, our HPLC-ED analysis revealed considerable variability among the tested strains with regard to their efficiency to decarboxylate levodopa. *E. faecium* and *E. faecalis* were drastically more efficient at converting levodopa to dopamine, compared to *L. brevis*. Growing *L. brevis* in different growth media did not change the levodopa decarboxylation efficacy (**Supplementary Figure 2B, C**).

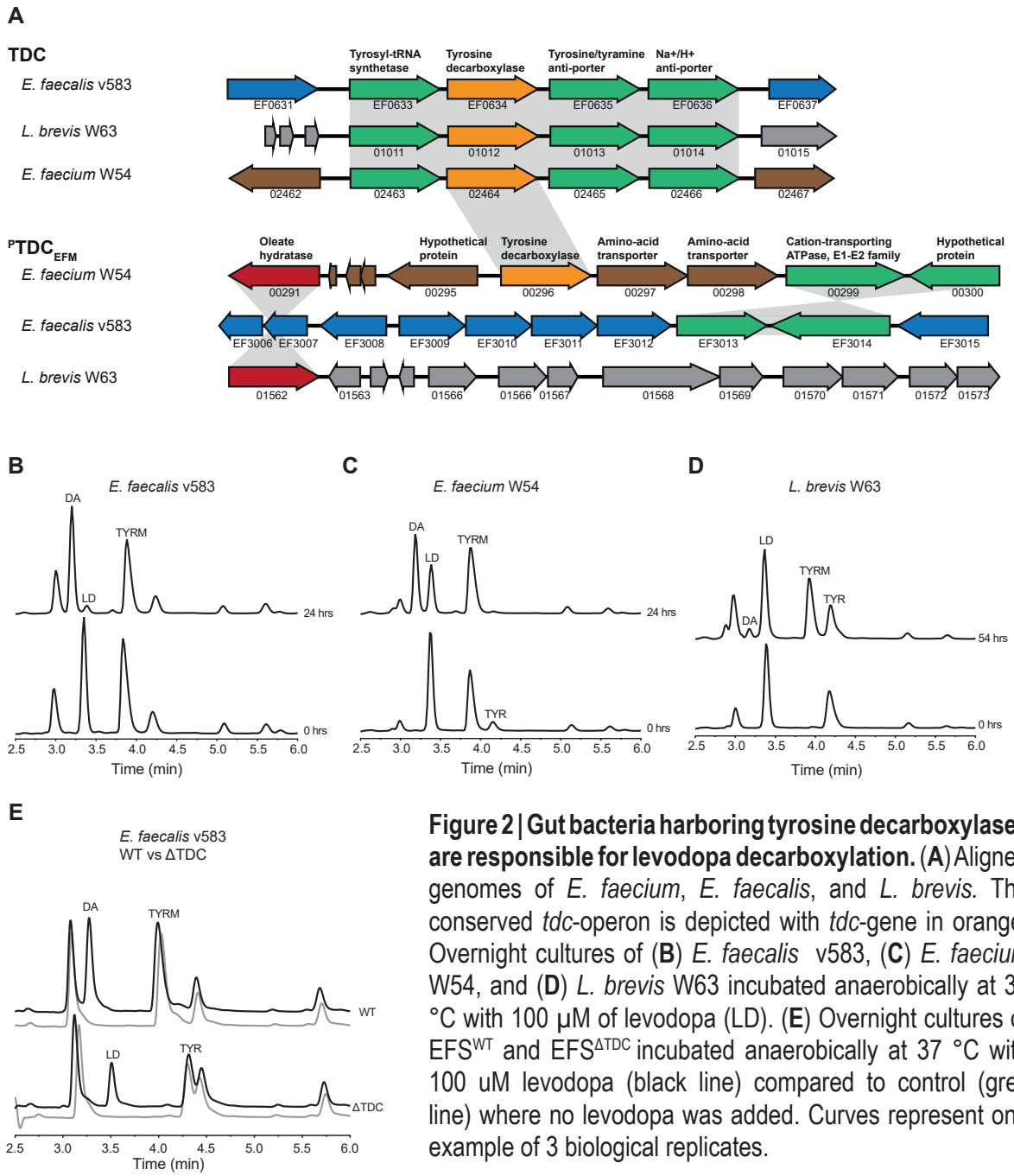

Figure 2 | Gut bacteria harboring tyrosine decarboxylases are responsible for levodopa decarboxylation. (**A**) Aligned genomes of *E. faecium*, *E. faecalis*, and *L. brevis.* The conserved *tdc*-operon is depicted with *tdc*-gene in orange. Overnight cultures of (**B**) *E. faecalis* v583, (**C**) *E. faecium* W54, and (**D**) *L. brevis* W63 incubated anaerobically at 37 °C with 100 µM of levodopa (LD). (**E**) Overnight cultures of EFS^{WT} and $EFS^{\Delta TDC}$ incubated anaerobically at 37 °C with 100 uM levodopa (black line) compared to control (grey line) where no levodopa was added. Curves represent one example of 3 biological replicates.

To eliminate the possibility that other bacterial amino acid decarboxylases are involved in levodopa conversion observed in the jejunal content we expanded our screening to include live bacterial species harboring PLP-dependent amino acid decarboxylases previously identified by Williams et al [20]. None of the tested bacterial strains encoding different amino acid decarboxylases could decarboxylate levodopa (**Supplementary Figure 2D-G, Supplementary Table 2**).

To verify that the TDC is solely responsible for levodopa decarboxylation in *Enterococcus*, wild type *E. faecalis* v583 (EFS^{WT}) was compared with a mutant strain ($EFS^{\Delta TDC}$) [17]. Overnight

incubation of EFS^{WT} and $EFS^{\Delta TDC}$ bacterial cells with levodopa resulted in production of dopamine in the supernatant of EFS^{WT} but not $EFS^{\Delta TDC}$ (**Figure 2E**), confirming the pivotal role of this gene in this conversion. Collectively, results show that TDC is encoded on genomes of gut bacterial species known to dominate the proximal small intestine and that this enzyme is exclusively responsible for converting levodopa to dopamine by these bacteria, although the efficiency of that conversion displays considerable species-dependent variability.

Tyrosine abundance does not prevent levodopa decarboxylation

To test whether the availability of the primary substrate for bacterial TDC (i.e., tyrosine) could inhibit the uptake and decarboxylation of levodopa, the growth, metabolites, and pH that was previously shown to affect the expression of *tdc* [17], of *E. faecium* W54 and *E. faecalis* v583 were analyzed over time. 100 µM levodopa was added to the bacterial cultures, whereas approximately 500 µM tyrosine was present in the growth media, which corresponds to the levels of tyrosine found in the jejunum[21]. Remarkably, levodopa and tyrosine were converted simultaneously, even in the presence of these excess levels of tyrosine (1:5 levodopa to tyrosine), albeit at a slower conversion rate for levodopa (**Figure 3A-B**). Notably, the decarboxylation reaction appeared operational throughout the exponential phase of growth for *E. faecalis*, whereas it is only observed in *E. faecium* when this bacterium entered the stationary phase of growth, suggesting differential regulation of the *tdc* gene expression in these species.

To further characterize the substrate specificity and kinetic parameters of the bacterial tyrosine decarboxylases, *tdc* genes from *E. faecalis* v583 (TDC_{EFS}) and *E. faecium* W54 (TDC_{EFM} and $^{P}TDC_{EFM}$) were expressed in *Escherichia coli* BL21 (DE3) and then purified. Michaelis-Menten kinetics indicated each of the studied enzymes had a significantly higher affinity (K_m) (**Figure 3C-I**) and catalytic efficiency (K_{cat}/K_m) for tyrosine than for levodopa (**Table 1**). Despite the differential substrate affinity, our findings illustrate that high levels of tyrosine do not prevent the decarboxylation of levodopa in batch culture.

Carbidopa does not inhibit bacterial decarboxylases

To assess the extent to which human DOPA decarboxylase inhibitors could affect bacterial decarboxylases, three human DOPA decarboxylase inhibitors (carbidopa, benserazide, and methyldopa) were tested on purified bacterial TDCs and on the corresponding bacterial batch cultures. Comparison of the inhibitory constants (K_i^{TDC}/K_i^{DDC}) demonstrates carbidopa to be a 1.4-1.9 x 10^4 times more potent inhibitor of human DOPA decarboxylase than bacterial TDCs (**Figure 4A, Supplementary Figure 3; Supplementary Table 3**). This is best illustrated by the observation that levodopa conversion by *E. faecium* W54 and *E. faecalis* v583 batch cultures (OD_{600}= ~2.0) was unaffected by co-incubation with carbidopa (equimolar or 4-fold carbidopa relative to levodopa) (**Figure 4B, C**, **Supplementary Figure 4A**). Analogously, benserazide and methyldopa did not inhibit the levodopa decarboxylation activity in *E. faecalis* or *E. faecium* (**Supplementary Figure 4B, C**).

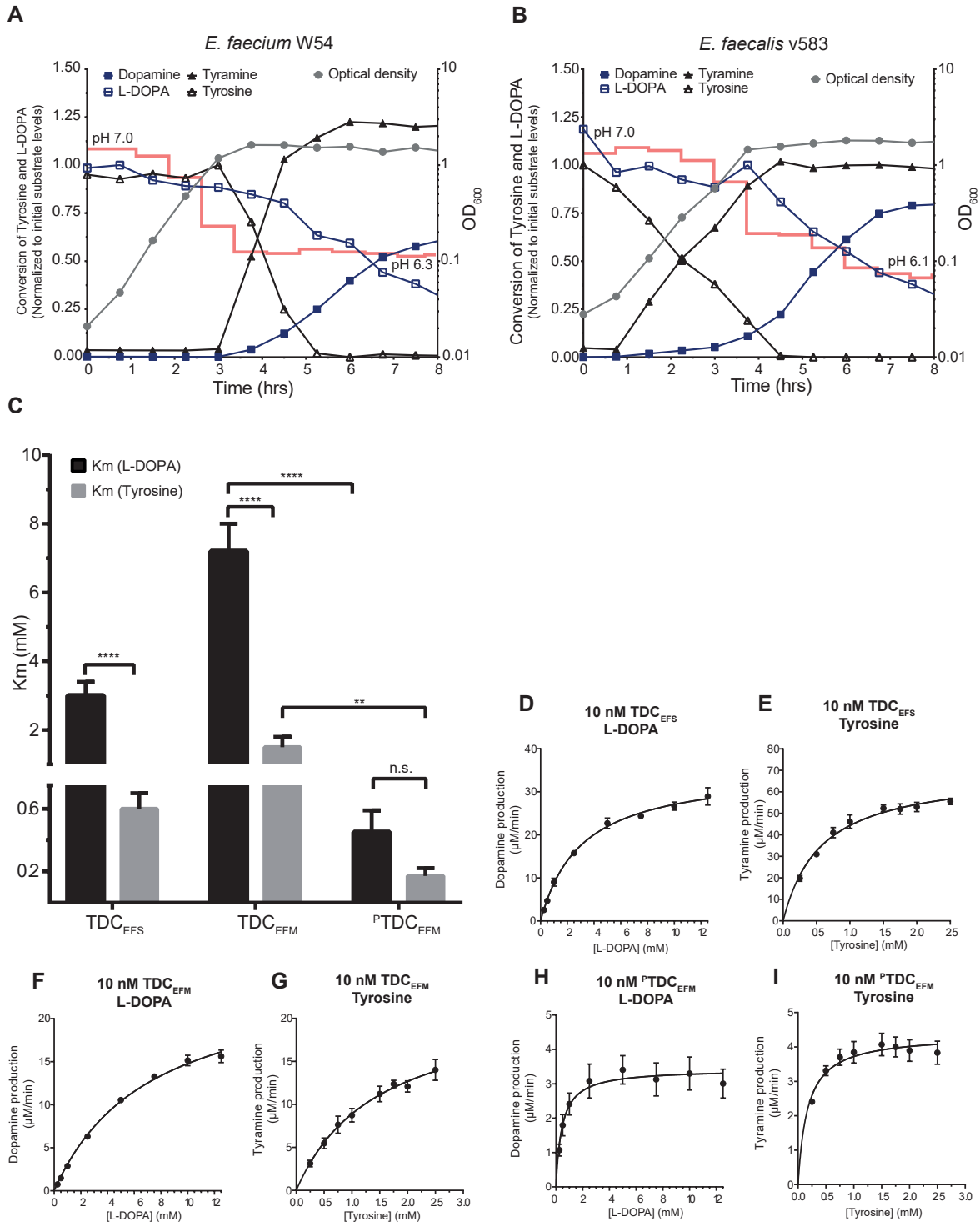

Figure 3 | Enterococci decarboxylate levodopa in presence of tyrosine despite higher affinity for tyrosine *in vitro*. Growth curve (grey circle, right Y-axis) of *E. faecium* W54 (**A**) and *E. faecalis* (**B**) plotted together with levodopa (open square), dopamine (closed square), tyrosine (open triangle), and tyramine (closed triangle) levels (left Y-axis). Concentrations of product and substrate were normalized to the initial levels of the corresponding substrate (100 µM supplemented levodopa and ~500 µM tyrosine present in the medium). pH of the culture is indicated over time as a red line. (**C**) Substrate affinity (Km) for levodopa and tyrosine for purified tyrosine decarboxylases from *E. faecalis* v583 (TDC_{EFS}), *E. faecium* W54 (TDC_{EFM}, $^{P}TDC_{EFM}$). (**D-I**) Michaelis-Menten kinetic curves for levodopa and tyrosine as substrate for TDC_{EFS} (**D,E**), TDC_{EFM} (**F,G**), and $^{P}TDC_{EFM}$ (**H,I**). (continued)

Figure 3 | Continued. Reactions were performed in triplicate using levodopa concentrations ranging from 0.5-12.5 mM and tyrosine concentrations ranging from 0.25-2.5 mM. The enzyme kinetic parameters were calculated using nonlinear Michaelis-Menten regression model. Error bars represent the SEM and significance was tested using 2-way-Anova, Fisher LSD test, (*=p<0.02 **=p<0.01 ****<0.0001).

Table 1 | Michaelis-Menten kinetic parameters

Levodopa	pH 5.0 TDC_{EFS}	pH 5.0 TDC_{EFM}	pH 4.5 $^{P}TDC_{EFM}$	pH 7.4 DDC
[E] (nM)	10	10	10	10
Km (mM)	3±0.4	7.2±0.8	0.4±0.1	0.1±0.01
Vmax (µM/min)	35.3±1.4	25.5±1.3	3.4±0.2	1.4±0.03
Kcat (min-1)	3531±137	2549±133	342.4±21	136.9±3
Kcat/Km (min-1/mM-1)	1160	352	764	1567
R^2	0.978	0.99	0.621	0.962

Tyrosine	pH 5.0 TDC_{EFS}	pH 5.0 TDC_{EFM}	pH 4.5 $^{P}TDC_{EFM}$
[E] (nM)	10	10	10
Km (mM)	0.6±0.1	1.5±0.3	0.2±0.05
Vmax (µM/min)	69.6±2.9	22±2.5	4.4±0.2
Kcat (min-1)	6963±288	2204±247	435.6±19.2
Kcat/Km (min-1/mM-1)	12216	1493	2558
R^2	0.928	0.902	0.589

Enzyme kinetic parameters were determined by Michaelis-Menten nonlinear regression model for levodopa and tyrosine as substrates. ± indicates the standard error.

These findings demonstrate the commonly applied inhibitors of human DOPA decarboxylase in levodopa combination therapy do not inhibit bacterial TDC dependent levodopa conversion, implying levodopa /carbidopa (levodopa) combination therapy for PD patients would not affect the efficacy of levodopa *in situ* by small intestinal bacteria.

PD dosage regimen correlates with *tdc* gene abundance

To determine whether the increased dosage regimen of levodopa treatment in PD patients could be attributed to the abundance of *tdc* genes in the gut microbiota, fecal samples were collected from male and female PD patients (**Supplementary Table 4**) on different doses of levodopa /carbidopa treatment (ranging from 300 up to 1100 mg levodopa per day). *tdc* gene-specific primers were used to quantify its relative abundance within the gut microbiota by qPCR and results were normalized to 16s rRNA gene to correct for difference in total bacterial counts among the stool samples (**Supplementary Figure 5**). Remarkably, Pearson *r* correlation analyses showed a strong positive correlation (r= 0.66, R^2= 0.44, *p value*= 0.037) between

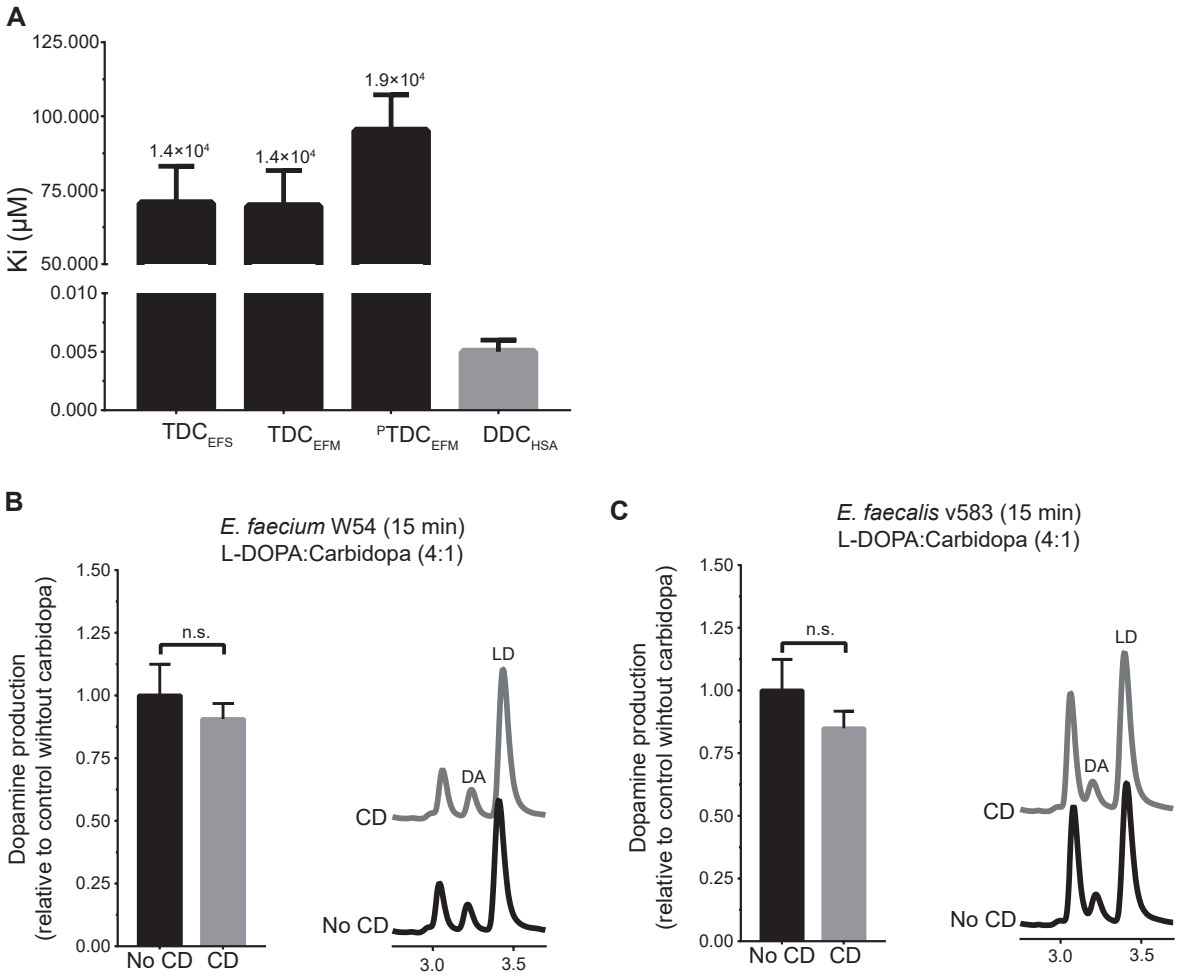

Figure 4 | Human DOPA decarboxylase inhibitor, carbidopa, does not inhibit bacterial tyrosine decarboxylases. (**A**) Inhibitory constants (Ki) of bacterial decarboxylases (black) and human DOPA decarboxylase (grey), with fold-difference between bacterial and human decarboxylase displayed on top of the bars. Quantitative comparison of dopamine (DA) production by E. faecium W54, (**B**) and E. faecalis v583, (**C**) at stationary phase after 15 min, with representative HPLC-ED curve. Bacterial cultures (n=3) were incubated with 100 μM levodopa (LD) or a 4:1 mixture (in weight) of levodopa and carbidopa (CD) (100 μM levodopa and 21.7 μM carbidopa). Error bars represent SEM (**A**) or SD (**B,C**) and significance was tested using a parametric unpaired T-test.

bacterial *tdc* gene relative abundance and levodopa /carbidopa treatment dose (**Figure 5A**), as well as with the duration of disease (**Figure 5B**, **Supplementary Table 5**). Collectively, the selective prevalence of *tdc* encoding genes in the genomes of signature microbes of the small intestine microbiota supports the notion that the results obtained from fecal samples are a valid representation of *tdc* gene abundance in the small intestinal microbiota. Moreover, the significant correlation of the relative *tdc* abundance in the fecal microbiota and the required levodopa /carbidopa dosage strongly supports a role for bacterial TDC in levodopa /carbidopa efficacy.

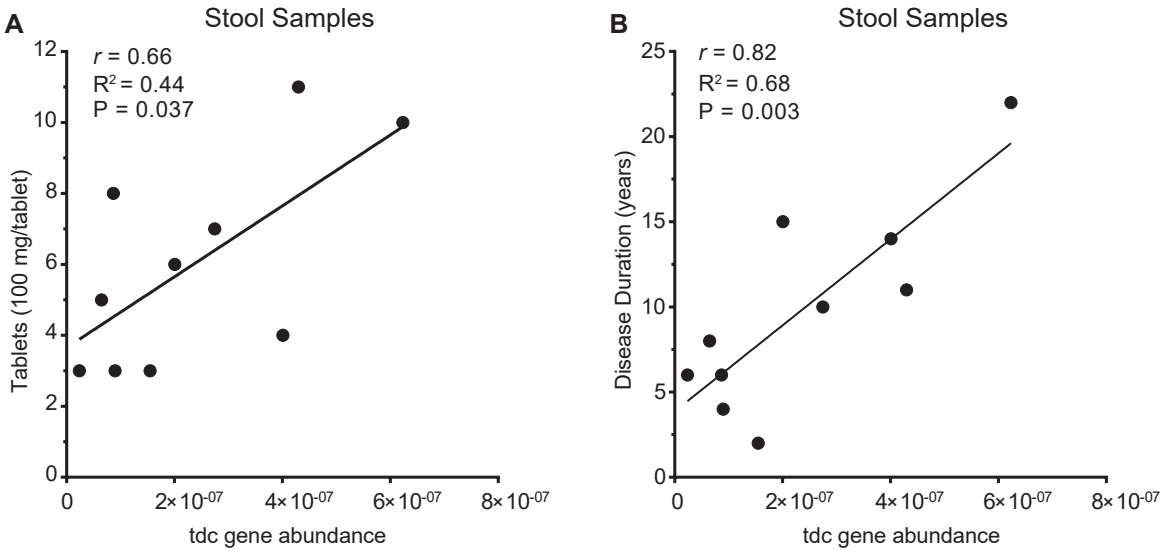

Figure 5 | Tyrosine decarboxylase gene abundance correlates with daily levodopa dose and disease duration in fecal samples of Parkinson's disease patients. (**A**) Scatter plot of *tdc* gene abundance measured by qPCR in fecal samples of PD patients (n=10) versus daily levodopa/carbidopa dosage fitted with linear regression model. (**B**) Scatter plot of *tdc* gene abundance from the same samples versus disease duration fitted with a linear regression model. Pearson's r analysis was used to determine significant correlations between tyrosine decarboxylase gene abundance and dosage (r=0.66, R^2=0.44, P value=0.037) or disease duration (r = 0.82, R^2 = 0.68, P value = 0.003).

At this stage, it is not demonstrated whether the relative abundance of *tdc* in fecal samples reflects its abundance in the proximal small intestine. This is of particular importance because levodopa is absorbed in the proximal small intestine, and reduction in its bioavailability by bacterial TDC activity in the context of PD patients' medication regimens would only be relevant in that intestinal region.

Higher *tdc* gene abundance restricts levodopa level in plasma

To further consolidate the concept that *tdc* gene abundance in proximal small intestinal microbiota affects peripheral levels of levodopa /carbidopa in blood and dopamine: levodopa / carbidopa ratio in the jejunal luminal content, male wild-type Groningen rats (n=18) rats were orally administered 15 mg levodopa /3.75 mg carbidopa per kg of body weight and sacrificed after 15 minutes (point of maximal levodopa bioavailability in rats [22]). Plasma levels of levodopa /carbidopa and its metabolite dopamine were measured by HPLC-ED, while relative abundance of the *tdc* gene within the small intestinal microbiota was quantified by gene-specific qPCR (**Supplementary Figure 5**). Strikingly, Pearson *r* correlation analyses showed that the ratio between dopamine and levodopa /carbidopa levels in the proximal jejunal content positively correlated with *tdc* gene abundance (r= 0.78, R^2= 0.61, P value = 0.0001), whereas the levodopa/carbidopa concentration in the proximal jejunal content negatively correlated with the abundance of the *tdc* gene (r= −0.68, R^2= 0.46, P value = 0.021) (**Figure 6A**). Moreover, plasma levels of levodopa /carbidopa displayed a strong negative correlation (r = −0.57, R^2 = 0.33, P value = 0.017) with the relative abundance of the *tdc* gene (**Figure 6B**). No basal levels of levodopa were detected in the measured samples by HPLC-ED.

To further support this correlation, plasma levels of levodopa/carbidopa from rats treated with EFS^{WT} (n=10) or $EFS^{\Delta TDC}$ (n=10) cells were determined after oral administration with levodopa/ carbidopa mixture (4:1). Rats treated with EFS^{WT} showed significant lower levels (*P* value <0.01) of levodopa/carbidopa in their plasma compared to rats treated with $EFS^{\Delta TDC}$ (**Figure 6C**). Collectively, these findings clearly show that levodopa /carbidopa uptake by the host is compromised by higher abundance of gut bacteria encoding for *tdc* genes in the upper region of the small intestine.

DISCUSSION

Our observation that the jejunal microbiota are able to convert levodopa to dopamine (**Figure 1**) was the basis of investigating the role of levodopa metabolizing bacteria in the context of the disparity in increased dosage regimen of levodopa /carbidopa treatment in a subset of PD patients (**Figure 5**) and the accompanying adverse side effects [23]. This study identifies a significant factor to explain the motor response (timing of movement-related potentials) fluctuations observed in PD patients requiring frequent levodopa /decarboxylase inhibitor administration.

Our primary outcome is that levodopa decarboxylation by small intestinal bacteria, in particular, members of bacilli, including the genera *Enterococcus* and *Lactobacillus*, which were previously identified as the predominant residents of the small intestine [24,25], would drastically reduce the levels of levodopa/decarboxylase inhibitor in the body, and thereby contribute to the observed higher dosages required in a subset of PD patients. Previously, reduced levodopa availability has been associated with *Helicobacter pylori* positive PD patients, which was explained by the observation that *H. pylori* could bind levodopa *in vitro* via surface adhesins [8]. However, this explanation is valid only for a small population of the PD patients, who suffer from stomach ulcers and thus have high abundance of *H. pylori.*

The impaired intestinal motility frequently observed in PD patients [26] could also result from altered levels of dopamine, the conversion product of bacterial *tdc* metabolism of levodopa [27] but has been also associated with small intestinal bacterial overgrowth [28], and worsening of motor response fluctuations thus requiring higher dosage frequency of levodopa/decarboxylase inhibitor treatment [29]. Moreover, the decreasing efficacy of levodopa treatment observed in PD patients might be explained by the overgrowth of small intestinal bacteria that metabolize levodopa resulting from proton pump inhibitors [30-32] for treatment of gastrointestinal symptoms. In particular, *Enterococcus* has been reported to dominate in proton pump inhibitors' induced small intestinal bacterial overgrowth [33]. Altogether, these factors will enhance a state of small intestinal bacterial overgrowth, and perpetuating a vicious circle leading to increased levodopa/decarboxylase inhibitor dosage requirement in a subset of PD patients (**Figure 7**). Finally, it is likely that prolonged levodopa/ decarboxylase inhibitor administration favors growth of *tdc* expressing bacteria in the proximal small intestine, resulting in higher levels of *tdc* further lowering the efficacy of levodopa. In fact, it has been shown that the fitness

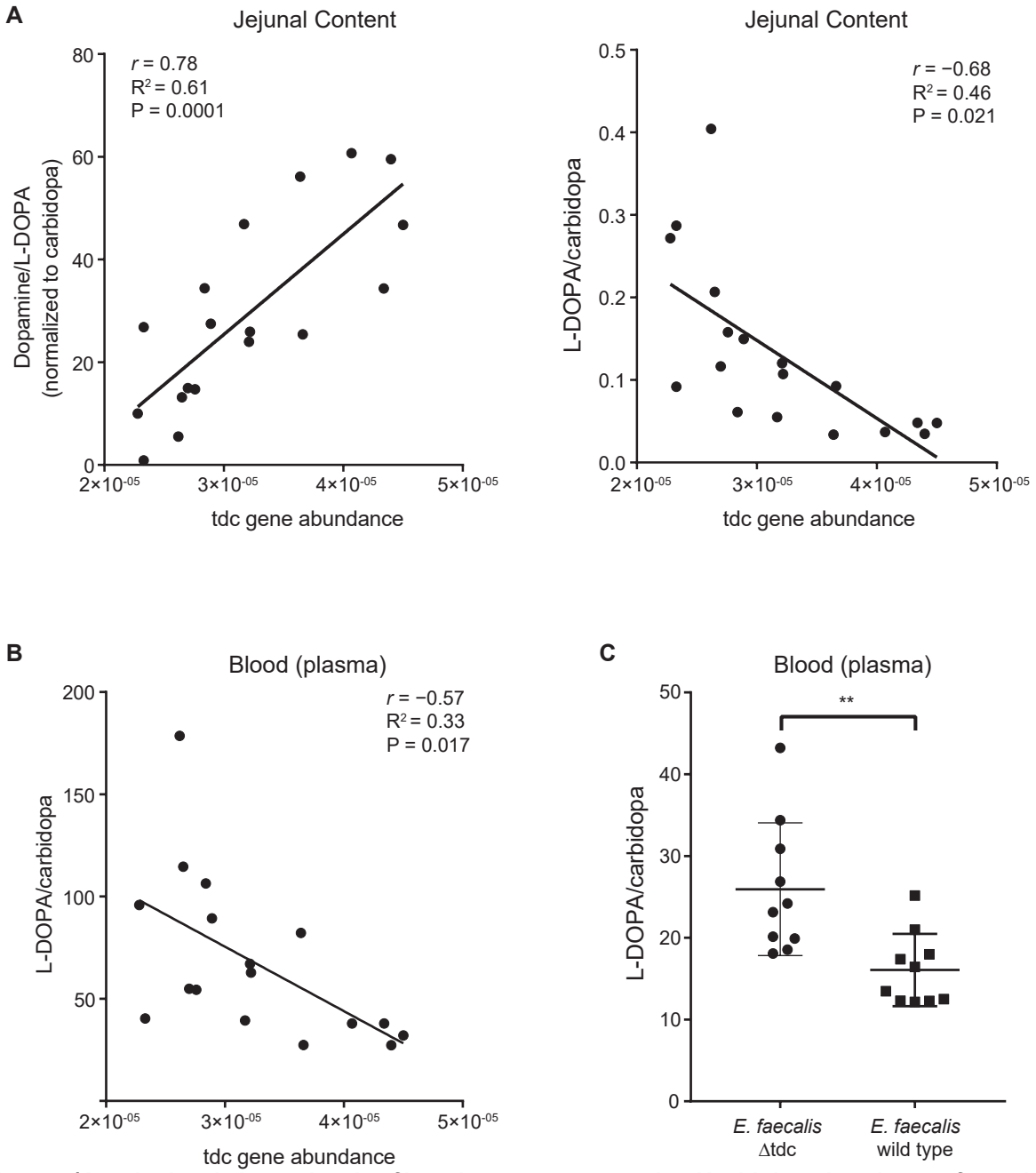

Figure 6 | Luminal and plasma levels of levodopa are compromised by higher abundance of tyrosine decarboxylase gene in the small intestine of rats. Scatter plot of *tdc* gene abundance measured by qPCR in jejunal content of wild-type Groningen rats (n=18) orally supplied with levodopa/ carbidopa mixture (4:1) versus (**A**) the dopamine: levodopa/carbidopa levels in the jejunal content, the levodopa/ carbidopa levels in the jejunal content, (**B**) or the levodopa/carbidopa levels in the plasma, fitted with a linear regression model. Intake of levodopa/carbidopa was corrected by using carbidopa as an internal standard. Pearson's r correlation was used to determine significant correlations between *tdc* abundance and jejunal dopamine levels (r = 0.78, R^2 = 0.61, P value = 0.0001), jejunal levodopa/carbidopa levels (r = −0.68, R^2 = 0.46 P value = 0.021), or plasma levodopa/carbidopa levels (r = −0.57, R^2 = 0.33, P value = 0.017). No levodopa/carbidopa, dopamine, or DOPAC were detected in the control group (n=5). (**C**) Significant difference in plasma levels of levodopa/carbidopa orally supplied to rats after treatment with EFS^{WT} (n=10) or $EFS^{\Delta TDC}$ (n=10). Significance was tested using parametric unpaired T-test (**=p<0.01).

of *E. faecalis* v583 in low pH depends on the *tdc*-operon [17], indicating long-term exposure to levodopa could contribute to selection for overgrowth of *tdc* encoding bacteria *in vivo* as supported by the positive correlation with *tdc* gene abundance observed in human stool samples (**Figure 5B**). This would explain the fluctuating motor response and subsequent increased levodopa/ decarboxylase inhibitor dosage regimen thus severity of its adverse effects such as dyskinesia during prolonged disease treatment [34].

While our further investigation into the kinetics of both bacterial and human decarboxylases support the effectiveness of carbidopa to inhibit the human DOPA decarboxylase, it also shows that the same drug fails to inhibit levodopa decarboxylation by bacterial TDC, probably due to the presence of an extra hydroxyl group on the benzene ring of carbidopa (**Figure 4, Supplementary Figure 3**) or ineffective transport of the inhibitor inside the bacterial cell. This suggests a better equilibration of levodopa treatment between patients could potentially be achieved by co-administration of an effective TDC inhibitor that targets both human and bacterial decarboxylases. Alternatively, we are currently evaluating regulation of *tdc* gene expression to help avoid the need for high levodopa dosing, thus minimizing its adverse side effects.

Notably, a few *Enterococcus* strains that harbor the *tdc* gene are marked as probiotics. The use of such strains as dietary supplements should be recognized in case of PD patients. More generally, our data support the increasing interest in the impact that gut microbiota metabolism may have on medical treatment and diet.

Collectively, our data show that levodopa conversion by bacterial TDC in the small intestine should be considered as a significant explanatory factor for the increased levodopa/ carbidopa dosage regimen required in a subset of PD patients. Although the data from PD patients are tentative due to small number of samples, this study strongly suggests these bacteria or their encoded *tdc* gene may potentially serve as a predictive biomarker to stratify PD patients for efficacy of levodopa treatment as supported by the significant (r = 0.66) correlation observed between the relative abundance of bacterial *tdc* genes in stool samples of patients and number of levodopa/carbidopa tablets required to treat individual PD patients (**Figure 5**). To overcome the limitation of the small number of samples from PD patients in this study, we are currently validating the development of such a simple cost-effective novel biomarker for optimal dosage of levodopa/ carbidopa and to prevent side-effects in a large longitudinal cohort of newly diagnosed PD patients, who are followed over long periods of time.

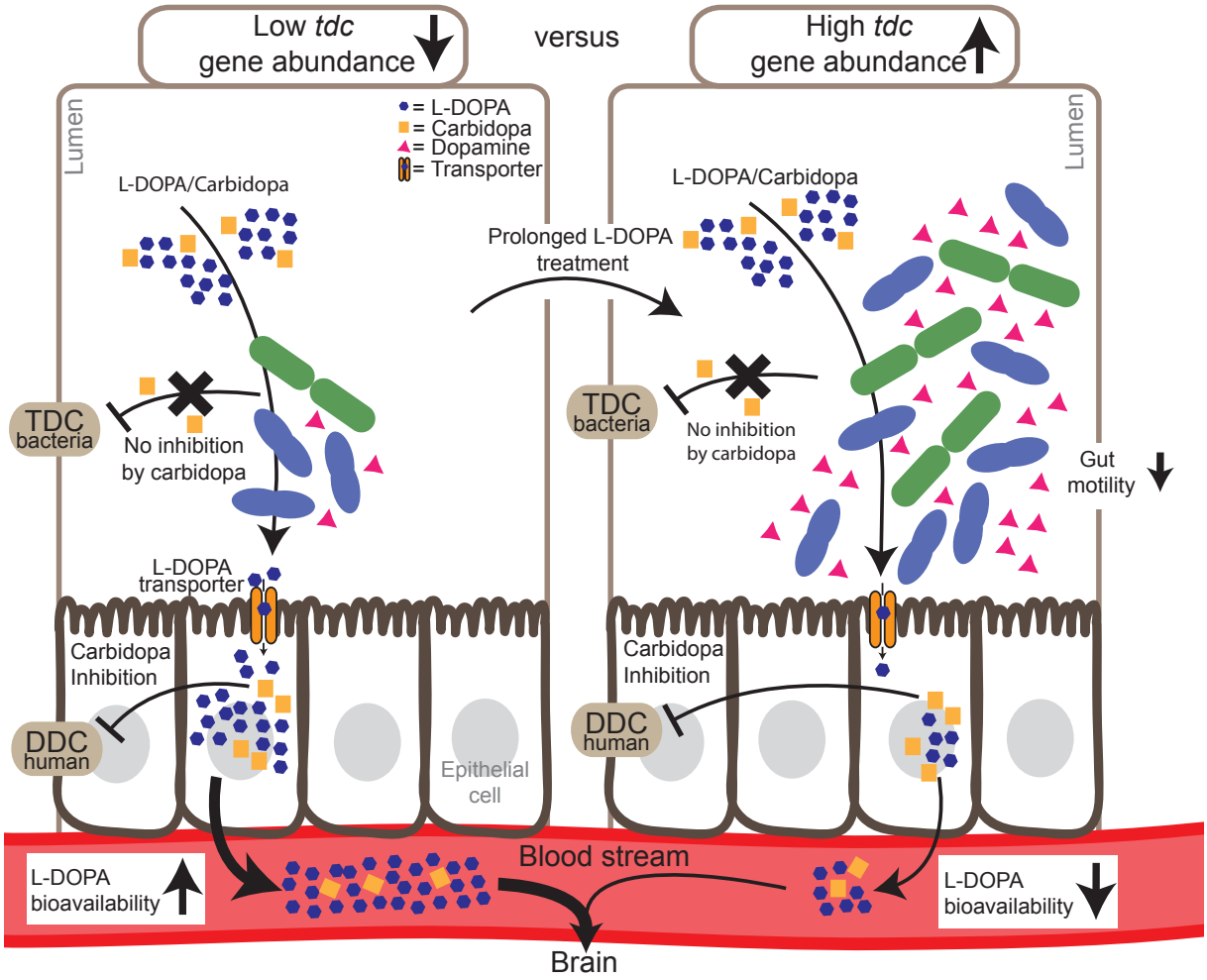

Figure 7 | Higher abundance of tyrosine decarboxylase can explain increased levodopa administration requirement in Parkinson's disease patients. A model representing two opposing situations, in which the proximal small intestine is colonized by low (left) or high abundance of tyrosine decarboxylase-encoding bacteria. The latter could result from or lead to increased individual L-DOPA dosage intake.

METHODS

Human fecal samples from patients with Parkinson's disease

Fecal samples from patients diagnosed with Parkinson's disease (n=10) on variable doses (300-1100mg levodopa per day) of levodopa/carbidopa treatment were acquired from the Movement Disorder Center at Rush University Medical Center, Chicago, Illinois, USA. Patients' characteristics were published previously [35] (more details are provided in Supplementary Table 4). Solid fecal samples were collected in anaerobic fecal bags and kept sealed in a cold environment until brought to the hospital where they were immediately stored at −80°C until analysis.

Rats

All animal procedures were approved by the Groningen University Committee of Animal experiments (approval number: AVD1050020184844), and were performed in adherence to the NIH Guide for the Care and Use of Laboratory Animals.

Twenty-five male wild-type Groningen rats (Groningen breed, male, age 18-24 weeks) housed 4-5 animals/cage had *ad libitum* access to water and food (RMH-B, AB Diets; Woerden, the Netherlands) in a temperature (21 ± 1°C) and humidity-controlled room (45–60% relative humidity), with a 12 h light/dark cycle (lights off at 1:00 p.m.). These outbred rats are very frequently used in behavioral studies[36] due to the high inter-individual variation (also in their microbiota composition), thus resembling, to some extent, the human inter-individual variation. On ten occasions over a period of three weeks, rats were taken from their social housing cage between circadian times 6 and 16.5, and put in an individual training cage (L×W×H = 25×25×40 cm) with a layer of their own sawdust without food and water. Ten minutes after transfer to these cages, rats were offered a drinking pipet in their cages with a 2.5 ml saccharine-solution (1.5 g/L, 12476, Sigma). Over the course of training, all rats learned to drink the saccharine-solution avidly. On the 11th occasion, the saccharine solution was used as vehicle for the levodopa/carbidopa mixture (15/3.75 mg/kg), which all rats drank within 15 seconds. Fifteen minutes after drinking the latter mixture (maximum bioavailability time point of levodopa in blood as previously described [22], the rats were anesthetized with isoflurane and sacrificed. Blood was withdrawn by heart puncture and placed in tubes pre-coated with 5 mM EDTA. The collected blood samples were centrifuged at 1500 × g for 10 minutes at 4°C and the plasma was stored at −80°C prior to levodopa, dopamine, and DOPAC extraction. Luminal contents were harvested from the entire rat jejunum by gentle pressing and were snap frozen in liquid N_2, stored at −80°C until used for qPCR, and extraction of levodopa and its metabolites. The Jejunum was distinguished from ileum by length (the intestinal tubes starting at 5 cm from stomach to cecum was divided into two; the proximal part was considered jejunum) Oral administration (by drinking, with saccharine as vehicle) of levodopa was corrected for by using carbidopa as an internal standard to correct for intake. Further, 5 rats were used as control and were administered a saccharine only solution (vehicle) to check for basal levels of levodopa, dopamine, and DOPAC levels or background HPLC-peaks. Jejunal content of control rats was used in *ex vivo* fermentation experiments (see incubation experiments of jejunal content section).

Treatment with EFS^{WT} and EFS$^{\Delta TDC}$ bacteria

Rats (n =20) were treated orally with 200 mg/kg body weight Rifaximin (R9904, Sigma) for 5 consecutive days as previously shown [29]. Subsequently, the rats were treated orally with 10^{10}-10^{11} CFU wild type (n=10) or Δ*tdc* (n=10) *E. faecalis* v583 cells (EFS^{WT} and EFS$^{\Delta TDC}$ respectively) for 5 other consecutive days. One day following the bacterial treatment, the rats were orally supplied with levodopa/ carbidopa mixture (4:1) as described above.

Bacteria

Escherichia coli DH5a or BL21 were routinely grown aerobically in Luria-Broth (LB) at 37°C degrees with continuous agitation. Other strains listed in **Supplementary Table 6** were grown anaerobically (10% H_2, 10% CO_2, 80% N_2) in a Don Whitley Scientific DG250 Workstation (LA Biosystems, Waalwijk, The Netherlands) at 37°C in an enriched beef broth based on SHIME medium [37] (**Supplementary Table 7**). Bacteria were inoculated from −80°C stocks and grown overnight. Before the experiment, cultures were diluted 1:100 in fresh medium from overnight cultures. levodopa (D9628, Sigma, The Netherlands), carbidopa (C1335, Sigma), benserazide (B7283, Sigma), or methyldopa (857416, Sigma) were supplemented during the lag or stationary phase depending on the experiment. Growth was followed by measuring the optical density (OD) at 600 nM in a spectrophotometer (UV1600PC, VWR International, Leuven, Belgium).

Cloning and heterologous gene expression

The human DOPA decarboxylase gene cloned in pET15b was ordered from GenScript (Piscataway, USA) (**Supplementary Table 6**). Tyrosine decarboxylase-encoding genes from *E. faecalis* v583 ($TDC_{EFS,}$ accession: EOT87933), *E. faecium* W54 (TDC_{EFM}, accession: MH358385; $^{P}TDC_{EFM}$, accession: MH358384) were amplified using Phusion High-fidelity DNA polymerase and primers listed in **Supplementary Table 8**. All amplified genes were cloned in pET15b, resulting in pSK18, pSK11, and pSK22, respectively (**Supplementary Table 6**). Plasmids were maintained in *E. coli* DH5α and verified by Sanger sequencing before transformation to *E. coli* BL21 (DE3). Overnight cultures were diluted 1:50 in fresh LB medium with the appropriate antibiotic and grown to OD_{600} = 0.7-0.8. Protein translation was induced with 1mM Isopropyl β-D-1-thiogalactopyranoside (IPTG, 11411446001, Roche Diagnostics) and cultures were incubated overnight at 18°C. Cells were washed with 1/5th of 1× ice-cold PBS and stored at −80 °C or directly used for protein isolation. Cell pellets were thawed on ice and resuspended in 1/50th of buffer A (300 mM NaCl; 10 mM imidazole; 50 mM KPO4, pH 7.5) containing 0.2 mg/mL lysozyme (105281, Merck) and 2 μg/mL DNAse (11284932001, Roche Diagnostics), and incubated for at least 10 minutes on ice before sonication (10 cycles of 15s with 30s cooling at 8 microns amplitude) using Soniprep-150 plus (Beun de Ronde, Abcoude, The Netherlands). Cell debris were removed by centrifugation at 20000 × *g* for 20 min at 4°C. The 6×his-tagged proteins were purified using a nickel-nitrilotriacetic acid (Ni-NTA) agarose matrix (30250, Qiagen). Cell-free extracts were loaded on 0.5 ml Ni-NTA matrixes and incubated on a roller shaker for 2 hours at 4°C. The Ni-NTA matrix was washed three times with 1.5 ml buffer B (300 mM NaCl; 20 mM imidazole; 50 mM KPO4, pH 7.5) before elution with buffer C (300 mM NaCl; 250 mM imidazole; 50 mM KPO4, pH 7.5). Imidazole was removed from purified protein fractions using Amicon Ultra centrifugal filters (UFC505024, Merck) and washed three times and reconstituted in buffer D (50 mM Tris-HCL; 300 mM NaCl; pH 7.5) for TDC_{EFS}, and $TDC_{EFM,}$ buffer E (100 mM KPO4; pH 7.4) for $^{P}TDC_{EFM}$ and buffer F (100 mM KPO4; 0.1 mM pyridoxal-5-phosphate; pH 7.4) for DDC. Protein concentrations were measured spectrophotometrically (Nanodrop 2000, Isogen, De Meern, The Netherlands) using

the predicted extinction coefficient and molecular weight from ExPASy ProtParam tool (www.web.expasy.org/protparam/).

Enzyme kinetics and IC50 curves

Enzyme kinetics were performed in 200 mM potassium acetate buffer containing 0.1 mM PLP (pyridoxal-5-phosphate, P9255, Sigma, The Netherlands) and 10 nM of enzyme at pH 5 for TDC_{EFS} and TDC_{EFM}, and pH 4.5 for $^{P}TDC_{EFM}$. Reactions were performed in triplicate using levodopa substrate ranges from 0.5-12.5 mM and tyrosine substrate ranges from 0.25-2.5 mM. Michaelis-Menten kinetic curves were fitted using GraphPad Prism 7. The human dopa decarboxylase kinetic reactions were performed in 100 mM potassium phosphate buffer at pH 7.4 containing 0.1 mM PLP and 10 nM enzyme concentrations with levodopa substrate ranges from 0.1-1.0 mM. Reactions were stopped with 0.7% $HClO_4$, filtered and analyzed on the HPLC-ED-system described below. For IC50 curves, the reaction was performed using levodopa as the substrate at concentrations lower or equal to the Km of the decarboxylases (DDC, 0.1 mM; TDC_{EFS} and TDC_{EFM}, 1.0 mM; $^{P}TDC_{EFM}$, 0.5 mM) with 10 different concentrations of carbidopa in triplicate (human dopa decarboxylase, 0.005-2.56 µM; bacterial tyrosine decarboxylases, 2-1024 µM).

HPLC-ED analysis and sample preparation

1 mL of ice-cold methanol was added to 0.25 mL cell suspensions. Cells and protein precipitates were removed by centrifugation at 20000 × *g* for 10 min at 4°C. Supernatant was transferred to a new tube and the methanol fraction was evaporated in a Savant speed-vacuum dryer (SPD131, Fisher Scientific, Landsmeer, The Netherlands) at 60°C for 1h 15 min. The aqueous fraction was reconstituted to 1 mL with 0.7% $HClO_4$. Samples were filtered and injected into the HPLC system (Jasco AS2059 plus autosampler, Jasco Benelux, Utrecht, The Netherlands; Knauer K-1001 pump, Separations, H. I. Ambacht, The Netherlands; Dionex ED40 electrochemical detector, Dionex, Sunnyvale, USA, with a glassy carbon working electrode (DC amperometry at 1.0 V or 0.8 V, with Ag/AgCl as reference electrode)). Samples were analyzed on a C18 column (Kinetex 5µM, C18 100 Å, 250 ×4.6 mm, Phenomenex, Utrecht, The Netherlands) using a gradient of water/methanol with 0.1% formic acid (0-10 min, 95−80% H_2O; 10-20 min, 80-5% H_2O; 20-23 min 5% H_2O; 23-31 min 95% H_2O). Data recording and analysis was performed using Chromeleon software (version 6.8 SR13).

Bioinformatics

TDC_{EFS} (NCBI accession: EOT87933) was BLASTed against the protein sequences from the NIH HMP data bank using search limits for Entrez Query "43021[BioProject]". All BLASTp hits were converted to a distance tree using NCBI TreeView (Parameters: Fast Minimum Evolution; Max Seq Difference, 0.9; Distance, Grishin). The tree was exported in Newick format and visualized in iTOL phylogentic display tool (http://itol.embl.de/). Whole genomes or contigs containing the *tdc* cluster were extracted from NCBI and aligned using Mauve multiple genome alignment tool (v 2.4.0, www.darlinglab.org/mauve/mauve.html).

Incubation experiments of jejunal content

Luminal contents from the jejunum of wild-type Groningen rats (n=5) were suspended in EBB (5% w/v) containing 1 mM levodopa and incubated for 24 hours in an anaerobic chamber at 37 °C prior to HPLC-ED analysis (DC amperometry at 0.8 V).

DNA extraction

DNA was extracted from fecal samples of Parkinson's patients and jejunal contents of rats using QIAGEN (Cat no. 51504) kit-based DNA isolation [38] with the following modifications: Fecal samples were suspended in 1 mL inhibitEX buffer (1:5 w/v) and transferred to screw-caped tubes containing 0.5 g of 0.1 mm and 3 mm glass beads. Samples were homogenized 3 × 30 sec with 1-minute intervals on ice in a mini bead-beater (Biospec, Bartlesville, USA) 3 times before proceeding according to manufacturer's protocol (Isolation of DNA from Stool for Pathogen Detection).

Quantification of bacterial tyrosine decarboxylase

To identify bacterial species carrying the *tdc* gene, a broad range of *tdc* genes from various bacterial genera were targeted as previously described [39] (**Supplementary Figure 5**). Quantitative PCR (qPCR) of *tdc* genes was performed on DNA extracted from each fecal sample of Parkinson's patients and rats' jejunal content using primers (Dec5f and Dec3r) targeting a 350bp region of the *tdc* gene. Primers targeting 16sRNA gene for all bacteria (Eub338 and Eub518) were used as an internal control (**Supplementary Table 8**). All qPCR experiments were performed in a Bio-Rad CFX96 RT-PCR system (Bio-Rad Laboratories, Veenendaal, The Netherlands) with iQ SYBR Green Supermix (170-8882, Bio-Rad) in triplicate on 20 ng DNA in 10 µL reactions using the manufacturer's protocol. qPCR was performed using the following parameters: 3 min at 95°C; 15 sec at 95°C, 1 min at 58°C, 40 cycles. A melting curve was determined at the end of each run to verify the specificity of the PCR amplicons. Data analysis was performed using the BioRad software. Ct[DEC] values were corrected with the internal control (Ct[16s]) and linearized using 2^-(Ct[DEC]-Ct[16s]) based on the 2^-ΔΔCt method [40].

Jejunal and plasma extraction of levodopa metabolites

Levodopa, dopamine, and DOPAC were extracted from each luminal jejunal content and plasma samples of rats using activated alumina powder (199966, Sigma) as previously described [41] with a few modifications. 50-200 µl blood plasma was used with 1µM DHBA (3, 4-dihydroxybenzylamine hydrobromide, 858781, Sigma) as an internal standard. For jejunal luminal content samples, an equal amount of water was added (w/v), and suspensions were vigorously mixed using a vortex. Suspensions were subsequently centrifuged at 20000 × *g* for 10 min at 4°C. 50-200 µL of supernatant was used for extraction. Samples were adjusted to pH 8.6 with 200−800µl TE buffer (2.5% EDTA; 1.5 M Tris/HCl pH 8.6) and 5-10 mg of alumina was added. Suspensions were mixed on a roller shaker at room temperature for 15 min and were thereafter centrifuged for 30s at 20000 × *g* and washed twice with 1 mL of H_2O by aspiration. levodopa and its metabolites were eluted using 0.7% $HClO_4$ and filtered before injection into

the HPLC-ED-system as described above (DC amperometry at 0.8 V).

Statistical analysis and (non)linear regression models

All statistical tests and (non)linear regression models were performed using GraphPad Prism 7. Statistical tests performed are unpaired T-tests, 2-way-ANOVA followed by a Fisher's LSD test. Specific tests and significance are indicated in the figure legends.

Data availability

The authors declare that all the data supporting the findings of this study are available within the paper and its supplementary information files. The sequences of the tyrosine decarboxylase genes from *E. faecium* W54 TDC_{EFM} and $^{P}TDC_{EFM}$ have been deposited under NCBI accession numbers MH358385, MH358384 respectively. The gene sequence of *E. faecalis* v583 TDC_{EFS} was already available under NCBI accession number EOT87933.

REFERENCES

1 Kahtrom, C. T., Pariente, N. & Weiss, U. Intestinal microbiota in health and disease. *Nature* **535**, 47, (2016).

2 Yano, J. M. *et al.* Indigenous bacteria from the gut microbiota regulate host serotonin biosynthesis. *Cell* **161**, 264-276, (2015).

3 Mao, K. *et al.* Innate and adaptive lymphocytes sequentially shape the gut microbiota and lipid metabolism. *Nature* **554**, 255-259, (2018).

4 Pusceddu, M. M. *et al.* N-3 Polyunsaturated Fatty Acids (PUFAs) Reverse the Impact of Early-Life Stress on the Gut Microbiota. *PloS one* **10**, e0139721, (2015).

5 El Aidy, S. *et al.* Temporal and spatial interplay of microbiota and intestinal mucosa drive establishment of immune homeostasis in conventionalized mice. *Mucosal immunology* **5**, 567-579, (2012).

6 Kelly, J. R. *et al.* Transferring the blues: Depression-associated gut microbiota induces neurobehavioural changes in the rat. *Journal of psychiatric research* **82**, 109-118, (2016).

7 Enright, E. F., Gahan, C. G., Joyce, S. A. & Griffin, B. T. The Impact of the Gut Microbiota on Drug Metabolism and Clinical Outcome. *The Yale journal of biology and medicine* **89**, 375-382 (2016).

8 Niehues, M. & Hensel, A. In-vitro interaction of L-dopa with bacterial adhesins of Helicobacter pylori: an explanation for clinicial differences in bioavailability? *The Journal of pharmacy and pharmacology* **61**, 1303-1307, (2009).

9 Pereira, P. A. B. *et al.* Oral and nasal microbiota in Parkinson's disease. *Parkinsonism & related disorders* **38**, 61-67, (2017).

10 Sampson, T. R. *et al.* Gut Microbiota Regulate Motor Deficits and Neuroinflammation in a Model of Parkinson's Disease. *Cell* **167**, 1469-1480.e1412, (2016).

11 Scheperjans, F. *et al.* Gut microbiota are related to Parkinson's disease and clinical phenotype. *Mov. Disord.* **30**, 350–358 (2015).

12 Deleu, D., Northway, M. G. & Hanssens, Y. Clinical pharmacokinetic and pharmacodynamic properties of drugs used in the treatment of Parkinson's disease. *Clinical pharmacokinetics* **41**, 261-309, (2002).

13 Pinder, R. M. Possible dopamine derivatives capable of crossing the blood-brain barrier in relation to Parkinsonism. *Nature* **228**, 358 (1970).

14 Katzenschlager, R. & Lees, A. J. Treatment of Parkinson's disease: levodopa as the first choice. *Journal of neurology* **249 Suppl 2**, Ii19-24, (2002).

15 Goldin, B. R., Peppercorn, M. A. & Goldman, P. Contributions of host and intestinal microflora in the metabolism of L-dopa by the rat. *J Pharmacol Exp Ther* **186**, 160-166 (1973).

16 Gundert-Remy, U. *et al.* Intestinal absorption of levodopa in man. *European journal of clinical pharmacology* **25**, 69-72 (1983).

17 Perez, M. *et al.* Tyramine biosynthesis is transcriptionally induced at low pH and improves the fitness of *Enterococcus faecalis* in acidic environments. *Applied microbiology and biotechnology* **99**, 3547-3558, (2015).

18 Zhu, H. *et al.* Crystal structure of tyrosine decarboxylase and identification of key residues involved in conformational swing and substrate binding. *Scientific reports* **6**, 27779, (2016).

19 Zhang, K. & Ni, Y. Tyrosine decarboxylase from *Lactobacillus brevis*: soluble expression and characterization. *Protein expression and purification* **94**, 33-39, (2014).

20 Williams, B. B. *et al.* Discovery and characterization of gut microbiota decarboxylases that can produce the neurotransmitter tryptamine. *Cell host & microbe* **16**, 495-503, (2014).

21 Adibi, S. A. & Mercer, D. W. Protein Digestion in Human Intestine as Reflected in Luminal, Mucosal, and Plasma Amino Acid Concentrations after Meals. *The Journal of clinical investigation* **52**, 1586-1594, (1973).

22 Bredberg, E., Lennernas, H. & Paalzow, L. Pharmacokinetics of levodopa and carbidopa in rats following different routes of administration. *Pharm Res* **11**, 549-555 (1994).

23 Tomlinson, C. L. *et al.* Systematic review of levodopa dose equivalency reporting in Parkinson's disease. *Mov. disord.* **25**, 2649-2653, (2010).

24 Zoetendal, E. G. *et al.* The human small intestinal microbiota is driven by rapid uptake and conversion of simple carbohydrates. *The ISME journal* **6**, 1415-1426, (2012).

25 El Aidy, S., van den Bogert, B. & Kleerebezem, M. The small intestine microbiota, nutritional modulation and relevance for health. *Curr Opin Biotechnol* **32c**, 14-20, (2014).

26 Pellegrini, C. *et al.* Gastric motor dysfunctions in Parkinson's disease: Current pre-clinical evidence. *Parkinsonism & related disorders* **21**, 1407-1414, (2015).

27 Valenzuela, J. E. & Dooley, C. P. Dopamine antagonists in the upper gastrointestinal tract. *Scandinavian journal of gastroenterology. Supplement* **96**, 127-136 (1984).

28 Gabrielli, M. *et al.* Prevalence of small intestinal bacterial overgrowth in Parkinson's disease. *Mov. disord.* **26**, 889-892, (2011).

29 Fasano, A. *et al.* The role of small intestinal bacterial overgrowth in Parkinson's disease. *Mov. disord.* **28**, 1241-1249, (2013).

30 Richter, J. E. The many manifestations of gastroesophageal reflux disease: presentation, evaluation, and treatment. *Gastroenterology clinics of North America* **36**, 577-599, viii-ix, (2007).

31 Tan, A. H. *et al.* Small intestinal bacterial overgrowth in Parkinson's disease. *Parkinsonism & related disorders* **20**, 535-540, (2014).

32 Pfeiffer, R. Beyond here be dragons: SIBO in Parkinson's disease. *Mov. Disord.* **28**, 1764-1765, (2013).

33 Freedberg, D. E. *et al.* Proton Pump Inhibitors Alter Specific Taxa in the Human Gastrointestinal Microbiome: A Crossover Trial. *Gastroenterology* **149**, 883-885.e889, (2015).

34 Kempster, P. A. *et al.* Patterns of levodopa response in Parkinson's disease: a clinico-pathological study. *Brain* **130**, 2123-2128, (2007).

35 Keshavarzian, A. *et al.* Colonic bacterial composition in Parkinson's disease. *Mov. Disord.* **30**, 1351–1360 (2015).

36 Koolhaas, J. M. *et al.* The resident-intruder paradigm: a standardized test for aggression, violence and social stress. *Journal of visualized experiments : JoVE*, e4367, (2013).

37 Auchtung, J. M., Robinson, C. D. & Britton, R. A. Cultivation of stable, reproducible microbial communities from different fecal donors using minibioreactor arrays (MBRAs). *Microbiome* **3**, 42, (2015).

38 Zoetendal, E. G. *et al.* Isolation of DNA from bacterial samples of the human gastrointestinal tract. *Nature protocols* **1**, 870-873, (2006).

39 Torriani, S. *et al.* Rapid detection and quantification of tyrosine decarboxylase gene (tdc) and its expression in gram-positive bacteria associated with fermented foods using PCR-based methods. *Journal of food protection* **71**, 93-101 (2008).

40 Livak, K. J. & Schmittgen, T. D. Analysis of relative gene expression data using real-time quantitative PCR and the 2(-Delta Delta C(T)) Method. *Methods (San Diego, Calif.)* **25**, 402-408, (2001).

41 Ganhao, M. F., Hattingh, J., Hurwitz, M. L. & Pitts, N. I. Evaluation of a simple plasma catecholamine extraction procedure prior to high-performance liquid chromatography and electrochemical detection. *Journal of chromatography* **564**, 55-66 (1991).

SUPPLEMENTARY INFORMATION

Supplemetary Information accompanies this paper at https://doi.org/10.1038/s41467-019-08294-y and in this thesis (see next page).

Acknowledgements

We thank Dr. Saskia van Hemert and Dr. Coline Gerritsen of Winclove Probiotics, Amsterdam, The Netherlands, for providing us *E. faecium* W54 and *L. brevis* W63 , as well as their sequencing data; Prof. Jan Kok of Department of Molecular genetics, University of Groningen, The Netherlands, and Dr. Miguel A. Alvarez of Instituto de Productos Lácteos de Asturias, Villaviciosa, Spain for providing the mutant strain *E. faecalis* v583; and Dr. Phillip A. Engen, Division of Digestive Disease and Nutrition, Section of Gastroenterology, Rush University Medical Center, USA for assisting in preparing fecal samples from Parkinson's patients for shipment, and Profs. Michiel Kleerebezem, Annick Mercenier, Host-microbe interactomics group, Wageningen University, The Netherlands for critical reading of our manuscript.

Funding

SEA is supported by a Rosalind Franklin Fellowship, co-funded by the European Union and University of Groningen, The Netherlands.

Authors Contributions

S.P.K. and S.E.A. conceived and designed the study. S.P.K., A.K.F., A.O.E.G., M.C., A.K., G.D., S.E.A. performed the experiments and S.P.K. and S.E.A. analyzed the data. S.P.K. and S.E.A. wrote the original manuscript that was reviewed by A.K.F., S.E.A., A.K., G.D.

Conflict of interest

The authors declare no competing interests.

SUPPLEMENTARY FIGURES

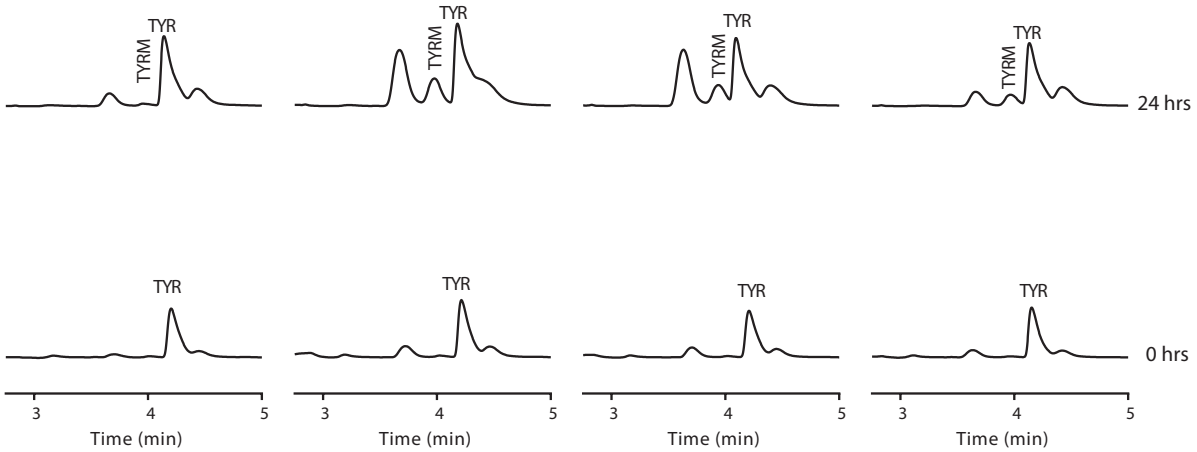

Supplementary Figure 1 | Corresponding control samples jejunal content incubation without levodopa. From left to right corresponding control samples, where H_2O was added instead of L-DOPA. Bacterial conversion of tyrosine (TYR) to tyramine (TYRM) during 24 hrs of incubation of jejunal content is visible. No dopamine is produced *de novo* or hydrolyzed from potential conjugated-forms of dopamine in the jejunal-content.

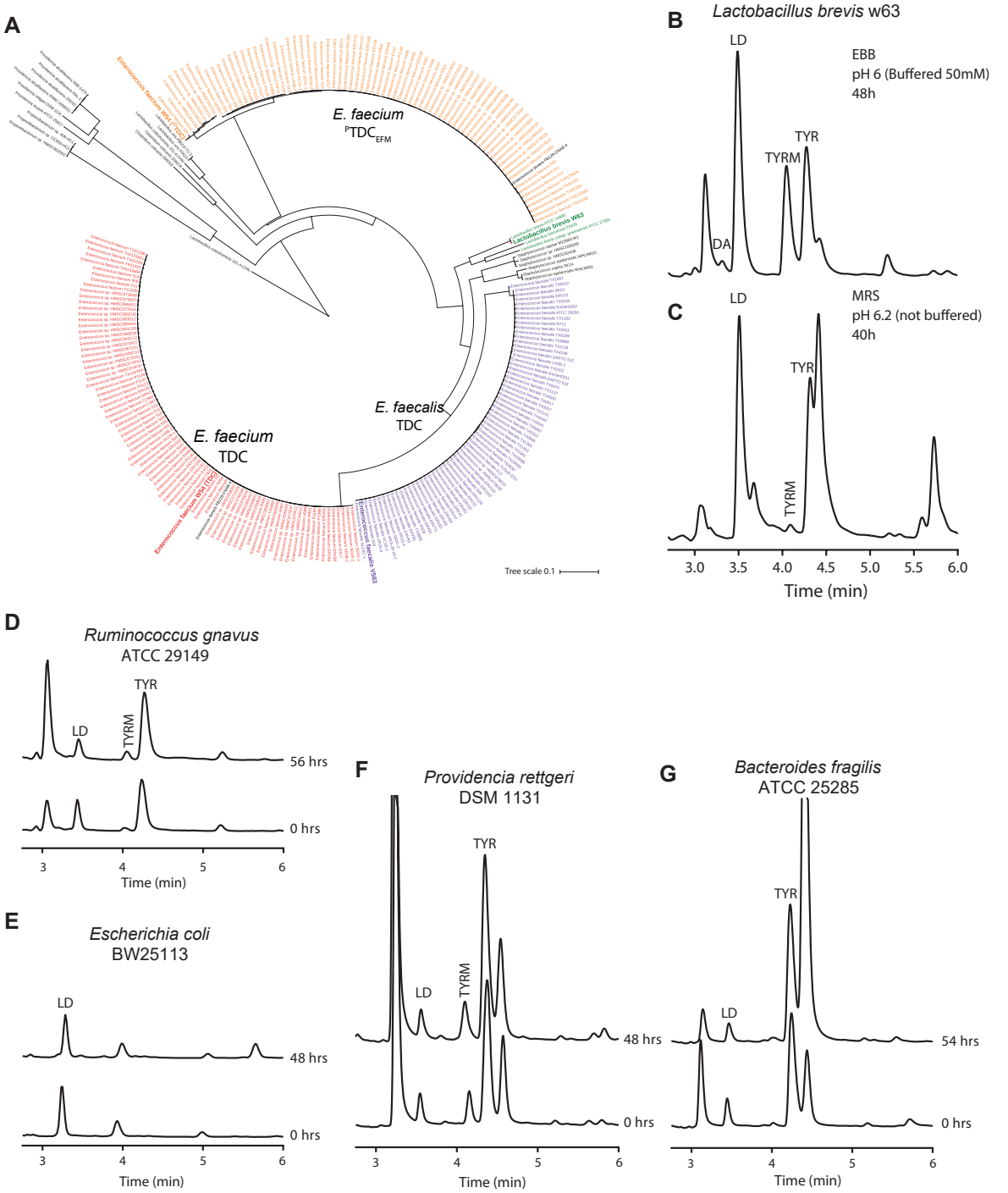

Supplementary Figure 2 | Microbiota harboring other PLP-dependent amino acid decarboxylases do not decarboxylate levodopa. (**A**) Phylogenetic analysis of TDC proteins from NIH Human Microbiome Project (HMP) protein database, TDC_{EFS} (EOT87933) was used as query. TDC protein sequences from strains employed in this study are depicted in bold. Live stationary cultures of *L. brevis* grown with levodopa in (**B**) MRS (De Man, Rogosa and Sharpe) or in (**C**) enriched beef broth (EBB) buffered at pH 6.0. (**D-G**) Gut associated bacteria harboring different amino acid decarboxylases, which were previously identified (**Supplementary Table 2**) were tested for their ability to convert levodopa in live stationary cultures

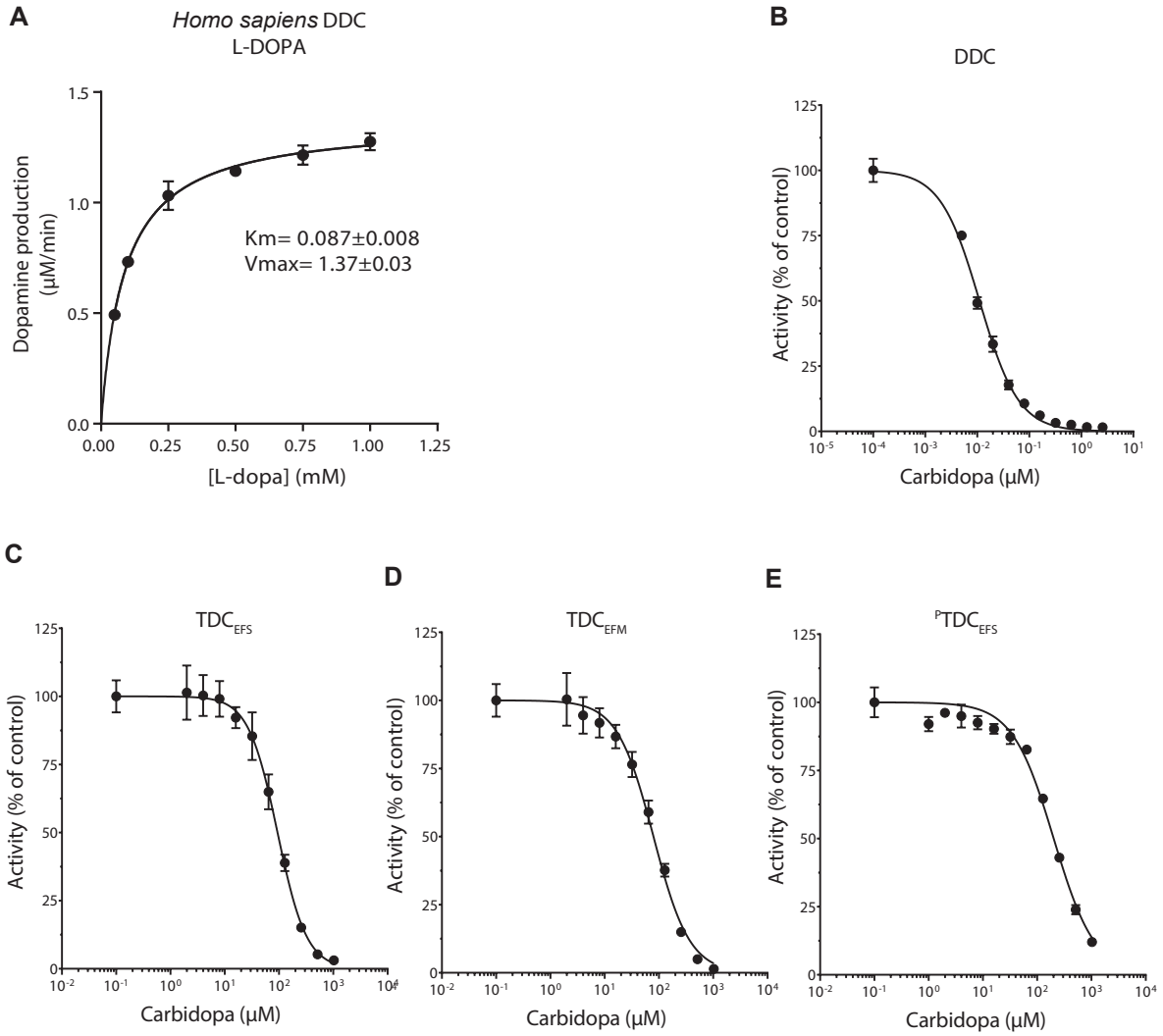

Supplementary Figure 3 | IC50 determination for human DOPA decarboxylase and bacterial tyrosine decarboxylases. (**A**) Kinetic curve with levodopa as substrate for human DOPA decarboxylase (DDC) to determine the inhibitory constant for carbidopa. Reactions were performed in triplicate using 10 nM of enzyme in 100 mM PO_4 with 100 µM PLP[3] with levodopa concentrations ranging from 0.1-1.0 mM. The enzyme kinetic parameters were calculated using nonlinear Michaelis-Menten regression model (for further kinetic parameters see **Table 1**). IC50 inhibitory curves using carbidopa as inhibitor for (**B**) DDC (0.005-2.56 µM carbidopa), (**C**) TDC_{EFS} (2-1024 µM carbidopa), (**D**) TDC_{EFM} (2-1024 µM carbidopa), (**E**) $^{P}TDC_{EFM}$ (2-1024 µM carbidiopa). Reactions were performed in triplicate and the parameters were determined by fitting a sigmoidal–curve ([inhibitor] vs. normalized response). Further parameters are listed in **Supplementary Table 3**.

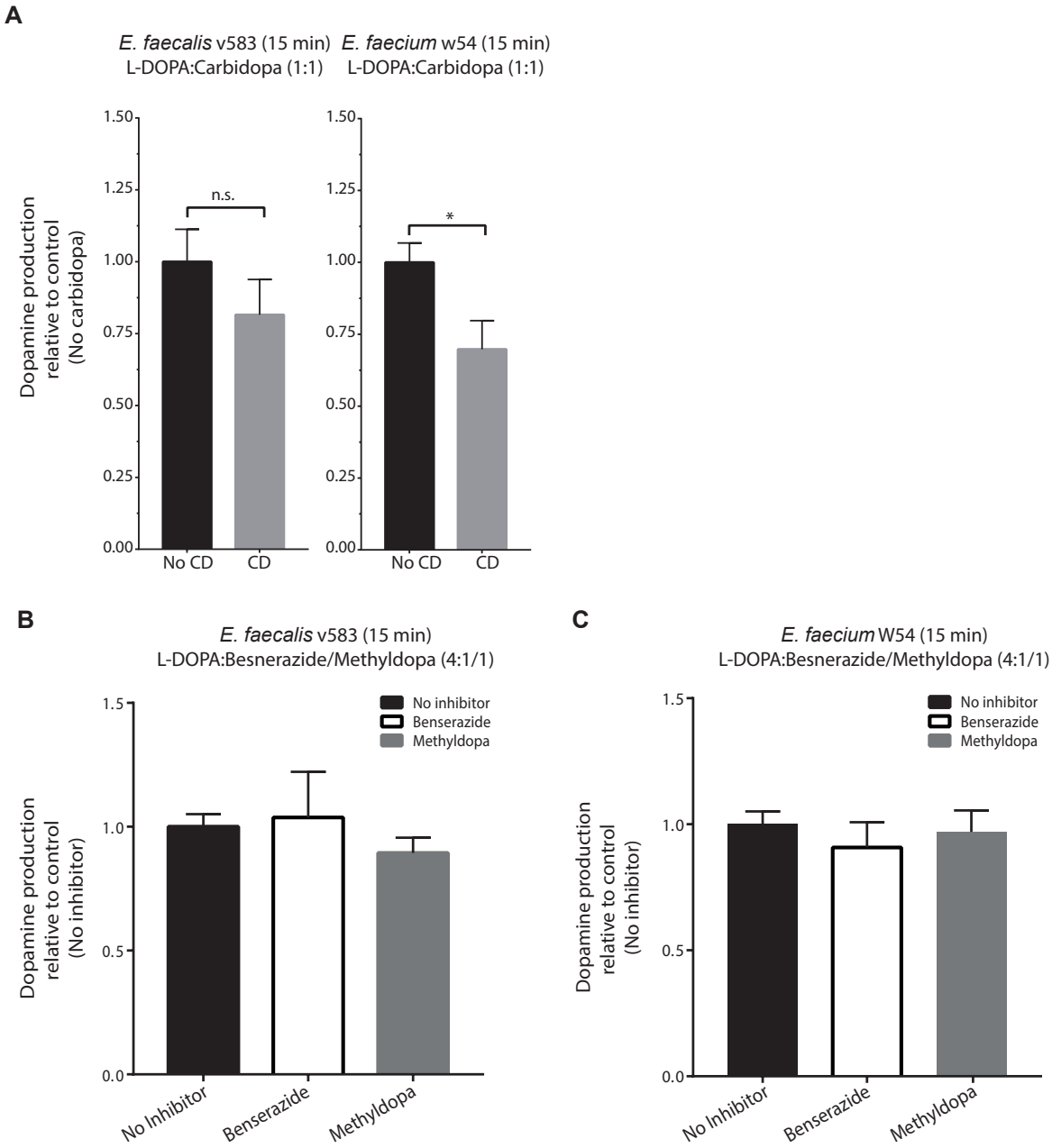

Supplementary Figure 4 | Human DOPA decarboxylase inhibitors are ineffective against the decarboxylase activity of live enterococci. Live stationary cultures of *E. faecalis* and *E. faecium* incubated for 15 minutes with (**A**) an equimolar ratio levodopa /carbidopa, (**B, C**) a 6:1 molar ratio (4:1 in weight) of levodopa /benserazide or 4.8:1 molar ratio (4:1 in weight) of levodopa/methyldopa (100/16.7/20,8 μM levodopa /benserazide/methyldopa). Samples were analyzed using HPLC-ED. Bar graphs show levels of dopamine production (relative to control, where no inhibitor was added) with and without the addition of inhibitor. Error bars represent the SEM and significance was tested using a parametric unpaired T-test (*=p<0.02).

a

```
5’-CGTTGTTGGTGTTGTTGGCACNACNGARGARG (Dec5f primer)
   *|||||*|||||*|||||**||||||||||||
5’-TGTTGTCGGTGTAGTTGGTTCTACTGAAGAAGGTGCCGTTGACTCAATCGATAAAAT
TATTGCTTTACGCGATGAATTAATGAAAGACGGTATTTACTATTATGTACACGTTGATGC
TGCTTATGGTGGTTATGGACGTGCCATCTTCTTAGACGAAGACAACAACTTCATCCCTTA
CGAAGATTTACAAGATGTTCACGAAGAATACGGTGTCTTCAAAGAGAAAAAAGAACACAT
TTCAAGAGAAGTGTATGATGCATATAAAGCAATCGAATTAGCAGAATCAGTAACAATTGA
CCCTCATAAAATGGGTTATATCCCTTATTCAGCTGGTGG-3’
          |||||||||||||||*|||||*|||||*||
         ATGGGNTAYRTTCCATATTCTGCTGGCGG-3’ (Dec3r primer)
```

b

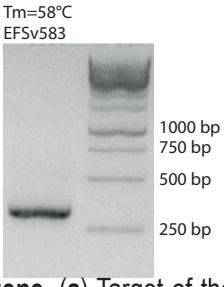

Supplementary Figure 5 | Primers (Dec5f and Dec3r) targeting *E. faecalis* v583 *tdc* gene. (**a**) Target of the Dec5f and Dec3r primers[2] are depicted for *Enterococcus faecalis* v583 with (**b**) the corresponding agarose gel of PCR amplification of 336 bp fragment of *tdc*.

Supplementary Figure 6 | Identification of conserved *tdc* paralogue protein (TDC_{EFM}) in all *E. faecium* strains analyzed. Identification of conserved *tdc* paralogue protein (TDC_{EFM}) in all *E. faecium* strains analyzed**.** Genome contigs harboring the *tdc* gene cluster of all *E. faecium* strains were extracted from NCBI and aligned using Mauve genome aligner. As comparison, the genome of *E. faecium* W54 is depicted above the alignment results. The paralog TDC from *E faecium* ($^{P}TDC_{EFM}$) is shown in orange. Black boxes indicate the TDC gene in all other strains, white bars indicate the single genes, and colored bars indicate conserved gene clusters.

SUPPLEMENTARY TABLES

Supplementary Table 1 | *Enterococcus* strains isolated from healthy subjects and clinical enterococcal isolates

	Number	Sample Type		Bile aesculin hydrolysis	Levodopa decarboxylation	Tyrosine decarboxylation
	29	Clinical	Stool	29	29	29
	34	Clinical	Urine	34	33	33
	14	Volunteer	Stool	14	10	10
Total	**77**			**77**	**72**	**72**

Enterococcus strains isolated from (1) fecal samples (collected from non-hospitalized subjects from clinical labs during their routine check up), (2) urine samples (collected from non-hospitalized patients suffering from urinary tract infection), and (3) healthy volunteers (age 2 to 79 years). All samples were isolated between January 2008-2018 in Beni-Suef City, Egypt. 72 out of 77 isolates were able to decarboxylate levodopa and tyrosine indicating that only 5 isolates are species or strains not encoding for tyrosine decarboxylase.

Supplementary Table 2 | List of microbiota harboring other PLP-dependent amino acid decarboxylases tested in this study

Reported tyrosine decarboxylation[4]	Cloned gene[4]	Associated protein accession	Definition	This study (Live bacterial culture)	Protein Identity*	Protein accession
-	BF 0393 (BF9343_0382)	CAH06161	Putative Glutamate decarboxylase	*Bacteroides fragilis* NCTC 9343 (=ATCC 25285)	100.00%	CAH06161
	Not tested	NA	Tyrosine decarboxylase	*Enterococcus faecalis* v583	NA	EOT87933
	Not tested	NA	Tyrosine decarboxylase	*Enterococcus faecium* W54	NA	MH358384, MH358385
-	ECD_03365	ACT45166	Glutamate decarboxylase	*Escherichia coli* BW25113	100.00%	AIN33843
-	LVIS_1847	ABJ64910	Glutamate decarboxylase	*Lactobacillus brevis* W63	NA	
++	LVIS_2213	ABJ65263	Tyrosine decarboxylase	*Lactobacillus brevis* W63	100.00%	MH3583846
-	LVIS_0079	ABJ63253	Glutamate decarboxylase	*Lactobacillus brevis* W63	NA	
+++	PROSTU_02509	EDU59320	putative tyrosine decarboxylase	*Providencia rettgeri* DSM1131	83%	EFE55437
+++	RUMGNA_01526	EDN78222	Tryptophan decarboxylase	*Ruminococcus gnauvs* ATCC29149	100.00%	EDN78222

* Protein identity from strain tested compared to cloned gene Williams et al. [4]. NA, not applicable.

Supplementary Table 3 | IC50 curve parameters

	DDC	TDC_{EFS}	TDC_{EFM}	$^{P}TDC_{EFM}$
[E] (nM)	10	10	10	10
[S] (μM)	100	1000	1000	500
[Km] (μM)	87.3	3043.0	7244.0	448.1
HillSlope	1.16	1.6	1.3	1.1
IC50 (μM)	0.01	93.8	79.2	201.3
Ki=IC50/(1+([S]/Km))	0.005	70.6	69.6	95.1
[IC50]/[s]	0.01%	9%	8%	40%

The parameters were determined by fitting a sigmoidal–curve ([inhibitor] vs. normalized response) using Graphpad Prism. Reactions were performed in triplicate.

Supplementary Table 4 | Sample information Parkinson's patients

ID	tdc-gene abundance	Levodopa/ carbidopa Tablets per Day	PD Onset (year) - First Diagnosed at Rush University	Disease Duration (years)	Date of Enrollment into Microbiota Research Study at Rush University	UPDRS*	Hy Stage**	Sex	Age	Race	BMI	Medication
Subject 1	1.55E-07	3 Tablets	2010	2	16-5-2012	35	2	Male	63	Caucasian	27.11	No; None
Subject 2	4.30E-07	11 Tablets	2001	11	25-10-2012	30	2.5	Male	50	Caucasian	24.28	No; None
Subject 3	6.48E-08	5 Tablets	2004	8	8-5-2012	36	2	Female	53	Caucasian	22.86	Yes; Naproxyn
Subject 4	8.97E-08	3 Tablets	2008	4	20-8-2012	13	2	Female	58	Caucasian	27.45	No; None
Subject 5	4.01E-07	4 Tablets	1998	14	20-9-2012	26	2	Female	68	Caucasian	23.92	Yes; Aspirin
Subject 6	2.37E-08	3 Tablets	2007	6	4-10-2012	35	2	Male	58	Caucasian	31.44	Yes; Aspirin
Subject 7	6.23E-07	10 Tablets	1991	22	14-6-2012	21	2	Female	57	Caucasian	18.01	No; None
Subject 8	8.69E-08	8 Tablets	2006	6	16-8-2012	27	2	Male	55	Caucasian	23.74	Yes; Aspirin
Subject 9	2.00E-07	6 Tablets	1997	15	18-9-2012	19	2	Male	82	Caucasian	29.12	No; None
Subject 10	2.75E-07	7 Tablets	2002	10	6-12-2012	40	2	Male	74	Asian	28.2	No; None

* Unified Parkinson Disease Rating Scale, ** Hoehn and Yahr Stage, BMI = Body Mass Index. According to medical records, all subjects were on the same levodopa/carbidopa dose thereafter their PD Onset (year) at Rush University Medical Center Neurology Department. Parkinson's disease was diagnosed according to the UK Brain Bank Criteria[5].

Supplementary Table 5 | Bivariate correlations

		Correlations								
		L-Dopa Tablets per Day	Disease Duration (years)	UPDRS	Hy Stage	Sex	Age	Race	BMI	Medi-cation
***tdc*-gene abundance**	**Pearson Correlation**	0.662*	0.823**	-0.195	0.351	-0.264	0.024	-0.071	-0.652*	-0.401
	Sig. (2-tailed)	0.037	0.003	0.589	0.320	0.461	0.949	0.845	0.041	0.251
	N	10	10	10	10	10	10	10	10	10

* Correlation is significant at the 0.05 level (2-tailed). ** Correlation is significant at the 0.01 level (2-tailed).

Supplementary Table 6 | Bacterial strains and Plasmids used in this study

Bacterial strains	Genotype	Reference
Escherichia coli DH5a	F^{-}; *endA1*; *glnV44*; *thi-1*; *recA*; *relA1*; *gyrA96*; *deoR*; *nupG*; *purB20*; φ80d-*lacZ*ΔM15; Δ(*lacZYA-argF*)U169; hsdR17(r_K^- m_K^+); λ^{-}	6
Escherichia coli BL21 (DE3)	*E. coli* str. B; F^{-}; *ompT*; *gal*; *dcm*; *lon*; *hsdS*-$_B$($r_B^-m_B^-$); λ(DE3 [*lacI lacUV5-T7p07 ind1 sam7 nin5*]) ; [*malB*$^+$]$_{K-12}$(λ^S)	7
Escherichia coli BW25113	*lacI*$^+$; *rrnB*$_{T14}$; Δ*lacZ*$_{WJ16}$; *hsdR*514 Δ*araBA-D*$_{AH33}$; Δ*rhaBAD*$_{LD78}$; *rph-1*; Δ*(araB–D)567*; Δ*(rhaD–B)568;* Δ*lacZ4787*(::*rrnB-3*)	8
E. faecalis v583/ATCC 700802		9
E. faecalis ΔTDC	*tyrS*:*nhaC* (Δ*tdcA*)	10
Enterococcus faecium W54		Winclove Probiotic B.V.
Lactobacillus brevis W63		Winclove Probiotic B.V.
Ruminococcus gnavus ATCC29149		ATCC
Providencia rettgeri DSM 1131		DSMZ
Bacteroides fragilis ATCC 25285		ATCC
Plasmids used	**Gene-insert**	
pET15b		Novagen
pSK11	pET15b-^{P}TDC$_{EFM}$	This study
pSK18	pET15b-TDC$_{EFS}$	This study
pSK22	pET15b-TDC$_{EFM}$	This study
pET15b- OHu25359C	pET15b-DDC cDNA	This study / GenScript

Supplementary Table 7 | Constituents of enriched beef broth (EBB) medium used in this study

Component	g/L
Glucose	2.000
NaCl	0.080
K_2HPO_4	5.310
KH_2PO_4	2.650
$NaHCO_3$	0.400
Beef extract	5.000
Yeast extract	3.000
Peptone	0.600
$CaCl_2$	0.008
$MgSO_4$	0.008
Cysteine	0.500
Hemin	0.005
Vitamin solution (1000x)	
D-biotin	0.0020
D-Pantothenic acid	0.0100
Ca2.Nicotinamide	0.0050
Vitamin B12	0.0005
Thiamin.HCl	0.0040
Para-aminobenzoic acid	0.0050
Riboflavin	0.0050
Folic acid	0.0020
Pyridoxyal-5-Phosphate	0.0100
Vitamin K1	0.0005
Trace Elements (1000x)	
EDTA	1.000
$ZnSO_4.7H_2O$	0.178
$MnSO_4.H_2O$	0.452
$FeSO_4.7H_2O$	0.100
$CoSO_4.7H_2O$	0.181
$CuSO_4.5H_2O$	0.010
H_3BO_3	0.010
$Na_2MoO_4.2H_2O$	0.010
$NiSO_4.6H_2O$	0.111

The KPO_4 solution is buffered at 50 mM pH7

Supplementary Table 8 | Primer sequences used in this study

Primers	5'-Sequence-'3	Target
sk075	AGGAGGCTCGAGAAAGATATGGATATCAAGGCCG	*E. feacium* W54 $^{P}TDC_{EFM}$
sk076	AGGAGGGGATCCCCAGTATCACCGAAACATCC	*E. feacium* W54 $^{P}TDC_{EFM}$
sk153	AGGAGGCTCGAGAAAAACGAAAAATTAGCAAAAGGCG	*E. faecalis* v583 TDC_{EFS}
sk154	AGCAGAGGATCCCAATCAGACGAACGTTCCCTC	*E. faecalis* v583 TDC_{EFS}
sk171	AGAGAGCTCGAGAGTGAATCATTGTCGAAAG	*E. feacium* W54 TDC_{EFM}
sk172	ATATATGGATCCCCAAACATGCGTCAGAAACAG	*E. feacium* W54 TDC_{EFM}
qPCR	**5'-Sequence-'3**	**Reference**
DEC5f	CGTTGTTGGTGTTGTTGGCACNACNGARGARG	[2]
DEC3r	CCGCCAGCAGAATATGGAAYRTANCCCAT	[2]
Eub338	ACTCCTACGGGAGGCAGCAG	[11]
Eub518	ATTACCGCGGCTGCTGG	[11]

Underlined sequences represent restriction sites used.

SUPPLEMENTARY METHODS

Screening for *Enterococcus* strains, isolated from healthy subjects and clinical isolates

Enterococcus strains were isolated from fecal or urine samples from clinical setting or from healthy volunteers (aged 2 to 79 years). All samples were collected between January 2008 and 2018 in Beni-Suef City, Egypt. A total of 77 *Enterococcus* spp. were isolated on bile esculin agar and observed microscopically after gram staining. The screening for decarboxylase activity was performed as described previously by Bover-Cid and Holzapfel [1] with levodopa or tyrosine added as a substrate to a final concentration of 1% to screen for production of dopamine and tyramine. All *Enterococcus* strains were spot inoculated on agar plates containing the substrates of interest and on control plates without any substrate. The plates were duplicated, either aerobically or anaerobically at 37°C. Plates were checked daily for 4 days to record the change in the indicator color from yellow to violet, indicative of production of tyramine and dopamine, respectively (**Supplementary Table 1**).

Fecal samples from patients with Parkinson's disease

All study subjects consented to the use of their samples for research. Parkinson's disease was diagnosed according to the UK Brain Bank Criteria. Exclusion criteria for Parkinson's disease subjects: (1) atypical or secondary Parkinsonism, (2) the use of probiotics or antibiotics within three months prior to sample collection, (3) primary gastrointestinal pathology, (4) unstable medical, neurological, or psychiatric illness, (5) low platelet count (<80k), uncorrectable prolonged PT (>15 sec. Solid fecal samples were collected via a home feces collection kit. Study patients were provided with the supplies and instructions for home feces collection using the BD Gaspak EZ Anaerobe Gas Generating Pouch System with Indicator (Ref 260683; Becton, Dickinson and Company, Sparks, MD) in order to minimize the exposure of the feces to high oxygen ambient atmosphere, which may alter the microbiota. Patients were asked to have a

bowel movement within 24 hours of their study visit. Patients kept the sealed anaerobic fecal bag in a cold environment, before bringing the anaerobic fecal bag to the hospital. Fecal samples were then immediately stored at -80°C until analysis.

Primers targeting bacterial tyrosine decarboxylase

In order to cover numerous bacterial species harboring the *tdc* gene, degenerate primers, Dec5f and Dec3r, previously designed to target 350bp region of the *tdc* gene from a variety of bacterial genera[2] were used for qPCR. Prior to qPCR experiments a normal PCR test on the genomic DNA *E. faecalis* v583 was performed using Phire Hot Start II DNA Polymerase (F125S, ThermoFisher) using the following PCR parameters: 3 min at 98°C; 15 sec at 98°C, 1 min at 58°C and 1 min at 72°C, for 35 cycles; 5 min at 72°C, to ensure primer specificity.

SUPPLEMENTARY REFERENCES

1 Bover-Cid, S. & Holzapfel, W. H. Improved screening procedure for biogenic amine production by lactic acid bacteria. *International journal of food microbiology* **53**, 33-41 (1999).

2 Torriani, S. *et al.* Rapid detection and quantification of tyrosine decarboxylase gene (*tdc*) and its expression in gram-positive bacteria associated with fermented foods using PCR-based methods. *Journal of food protection* **71**, 93-101 (2008).

3 Montioli, R., Cellini, B. & Borri Voltattorni, C. Molecular insights into the pathogenicity of variants associated with the aromatic amino acid decarboxylase deficiency. *Journal of inherited metabolic disease* **34**, 1213-1224, (2011).

4 Williams, B. B. *et al.* Discovery and characterization of gut microbiota decarboxylases that can produce the neurotransmitter tryptamine. *Cell host & microbe* **16**, 495-503, (2014).

5 Keshavarzian, A. *et al.* Colonic bacterial composition in Parkinson's disease. *Mov. Disord.* **30**, 1351-1360, (2015).

6 Grant, S. G., Jessee, J., Bloom, F. R. & Hanahan, D. Differential plasmid rescue from transgenic mouse DNAs into Escherichia coli methylation-restriction mutants. *Proc. Natl. Acad. Sci. U. S. A.* **87**, 4645-4649 (1990).

7 Wood, W. B. Host specificity of DNA produced by Escherichia coli: bacterial mutations affecting the restriction and modification of DNA. *Journal of molecular biology* **16**, 118-133 (1966).

8 Datsenko, K. A. & Wanner, B. L. One-step inactivation of chromosomal genes in Escherichia coli K-12 using PCR products. *Proc. Natl. Acad. Sci. U. S. A.* **97**, 6640-6645, (2000).

9 Sahm, D. F. *et al.* In vitro susceptibility studies of vancomycin-resistant *Enterococcus faecalis*. *Antimicrobial agents and chemotherapy* **33**, 1588-1591 (1989).

10 Perez, M. *et al.* Tyramine biosynthesis is transcriptionally induced at low pH and improves the fitness of *Enterococcus faecalis* in acidic environments. *Applied microbiology and biotechnology* **99**, 3547-3558, (2015).

11 Fierer, N., Jackson, J. A., Vilgalys, R. & Jackson, R. B. Assessment of Soil Microbial Community Structure by Use of Taxon-Specific Quantitative PCR Assays. Appl. Environ. Microbiol. **71**, 4117–4120 (2005).

Back to table of contents

CHAPTER 3

ARTICLE

Gut Bacterial Deamination of Residual Levodopa Medication for Parkinson's Disease

Sebastiaan P. van Kessel[1], Hiltje R. de Jong[1], Simon L. Winkel[1], Sander S. van Leeuwen[1†], Sieger A. Nelemans[2], Hjalmar Permentier[3], Ali Keshavarzian[4] and Sahar El Aidy[1*]

BMC Biology, 2020, 18, 137
DOI: 10.1186/s12915-020-00876-3

[1]Host-Microbe Interactions, Groningen Biomolecular Sciences and Biotechnology Institute (GBB), University of Groningen, Nijenborgh 7, 9747 AG Groningen, The Netherlands.

[2]Department of Molecular Neurobiology, Groningen Institute for Evolutionary Life Sciences (GELIFES), University of Groningen, Nijenborgh 7, 9747 AG Groningen, The Netherlands.

[3]Interfaculty Mass Spectrometry Center, University of Groningen, Groningen, The Netherlands.

[4]Division of Digestive Disease and Nutrition, Section of Gastroenterology, Department of Internal Medicine, Rush University Medical Center, 1725 W. Harrison, Suite 206, Chicago, IL 60612, USA.

[†]Current Address: Department of Laboratory Medicine, Cluster Human Nutrition & Health, University Medical Center Groningen (UMCG), Hanzeplein 1, 9713 GZ Groningen, The Netherlands.

*Correspondence: Sahar El Aidy, sahar.elaidy@rug.nl

Gut Bacterial Deamination of Residual Levodopa Medication for Parkinson's Disease

Sebastiaan P. van Kessel, Hiltje R. de Jong, Simon L. Winkel, Sander S. van Leeuwen, Sieger A. Nelemans, Hjalmar Permentier, Ali Keshavarzian and Sahar El Aidy

ABSTRACT

Background: Parkinson's disease (PD) is a progressive neurodegenerative disorder characterized by both motor and non-motor symptoms. Gastrointestinal tract dysfunction is one of the non-motor features, where constipation is reported as the most common gastrointestinal symptom. Aromatic bacterial metabolites are attracting considerable attention due to their impact on gut homeostasis and host's physiology. In particular, *Clostridium sporogenes* is a key contributor to the production of these bioactive metabolites in the human gut. ***Results:*** Here, we show that *C. sporogenes* deaminates levodopa, the main treatment in Parkinson's disease, and identify the aromatic aminotransferase responsible for the initiation of the deamination pathway. The deaminated metabolite from levodopa, 3-(3,4-dihydroxyphenyl)propionic acid, elicits an inhibitory effect on ileal motility in an *ex vivo* model. We detected 3-(3,4-dihydroxyphenyl) propionic acid in fecal samples of Parkinson's disease patients on levodopa medication and found that this metabolite is actively produced by the gut microbiota in those stool samples. ***Conclusions:*** Levodopa is deaminated by the gut bacterium *C. sporogenes* producing a metabolite that inhibits ileal motility *ex vivo*. Overall, this study underpins the importance of the metabolic pathways of the gut microbiome involved in drug metabolism not only to preserve drug effectiveness, but also to avoid potential side effects of bacterial breakdown products of the unabsorbed residue of medication.

BMC Biology, 2020, 18, 137
DOI: 10.1186/s12915-020-00876-3

BACKGROUND

Gut bacteria produce a wide range of small bioactive molecules from different chemical classes, including aromatic amino acids [1]. Bacterial products from aromatic amino acid degradation have been shown to play a critical role in intestinal barrier function, immune modulation and gut motility [2–6]. In the lower part of the gastrointestinal (GI) tract, where oxygen is limited, aromatic amino acid degradation by anaerobic bacteria involves reductive or oxidative deamination [7] resulting in production of aromatic metabolites [8–11]. Although the enzymes involved in the deamination pathway of the aromatic amino acids tryptophan, phenylalanine and tyrosine have been described [11–13], the enzyme involved in the initial transamination step remains unknown.

Recently, small intestinal (SI) microbiota have been implicated in the interference with levodopa drug availability [14,15]. Early *in vivo* studies showed that ~90% of levodopa is transported to the circulatory system [16–18], leaving a ~10% unabsorbed fraction of residual levodopa that can act as substrate for other bacterial species associated with the lower, more anaerobic regions of the GI-tract [19]. Such bacterial-residual drug interaction might act as bioactive metabolites with an impact on gut homeostasis.

Parkinson's disease (PD) is often associated with non-motor symptoms especially in the GI-tract. GI-tract dysfunction such as constipation, drooling and swallowing disorders occur frequently in PD patients, especially constipation, which is reported in 80-90% of the PD patients [20]. Importantly, chronic idiopathic constipation is associated with SI motor abnormalities in the esophagus, stomach, jejunum and ileum [21,22] and patients with constipation have a longer SI transit time compared to controls [22]. Only recently, SI dysfunction in PD was studied showing that the transit time in the SI was significantly longer in PD patients compared to healthy controls (HC) [23,24]. Using wireless electromagnetic capsules, the SI transit time was reported to be significantly higher in PD patients (400 min; n=22) compared to HC (295 min, n=15) [24].

This study uncovers the aminotransferase responsible for initiating the deamination pathway involved in the transamination of (among others) levodopa and shows that *C. sporogenes* can effectively deaminate levodopa to 3-(3,4-dihydroxyphenyl)propionic acid through the aromatic amino acid deamination pathway [11]. We show that the deamination product of gut bacterial degradation of the unabsorbed residues of levodopa in fecal samples from PD patients reduces ileal motility *ex vivo*. Our results highlight the urgency for further research on the effects of bacterial conversion of the unabsorbed residues of medication, which may affect host physiology.

RESULTS

Clostridium sporogenes deaminates levodopa through its deamination pathway

C. sporogenes is able to deaminate proteinogenic aromatic amino acids (PAAA) through an anaerobic deamination pathway (**Figure 1A**) [11–13]. We hypothesized that levodopa, a non-proteinogenic amino acid (NPAAA) and the main treatment in PD could be deaminated through the same pathway. Together with another NPAAA, 5-hydroxytryptophan (5-HTP, precursor

of serotonin, over-the-counter available drug used to treat depression, obesity, insomnia and chronic headaches [25]), as an analogous control compound derived from tryptophan, we screened for deamination of these compounds in batch cultures of *C. sporogenes*. Cultures were incubated with 100 µM levodopa or 5-HTP in combination with PAAAs from the growth medium and were followed over a period of 48 hours. Analysis of the samples using High Pressure Liquid Chromatography (HPLC) coupled to an electrochemical detector (ED) revealed that levodopa is completely converted within 24 h to a new metabolite, which was identified by $^{1}H/^{13}C$-NMR and LC-MS as 3-(3,4-dihydroxyphenyl)propionic acid, DHPPA (**Figure 1B-C, Supplementary Figure 1A-C**). Furthermore, the incubations showed that the PAAAs available from the growth medium did not prevent the deamination of levodopa and that, during the incubation for 48 h, DHPPA remained stable. Similarly, 5-HTP was converted into two new unknown peaks (**Supplementary Figure 2A-B**), albeit to a much lesser extent compared to levodopa. Only the first peak could be detected and assigned by LC-MS as 5-hydroxyindole-3-lactic acid (5-HILA) by its predicted exact mass (**Supplementary Figure 2C**). The other peak is potentially 5-hydroxyindole-3-propionic acid (5-HIPA), described below.

To further investigate the involvement of the deamination pathway in levodopa and 5-HTP deamination, the enzyme responsible for the dehydratase reaction (encoded by the *fldC* gene [11–13]) was disrupted using the ClosTron mutagenesis system (**Supplementary Figure 2D**) [26]. The resulting strain *C. sporogenes Ll.LtrB-ery^{R}ΩfldC* (CS$^{\Omega fldC}$) was incubated with levodopa, and the PAAAs from the growth medium. Tryptophan and tyrosine were converted to their intermediates ILA (indole-3-lactic acid) and 4-HPLA (3-(4-hydroxyphenyl)lactic acid), respectively, as previously shown [11]. Analogous to tryptophan and tyrosine, levodopa was no longer deaminated to DHPPA but to its intermediate product 3-(3,4-dihydroxyphenyl)lactic

(See figure on next page.)

Figure 1 | Levodopa is deaminated by *Clostridium sporogenes*. (**A**) Full reductive deamination pathway of *C. sporogenes* is depicted resulting in the full deamination (R-propionic acid) of (non)-proteinogenic aromatic amino acids (N)PAAA. The red arrow indicates a disrupted deamination pathway of *C. sporogenes*, where the dehydratase subunit *fldC* is mutagenized, resulting in a pool of partially deaminated metabolites (R-lactic acid) by *C. sporogenes*. (**B**) HPLC-ED curves from supernatant of a *C. sporogenes* batch culture conversion of levodopa (3-(3,4-dihydroxyphenyl)alanine) overtime. At the beginning of growth (timepoint 0 h) 100 µM of levodopa (blue) is added to the culture medium, the black line in the chromatogram depicts the control samples. In 24 h, levodopa is completely converted to DHPPA (3-(3,4-dihydroxyphenyl)propionic acid), the deaminated product of levodopa. Other aromatic amino acids from the medium, tryptophan and tyrosine (which are detectable with ED), are converted to the deaminated products IPA (indole-3-propionic acid) and 4-HPPA (3-(4-hydroxyphenyl)propionic acid). (**C**) Quantification (n=3) of levodopa conversion to DHPPA by *C. sporogenes* wild type (also see **Supplementary Table 1**). (**D**) Analysis of the supernatant of CS$^{\Omega fldC}$ shows that levodopa is not deaminated to DHPPA but to its intermediate product DHPLA (3-(3,4-dihydroxyphenyl)lactic acid) within 24 h. Tryptophan and tyrosine are converted to their intermediates ILA (indole-3-lactic acid) and 4-HPLA (3-(4-hydroxyphenyl)lactic acid), respectively. (**E**) Quantification (n=3) of levodopa conversion to DHPLA by *C. sporogenes* Ω*fldC* (also see **Supplementary Table 1**). All experiments were performed in 3 independent biological replicates and means with error bars representing the SEM are depicted.

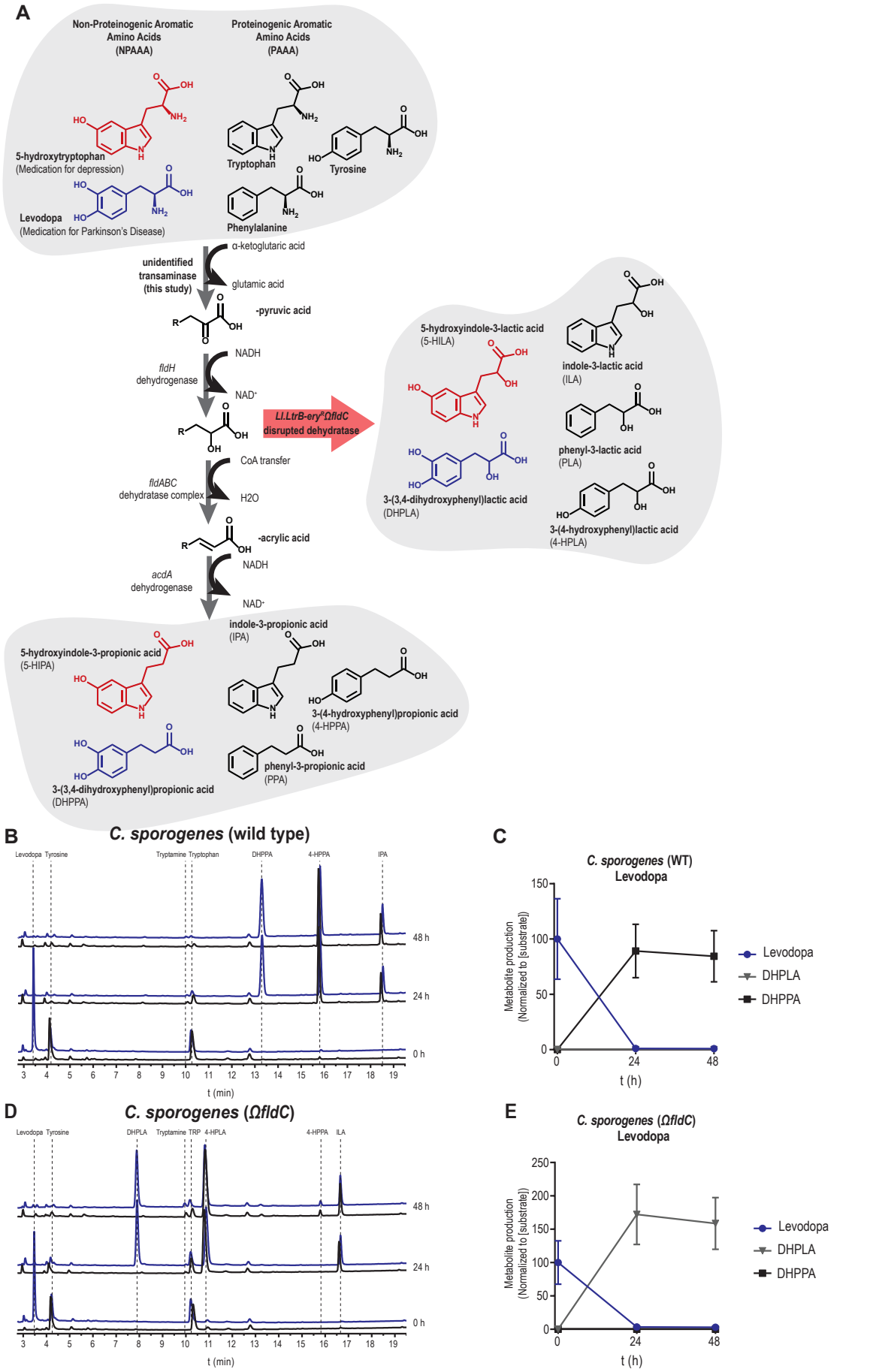

Figure 1 | Levodopa is deaminated by *Clostridium sporogenes*. (See legend on previous page.)

acid (DHPLA) (**Figure 1D-E**). Only a slight production of 4-HPPA (from tyrosine) is observed after 48 h, presumably because of the substitution of FldABC by the similar HadABC proteins from the *had*-operon in *C. sporogenes* [11,12]. HPLC-ED analysis of the 5-HILA production from 5-HTP by the *fldC* mutant was hampered by the production of coeluting 4-HPLA, the intermediate deamination product produced from tyrosine (described above). However, the analysis revealed that the second unknown peak produced from 5-HTP was no longer produced by $CS^{\Omega fldC}$ (**Supplementary Figure S2E-F**), demonstrating that 5-HTP conversion is affected and suggesting that the unknown product is 5-hydroxyindole-3-propionic acid (5-HIPA). Overall, the results show that the deamination pathway from *C. sporogenes* is not only involved in the deamination of PAAAs but also is in the deamination of the NPAAAs, levodopa and 5-HTP.

Identification of the aromatic aminotransferase responsible for initiation of the deamination pathway

The aromatic aminotransferase responsible for the transamination of levodopa and the other (N)PAAAs, is crucial for the initiation of the reductive deamination pathway and for the full deamination of the substrates by the dehydrogenases (FldH and AcdA) and dehydratase (FldABC) (**Figure 1A**). However, the gene encoding this transaminase remains unidentified. To further investigate this critical step in the pathway, all nine class I/II aminotransferases encoded by *C. sporogenes* were cloned, purified and screened for their activity on levodopa and the other (N)PAAAs. Screening revealed a single aminotransferase (EDU38870 encoded by CLOSPO_01732) to be involved in their transamination (**Figure 2A**). To verify whether other aminotransferases could substitute for the identified aminotransferase *in vivo*, CLOSPO_01732 was disrupted (resulting in $CS^{\Omega CLOSPO\_01732}$ (**Supplementary Figure 3A**)) and a targeted metabolomic analysis of all the (N)PAAA metabolites was performed using HPLC-ED (except metabolites from phenylalanine, which were quantified using HPLC-UV). The disruption of *fldC* or *CLOSPO_01732* resulted in only a minor reduction of the exponential growth rate in rich broth (Doubling time is 55.1±1.2 min and 64.1±1.1 min respectively compared to wild type 44.3±1.2 min) all reaching stationary phase within 12 hr (**Supplementary Figure 3B**). Comparing the metabolic profiles from wild type *C. sporogenes* (CS^{WT}), $CS^{\Omega fldC}$ and $CS^{\Omega CLOSPO\_01732}$ demonstrated that none of the other tested aminotransferases could take over this transaminase reaction effectively, except for the substrate phenylalanine (**Figure 2B, Supplementary Table 1**). Disrupting CLOSPO_01732 significantly reduced the production of phenyl-3-propionic acid (PPA), 3-(4-hydroxyphenyl)propionic acid (4-HPPA), indole-3-propionic acid (IPA), and 3-(3,4-dihydroxyphenyl)propionic acid (DHPPA) by 16.4%, 79.0%, 97.2%, 97.7%, respectively compared to CS^{WT} within 24-48 h (**Supplementary Table 1**). Presumably, the transamination of phenylalanine is substituted by EDU37030 as this aminotransferase also showed phenylalanine-converting activity *in vitro* (**Figure 2A**). Interestingly, $CS^{\Omega CLOSPO\_01732}$ produces significantly higher amounts of tryptamine (4 to 6-fold

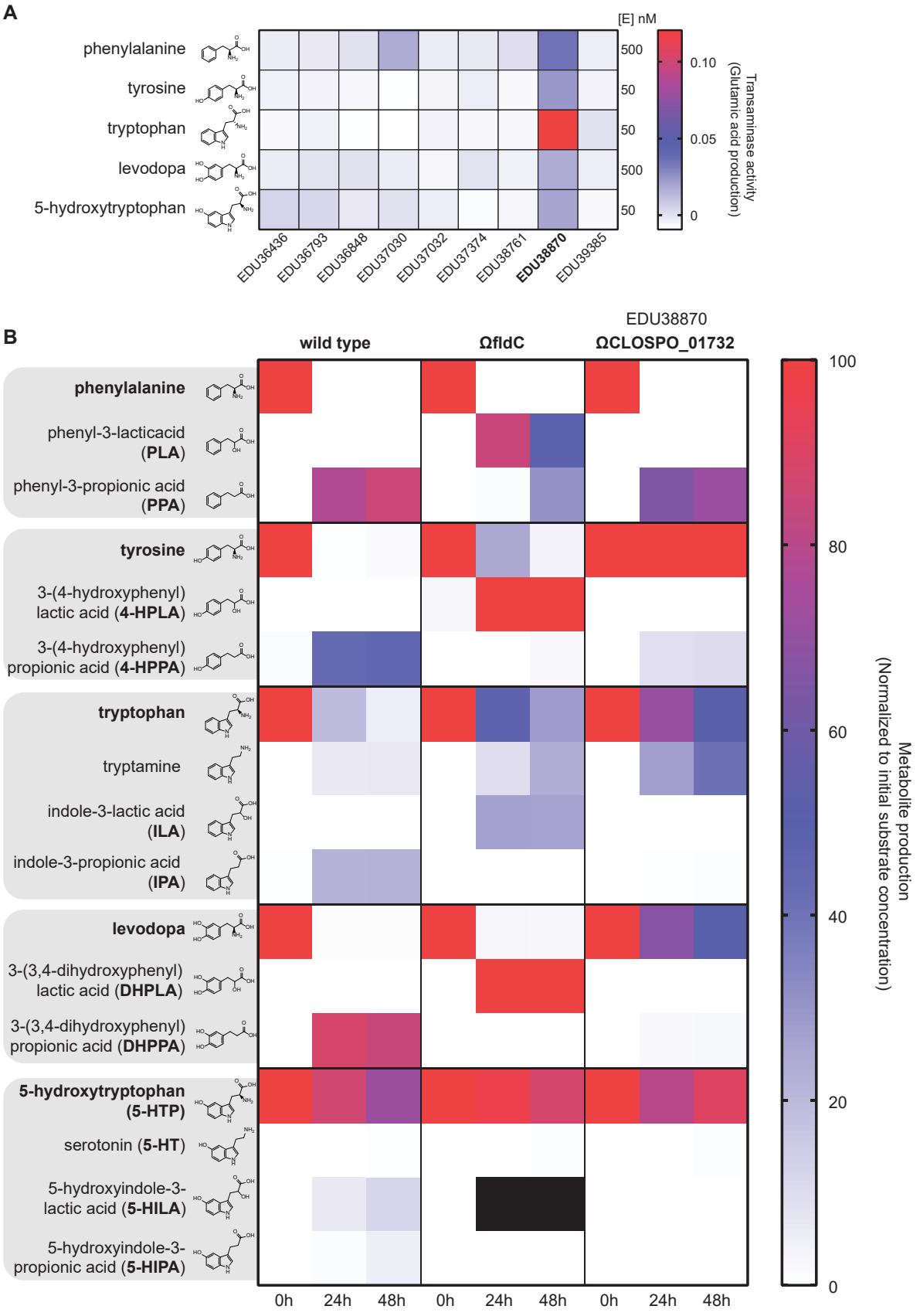

Figure 2 | Identification of the aromatic amino transferase initiating the deamination pathway. (See legend on next page.)

(See figure on previous page.)
Figure 2 | Identification of the aromatic amino transferase initiating the deamination pathway. In order to identify which aminotransferase is responsible for the initial transaminase reaction all class I/II aminotransferase were cloned and purified to test the activity against (N)PAAAs. (**A**) Transaminase activity (production of glutamate) for all substrates is depicted. EDU38870 (CLOSPO_01732) was involved in all transaminase reactions. EDU37030 showed similar activity as EDU38870, for phenylalanine. Experiment was performed in technical duplicates to screen for candidate genes for mutagenesis in *C. sporogenes*. (**B**) Targeted metabolic quantification of deamination products from CS^{WT}, $CS^{\Omega fldC}$, $CS^{\Omega CLOSPO\_01732}$ reveals that EDU38870 is involved in the transamination of all for all tested (N)PAAAs. All quantified deamination products are normalized to their initial substrate concentration and the data represents 3 independent biological replicates. Corresponding values are reported and metabolite concentration differences between WT and *ΩfldC* or ΩCLOSPO_01732 were tested for significance using Student's t-Test, in **Supplementary Table 1**. Black squares indicate that quantification was not possible because of a coeluting HPLC-ED peak. As no commercial standards are available for 5-HILA and 5-HIPA, the peaks were quantified assuming a similar ED-detector response as for 5-HTP.

increase at 24 and 48 h, respectively) compared to CS^{WT}, reflecting a reduced competition for the same substrate by different enzymes (**Figure 2B**, **Supplementary Table 1)**. Analogous to tryptamine, $CS^{\Omega CLOSPO\_01732}$ produced significantly more serotonin compared to CS^{WT} at 48 h when incubated with 5-HTP (**Figure 2B**, **Supplementary Figure 3C, Supplementary Table 1**), though to a much lesser extent (~1% of substrate added) compared to tryptamine. Collectively, the data show that the aromatic aminotransferase (EDU38870), is involved in the initiation of the aromatic amino acid deamination pathway and is crucial for the production of DHPPA, 5-HILA, 5-HIPA, and as well as the previously described metabolites to be circulating in the blood, IPA, and 4-HPPA (Dodd *et al*. [11]).

3-(3,4-dihydroxyphenyl)propionic acid elicits an inhibitory effect on ileal muscle contractions *ex vivo*

Because levodopa is the main treatment of PD patients, and is efficiently deaminated to DHPPA within 24 h by the *C. sporogenes* deamination pathway compared to 5-HTP, we further focused on levodopa and its deamination products. DHPPA is a phenolic acid (a molecule in the class polyphenols) and recent findings demonstrated an association between bacterial-derived polyphenol metabolites and gut-transit times in humans [27]. Levodopa is mainly absorbed in the proximal small intestine, but significant amounts can reach the distal part of the intestinal tract [17], and these levels increase with age [28]. As levodopa is taken orally, the first intestinal site where anaerobic bacteria such as *C. sporogenes* (*Clostridium* Cluster I) can encounter relevant levels of levodopa is the ileum. Studies on asymptomatic ileostomy subjects established that the core ileal microbiota consists of (facultative) anaerobes including species from *Clostridium* Cluster I [29,30]. Moreover, the transit time in the SI has been shown to be significantly longer in PD patients compared to healthy controls (with a median increase of 1.75 hours in PD patients) [23,24]. To this end, we tested whether DHPPA (100 µM) could affect the muscle contractility in the ileum. Ileal rings of wild type C57BL/6J mice were suspended in an *ex vivo* organ bath system to test the effect of DHPPA on muscle contractions. Our initial results indicated that DHPPA displayed an inhibiting effect on natural ileal contractility (**Supplementary Figure 4A**).

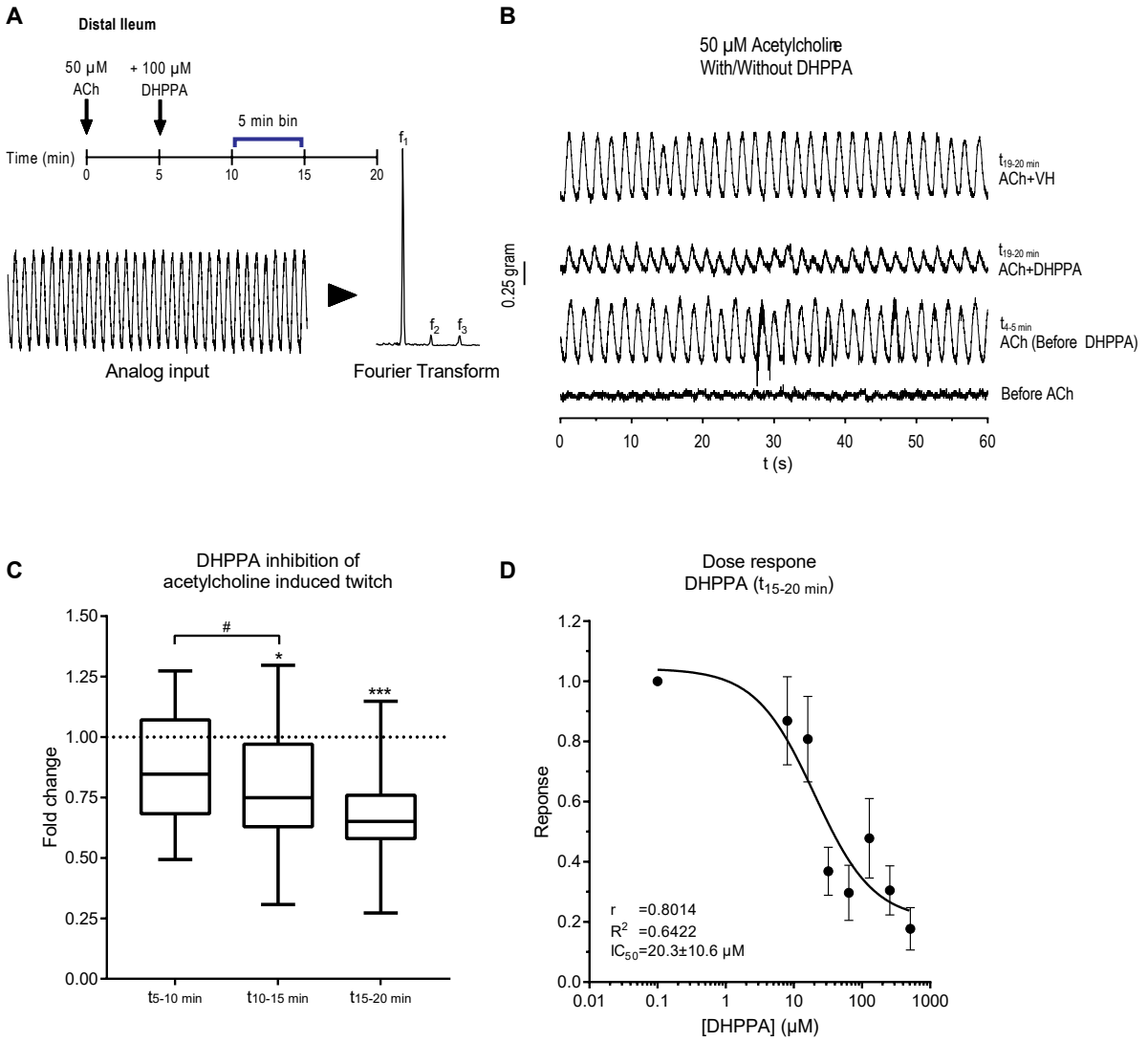

Figure 3. DHPPA inhibits the acetylcholine-induced twitch from mouse ileum. (**A**) Experimental setup, where 5 min after adding 50 µM acetylcholine, 100 µM DHPPA is added. The panel below indicates how the amplitude of the frequencies of the observed oscillations (from 5 minute bins) are extracted by a Fourier transform of the analog input. (**B**) A representative 1 min recording trace before and after the addition of acetylcholine and DHPPA or vehicle (VH) is shown. ACh, acetylcholine; VH, vehicle (0.05% ethanol). (**C**) Inhibition of DHPPA on acetylcholine-induced twitch binned in intervals of 5 minutes shows a decrease in contractility over time (n=6 biological replicates and experiments were repeated 1-4 times per tissue). Significance was tested using repeated measures (RM) 1-way-ANOVA followed by a Tukey's test (*=p<0.0021 ***=p<0.0002 #=p<0.0021). Box represents the median with interquartile range and whiskers represent the maxima and minima. (**D**) Dose response curve of DHPPA on the acetylcholine-induced twitch at the $t_{15\text{-}20}$ minute bin (n=4 biological replicates) with a half maximal inhibitory concentration (IC_{50}) of 20.3±10.6 µM.

Because acetylcholine is the neurotransmitter constantly produced from the excitatory muscle motor neurons to induce gut smooth muscle contractility [31], we tested whether DHPPA could have an inhibiting effect on acetylcholine-induced contractility in the ileum. The differences in amplitude of the contractions were quantified by measuring the decrease of the observed frequencies after a Fourier transform of 5 min intervals (**Figure 3A**). Ileal tissue preparations were tested by initiating an acetylcholinergic twitch by adding 50 µM of acetylcholine (a

concentration saturating the muscarinic receptors (Kd=1.7±0.18 μM [32]). After five minutes, 100 μM DHPPA (a concentration resembling the higher levels detected in fecal samples of PD patients, see below) was added and contractions were followed further over a period of 15 minutes. One-minute traces of the contractility representing one of the experiments are shown before and after addition of acetylcholine, DHPPA or vehicle (**Figure 3B**). A significant decrease in the amplitude (binned in 5 min intervals) of the acetylcholinergic twitch by DHPPA was observed at the 10-15 min (maximal reduction 69%) and 15-20 min interval (maximal reduction 73%) (**Figure 3C**). In order to determine the potency of DHPPA, a dose response curve with DHPPA was performed and showed a half maximal inhibitory concentration (IC_{50}) of 20.3±10.6 μM (**Figure 3D**). In contrast to DHPPA, incubations with levodopa did not show any significant effect on the acetylcholinergic twitch (**Supplementary Figure 4B).** Collectively the data shows that DHPPA can inhibit the acetylcholine-induced muscle contractility of mouse ileum *ex vivo*.

Active levodopa deamination pathway in fecal suspensions of patients with Parkinson's disease

We hypothesized that if *C. sporogenes* or other bacteria with the deamination pathway (*C. botulinum*, *Peptostreptococcus anaerobius* or *Clostridium cadaveris* [11]) are present in the GI-tract of PD patients on levodopa/carbidopa treatment, those patients might have considerable amounts of DHPPA in their distal GI-tract. Because DHPPA can be a product of gut bacterial metabolism of polyphenolic rich foods in the colon such as coffee and fruit (Jenner et al., 2005), fecal samples from 10 PD patients were compared to 10 age-matched HC. Samples were collected in a previous study and there were no significant difference in in macronutrients, dietary fiber, or total calorie intake between groups [34]. Using a catechol extraction targeted for the quantification of DHPPA we found that the DHPPA concentrations were significantly higher in PD patient's fecal samples compared to HC (**Figure 4A**). Identification of DHPPA was confirmed by LC-MS (**Supplementary Table 2**). The higher amounts (2.2 fold increase) of DHPPA observed in the fecal samples of PD patients are likely to result from levodopa metabolized by the anaerobic bacteria, deaminating levodopa through the FldBC dehydratase (**Figure 1A**). In order to investigate the presence and activity of the anaerobic deamination pathway in fecal samples, the dehydration of the intermediate levodopa metabolite, DHPLA (**Figure 1A**) was tested. The levodopa intermediate DHPLA was used as substrate instead of levodopa to prevent an *in vitro* substrate bias for bacteria that can decarboxylate levodopa to dopamine [14,15]. Moreover, FldABC is the key protein complex responsible for the production of DHPPA. Screening for the identified transaminase or FldH dehydrogenase upstream of FldABC would not be relevant as many bacterial species harbor these type of enzymes (**Supplementary Figure 5**). Hence, fecal suspensions (10% w/v) from PD and HC were incubated anaerobically with DHPLA, and samples were collected at 0, 20, and 45 h and were analyzed by HPLC-ED. After 20 h, DHPPA was detected in fecal samples from PD patients, as well as in fecal samples of HC when supplied

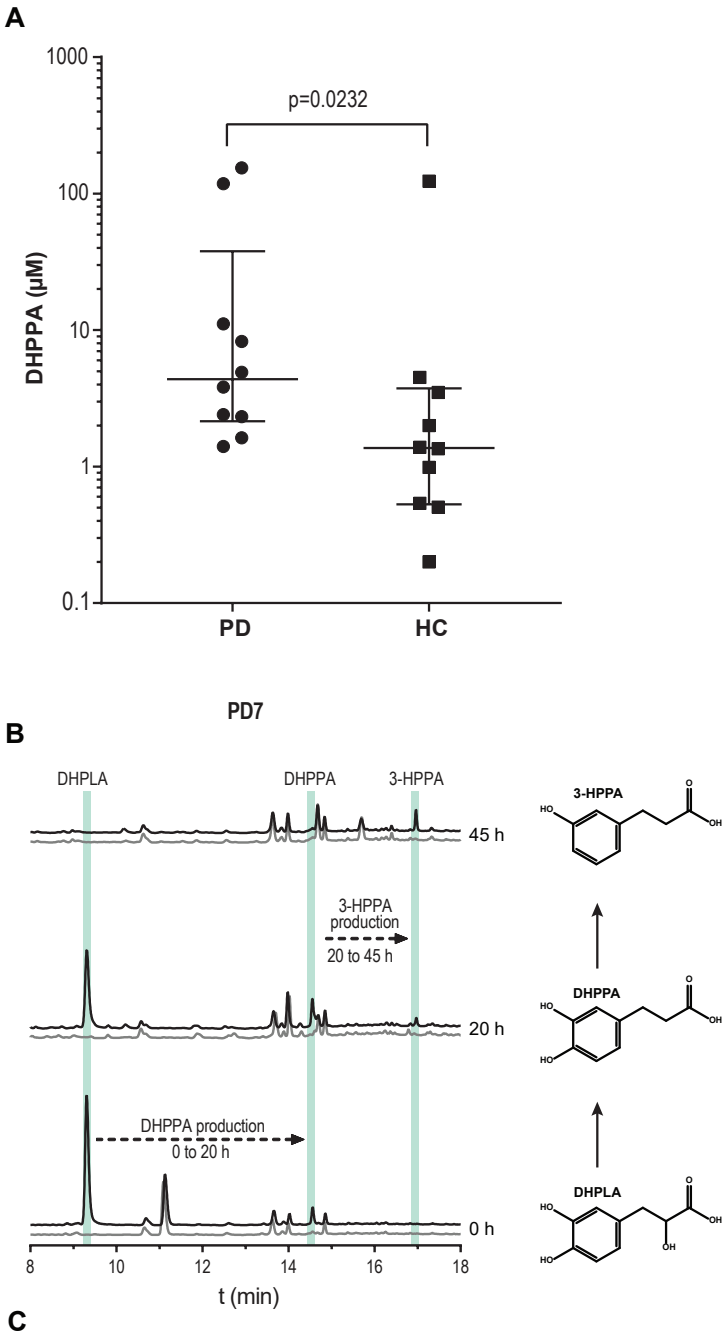

Figure 4. Higher DHPPA levels in PD patients and active levodopa deamination pathway in PD fecal suspensions. (See legend on next page.)

(See figure on previous page.)
Figure 4. Higher DHPPA levels in PD patients and active levodopa deamination pathway in PD fecal suspensions. (**A**) DHPPA was extracted from fecal samples of PD patients (n=10) and age-matched healthy controls (n=10) using activated alumina beads and concentrations were quantified using a standard curve of DHPPA on the HPLC-ED with 3,4-dihydroxybenzylamine as internal standard. DHPPA concentrations are depicted on the logarithmic y-axis and individual levels are indicated and compared between Parkinson's disease patients (PD) and age-matched healthy controls (HC). The cross-header represents the median (PD, 4.36 µM; HC, 1.37 µM) and the interquartile range (PD, 2.15-37.90 µM; HC, 0.53-3.75 µM). Significance was tested using an unpaired nonparametric Mann-Whitney test (p=0.0232) (**B**) A representative HPLC-ED chromatogram of fecal-suspension from PD7 where DHPPA is produced from DHPLA (black) after 20 h and is further metabolized to 3-HPPA after 45 h of incubation. The control, without the addition of DHPLA is indicated in grey. The green bars indicate the retention time of the standards indicated . (**C**) Metabolite profiles of the PD fecal suspensions that produced DHPPA/3-HPPA within 20-45h (70%) are merged as replicates. Lines represent the mean and the shadings the SEM, a zoom in graph of DHPPA and 3-HPPA is depicted on the right.

with the substrate levodopa (**Figure 4B, Supplementary Figure 6A**). Moreover, DHPPA was further converted to the downstream dehydroxylated metabolite of DHPPA, 3-(3-hydroxyphenyl) propionic acid (3-HPPA) over time (**Figure 4B, Supplementary Figure 6A**). Because DHPPA is further converted to 3-HPPA *in vitro* we quantified both the production of DHPPA and/or 3-HPPA in the fecal incubations as measure for the presence of an active deamination pathway. Metabolic profiles of PD or HC samples that produced DHPPA/3-HPPA overtime were quantified and merged (**Figure 4C, Supplementary Figure 6B**), showing that DHPPA is produced first, and is further metabolized to 3-HPPA. The production of DHPPA or 3-HPPA was observed in 50% and 20% of the PD patient's and HC fecal-suspensions, respectively after 20 h and in 70% and 50% PD patient's and HC fecal-suspensions, respectively after 45 h (**Supplementary Figure 6C).** The production of 3-HPPA *in vitro* is likely to be performed by *Eggerthella lenta*, which has been shown to perform *p*-dehydroxylations [35]. Indeed *in vitro* culturing of *E. lenta* showed *p*-dehydroxylation of DHPPA (**Supplementary Figure 7A** [35,36]). Because DHPPA is further converted to 3-HPPA *in vitro,* we examined whether 3-HPPA could elicit a similar effect on the acetylcholine induced contractions in ileum. Unlike, DHPPA, 3-HPPA did not elicit a significant effect on the acetylcholine induced twitch (**Supplementary Figure 7B** [35,36]).
Furthermore, to investigate the genomic abundance levels of bacteria capable of deaminating (N)PAAAs, we analyzed the 16s rDNA sequence data of the fecal samples of patients with Parkinson disease [34] that were employed in this study (**Supplementary Results** [11–13,37]**, Supplementary Figure 8**). A significant positive correlation (r= 0.62, R^2= 0.38, p= 0.02) was found between bacteria with the deamination pathway and DHPPA/3HPPA production in fecal incubation samples at 20 h (**Supplementary Figure 8E**). Taken together, the results show that DHPPA can be produced by the microbiota via anaerobic deamination of levodopa. Moreover, our findings indicate that 3-HPPA originates from DHPPA via dehydroxylation potentially by *Eggerthella lenta* and that the aromatic deamination pathway, as measured by the production of DHPPA or 3-HPPA, is active and present in at least 70% of the PD samples.

DISCUSSION

Identifying bacterial pathways and elucidating their potential impact on bacterial drug metabolism is crucial in order, not only, to maximize medication efficacy, but also to recognize and eventually prevent potential side effects that might affect the host's physiology on an individual basis [14,36,38,39]. Here we disclosed the reductive anaerobic deamination pathway in *C. sporogenes* by identifying its initiating enzyme, the aromatic aminotransferase, and expanded the pathway's relevance by demonstrating its capacity to convert two clinically important NPAAAs, levodopa and 5-HTP. We showed that *C. sporogenes* is able to completely deaminate levodopa to DHPPA and to a much lesser extent 5-HTP (**Figures 1-2, Supplementary Figure 1-3, Supplementary Table 1**). Disrupting the bacterial transaminase encoding gene abolished the production of deaminated products, and increased the production of neuromodulators such as tryptamine and, to much lesser extent, serotonin (**Figure 2, Supplementary Figure 3C and Supplementary Table 1**). Tryptamine is a natural product produced by *C. sporogenes* that has been proposed to modulate gut transit time [40]. The application of engineered gut bacteria as a therapeutic strategy to modulate GI-motility or host physiology has been also proposed recently in two proof-of-concept studies; by heterologous expression of *Ruminococcus gnavus* tryptophan decarboxylase in *Bacteroides thetaiotamicron* [5] and by modification of the metabolic output of bioactive compounds in an engineered *fldC* deficient *C. sporogenes* strain [11]. However, translation of these studies into applications is hindered by restrictions on the application of genetically engineered microorganisms (GMOs) *per se*, and the complexity of introducing these GMOs into an existing gut microbiota ecosystem. Selective therapeutic blockage of the aminotransferase identified in this study may provide an attractive alternative solution to modify gut microbiota metabolism.

PD patients encounter increased gut transit time; thus, an additional inhibition of acetylcholine-induced contraction could result in further slowing down of gut transit rates. The inhibitory effect of DHPPA on the acetylcholine-induced ileal muscle contractions (**Figure 3**), higher DHPPA levels in fecal samples of PD patients compared to HC (**Figure 4**), and an active deamination pathway of levodopa during fecal-incubations of PD patients (**Figure 4**) demonstrate active deamination of levodopa in the distal GI-tract of PD patients and suggest potential side effects of this bacterial by-product of the unabsorbed residue of the medication. DHPPA shares similarity with dopamine structure except of the terminal amine group, which is substituted by a carboxyl group in DHPPA. Dopamine, and dopamine agonists, have been shown to inhibit methacholine (analog of acetylcholine) induced contraction, which is not mediated via dopamine receptors, in guinea pig jejunum in similar concentration ranges to DHPPA (EC_{50} relaxation by dopamine ~290 μM) [41], indicating that DHPPA might act on a similar mechanism. Collectively, although further research is needed to unravel the underlying mechanism, our results show that DHPPA inhibits the acetylcholine-induced muscle contractions in the ileum with implications on intestinal motility, often observed in PD patients.

CONCLUSIONS

The present study shows that *C. sporogenes* can effectively deaminate unabsorbed residues of levodopa in fecal samples from PD patients to 3-(3,4-dihydroxyphenyl)propionic acid, which reduces ileal motility *ex vivo*. Overall, our results highlight the urgency to unravel potential effects of gut bacterial processing of (unabsorbed residues of) medication, such as levodopa.

METHODS

Growth and incubation of *Clostridium sporogenes* and *Eggerthella lenta*

Clostridium sporogenes ATCC15579 was grown in enriched beef broth (EBB) with 2 g/L glucose [14] and 0.1% Tween 80 (EBB/T) anaerobically (10% H_2, 10% CO_2, 80% N_2) in a Don Whitley Scientific DG250 Workstation (LA Biosystems, Waalwijk, The Netherlands) at 37 °C. *Eggerthella lenta* DSM2243 was grown in modified DSMZ medium 78 (DSMZ 78: Beef extract, 10.0 g/L; Casitone, 30.0 g/L; Yeast extract, 5.0 g/L; K_2HPO_4, 5.0 g/L; Tween 80, 0.1%; Menadione (Vitamin K3), 1 µg/ml; Cysteine, 0.5 g/L; Hemin, 5 mg/L; L-Arginine 0.1-1.5%) anaerobically (1.5% H_2, 5% CO_2, balance with N_2) in a Coy Laboratory Anaerobic Chamber (neoLab Migge GmbH, Heidelberg, Germany) at 37 °C in a tube shaker at 500 RPM. Upon use, bacteria were inoculated from -80 °C stored glycerol stocks in the appropriate media and grown for 18-24 h for *C. sporogenes* and 24-40 h for *E. lenta*. Overnight turbid cultures were then diluted 1/50 in an appropriate volume EBB/T or CMM for further experiments with 100 µM levodopa (D9628, Sigma), 5-hydroxytrytophan (H9772, Sigma), 50 µM 3-(3,4-dihydroxyphenyl) propionic acid (102601, Sigma) or H_2O as control. All experiments were performed in triplicate (3 biological replicates)

Protein production and purification

Transaminase-encoding genes from *C. sporogenes* (**Supplementary Table 3**) were amplified using Phusion High-fidelity DNA polymerase and primers listed in **Supplementary Table 3**. All amplified genes were cloned in pET15b, except for EDU37032 which was cloned in pET28b (**Supplementary Table 3)**. Plasmids were maintained in *E. coli* DH5α and verified by Sanger sequencing before transformation to *E. coli* BL21 (DE3). Overnight cultures were diluted 1:50 in fresh LB medium with the appropriate antibiotic and grown to OD600 = 0.7–0.8 shaking at 37 °C. Protein translation was induced with 1 mM Isopropyl β-D-1-thiogalactopyranoside (IPTG, 11411446001, Roche Diagnostics) and cultures were incubated overnight at 18 °C. The cells were washed with 1/5th of the volume in 1× ice-cold PBS and stored at −80 °C or directly used for protein isolation. Cell pellets were thawed on ice and resuspended in 1/50th of buffer A (300 mM NaCl; 10 mM imidazole; 50 mM KPO4, pH 8.0) containing 0.2 mg/mL lysozyme (105281, Merck) and 2 µg/mL DNAse (11284932001, Roche Diagnostics), and incubated for at least 10 min on ice before sonication (10 cycles of 15 s with 30 s cooling at 8 microns amplitude) using Soniprep-150 plus (Beun de Ronde, Abcoude, The Netherlands). Cell debris was removed by centrifugation at 20,000 × g for 20 min at 4 °C. The 6 × his-tagged proteins were purified using

a nickel-nitrilotriacetic acid (Ni-NTA) agarose matrix (30250, Qiagen). Cell-free extracts were loaded on 0.5 ml Ni-NTA matrixes and incubated on a roller shaker for 2 h at 4 °C. The Ni-NTA matrix was washed three times with 1.5 mL buffer B (300 mM NaCl; 20 mM imidazole; 50 mM KPO4, pH 8.0) before elution with buffer C (300 mM NaCl; 250 mM imidazole; 50 mM KPO4, pH 8.0). Imidazole was removed from purified protein fractions using Amicon Ultra centrifugal filters (UFC505024, Merck) and washed three times and reconstituted in buffer D (50 mM Tris-HCl; 300 mM NaCl; pH 7.5). Protein concentrations were measured spectrophotometrically (Nanodrop 2000, Isogen, De Meern, The Netherlands) using the predicted extinction coefficient and molecular weight from ExPASy ProtParam tool (www.web.expasy.org/protparam/).

Transaminase activity test

Purified transaminases were incubated with 1 mM substrate, 2 mM α-ketoglutaric acid, and 0.1 mM PLP (pyridoxal-5-phosphate, P9255, Sigma, The Netherlands) in buffer D with an enzyme concentration of 50 nM for tyrosine, tryptophan, or 5-HTP as substrate and an enzyme concentration of 500 nM for phenylalanine and levodopa as substrate. Enzyme reactions were incubated for 0.5 h at 37 °C, the reactions were stopped with 0.7% (v/v) perchloric acid (1:1). Transaminase activity was tested using an L-glutamic acid detection kit (K-GLUT, Megazyme Inc., Wicklow, Ireland), according to the manufacture's microplate assay procedure with some modifications. The supplied buffer was substituted for buffer D (described above, to prevent oxidation of the substrates/products). A reaction mix was prepared mixing 50 µL buffer D; 10 µL quenched sample reaction mixture, 20 µL NAD^+/iodonitrotetrazolium chloride solution, 5 µL diaphorase solution, 5 µL glutamate dehydrogenase (GIDH) solution and reconstituted to a final volume of 290 µL with H2O. Absorbance at 492 nm was measured after 10 minutes of incubation using a microplate reader (Synergy HTX spectrophotometer, BioTek, BioSPX, The Netherlands) and background was subtracted from initial read before addition of GIDH solution

Targeted mutagenesis

Gene disruptions in *Clostridum sporogenes* were performed using the ClosTron system [42,43]. This system facilitates targeted mutagenesis using the group-II *Ll.LtrB* intron of *Lactococcus lactis*. Introns targeting *fldC* (CLOSPO_311) or CLOSPO_1732 (encoding for the transaminase) were designed using the ClosTron intron design tool (http://www.clostron.com) and were ordered in pMTL007C-E2 from ATUM (Newark, California, United States) resulting in pMTL007C-E2_Cs-fldC-561a and pMTL007C-E2_Cs-CLOSPO_1732-493s respectively. Plasmids were transferred to *C. sporogenes* by conjugation as described before [43] using *E. coli* CA434 (*E. coli* HB101 (Bio-Rad Laboratories, The Netherlands) harboring the broad host $IncP\beta^+$ conjugational plasmid pRK24 [44] as donor strain. *E. coli* CA434 harboring pMTL007C-E2_Cs-fldC-561a or pMTL007C-E2_Cs-CLOSPO_1732-493s was grown in Luria Broth (LB) with 10 µg/mL tetracycline and 25 µg/mL chloramphenicol (to select for pRK24 and PMTL007C-E2 respectively). Cell suspensions of 1 mL of overnight culture were washed once with PBS and the cell pellet was resuspended in 200 µL of *C. sporogenes* overnight cell suspension. The bacterial-

mixture was spotted (in drops of 10 µL) on trypticase soy agar (TSA) plates and incubated for 24 h anaerobically at 37 °C. Sequentially, 1 mL of PBS was added to the spotted plates and the donor-recipient mix was scraped of the plate, sequentially the scraped-off suspension was distributed over TSA plates containing 50 µg/mL neomycin (to prevent growth of *E. coli*) and 15 µg/mL chloramphenicol to select for *C. sporogenes* conjugants. Chloramphenicol resistant colonies of *C. sporogenes* were re-streaked on TSA plates containing 50 µg/mL neomycin and 2.5 µg/mL erythromycin (to select for intron insertion) for several times. To makes sure the plasmid was integrated, colonies were checked and selected for their sensitivity towards chloramphenicol and the genomic DNA was verified using PCR (**Supplementary Figure 1F, and 2A**)

Fecal samples from patients with Parkinson's disease and age-matched healthy controls

Fecal samples from patients diagnosed with PD (n = 10) and age-matched healthy controls (n = 10) were acquired from the Movement Disorder Center at Rush University Medical Center, Chicago, Illinois, USA published previously [34]. All study subjects consented to the use of their samples for research. PD was diagnosed according to the UK Brain Bank Criteria as previously described [34]. Study subjects were provided with the supplies and instructions for home feces collection using the BD Gaspak EZ Anaerobe Gas Generating Pouch System with Indicator (Ref 260683; Becton, Dickinson and Company, Sparks, MD) in order to minimize the exposure of the feces to high oxygen ambient atmosphere, which may alter the microbiota. Subjects were asked to have a bowel movement within 24 h of their study visit. Subjects kept the sealed anaerobic fecal bag in a cold environment, before bringing the anaerobic fecal bag to the hospital. Fecal samples were then immediately stored at -80°C until analysis.

Fecal metabolite incubations from PD patients and HC subjects

Stool samples were suspended 1:1 (w/v) in EBB/T and incubated anaerobically (10% H_2, 10% CO_2, 80% N_2) in a Don Whitley Scientific DG250 Workstation (LA Biosystems, Waalwijk, The Netherlands) at 37 °C with 100 µM Sodium 3-(3,4-dihydroxyphenyl)-DL-lactate (39363,Sigma). Samples were taken at 0, 20, and 45 h and analyzed on HPLC-ED as described below.

HPLC-ED/UV analysis and sample preparation

For bacterial cell suspensions, 1 mL of methanol was added to 0.25 mL of cell suspension and stored at -20 °C until further use. For fecal metabolite incubations, 300 µl of methanol was added to 75 µL of fecal suspension and stored at -20°C until further use. Metabolites from stool samples were extracted by suspending the stool 1:1 (w/v) in water, followed by homogenization by vigorously vortexing while keeping samples as cold as possible. Homogenized suspensions were centrifuged at 3500 × *g* for 20 min at 4°C and sequentially 1.6 mL of methanol was added to 0.4 mL of supernatant. From bacterial, fecal incubation or stool samples cells and protein precipitates were removed by centrifugation at 20000 × *g* for 10 min at 4°C. Supernatant was transferred to a new tube and the methanol fraction was evaporated in a Savant speed-vacuum dryer (SPD131, Fisher Scientific, Landsmeer, The Netherlands) at 60°C for 1.5-2 h. The

aqueous fraction was reconstituted with 0.7% $HClO_4$ to the appropriate volume. Samples were filtered and injected into the HPLC-ED system (Alliance Separations Module 2695, Waters Chromatography B.V, Etten-Leur, The Netherlands; Dionex ED40 electrochemical detector, Dionex, Sunnyvale, USA, with a glassy carbon working electrode (DC amperometry at 0.8 or 1.0 V, with Ag/AgCl as reference electrode)). Samples were analyzed on a C18 column (Kinetex 5µM, C18 100 Å, 250 × 4.6 mm, Phenomenex, Utrecht, The Netherlands) using a gradient of water/methanol with 0.1% formic acid (0-10 min, 95−80% H_2O; 10-20 min, 80-5% H_2O; 20-23 min 5% H_2O; 23-31 min 95% H_2O). Fecal suspension metabolites were injected twice and analyzed at DC amperometry at 0.8 V (for DHPPA) and at 1.0 V (for 3-HPPA). Lowering the voltage makes the detection more selective for more readily oxidizable compounds [45] such as DHPPA, but making 3-HPPA invisible for detection. For the detection of the *C. sporogenes* metabolites and for peak isolation another HPLC-ED system was used (Jasco AS2059 plus autosampler, Jasco Benelux, Utrecht, The Netherlands; Knauer K-1001 pump, Separations, H. I. Ambacht, The Netherlands) with the same detector (ED40) and the same gradient as described above. Phenylalanine metabolites were detected by injecting the same samples in an HPLC-UV system (Alliance Separations Module 2695, Waters Chromatography B.V, Etten-Leur, The Netherlands; TSP UV6000LP UV-detector (wavelength: 260 nM) Thermo Scientific, The Netherlands). Samples for peak isolation were separated on a Vydac Semi-preparative C18 column (218TP510, 5 µm, 300 Å, 10 mm × 250 mm, VWR International B.V, Amsterdam, The Netherlands) at 3 ml/min using the same gradient as above. Data recording and analysis was performed using Chromeleon software (version 6.8 SR13). Significance was tested using a Two-sample equal variance (homoscedastic) Student's t-Test (Microsoft Excel 2019 version 1808).

Catechol extraction from stool for DHPPA quantification

Catechols were extracted from PD patients and HC stool samples using activated alumina powder (199966, Sigma) as previously described [14] with a few modifications. A volume of 200 µl 50% stool suspension (described above) was used with 1 mM DHBA (3,4-dihydroxybenzylamine hydrobromide, 858781, Sigma) as an internal standard. Samples were adjusted to pH 8.6 with 800 µL TE buffer (2.5% EDTA; 1.5 M Tris/HCl pH 8.6) and 5–10 mg of alumina was added. Suspensions were mixed on a roller shaker at room temperature for 20 min and were sequentially centrifuged for 30 s at 20,000× g and washed three times with 1 mL of H_2O by aspiration. Catechols were eluted using 0.7% $HClO_4$ and filtered before injection into the HPLC-ED-system as described above (DC amperometry at 0.8 V). A standard curve was injected to quantify the concentrations of DHPPA in 50% (w/v) stool samples. Significance was tested using an unpaired nonparametric Mann-Whitney test (GraphPad Prism version 7).

Organ-bath experiments

Distal ileal samples were harvested from wild type adult (18-20 weeks) male C57BL/6J mice that were sacrificed for another purpose. Harvested tissue was immediately removed, placed

and washed in 0.85% NaCl. Approximately 3 mm rings were cut and were placed in an organ bath (Tissue Bath Station with SSL63L force transducer, Biopac Systems Inc. Varna, Bulgaria) filled with Krebs–Henseleit solution (NaCl, 7.02 g/L; KCl, 0.44 g/L; $CaCl_2.2H_2O$, 0.37 g/L; $MgCl_2.6H_2O$, 0.25 g/L; $NaH_2PO_4.H_2O$ 0.17 g/L; Glucose, 2.06 g/L; $NaHCO_3$, 2.12 g/L) gassed with Carbogen gas mixture (5 % CO_2, balanced with O_2) at 37 °C. Ileal rings were equilibrated for at least 45-60 min with replacement of Krebs–Henseleit solution approximately every 15 min. Sequentially, 50 µM of acetylcholine (ACh) (Sigma, A2661) was added to induce a stable repetitive muscle twitch response, and after ~5 min 100 µM of DHPPA (102601, Sigma) (n=6 biological replicates, 1-4 technical replicates), 3-HPPA (91779, Sigma) (n=4 biological replicates, 2 technical replicates), or levodopa (D9628, Sigma) (n=3 biological replicates, 2 technical replicates) was added for ~15 min before the ileal rings were washed. This step was repeated 1-4 times per ileal preparation. As control, ACh was added for at least 20 min with or without 0.05% ethanol (solvent of DHPPA) after 5 min to check for spontaneous decrease. For the dose response curve (n= 4 biological replicates), every 15 minutes the cumulative dose of DHPPA was increased by 2-fold ranging from 8 to 512 µM. Data was recorded and analyzed in BioPac Student Lab 4.1 (Build: Feb 12, 2015). Frequencies were extracted performing a fast Fourier transform (FFT) on bins of 5 minute intervals. The maximum amplitude of all the observed frequencies were extracted and the average decrease of all frequencies overtime were calculated. Significance was tested using repeated measures (RM) 1-way-ANOVA followed by a Tukey's test (GraphPad Prism version 7).

NMR

Samples were exchanged once with 99.9 atom% D_2O with intermediate lyophilization, finally dissolved in 650 µL D_2O. One- and two-dimensional ^{1}H and ^{13}C NMR spectra were recorded at a probe temperature of 25°C on a Varian Inova 500 spectrometer (NMR Department, University of Groningen). Chemical shifts are expressed in ppm in reference to external acetone (δ ^{1}H 2.225; δ ^{13}C 31.08). 1D 500-MHz 1H NMR spectra were recorded with 5000 Hz spectral width at 16 k complex data points, using a WET1D pulse to suppress the HOD signal. Homonuclear decoupled ^{1}D 125 MHz ^{13}C NMR spectra were recorded with 31,000 Hz spectral width at 64k complex data points. 2D ^{1}H-^{13}C HSQC spectroscopy was performed using multiplicity editing, rendering CH_2 signals in the negative plane, while CH and CH_3 remain in the positive plain. 2D ^{13}C-^{1}H HMBC spectroscopy was performed suppressing single-bond correlations. Spectra were processed using MestReNova v9.1 (Mestrelabs Research SL, Santiago de Compostela, Spain).

LC-MS

HPLC-MS analysis was performed using an Accella1250 HPLC system coupled with the benchtop ESI-MS Orbitrap Exactive (Thermo Fisher Scientific, San Jose, CA, USA) in negative and positive ion mode. Samples were analyzed on a C18 column (Shim Pack Shimadzu XR-ODS 3 × 75 mm) using a gradient of water/acetonitrile with 0.1% formic acid (0-5 min, 98−90% H_2O; 5-10 min, 90-5% H_2O; 10-13 min 5% H_2O; 13-14 min 98% H_2O). Data analysis was

performed using Qual Browser Thermo Xcalibur software (version 2.2 SP1.48).

HPLC-MS analysis of alumina extraction samples was performed using an Waters Acquity Class-I UPLC (Waters Chromatography B.V, Etten-Leur, The Netherlands) system coupled to a MaXis Plus Q-TOF (Bruker, Billerica, MA, USA) on negative ion mode with post-column addition of 3 µl/min ESI Tune Mix (G1969-85000; Agilent Technologies, Middelburg, The Netherlands) for mass calibration. Samples were analyzed on a C18 column (Shim Pack Shimadzu XR-ODS 3 × 75 mm) using a gradient of water/acetonitrile with 0.1% formic acid (0-5 min, 98−90% H_2O; 5-10 min, 90-5% H_2O; 10-13 min 5% H_2O; 13-15 min 2% H_2O; 15-17 min 98% H_2O). Data analysis was performed using Bruker Compass Data Analysis (version 4.2 SR1).

Bioinformatics

Phylogenetic trees. Proteins were BLASTed against a local BLAST database constructed from the protein sequences of the NIH Human Microbiome Project (HMP) Roadmap project (PRJNA43021) using BLAST 2.9.0+, NCBI. The top 100 BLASTp hits were aligned in the Constraint-based Multiple Alignment Tool (COBALT, NCBI) and converted to a distance tree using NCBI TreeView (Parameters: Fast Minimum Evolution; Max Seq Difference, 0.85; Distance, Grishin).

Sequence data analysis. The demultiplexed paired-end sequence data from stool and sigmoid colon samples of PD patients and healthy controls from Keshavarzian *et al*. [34] (bioproject PRJNA268515) were analyzed using Kraken2 (v2.0.9, April 7, 2020), a *k*-mer taxonomic classification system [46], using the standard Kraken2-database. To further estimate the species abundance the Kraken2 output was analyzed with Bracken (Bayesian Reestimation of Abundance with KrakEN; v2.6.0, April 3, 2020) [47]. The number of mapped reads from bacteria with the *fld*-gene cluster [11] were extracted from the Bracken results and the abundance was calculated relative to the total number of mapped bacterial reads.

REFERENCES

1. Donia, M. S. & Fischbach, M. A. Small molecules from the human microbiota. *Science* **349**, 1254766 (2015).
2. Bansal, T., Alaniz, R. C., Wood, T. K. & Jayaraman, A. The bacterial signal indole increases epithelial-cell tight-junction resistance and attenuates indicators of inflammation. *Proc. Natl. Acad. Sci.* **107**, 228–233 (2010).
3. Schiering, C. *et al.* Feedback control of AHR signalling regulates intestinal immunity. *Nature* **542**, 242–245 (2017).
4. Yano, J. M. *et al.* Indigenous Bacteria from the Gut Microbiota Regulate Host Serotonin Biosynthesis. *Cell* **161**, 264–276 (2015).

5. Bhattarai, Y. *et al.* Gut Microbiota-Produced Tryptamine Activates an Epithelial G-Protein-Coupled Receptor to Increase Colonic Secretion. *Cell Host Microbe* **23**, 775-785.e5 (2018).
6. Venkatesh, M. *et al.* Symbiotic bacterial metabolites regulate gastrointestinal barrier function via the xenobiotic sensor PXR and toll-like receptor 4. *Immunity* **41**, 296–310 (2014).
7. Barker, H. A. Amino Acid Degradation by Anaerobic Bacteria. *Annu. Rev. Biochem.* **50**, 23–40 (1981).
8. Yvon, M., Thirouin, S., Rijnen, L., Fromentier, D. & Gripon, J. An aminotransferase from *Lactococcus lactis* initiates conversion of amino acids to cheese flavor compounds. *Appl. Envir. Microbiol.* **63**, 414–419 (1997).
9. Nierop Groot, M. N. & De Bont, J. A. M. Conversion of phenylalanine to benzaldehyde initiated by an aminotransferase in *Lactobacillus plantarum*. *Appl. Environ. Microbiol.* **64**, 3009–3013 (1998).
10. Elsden, S. R., Hilton, M. G. & Waller, J. M. The end products of the metabolism of aromatic amino acids by clostridia. *Arch. Microbiol.* **107**, 283–288 (1976).
11. Dodd, D. *et al.* A gut bacterial pathway metabolizes aromatic amino acids into nine circulating metabolites. *Nature* **551**, 648–652 (2017).
12. Dickert, S., Pierik, A. J. & Buckel, W. Molecular characterization of phenyllactate dehydratase and its initiator from *Clostridium sporogenes*. *Mol. Microbiol.* **44**, 49–60 (2002).
13. Dickert, S., Pierik, A. J., Linder, D. & Buckel, W. The involvement of coenzyme A esters in the dehydration of (*R*)-phenyllactate to (*E*)-cinnamate by *Clostridium sporogenes*. *Eur. J. Biochem.* **267**, 3874–3884 (2000).
14. van Kessel, S. P. *et al.* Gut bacterial tyrosine decarboxylases restrict levels of levodopa in the treatment of Parkinson's disease. *Nat. Commun.* **10**, 310 (2019).
15. Maini Rekdal, V., Bess, E. N., Bisanz, J. E., Turnbaugh, P. J. & Balskus, E. P. Discovery and inhibition of an interspecies gut bacterial pathway for Levodopa metabolism. *Science* **364**, eaau6323 (2019).
16. Bianchine, J. R., Messiha, F. S. & Hsu, T. H. Peripheral aromatic L-amino acids decarboxylase inhibitor in parkinsonism. II. Effect on metabolism of L-2-14 C-dopa. *Clin. Pharmacol. Ther.* **13**, 584–94 (1972).
17. Morgan, J. P. Metabolism of Levodopa in Patients With Parkinson's Disease. *Arch. Neurol.* **25**, 39 (1971).
18. Sasahara, K. *et al.* Dosage form design for improvement of bioavailability of levodopa IV: Possible causes of low bioavailability of oral levodopa in dogs. *J. Pharm. Sci.* **70**, 730–733 (1981).

19. Goldin, B. R., Peppercorn, M. A. & Goldman, P. Contributions of host and intestinal microflora in the metabolism of L-dopa by the rat. *J. Pharmacol. Exp. Ther.* **186**, 160–6 (1973).
20. Fasano, A., Visanji, N. P., Liu, L. W. C., Lang, A. E. & Pfeiffer, R. F. Gastrointestinal dysfunction in Parkinson's disease. *Lancet Neurol.* **14**, 625–639 (2015).
21. Panagamuwa, B., Kumar, D., Ortiz, J. & Keighley, M. R. B. Motor abnormalities in the terminal ileum of patients with chronic idiopathic constipation. *Br. J. Surg.* **81**, 1685–1688 (1994).
22. Van Der Sijp, J. R. M. *et al.* Disturbed gastric and small bowel transit in severe idiopathic constipation. *Dig. Dis. Sci.* **38**, 837–844 (1993).
23. Dutkiewicz, J. *et al.* Small intestine dysfunction in Parkinson's disease. *J. Neural Transm.* **122**, 1659–1661 (2015).
24. Knudsen, K. *et al.* Gastrointestinal Transit Time in Parkinson's Disease Using a Magnetic Tracking System. *J. Parkinsons. Dis.* **7**, 471–479 (2017).
25. Das, Y. T., Bagchi, M., Bagchi, D. & Preuss, H. G. Safety of 5-hydroxy-L-tryptophan. *Toxicol. Lett.* **150**, 111–122 (2004).
26. Heap, J. T. *et al.* The ClosTron: Mutagenesis in *Clostridium* refined and streamlined. *J. Microbiol. Methods* **80**, 49–55 (2010).
27. Roager, H. M. *et al.* Colonic transit time is related to bacterial metabolism and mucosal turnover in the gut. *Nat. Microbiol.* **1**, 16093 (2016).
28. Iwamoto, K., Watanabe, J., Yamada, M., Atsumi, F. & Matsushita, T. Effect of age on gastrointestinal and hepatic first-pass effects of levodopa in rats. *J. Pharm. Pharmacol.* **39**, 421–425 (1987).
29. Zoetendal, E. G. *et al.* The human small intestinal microbiota is driven by rapid uptake and conversion of simple carbohydrates. *ISME J.* **6**, 1415–1426 (2012).
30. Booijink, C. C. G. M. *et al.* High temporal and inter-individual variation detected in the human ileal microbiota. *Environ. Microbiol.* **12**, 3213–3227 (2010).
31. Costa, M., Brookes, S. J. & Hennig, G. W. Anatomy and physiology of the enteric nervous system. *Gut* **47 Suppl 4**, iv15-9; discussion iv26 (2000).
32. Ringdahl, B. Dissociation constants and relative efficacies of acetylcholine, (+)- and (-)-methacholine at muscarinic receptors in the guinea-pig ileum. *Br. J. Pharmacol.* **89**, 7–13 (1986).
33. Jenner, A. M., Rafter, J. & Halliwell, B. Human fecal water content of phenolics: The extent of colonic exposure to aromatic compounds. *Free Radic. Biol. Med.* **38**, 763–772 (2005).
34. Keshavarzian, A. *et al.* Colonic bacterial composition in Parkinson's disease. *Mov. Disord.* **30**, 1351–1360 (2015).

35. Jin, J. S. & Hattori, M. Isolation and characterization of a human intestinal bacterium Eggerthella sp. CAT-1 capable of cleaving the C-Ring of (+)-catechin and (-)-Epicatechin, followed by p-dehydroxylation of the B-ring. *Biol. Pharm. Bull.* **35**, 2252–2256 (2012).
36. Haiser, H. J. *et al.* Predicting and manipulating cardiac drug inactivation by the human gut bacterium *Eggerthella lenta*. *Science* **341**, 295–8 (2013).
37. Kalia, V. C. *et al.* Analysis of the unexplored features of rrs (16S rDNA) of the Genus *Clostridium*. *BMC Genomics* **12**, (2011).
38. Niehues, M. & Hensel, A. In-vitro interaction of L-dopa with bacterial adhesins of *Helicobacter pylori*: an explanation for clinicial differences in bioavailability? *J. Pharm. Pharmacol.* **61**, 1303–7 (2009).
39. Zimmermann, M., Zimmermann-Kogadeeva, M., Wegmann, R. & Goodman, A. L. Separating host and microbiome contributions to drug pharmacokinetics and toxicity. *Science* **363**, eaat9931 (2019).
40. Williams, B. B. *et al.* Discovery and Characterization of Gut Microbiota Decarboxylases that Can Produce the Neurotransmitter Tryptamine. *Cell Host Microbe* **16**, 495–503 (2014).
41. Lucchelli, A., Boselli, C. & Grana, E. Dopamine-induced relaxation of the guinea-pig isolated jejunum is not mediated through dopamine receptors. *Pharmacol. Res.* **22**, 433–44 (1990).
42. Heap, J. T., Pennington, O. J., Cartman, S. T., Carter, G. P. & Minton, N. P. The ClosTron : A universal gene knock-out system for the genus *Clostridium*. **70**, 452–464 (2007).
43. Heap, J. T., Pennington, O. J., Cartman, S. T. & Minton, N. P. A modular system for *Clostridium* shuttle plasmids. *J. Microbiol. Methods* **78**, 79–85 (2009).
44. Williams, D. R., Young, D. I. & Young, M. Conjugative plasmid transfer from *Escherichia coli* to *Clostridium acetobutylicum*. *J. Gen. Microbiol.* **136**, 819–826 (1990).
45. Nagatsu, T. & Kojima, K. Application of electrochemical detection in high-performance liquid chromatography to the assay of biologically active compounds. *TrAC Trends Anal. Chem.* **7**, 21–27 (1988).
46. Wood, D. E., Lu, J. & Langmead, B. Improved metagenomic analysis with Kraken 2. *Genome Biol.* **20**, 1–13 (2019).
47. Lu, J., Breitwieser, F. P., Thielen, P. & Salzberg, S. L. Bracken: Estimating species abundance in metagenomics data. *PeerJ Comput. Sci.* **2017**, 1–17 (2017).

SUPPLEMENTARY INFORMATION

Supplementary information accompanies this paper at https://doi.org/10.1186/s12915-020-00876-3 and in this thesis (see next page).

Acknowledgements

We thank Mr. Walid Maho, Interfaculty Mass Spectrometry Center, University of Groningen, The Netherlands for running and analyzing the samples on the LC-MS and Prof. dr. Michiel Kleerebezem, Host-microbe interactomics group, Wageningen University, The Netherlands, for critical reading of our manuscript.

Authors' Contributions

S.P.K. and S.E.A conceived and designed the study. S.P.K., H.R.J., S.L.W., S.S.L., S.A.N., H.P., A.K. performed the experiments and S.P.K., S.S.L., H.P., and S.E.A. analyzed the data. S.P.K. and S.E.A. wrote the original manuscript that was reviewed by S.S.L., S.A.N., H.P., A.K. Funding was acquired by S.E.A. All authors read and approved the final manuscript.

Funding

S.E.A is supported by a Rosalind Franklin Fellowship, co-funded by the European Union and University of Groningen, The Netherlands.

Availability of data and materials

All data generated or analyzed during this study are included in this published article and its supplementary information files. The metagenomic sequence data collected by Keshavarzian *et al*. [34] were deposited under BioProject number PRJNA268515.

Conflict of interest

The authors declare no competing interests.

Ethics Approval and Consent to Participate.

Samples from participants were used from Keshavarzian *et al*. [34] (bioproject PRJNA268515), where all subjects consented to use of their samples for research.

SUPPLEMENTARY RESULTS

Metagenomic analysis of deaminating bacteria and *E. lenta* in PD and HC fecal and mucosal samples

Measuring activity in fecal incubations shows that live bacteria express and produce enzymes that are capable of metabolic conversions, metagenomics on the other hand will only provide information whether a bacterium is present (death or alive) but no information on the activity of a certain metabolic pathway. Although its drawbacks it is of value to investigate the genomic abundance levels of bacteria capable of deaminating (N)PAAAs. In order to determine the relative abundance of deaminating bacteria, the 16s rDNA metagenomic sequence data from stool and sigmoid colon mucosa samples of PD patients and healthy controls from Keshavarzian *et al*. [34] (bioproject PRJNA268515) were analyzed using Kraken2, a *k*-mer taxonomic classification system followed by Bracken (Bayesian Reestimation of Abundance with KrakEN) that computes the abundance of species. We extracted the bacteria that are known to be capable of deaminating (N)PAAAs [11–13] and *E. lenta* and compared their relative abundance between PD and HC samples.

In all fecal samples (prevalence = 1.0) *Clostridium botulinum* was detected. *E. lenta* was detected in 91% and 87% (prevalence = 0.91 and 0.87) of PD and HC samples, respectively. *C. sporogenes* was found in 2.9% of the PD samples only, although many *C. sporogenes* reads might be wrongly associated with the *C. botulinum* clade as, based on 16S rDNA, they are occurring in a single phylogenetic clade and some strains share high sequence similarity (≥ 99.8 %) of their 16S rRNA [12, 37]. Moreover, some *C. sporogenes* sequences show exact homology with *C. botulinum* based on 16S rDNA *in silico* restriction enzyme analysis [37]. No reads were associated with *Clostridium cadaveris* or *Peptostrepotococcus anaerobius*. Furthermore, comparing the relative abundance of *C. botulinum* or *E. lenta* between PD and HC, no significant differences were observed between PD and HC fecal or mucosal samples (**Supplementary Figure 8A-D**), which is in agreement with the observed similar activity in PD and HC samples (**Supplementary Figure 6C**).

In order to investigate whether the DHPPA/3HPPA production in the fecal incubations are associated with higher levels of *C. botulinum* a correlation analysis was performed. The analysis showed a significant positive correlation (r= 0.62, R^2= 0.38, p= 0.02) between the relative abundance of *C. botulinum* and DHPPA/3HPPA production in fecal incubation samples at 20 h (**Supplementary Figure 8E**). No significant correlation between the DHPPA levels extracted from the PD samples (**Figure 4A**) and *C. botulinum* was observed (r=-0.05, R^2=0.003, p=0.89), indicating that some DHPPA might have originated from other sources, which is in agreement with the fact that DHPPA is also observed in the HC samples (**Figure 4A**).

SUPPLEMENTARY FIGURES

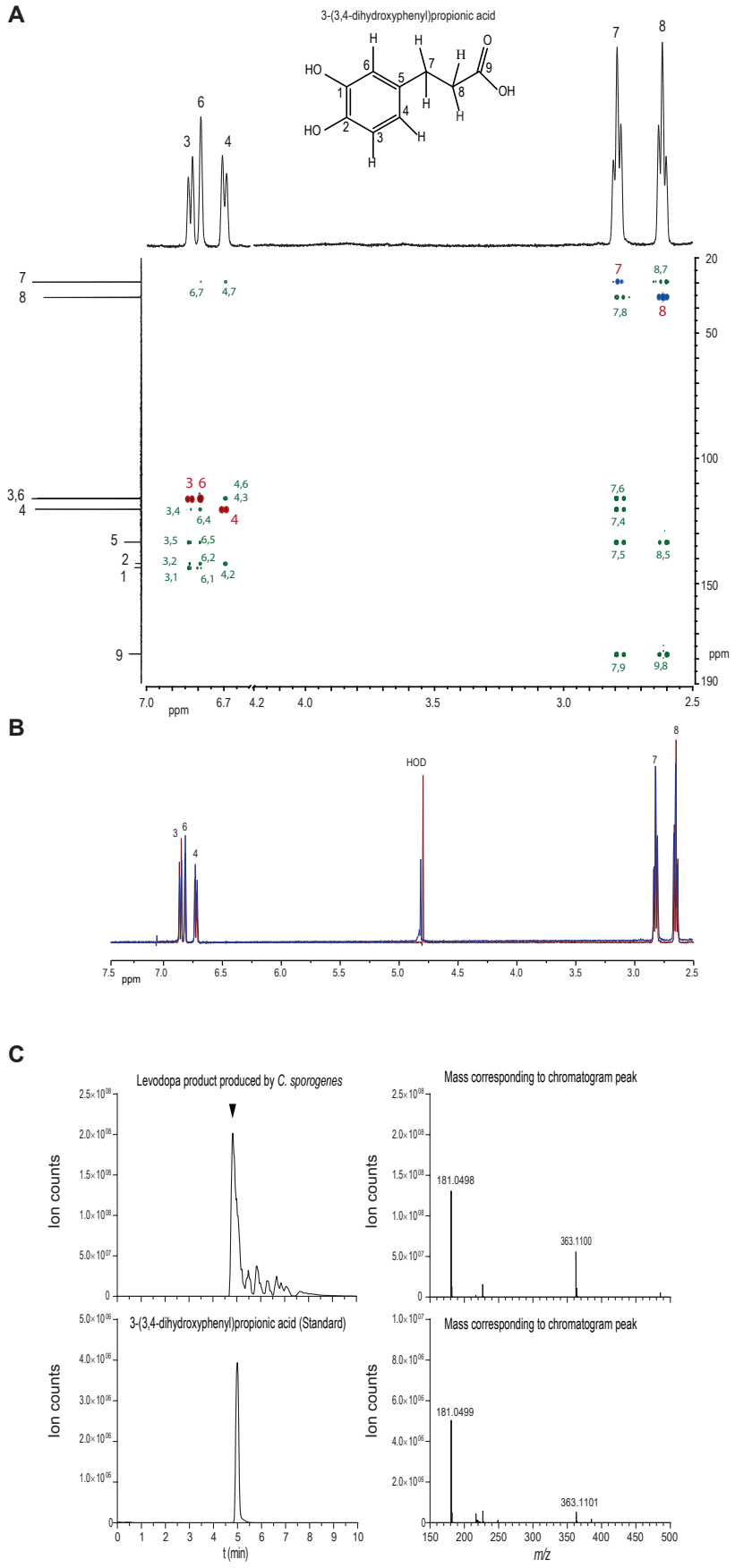

Figure S1 | NMR and MS confirmation of levodopa product, 3-(3,4-dihydroxyphenyl)propionic acid
(See legend on next page)

(See figure on previous page)

Figure S1 | NMR and MS confirmation of levodopa product, 3-(3,4-dihydroxyphenyl)propionic acid. (A) The isolated L-DOPA product was analysed by ^{1}H and ^{13}C NMR spectroscopy. The 1D ^{1}H NMR spectrum showed 5 distinct peaks; δ 6.86 (*d J* 8.2 Hz; 1; H-3), δ 6.82 (*s*; 1; H-6), δ 6.72 (*d J* 8.6 Hz; 1; H-4), δ 2.82 (*t J* 7.2 Hz; 2; H-7), δ 2.64 (*t J* 7.2 Hz; 2; H-8). The 1D ^{13}C NMR spectrum showed 9 peaks δ 178.47 (C-9), δ 143.80 (C-1), δ 142.08 (C-2), δ 133.69 (C-5), δ 120.46 (C-4), δ 116.26 (C-3), δ 116.07 (C-6), δ 35.80 (C-8) and δ 26.63 (C-7). The 2D ^{1}H-^{13}C gHSCQ spectrum showed positive peaks (red) corresponding with single proton CH correlations at δ 6.86;116.26 (H-3;C-3), δ 6.82;116.08 (H-6;C-6) and δ 6.72;120.46 (H-4;C-4) and negative peaks (blue) corresponding to CH_2 correlations at δ 2.82;26.63 (H-7;C-7) and δ 2.64;35.80 (H-8;C-8). The 2- and 3-bond ^{1}H-^{13}C correlations in the 2D ^{1}H-^{13}C HMBC spectrum (green) are marked, allowing the build-up of the compound, fitting the structure of 3-(3,4-dihydroxyphenyl)propionic acid (DHPPA). (**B**) The identity of DHPPA as assigned by 1D and 2D NMR spectroscopy was further confirmed by comparison of the 1D ^{1}H NMR spectra of the commercially available standard of DHPPA in blue, with the isolated product in red. (**C**) LC-ESI-MS in negative mode showing the exact same mass and retention time as the commercially available standard of DHPPA.

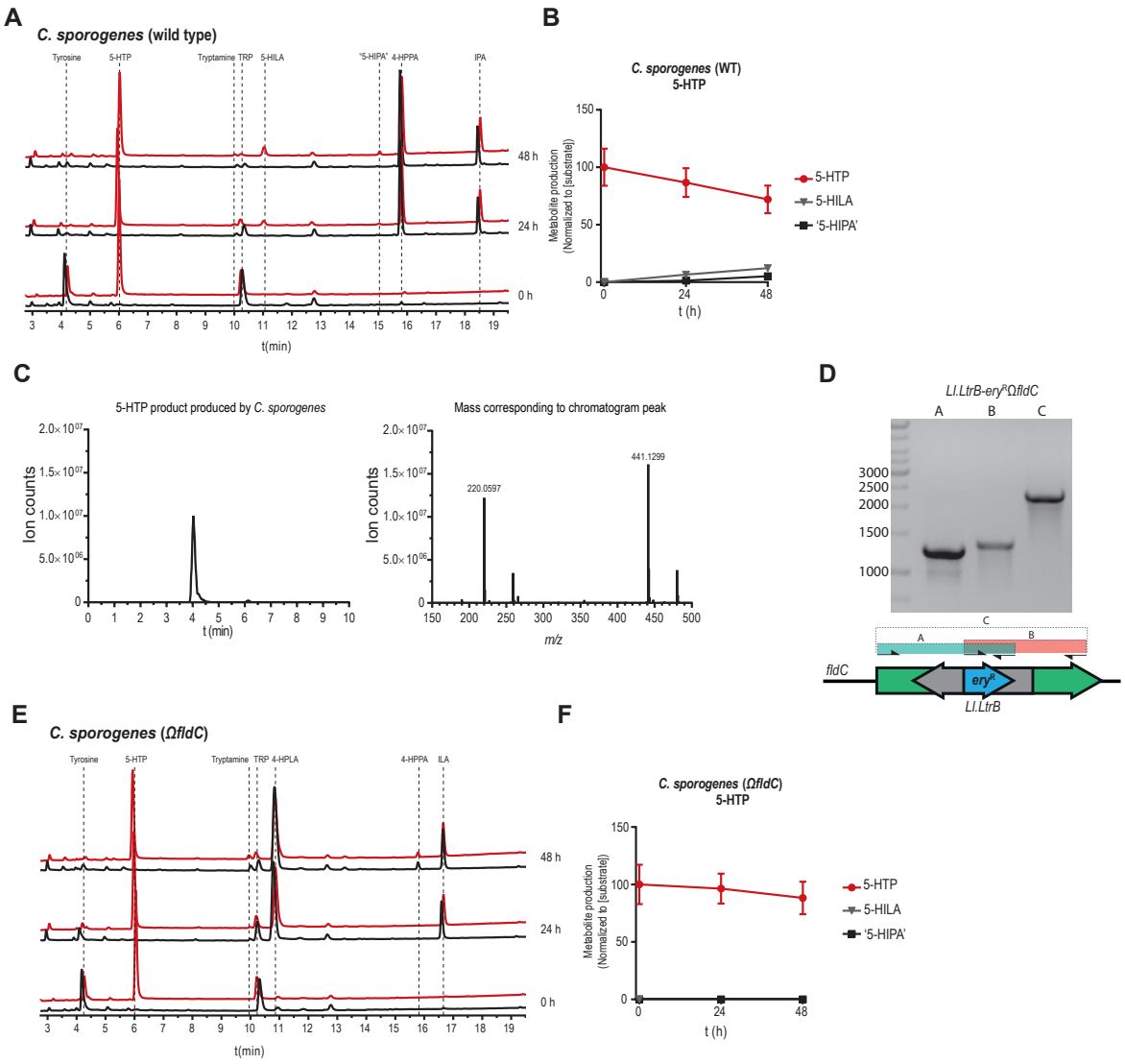

Figure S2 | 5-HTP conversion by *Clostridium sporogenes*. (**A and B**) HPLC-ED curves and quantification (n=3) from supernatant of a *C. sporogenes* batch culture conversion of 5-HTP (5-hydroxy-L-tryptophan) overtime. At the beginning of growth (timepoint 0 h), 100 µM of 5-HTP (red) was added to the culture medium, the black line in the chromatogram depicts the control samples. In 24 h, 5-HTP was converted, to a minor extent, to 5-HILA (5-hydroxyindole-3-lactic acid), as determined by LC-MS and potentially to 5-HIPA (5-hydroxyindole-3-propionic acid), as this peak was absent in $CS^{\Omega fldC}$ incubations. (**B**) Quantification (n=3) of 5-HTP conversion by *C. sporogenes* wild type (also see **Supplementary Table 1**). (**C**) LC-ESI-MS analysis shows the mass of the first peak produced by CS^{WT} from 5-HTP isolated from the HPLC-ED corresponding to the mass of 5-HILA (predicted exact mass 221.069-[H^+]). (**D**) Primers targeting the erythromycin cassette in *LI.LtrB* intron and primers binding outside the cassette were used to confirm the disruption of the *fldC.* (**E**) HPLC-ED chromatograms of $CS^{\Omega fldC}$ incubation with 100 µM of 5-HTP (red) or control (black); no 5-HIPA is detected and tryptophan and tyrosine are converted to their intermediates ILA (indole-3-lactic acid) and 4-HPLA (3-(4-hydroxyphenyl)lactic acid), respectively. The detection of 5-HILA is hampered by the coeluting 4-HPLA. (**F**) Quantification (n=3) of 5-HTP conversion to by *C. sporogenes* Ω*fldC* (also see **Supplementary Table 1**). (**A, B, E** and **F**) All experiments were performed in 3 independent biological replicates and means with error bars representing the SEM are depicted.

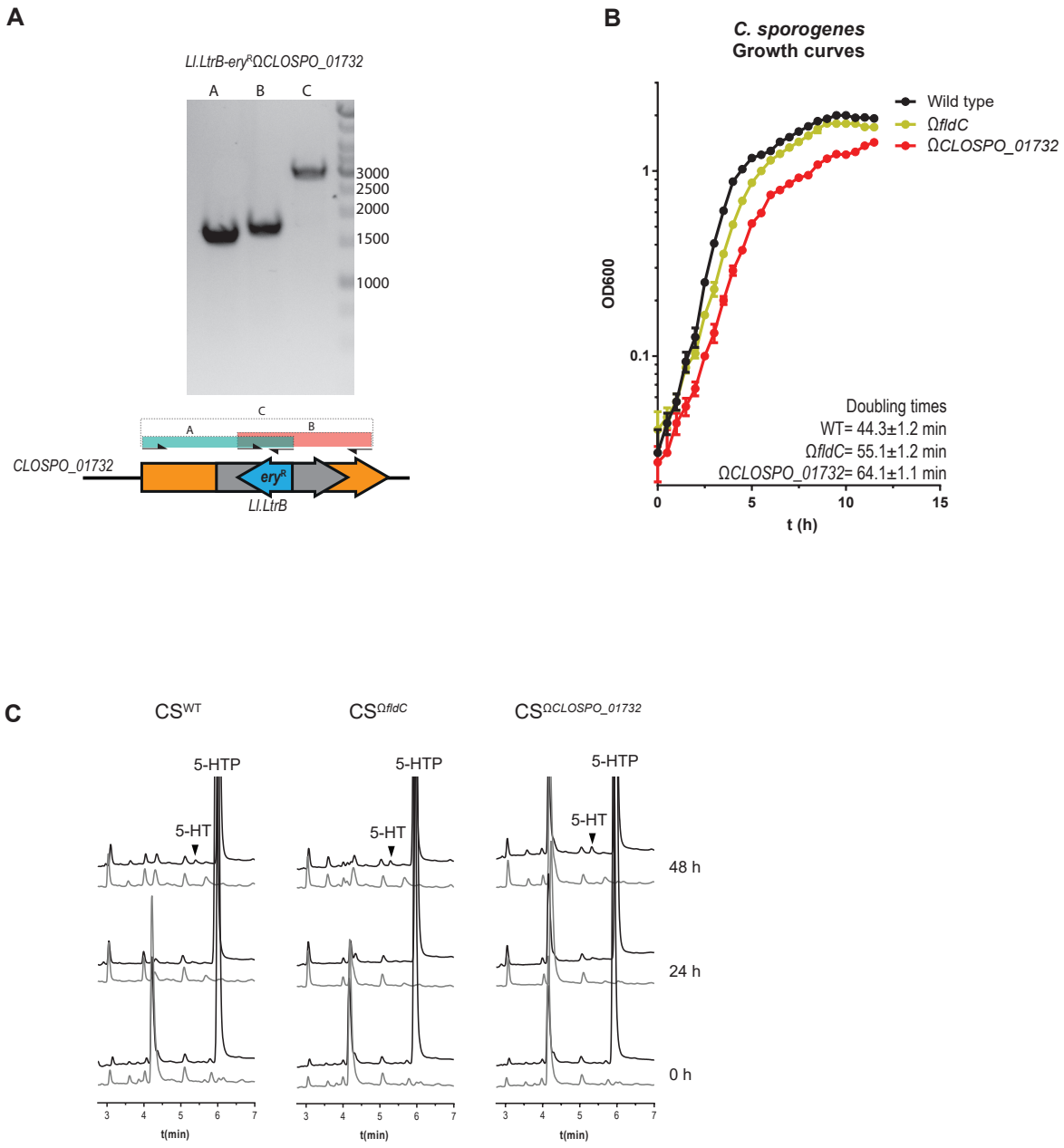

Figure S3 | Growth curves of CS$^{\Omega fldC}$ and CS$^{\Omega CLOSPO_01732}$, and 5-HT production. (**A**) Primers targeting the erythromycin cassette in *Ll.LtrB* intron and primers binding outside the cassette were used to confirm the disruption of the *fldC* and *CLOSPO_01732*. (**B**) Growth-curves of CS^{WT}, CS$^{\Omega fldC}$ and CS$^{\Omega CLOSPO_01732}$ showing minor but significant increase in doubling time in the first part of the growth curve. However, all strains reached stationary phase within 12 h. Experiment was performed in triplicate and points and error bars represent the mean with SD (**C**) A minor production of 5-HT (serotonin) is observed in all strains after 48 h, this graph represents 3 independent replicates, see **Supplementary Table 1** for comparison between CS$^{\Omega fldC}$ and CS$^{\Omega CLOSPO_01732}$ with wild type.

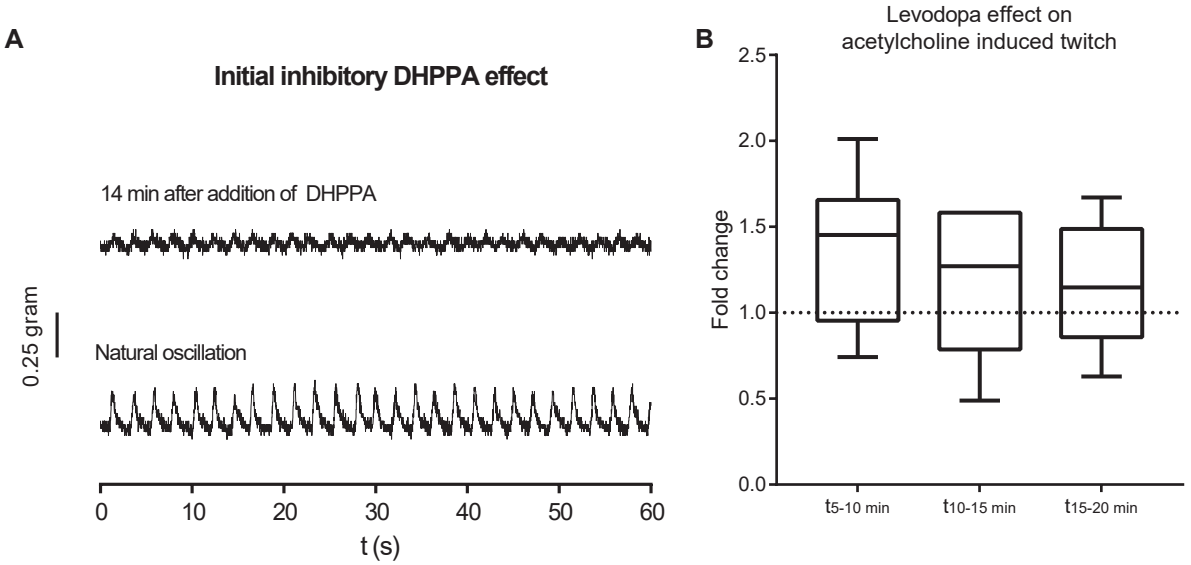

Figure S4 | Initial effect of DHPPA on natural ileal contractility and no effect of levodopa on acetylcholine induced twitch. (A) During a period of natural oscillations of contracting ileum 100 μM of DHPPA was added. The amplitude of the contractions decreased and the trace from 14-15 minutes after DHPPA addition is depicted. **(B)** Levodopa has no significant effect on the acetylcholine induced twitch binned in intervals of 5 minutes (n=3 biological replicates and experiments were repeated 2 times per tissue). Significance was tested using repeated measures (RM) 1-way-ANOVA followed by a Tukey's test. Box represents the median with interquartile range and whiskers represent the maxima and minima.

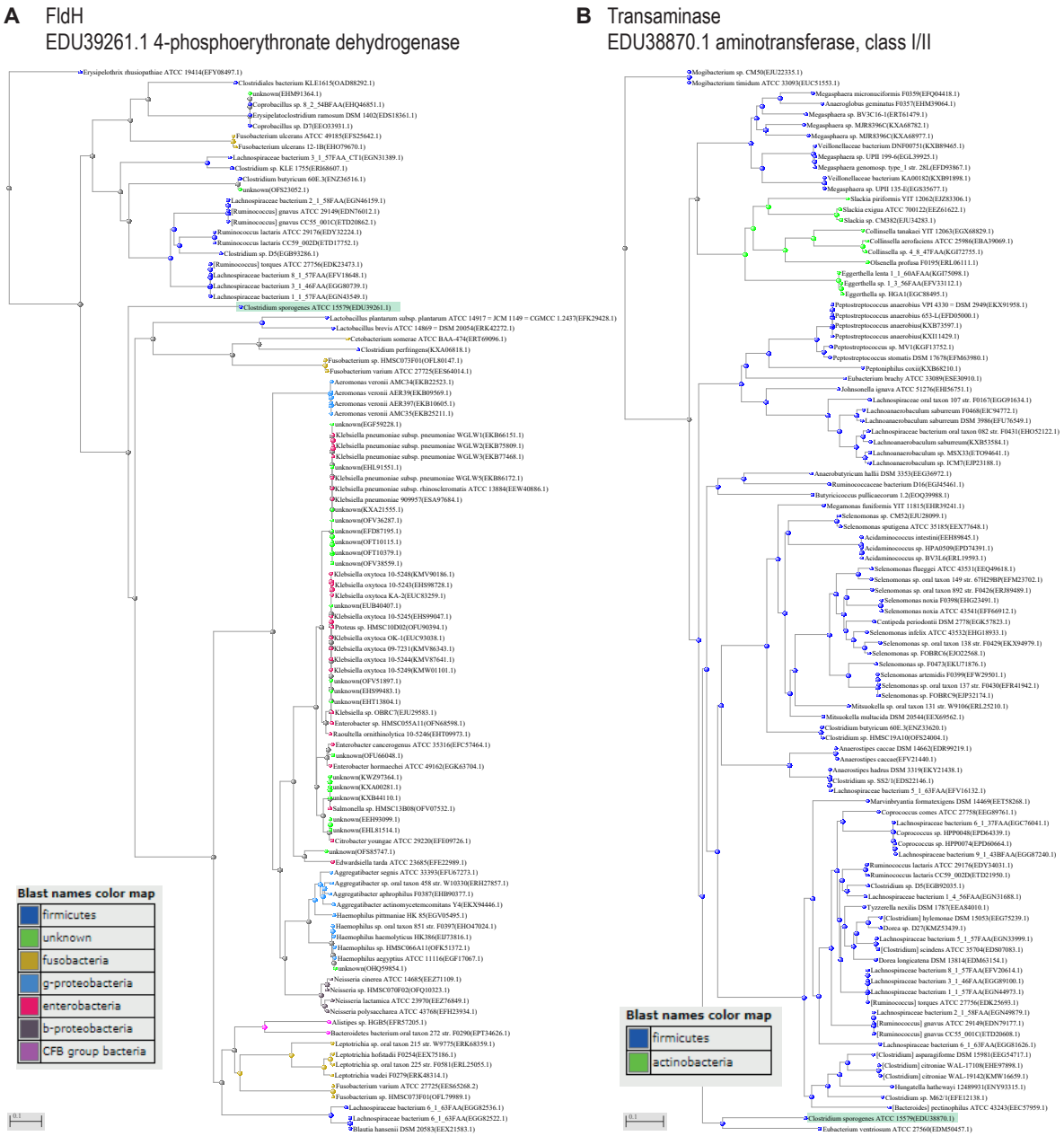

Figure S5 | Phylogenetic tree of *C. sporogenes* FldH and EDU38870. Proteins were BLASTed against the protein sequences from the NIH Human Microbiome Project (HMP) Road map project (PRJNA43021). The top 100 BLASTp hits were aligned in the Constraint-based Multiple Alignment Tool (COBALT) and converted to a distance tree using NCBI TreeView (Parameters: Fast Minimum Evolution; Max Seq Difference, 0.85; Distance, Grishin). In (**A** and **B**) a phylogenetic tree of the top 100 BLASTp hits are depicted for FldH and EDU38870 with *C. sporogenes* indicated by the green bar.

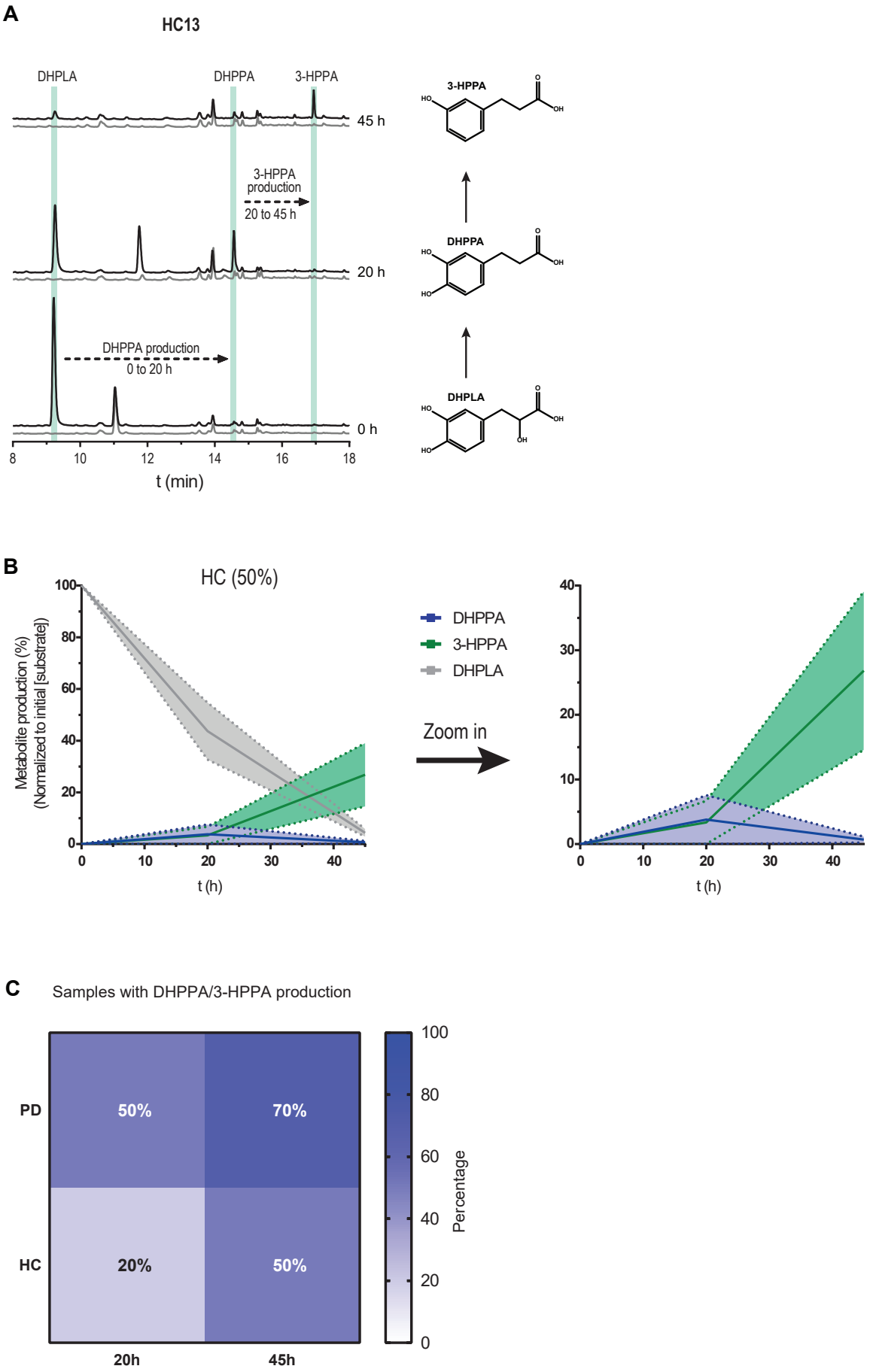

Figure S6 | Fecal-incubations from healthy age-matched controls. (See legend on next page.)

(See figure on previous page.)
Figure S6 | Fecal-incubations from healthy age-matched controls. (**A**) A representative HPLC-ED chromatogram of fecal-suspension from HC13 where DHPPA is produced from DHPLA (black) after 20 h and is further metabolized to 3-HPPA after 45 h of incubation. The control, without the addition of DHPLA is indicated in grey. Green bars indicate the retention time of the standards indicated. (**B**) Metabolite profiles of the HC fecal suspensions that produced DHPPA or 3-HPPA within 20-45h (50%) are merged as replicates. Lines represent the mean and the shadings the SEM, a zoom in graph of DHPPA and 3-HPPA is depicted on the right. (**C**) DHPPA or 3-HPPA was quantified as measure for active deamination pathway in the fecal-suspensions. DHPPA or 3-HPPA is produced in 50% and 70% of the PD patient's fecal-suspensions and in 20% and 50% of the HC's fecal-suspensions in 20 and 45 h respectively.

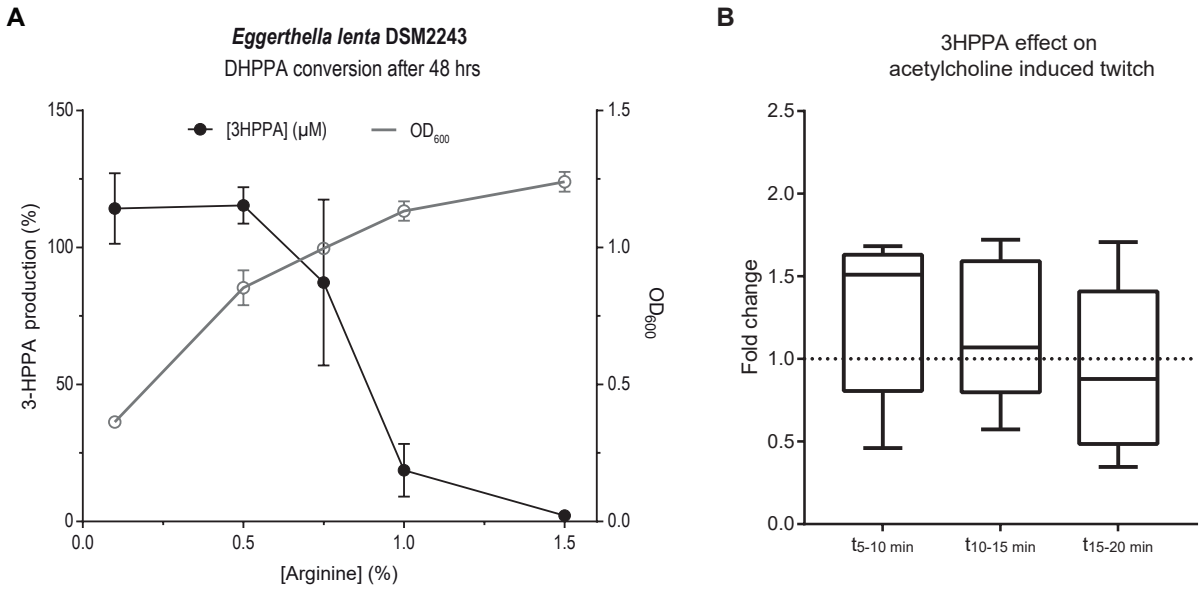

Figure S7 | 3-HPPA is produced by *E. lenta* (**A**) *Eggerthella lenta* has been shown to be able to perform *p*-dehydroxylation of the catecholic B-ring from (+)-catechin and (-)-epicatechin [35] (Jin and Hattori, 2012), a moiety resembling DHPPA. To test whether *E. lenta* could produce 3-HPPA from the dehydroxylation of DHPPA, *E. lenta* DSM 2243 was grown at various concentrations of arginine, which was previously shown to improve growth densities [36] (Haiser et al., 2013). The dehydroxylation of DHPPA to 3-HPPA by *Eggerthella lenta* DSM2243, which is dependent on the arginine concentration in the medium, is shown. The left y-axis indicates 3-HPPA production normalized to initial substrate (DHPPA) concentration. The right y-axis indicates the optical density (OD) at 600 nm. The x-axis indicates the increasing arginine concentration supplied to the medium before 48 h of incubation with 50 µM of DHPPA. At low arginine concentrations, *E. lenta* DSM2243 was capable of dehydroxylation of DHPPA to 3-HPPA, which was inhibited at higher arginine concentrations. Graph represents 3 independent biological replicates and mean with error bars representing the SEM are depicted. (**B**) 3-HPPA has no significant effect on the acetylcholine induced twitch binned in intervals of 5 minutes (n=4 biological replicates and experiments were repeated 2 times per tissue). Significance was tested using repeated measures (RM) 1-way-ANOVA followed by a Tukey's test. Box represents the median with interquartile range and whiskers represent the maxima and minima.

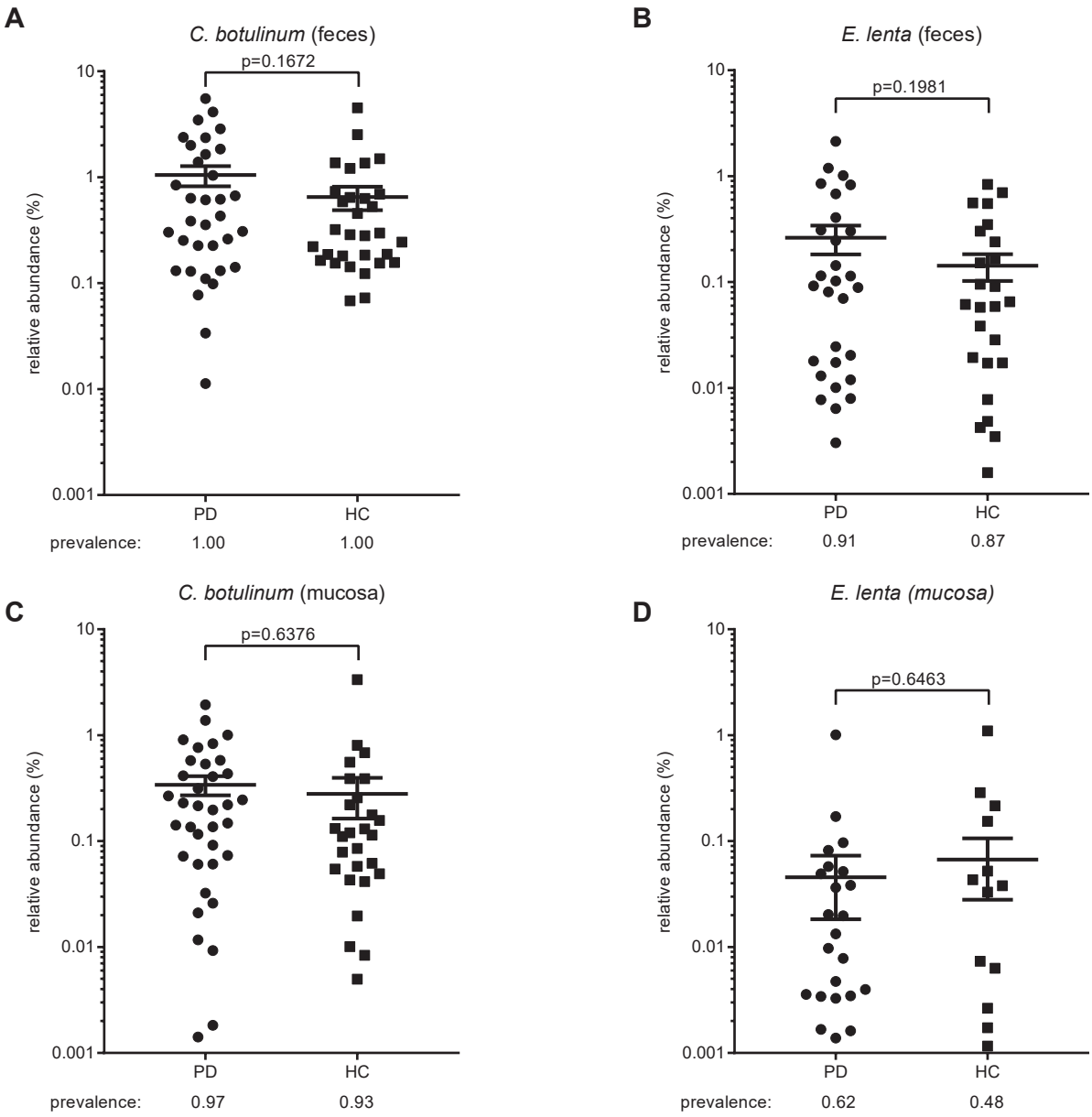

Figure S8 | Analysis of 16s rDNA metagenomics data of deaminating bacteria and *E. lenta* in PD and HC fecal and mucosal samples. (**A**) Relative abundance of *Clostridium botulinum* and (B) *Eggerthella lenta* in PD (feces, n= 34; mucosa, n= 37) and HC (feces, n= 31; mucosa, n=29) fecal samples. (**C**) Relative abundance of *Clostridium botulinum* and (**D**) *Eggerthella lenta* in sigmoid colon mucosa samples from .The cross-header represents the mean and the SEM. (**E**) Linear regression analysis of DHPPA/3HPPA production in PD (n= 9) and HC (n=4) fecal sample incubations at 20 h versus the relative abundance of *C. botulinum* in those samples.

Table S1 | Values and statistical results corresponding to Figure 2B

	WT			ΩfldC			ΩCLOSPO_01732		
	0 h	24 h	48 h	0 h	24 h	48 h	0 h	24 h	48 h
Phenylalanine	100.0 ± 17.7	n.d.	n.d.	100.0 ± 15.9	n.d.	n.d.	100.0 ± 4.6	n.d.	n.d.
PLA	n.d.	n.d.	n.d.	n.d.	84.7 ± 13.2*	48.4 ± 9.1*	n.d.	n.d.	n.d.
PPA	n.d.	77.6 ± 3.3	85.6 ± 0.7	n.d.	1.5 ± 0.3****	30.7 ± 4.1***	n.d.	64.9 ± 3.8#	71.6 ± 3.1*
Tyrosine	100.0 ± 23.0	0.4 ± 0.2	1.7 ± 1.0	100.0 ± 16.8	25.1 ± 12#	4 ± 0.7	100.0 ± 18.1	110.9 ± 15.9*	109.3 ± 18.2*
4-HPLA	n.d.	n.d.	n.d.	3.2 ± 0.7*	106.9 ± 15.3*	113.4 ± 15.0**	n.d.	n.d.	n.d.
4-HPPA	1.5 ± 0.3	43.7 ± 5.0	45.6 ± 4.9	n.d.*	n.d.**	2.3 ± 1.1**	n.d.*	9.2 ± 0.6*	10.2 ± 0.4**
Tryptophan	100.0 ± 21.4	19.6 ± 10.0	5.4 ± 4.1	100.0 ± 20.3	47.3 ± 15.3	28.3 ± 9.3#	100.0 ± 16.6	70.7 ± 17.5#	50.9 ± 13.6*
Tryptamine	n.d.	6.7 ± 2.3	7.0 ± 1.9	n.d.	9.6 ± 2.4	23.5 ± 2.6*	n.d.	27.8 ± 1.2**	40.8 ± 4.4**
ILA	n.d.	n.d.	n.d.	n.d.	27.2 ± 1.9***	27.0 ± 2.9**	n.d.	n.d.	n.d.
IPA	0.6 ± 0.2	21.7 ± 1.3	22.2 ± 1.8	n.d.*	n.d.****	n.d.**	n.d.*	0.6 ± 0.03****	0.8 ± 0.1**
Levodopa	100.0 ± 36.4	1.0 ± 0.5	0.9 ± 0.4	100.0 ± 32.7	3.4 ± 1.1#	2.9 ± 0.9#	100.0 ± 23.1	67.5 ± 10.4*	50.3 ± 8.5*
DHPLA	n.d.	n.d.	n.d.	n.d.	172.1 ± 45.2*	158.6 ± 38.8*	n.d.	n.d.	n.d.
DHPPA	n.d.	89.2 ± 24.1	84.4 ± 23.1	n.d.	n.d.*	n.d.*	n.d.	2.1 ± 0.1*	2.6 ± 0.6*
5-HTP	100.0 ± 16.2	86.7 ± 12.6	72.1 ± 12.0	100.0 ± 17.1	96.4 ± 13	88.3 ± 14.2	100.0 ± 15.4	79.7 ± 30.9	91.0 ± 14.8
Serotonin	0.04 ± 0.04	0.21 ± 0.03	0.47 ± 0.07	0.04 ± 0.04	0.15 ± 0.05	0.7 ± 0.11	0.06 ± 0.03	0.23 ± 0.06	1.07 ± 0.12*
5-HILA	n.d.	6.6 ± 0.4	12.1 ± 0.5	n.d.	n.d.***	n.d.****	n.d.	n.d.***	n.d.****
"5-HIPA"	n.d.	1.3 ± 0.3	5.2 ± 1.3	n.d.	n.d.*	n.d.*	n.d.	n.d.*	n.d.*

n.d., not detected; Deamination products are normalized to their initial substrate concentrations (100%). ± values indicate SEM (n=3). Significance was tested between WT and ΩfldC or ΩCLOSPO_01732 using a Two-sample equal variance (homoscedastic) Student's t-Test (Microsoft Excel 2019 version 1808). *=p<0.05, **=p<0.0021, ***=p<0.0002, ****=p<0.0001, #=p<0.1234 (not significant).
PLA, 3-phenyllactic acid; PPA, 3-phenylpropionic acid; 4-HPLA, 3-(4-hydroxyphenyl)lactic acid; 4-HPPA, 3-(4-hydroxyphenyl)propionic acid; ILA, 3-indolelactic acid; IPA, 3-indolepropionic acid; DHLA 3-(3,4-dihydroxyphenyl)lactic acid; DHPPA, 3-(3,4-dihydroxyphenyl)propionic acid; 5-HTP, 5-hydroxytryptophan; 5-HILA, 5-hydroxyindole-3-lactic acid; 5-HIPA, 5-hydroxyindole-3-propionic acid;

Table S2 | MS confirms that DHPPA is extracted from PD and HC samples using alumina extraction method.

Sample	M-H	ppm error	DHPPA quantification alumina extraction (µM)
DHPPA	181.0507	5.1	
P1	181.0509	7.5	118.2
P2	181.0504	4.7	4.9
P3	181.0504	4.7	1.6
P4	181.0505	5.3	3.8
P5	181.0503	4.2	2.3
P6	181.0509	7.3	154.3
P7	ND		1.4
P8	181.0506	5.8	8.2
P9	181.0505	5.3	11.1
P10	181.0504	4.7	2.4
HC11	181.0506	5.8	2.0
HC12	181.0504	4.7	1.4
HC13	ND		0.5
HC14	181.0506	5.8	1.0
HC15	ND		0.2
HC16	ND		3.5
HC17	181.508	6.9	1.4
HC18	ND		0.5
HC19	181.0507	5.1	4.5
HC20	181.0509	7.3	123.5

Table S3 | Plasmids and primers used in this study

Plasmid	Description	Reference
pET15b	His-Tag, amp^R	Novagen
pET28b	His-Tag, kan^R	Novagen
pSK023	pET15b-EDU36436	This study
pSK024	pET15b- EDU36793	This study
pSK025	pET15b-EDU36848	This study
pSK026	pET15b-EDU37030	This study
pSK027	pET28b-EDU37032	This study
pSK028	pET15b-EDU37374	This study
pSK029	pET15b-EDU38761	This study
pSK030	pET15b-EDU38870	This study
pSK031	pET15b-EDU39385	This study

Accession	Locus Tag	Primers used for cloning (5'-3')
EDU36436	CLOSPO_02604	sk173 FW: GCTACGCATATGAAGTTATCTAAAAAAGCAGTAG sk174 RV: ATTATTCTCGAGCTTTCTAACATTTTATCCACCTC
EDU36793	CLOSPO_02962	sk177 FW: GCGCGCCATATGAAAAATAAATTTTTAGCCTATAAG sk178 RV: AATAATCTCGAGCCTCTGAAGCCAAGAAATCTG
EDU36848	CLOSPO_03017	sk179 FW: CGCGCGCATATGAAATATGATTTTGATGAAATC sk180 RV: AATAATCTCGAGGCATTTCATAAAAACCCTAGC
EDU37030	CLOSPO_03199	sk181 FW: GGCCGCCATATGAAATTTTCAAAAAGAATATCTGACAT sk182 RV: ACGTACCTCGAGGGGTAAGTTCTGAAAATAAAGTA
EDU37032	CLOSPO_03201	sk215 FW: CGCGCGCTAGCGTGTTATTTAATGACAAATTAAGAC sk217 RV: GCGCGCCTCGAGTTTATAATATTTATCTA-AAACTTTACCTAATC
EDU37374	CLOSPO_03543	sk185 FW: GCGCGCCATATGAAGTATAATTTTGACAAAGTAG sk186 RV: GTACACCTCGAGTCCCTCCCATAATTTCAC
EDU38761	CLOSPO_01623	sk191 FW: GCAAGCCATATGTTGTTTAAAAAAGGTGGTATTTAT sk192 RV: AAGAATCTCGAGCTTCACTTTAAAGGGAATTTTC
EDU38870	CLOSPO_01732	sk193 FW: GCCGGCCATATGATTTCAAATGAAATGCTTAATC sk194 RV: AGTATACTCGAGCAGTTAATTAGCGGTTGTCC
EDU39385	CLOSPO_00463	sk197 FW: GCGCATCATATGGATTATATGAAAACTCAAGAAG sk198 RV: AGTAATCTCGAGTCTCAACCTTTAAAGAATGTTAAG

*restrictions sites are underlined

Back to table of contents

CHAPTER 4

Parkinson's Disease Medication Alters Rat Small Intestinal Motility and Microbiota Composition

Sebastiaan P. van Kessel[1], Amber Bullock[1], Gertjan van Dijk[2], and Sahar El Aidy[1*]

Unpublished
bioRxiv 2021
DOI: 10.1101/2021.07.19.452878

[1]Host-Microbe Interactions, Groningen Biomolecular Sciences and Biotechnology Institute (GBB), University of Groningen, Nijenborgh 7, 9747 AG Groningen, The Netherlands.
[2]Department of Behavioral Neuroscience, Groningen Institute for Evolutionary Life Sciences (GELIFES), University of Groningen, Nijenborgh 7, 9747 AG Groningen, The Netherlands.

*Correspondence: Sahar El Aidy, sahar.elaidy@rug.nl

Parkinson's Disease Medication Alters Rat Small Intestinal Motility and Microbiota Composition

Sebastiaan P. van Kessel, Amber Bullock, Gertjan van Dijk, and Sahar El Aidy

ABSTRACT Parkinson's disease has been associated with altered gastrointestinal function and microbiota composition. Altered gastrointestinal function is key in the development of small intestinal bacterial overgrowth, which is a comorbidity often observed in PD patients. Although, PD medication could be an important confounder in the reported alterations, relatively few studies investigated its effect on the microbiota composition or the gastrointestinal function at the site of drug absorption. To this end, wild-type Groningen rats were employed and treated with dopamine, pramipexole (in combination with levodopa/carbidopa), or ropinirole (in combination with levodopa/carbidopa) for 14 sequential days. Dopamine agonists in combination with levodopa/carbidopa showed a significant reduction in the small intestinal motility and an increase in bacterial overgrowth in the ileum. Furthermore, significant alterations in microbial taxa were observed between the treated and vehicle groups, analogous to the changes reported in human PD vs HC microbiota studies, including; an increase in *Lactobacillus* and *Bifidobacterium,* and decrease in *Lachnospiraceae* and *Prevotellaceae*. Overall, the results highlight the importance of PD medication in microbiota research and comorbidities, including gastrointestinal dysfunction and small intestinal bacterial overgrowth , both of which are strongly associated with PD.

Unpublished
bioRxiv 2021
DOI: 10.1101/2021.07.19.452878

INTRODUCTION

The microbiome composition of Parkinson's disease (PD) patients subjects have been studied in many, mainly cross-sectional, studies in the past couple years, in comparison to compared to matching-healthy control (HC) [1,2,11–16,3–10]. However, there is low consensus among the findings in these reports. Recently, the sequencing data from most of these studies have been pooled and re-analyzed in order to identify common alterations in the gut microbiota of PD patients [17]. Romano *et al.* concluded that it was impossible to determine whether the microbial associations were causally linked to PD in the pooled data analysis due to confounding factors such as PD medication, which was considerably variable among studies [17]. Indeed PD medication is a major differentiating factor between PD patients and HC subjects and only a few studies [1,3,6,8,14] investigated or reported the effect of medication on the microbiota profiles.

Most PD medications are affecting the dopaminergic-system in the brain, thus intrinsically influence peripheral dopaminergic systems in the enteric nervous system (ENS) [18,19] and the immune system [20,21] as well. Dopamine and/or dopamine agonists affect the gut-motility in rodents, dogs, and humans [22] and references in there [23,24,33–36,25–32]. Gut motility is inferred by Bristol-Stool Score, which is known to be major contributor to the variation in the fecal microbiota composition [37]. Many PD patients experience non-motor symptoms, including gastrointestinal (GI) dysfunction, such as constipation [38]. Small intestinal motility, also affected in PD patients [39,40], is one of the causes of small-intestinal bacterial overgrowth (SIBO) [41], which is prevalent (up to 54.5 %) and significantly higher in PD patients [42–44]. Recently PD medication has been also associated with the development of GI-symptoms [45] or GI-transit [46] in PD patients. Analogously, we showed that the unabsorbed residues of levodopa that reach the distal small intestine is converted to a bioactive molecule, which reduces ileal contractility in mice *ex vivo* [47]. Nonetheless, whether PD medication is also associated with alterations in microbiota composition, small-intestinal gut motility, and bacterial overgrowth is unknown.

In this study, we show that, in rats, commonly prescribed PD medications pramipexole and ropinirole in combination with levodopa/carbidopa have a profound effect on the small intestinal motility and microbiota composition, often found differentially altered in PD microbiota studies.

RESULTS

PD medication affects small-intestinal motility in wild-type Groningen rats

To test whether the commonly prescribed PD medication affects the small-intestinal motility, wild-type Groningen (WTG) rats were employed and were treated for 14 sequential days with dopamine (D), pramipexole (P, in combination with levodopa/carbidopa as co-prescribed for PD patients), ropinirole (R, in combination with levodopa/carbidopa), or vehicle (VH). Although dopamine is not used as a treatment for PD, it was included in the study to act as a control for the dopamine agonist groups. Moreover, PD patients usually have a higher exposure (2.5-40 fold) to dopamine than HC subjects [48–50]. On the last treatment day, animals were sacrificed 18.5±0.68 minutes after they started drinking continuously (no differences in time of sacrifice

were observed between groups: D, 18.55±0.69; P, 18.68±0.80; R, 18.4±0.67; VH, 18.28±0.47; One-way-ANOVA statistics, F=0.4977, P-value= 0.6865). The small intestine was sectioned into 7 pieces and their contents were assessed for carmine red spectrophotometrically. Carmine red detection was scored binary per segment (detection scored 1; no detection scored 0) and the geometric center, a sensitive and reliable measure of intestinal transit [51] was determined (**Figure 1A**). Pramipexole and ropinirole groups showed a significant decrease in the geometric center compared to the vehicle, indicative of a reduced small-intestinal motility (**Figure 1B**). In contrast, the dopamine-treated group did not show a significant effect on the small intestinal motility although 75% (up to the 3rd quartile) of the points were below the median of the vehicle group. These findings indicate that PD treatment seem to affect small intestinal motility, which may influence the bacterial composition and cause an increase in SIBO at the site of drug absorption.

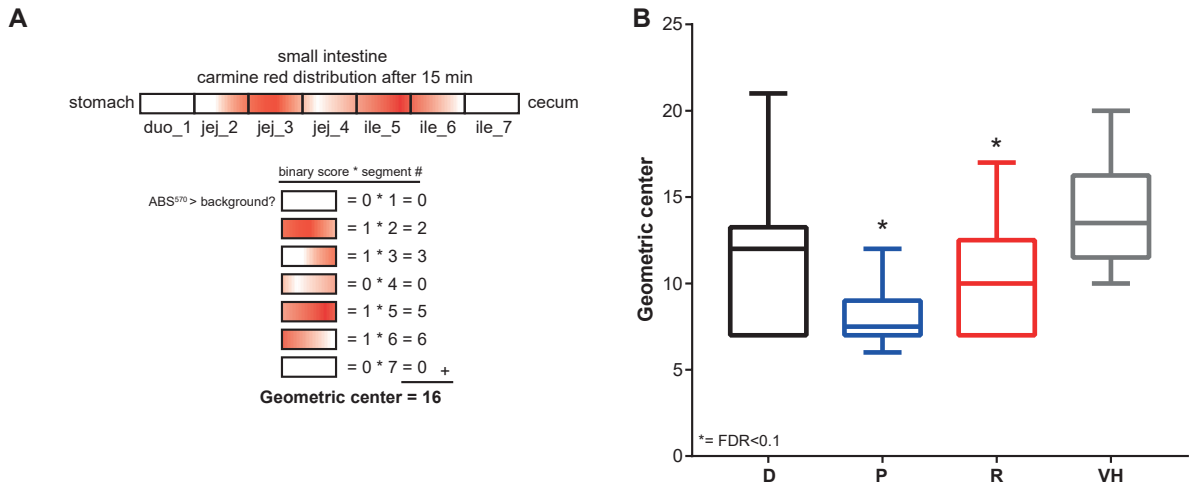

Figure 1. Small intestinal motility is affected by PD medication treatment. (**A**) A schematic representation of the small-intestine is depicted. Each rectangle represents the different sections assessed of the small intestine, where carmine red distribution in the small-intestine is depicted in red. Each segment was scored binary and multiplied by the segment number resulting in the geometric center. (**B**) the geometric center per treated group is depicted. D, dopamine; P, pramipexole; R, ropinirole; VH, vehicle (10% sucrose). Boxes represent the median with interquartile range, and whiskers represent the maxima and minima. Significance compared to VH (asterisks) was tested with One-way-ANOVA followed by Fisher's LSD test with FDR correction.

Increased bacterial counts in the ileal contents of rats treated with PD medication

Because the observed reduction in small intestinal motility is known to affect the bacterial loads [41], we determined the colony-forming units (CFU) in the jejunal and ileal content, respectively (**Figure 1A**). The content was spotted on chopped meat media plates and were incubated aerobically or anaerobically for 48 h at 37 °C before CFUs were counted. In the jejunum, no significant differences were observed between the treated and the vehicle groups (**Figure 2A-C**). In contrast, there was a significant increase of bacterial counts in the ileal content of the treated groups compared to the vehicle (**Figure 2D-F**). The ropinirole-treated animals had

significantly higher bacterial counts on both the aerobic (p = 0.024, q = 0.073) and anaerobic (p = 0.020, q = 0.061) incubated plates (**Figure 2D-E**). Subtracting the aerobic counts from the anaerobic counts, indicative of strict anaerobic counts, showed no significant difference implying that the facultative anaerobes maybe contributing to the bacterial increase observed in the ropinirole-treated group (**Figure 2F**). In the pramipexole-treated animals, a borderline not significant (p = 0.054, q = 0.080) increase was observed on the anaerobically incubated plates (**Figure 2E**). Similarly, the strict anaerobic counts showed a borderline not significant increase in bacterial counts (p = 0.046, q = 0.138) (**Figure 2F**), indicating that strict anaerobes in the pramipexole-treated group may contribute to the observed bacterial higher counts. Collectively, the results imply that the reduced gut-motility caused by PD medication is plausibly the cause of the observed increase in bacterial counts in the ileum of treated groups.

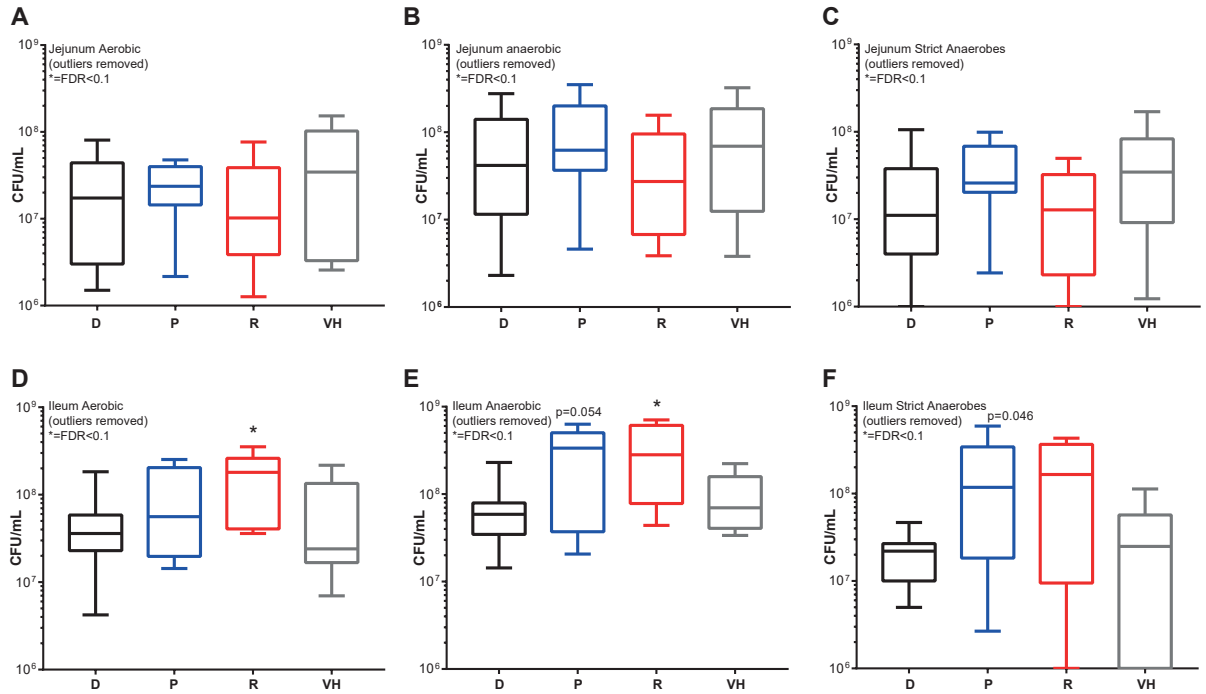

Figure 2. Significantly higher bacterial counts in the ileum of PD medication treated rats. Colony forming units (CFUs) were counted after 48 h aerobic or anaerobic incubation of jejunal and ileal content. (**A-C**) the jejunal and (**D-F**) ileal CFU/mL are depicted. (**A,D**), (**B,E**), and (**C,F**) depicts the aerobic, anaerobic and strict anaerobic (anaerobic-aerobic counts) CFU/mL, respectively. D, dopamine; P, pramipexole; R, ropinirole; VH, vehicle (10% sucrose). Boxes represent the median with interquartile range, and whiskers represent the maxima and minima. Extreme outliers were removed using the ROUT method (Q=0.1%). Significance compared to VH (asterisks) was tested with One-way-ANOVA followed by Fisher's LSD test with FDR correction.

PD medication affects the microbiota composition potentially through gut motility alterations

Next, we investigated whether the PD medication resulted in altered small intestinal microbiota composition directly or indirectly through the altered gut motility. To this end, we performed amplicon metagenomic sequencing on the V3-V4 regions of the bacterial 16s genes. Interestingly, the richness in the jejunum, but not in the ileum, was significantly different in the pramipexole-

and ropinirole-treated groups compared to the vehicle (**Figure 3A-B**). The Shannon's and Simpson's diversity indices showed marginal changes in the jejunum between the treated and vehicle groups (**Figure 3C**). In ileum the Simpson's index, but not inverse Simpson's index, was significantly higher in the ropinirole-treated group compared to the vehicle (**Figure 3D**). The data highlight an increase in the species richness only in the jejunum upon treatment with DA agonists, while the diversity did not change along the small intestine.

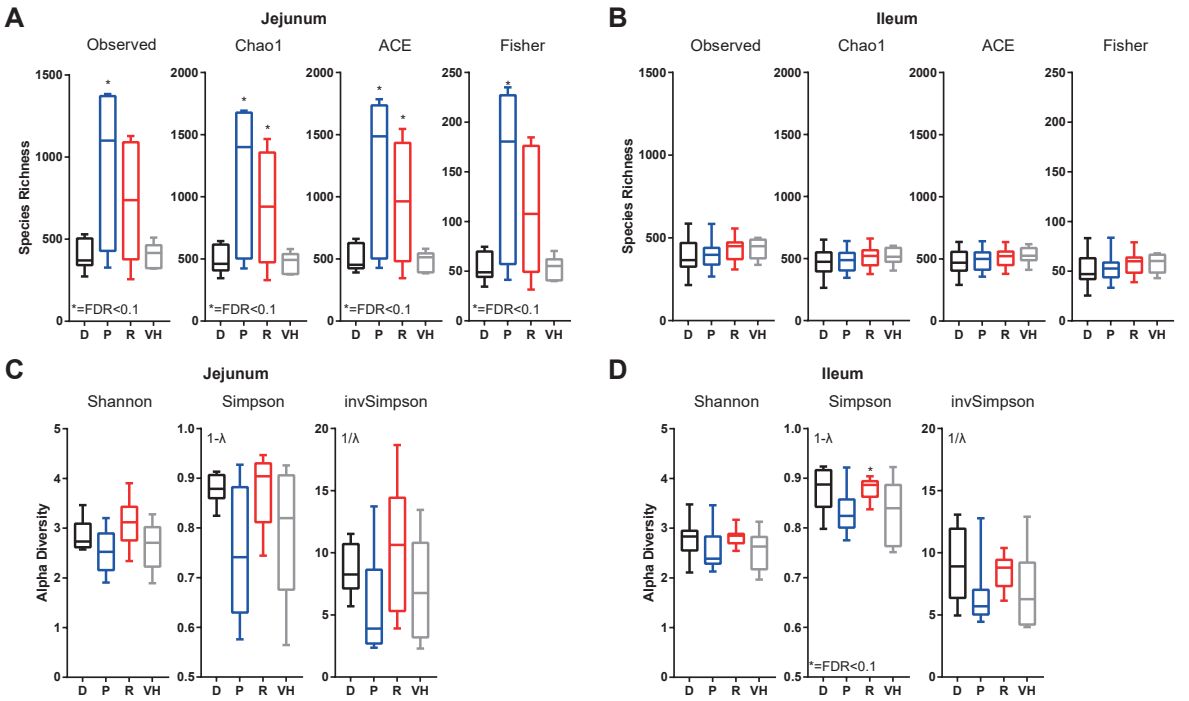

Figure 3. Species richness is significantly increased in the PD medication treated groups. (**A,B**) represent the species richness (Observed, Chao1, ACE and Fisher) of the jejunum (**A**) and ileum (**B**). (**C,D**) represent the alpha diversity (Shannon and Simpson) of the jejunum (**C**) and ileum (**D**). D, dopamine; P, pramipexole; R, ropinirole; VH , vehicle (10% sucrose). Boxes represent the median with interquartile range, and whiskers represent the maxima and minima. Significance compared to VH (asterisks) was tested with One-way-ANOVA followed by Fisher's LSD test with FDR correction.

To determine whether the jejunal and ileal microbiota compositions are distinct from each other, ß-diversity analyses using Principal Coordinate analysis (PCoA) with UniFrac distance was performed. The analysis revealed a significant difference within each treated group in both jejunal and ileal microbiota composition, respectively (**Supplementary Figure 1A-D**). The outcome indicates that there is a difference in the microbial composition between the tested small-intestinal locations independent of the treatment.

Because of the natural difference in microbiota composition of the jejunum and ileum, we separated the analysis based on location. The analysis showed that the treatment had a significant effect on the microbiota composition in both jejunum (R^2= 0.223, p= 0.001) and ileum (R^2= 0.197, p= 0.002) (**Figure 4A-B**). Because the gut motility was significantly affected in the dopamine agonist-treated groups (**Figure 1B**), the geometric center was also tested for its contribution. Indeed, the changes in geometric center contributed significantly in jejunum and ileum (R^2= 0.1, p=0.020 and R^2= 0.06, p=0.042 respectively) (**Figure 4A-B**).

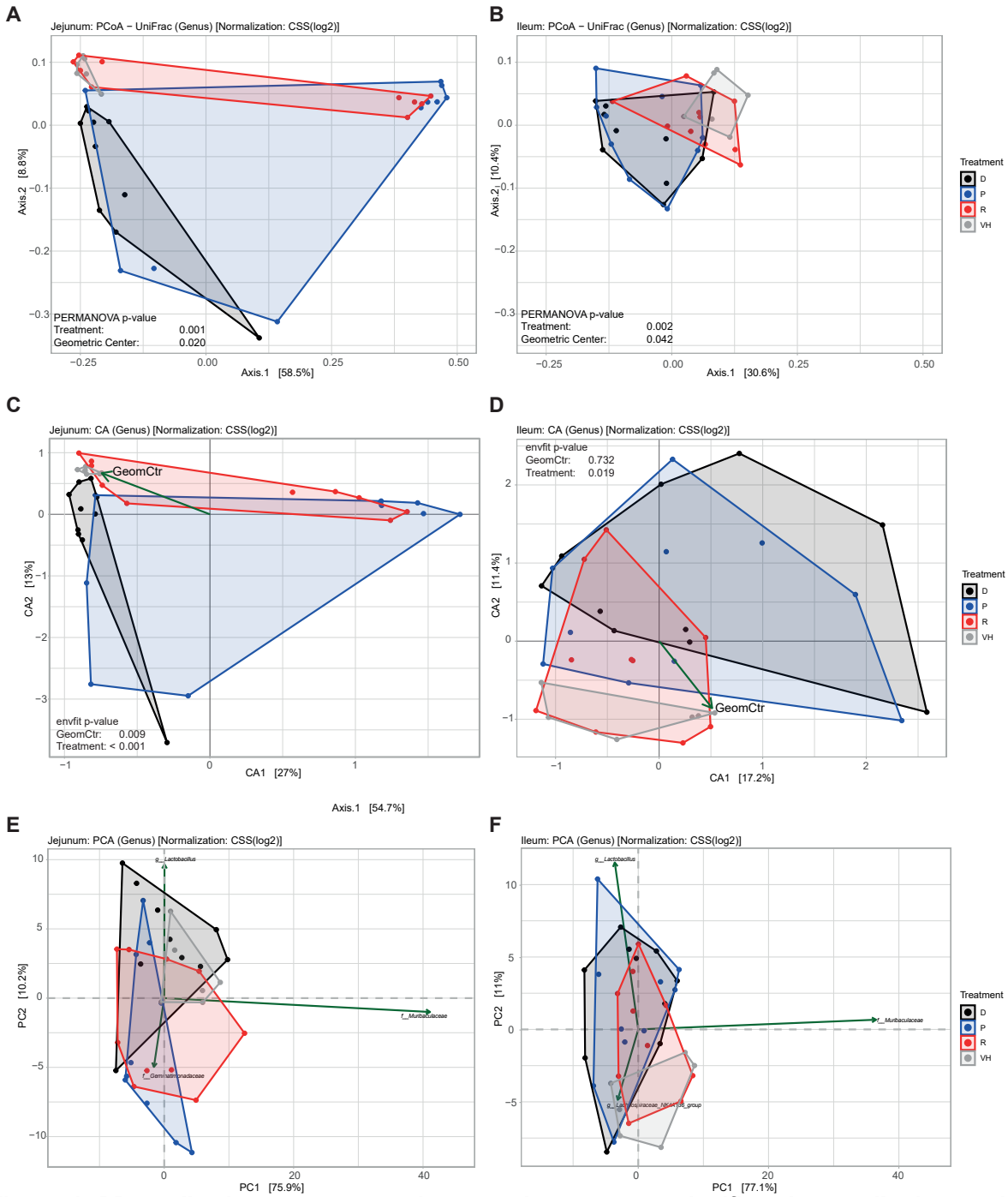

Figure 4. PD medication treatment and geometric center are significantly contributing to the variation in the microbiota composition. (**A,B**) depict a Principal Coordinate Analysis (PCoA) using unweighted UniFrac distances at genus level using CSS scaled data of jejunum (**A**) and Ileum (**B**). (**C,D**) depict a Correspondence Analysis (CA) at genus level using CSS scaled data of jejunum (**C**) and Ileum (**D**) with arrows indicating the direction of the geometric center towards the vehicle group. (**E,F**) depict a Principal Component Analysis (PCA) at genus level using CSS scaled data of jejunum (**E**) and Ileum (**F**). Arrows represent the top 3 contributing genera to the variation of PC1 and PC2. D, dopamine; P, pramipexole; R, ropinirole; VH, vehicle (10% sucrose). Significant contribution of the variables to the variance of the PCoA was tested with Permutational Multivariate ANOVA (PERMANOVA) and the significant contribution of the environmental vectors was tested with permutational test from *envfit* function from R package *vegan*.

Additionally, correspondence analysis (CA), another ordination technique used in exploring microbial ecology, was performed and fitted with the treatment and geometric center as dependent variables (**Figure 4C-D**). For both jejunum and ileum, treatment was a significant factor (envfit $R^2 = 0.341$, p-value = <0.001 and $R^2 = 0.196$, p = 0.019 respectively). Importantly, the changes in gut motility measured by geometric center were strongly associated with the direction of the vehicle (envfit p-value = 0.009, $R^2 = 0.263$ **Figure 4C**), indicative of the faster gut transit observed in the vehicle group. The results imply that, especially in the jejunum, the reduced gut-motility is associated with the altered microbiota composition, both of which are caused by PD medication.

Combining both the locations and treatments showed that dopamine-, pramipexole-, and 50% of the ropinirole-treated groups cluster distant from ileum and vehicle, while the other half of the ropinirole-treated animals cluster similar to vehicle and ileum (**Supplementary Figure 1E**). Both jejunal and ileal samples from vehicle cluster closer together (PERMANOVA for location: $R^2 = 0.199$, p = 0.01 VH vs mean $R^2 = 0.294$, p=0.001 in treatment groups). Overall the results indicate that the PD medication and dopamine treatments have the strongest effect on the jejunal microbial composition, which may be due to the changes in gut motility described above.

Using PCA (Principal Component Analysis), to identify taxa that associated most to the variation of the microbiota profiles, *Muribaculaceae* showed the strongest association with PC1 (explaining 75.9% and 77.1% of the variation in jejunum and ileum, respectively), and that *Lactobacillus* had the strongest association with PC2 (explaining 10.2% and 11.0% of the variation in jejunum and ileum, respectively) (**Figure 4E-F**). In ileum, *Lactobacillus* is associated with the same axis (PC2) that separates the treated groups from the vehicle group (**Figure 4F**).

Differential abundance analyses identify important taxa often reported to be altered in PD patients

The ordination analyses revealed the PD treatments to have a profound effect on the microbiota composition. To identify which bacterial taxa are significantly affected by the treatment, we continued with differential abundance analysis. Focusing on the top 10 most abundant taxa in in all groups, *Muribaculaceae spp* (previously known as S24-7, most often isolated from *Murinae* species but are also found in humans [52]) and *Lactobacillus spp* appeared to be the most prominent members in both jejunum and ileum (**Figure 5A-B**). From the top 10 taxa in jejunum, only *Romboutsia spp.* were significantly decreased (Dunnett's test p= 0.022) in the pramipexole-treated group compared to the vehicle (**Figure 5A**). In ileum, *Lachnospiraceae spp.* were decreased in both dopamine- and pramipexole-treated groups (Dunnett's test p=0.033 and 0.034 respectively), while *Enterorhabdus spp.* were decreased in the dopamine-treated group, and *Allobaculum spp.* increased in the pramipexole-treated group (Dunnett's test p=0.011, and 0.002 respectively), compared to vehicle (**Figure 5B**). Remarkably, in the

dopamine-, pramipexole- and ropinirole-treated groups, *Lactobacillus spp*. in the ileum was significantly increased compared to the vehicle group (Dunnett's test p=0.001, 0.003 and, 0.047, respectively) (**Figure 5B**), which is in agreement with the observation that *Lactobacillus* is associated with PC2, which separates the treatment groups from the vehicle group (**Figure 4F**).

Next, we used LEfSe (Linear discriminant analysis Effect Size) [53] and the zero-inflated log-normal model form the metagenomeSeq R-package [54] for differential abundance analysis on OTU level. From the LEfSe analyses, (**Figure 5C-H**) the main discriminant feature separating the vehicle from the other treatment groups are species from the *Muribaculaceae* family in both jejunum and ileum. The main discriminant feature separating the treatment groups from the vehicle group are species from the *Lactobacillus* genus, agreeing with the results observed in **Figure 4F and 5B**. From the metagenomeSeq analyses (**Figure 5J-N**) almost no significant differential abundant taxa were observed in the ropinirole group. As with the LEfSe analysis, species from the *Muribaculaceae* family are decreased in jejunum and ileum. *Lactobacillus* in the ileum is increased only in the dopamine-treated group. Focusing further on the shared differential taxa from the LEfSe and metagenomeSeq analyses (**Figure 5C-N**), species from the *Prevotellaceae*, *Lachnospiraceae* and *Muribaculaceae* family in jejunum or ileum were decreased in almost all treated groups compared to the vehicle group. Species from the *Lactobacillus* genus seemed to be increased especially in the LEfSe analysis but also in the metagenomeSeq analysis (in ileum of the dopamine-treated group and in the jejunum of the pramipexole-treated group (**Supplementary Table 1**)). Other increased differential taxa are *Bifidobacterium* in the ileum of the pramipexole-treated group and *Enterococcus* in the jejunum of the dopamine-treated group.

The increase in *Enterococcus* and *Lactobacillus* might be relevant for the levodopa decarboxylation activity in the jejunum, as species from these genera have been shown to decarboxylate levodopa and could restrict the available levels in the blood [55]. We tested the decarboxylation activity of levodopa (LDC) in the jejunal and ileal samples and the levodopa uptake. However no significant difference was observed between the tested groups (**Supplementary Figure 2A-C**), Interestingly, spearman correlation analyses between the top 50 most abundant OTUs in the jejunum and levels of the levodopa/carbidopa in the plasma showed negative correlations between OTUs from the *Lactobacillus* genus only, and the levodopa/carbidopa plasma levels (**Supplementary Figure 2D**). However, after FDR correction, only one OTU remained significant and no positive correlations were observed between the LDC activity in the jejunum and these *Lactobacillus* OTUs (**Supplementary Figure 2E**).

Overall, these findings are highly relevant as *Prevotellaceae* and *Lachnospiraceae* taxa are often reported to be decreased, while *Lactobacillus* and *Bifidobacterium* taxa are often reported to be increased, between PD patients and HC subjects.

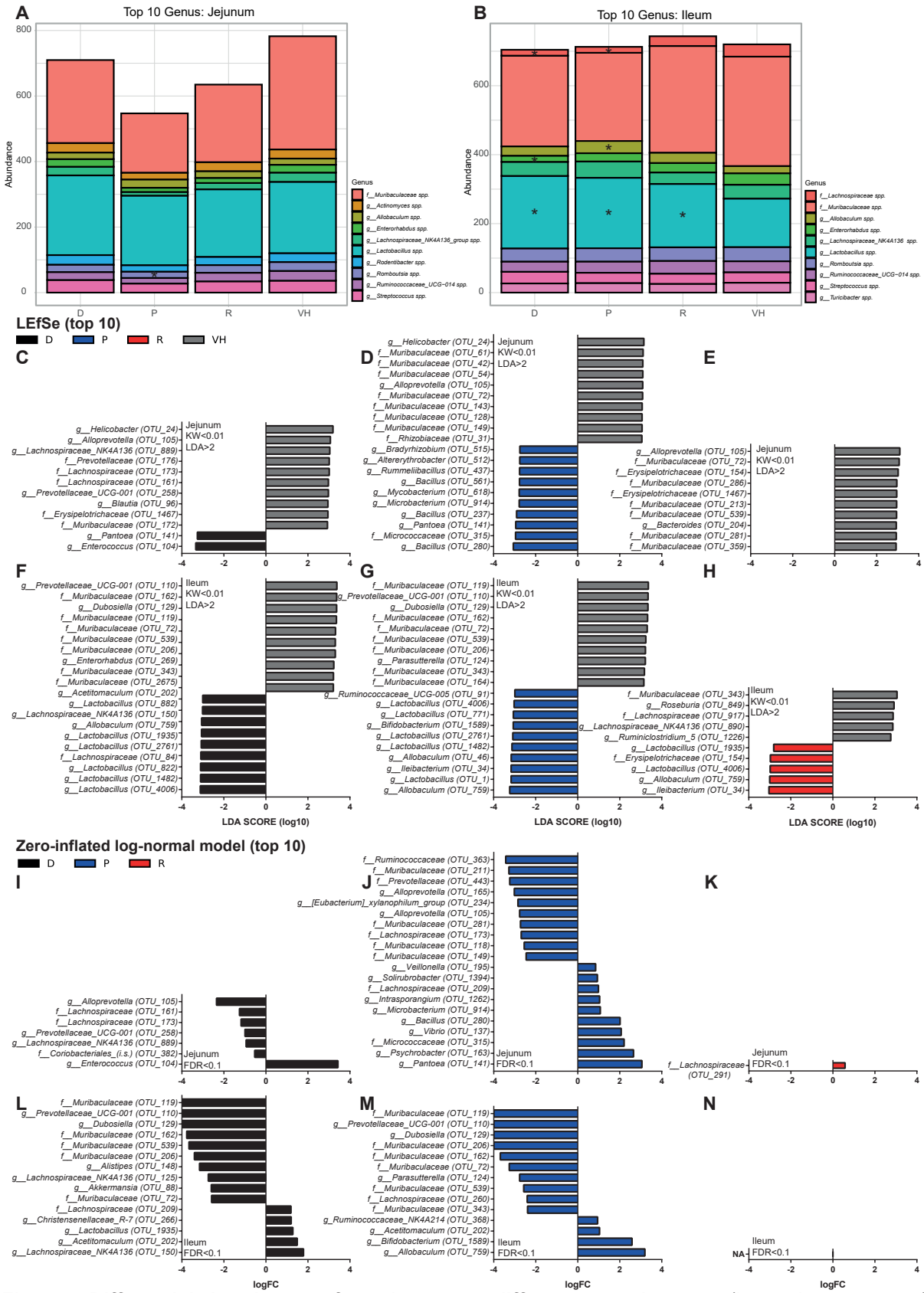

Figure 5. Differential abundances of species among different treated groups. (Legend on next page)

(Figure on previous page)

Figure 5. Differential abundances of species among different treated groups. (**A**,**B**) represent a stacked bar plot with mean genus levels using CSS scaled data from the top 10 taxa are from jejunum (**A**) and ileum (**B**). The asterisks indicate statistical significance compared to VH group tested using one-way-ANOVA followed with Dunnett's test. (**C-H**) represent LEfSe analysis (top 10) of the different treated groups of jejunum (**C-E**) and ileum (**F-H**). Significance was tested using one-way-ANOVA followed by a Kruskal-Wallis (KW) test and Linear Discriminant Analysis (LDA). A significant feature was considered when KW p-value<0.01 and Log(LDA score)>2. (**I-N**) represent differential abundance analysis (top 10) using the zero-inflated log-normal model from the *metagenomeSeq* R package of the different treatment groups of jejunum (**I-K**) and ileum (**L-N**). A significant feature was considered when FDR<0.1. D, dopamine; P, pramipexole; R, ropinirole; VH, vehicle (10% sucrose). For all the significant extracted features see **Supplementary Table 1**.

DISCUSSION

This study unraveled the effect of PD medications, pramipexole or ropinirole in combination with levodopa/carbidopa on the small-intestinal motility and the associated alteration in the bacterial counts, in the ileum (**Figures 1, 2**). Small intestinal motility is one of the factors influencing small-intestinal bacterial overgrowth [41], and is prevalent in PD patients [42–44]. PD medication has been shown to be associated with GI symptoms [45] and reduced transit times [46]. Here, we showed that the PD medication, besides its effect on gut motility, affect the microbial profile (**Figure 3, 4**). Dopamine, which is not used as PD treatment, as it cannot pass the blood-brain barrier, but can still be produced from levodopa endogenously, by the human dopa decarboxylase (DDC) or exogenously via bacterial tyrosine decarboxylases (TDC) in the periphery [55] also affected the microbiota profile (**Figure 4-5**). In fact PD patients have 2.5-40 times higher levels of (sulfonated) dopamine levels in their blood compared to HC or drug naïve PD patients [48–50]. Despite the substantial number of reports describing an effect of dopamine on gut motility [23,24,33–36,25–32], dopamine did not exert a significant effect on the gut-motility our study (**Figure 1**). This could be due to the metabolism during the absorption process. For example, the first-pass metabolism of dopamine is predominant in the intestine of dogs and its oral bioavailability was only approximately 3% with a half-life of 10.8 minutes [56]. The observation that 75% of the points in the dopamine group are below the median of the VH group (**Figure 1**) still implies that dopamine could affect gut motility, but in a less pronounced manner compared to dopamine agonists. In contrast to dopamine, pramipexole and ropinirole have a much higher bioavailability with a longer half-life compared to dopamine. Pramipexole has an oral bioavailability of ~90%, a long half-life (between 11.6-14.1 hours), minimal metabolism (70-78% excreted unchanged in urine) and is primarily eliminated renally [57]. Ropinirole has an oral bioavailability of ~50%, a shorter half-life of approximately 6 hours (ranging from 2 to 10 hours) and only 10% is excreted unchanged in urine and cleared by hepatic metabolism [58].

Importantly gut-motility contributed significantly to the variation observed in the microbiota profiles (**Figure 4 A-D**) and faster transit times (higher geometric center) associated closely to the vehicle group (**Figure 4 C-D**). Both dopamine and its agonists treated groups share similar

differentially abundant taxa (**Figure 5**), implying that dopamine, pramipexole, and ropinirole act through similar mechanisms, likely altered gut motility, consequently, differentiating the microbiota composition. These drugs could also elicit a direct effect on the microbiota, which warrants further elucidation.

Especially in the jejunum, the microbial changes were substantial (**Figure 3, Figure 4A and Supplementary Figure 1E**. The impact on the jejunal microbiota composition could be due to the rapid absorption in the proximal small intestine [56,58,59], resulting in the highest local drug concentration in the proximal small intestine.

The often-reported increase in *Lactobacillus*, *Bifidobacterium, Akkermansia*, and the decrease in *Lachnospiraceae* and *Prevotellaceae* have been reported as a common finding among the several studies investigating the fecal gut microbiota composition between PD patients and HC subjects [17]. Remarkably, for most of these altered taxa (except Akkermansia) a similar alteration was observed in the small intestine of the healthy rat model employed in this study (i.e. not PD model). This implies that the observed changes in microbiota composition in PD is, at least partly, due to the PD medications. The alterations in the small intestine could reflect those in the human fecal samples as 85.9% of the taxa are shared between small-intestine and feces and correlate significantly (Spearman's $R=0.69$, $R^2=0.48$, $p<2.2E-16$ on log transformed data, calculated from Table S3 in Li *et al.* [60]) and are ultimately washed-out through the large-intestine.

Especially, *Lactobacillus spp*. were found with the LEfSe analysis to be the discriminating factor from the vehicle in the ileum in all treatments. This is in agreement with the pooled data study of Romano *et al*. [17], where this genus was also the most strongly enriched in PD patients.

Despite the increase in *Lactobacillus* and *Enterococcus* in the jejunum, no significantly increased LDC activity or reduced levodopa uptake levels were observed per group. Remarkably, combining all samples resulted in significant negative correlations between *Lactobacillus* species and uptake of levodopa, however no positive correlations were observed between the LDC activity implying that the treatment period of 14 days was not long enough to observe significant changes, our activity measure was either to selective or that other unknown factors play a role in the association with the reduced uptake observed (**Supplementary Figure 2**).

Overall, this study showed the impact of commonly prescribed PD medications and dopamine on the small-intestinal motility, bacterial overgrowth and microbiota composition. Importantly, the microbial alterations observed in our healthy rat model (i.e. not PD model) in the small-intestine reflect the fecal microbial alterations observed in human cross-sectional studies comparing PD with HC subjects, and shows the importance of taking the PD medications in consideration in the assessments of the PD microbiota. Finally, we showed significant factors that link PD medication, altered microbiota profiles, and gut motility, which could lead to small intestinal bacterial overgrowth.

METHODS

Rat experiments

All animal procedures were approved by the Groningen University Committee of Animal experiments (approval number: AVD1050020197786) and were performed in adherence to the NIH Guide for the Care and Use of Laboratory Animals.

Thirty-six adult male WTG rats (Groningen breed, age 22 to 27 weeks) housed 2 to 4 animals/cage had ad libitum access to water and food (Altromin 1414) in a temperature (21 ± 1 °C) and humidity-controlled room (~60% relative humidity), with a 12-h light/dark cycle.

The rats were trained on drinking 10% (w/v) sucrose solution from a burette as followed. On 9-13 occasions over a period of 2-3 weeks, rats were taken from their social housing cage in the beginning (within 1 hour) of the dark-phase cycle and placed in an individual training cage (L × W × H = 25 × 25 × 40 cm), without bedding, food, or water. Ten minutes after transfer to the training cages, rats were given a drinking burette with a 2.5-mL sucrose solution (10% w/v). On 2-4 training occasions, 1.2 % carmine red (C1022, Sigma) was added to the sucrose solution. Over the course of training, all rats were trained to drink the sucrose solution avidly. After 2-3 weeks, when the training was complete, animals were designated at random to four different treatments groups, dopamine (D, n=10), pramipexole/levodopa/carbidopa (P, n=10), ropinirole/levodopa/carbidopa (R, n=10), and vehicle (VH, n=6) animals were at least from 2-3 different cages, but treated per cage because of coprophagy. Rats in the designated groups were treated for 14 consecutive days with on average 1.5 mg/kg dopamine (H8502, Sigma), 0.0625 mg/kg pramipexole (A1237, Sigma) with 7.5/1.875 mg/kg levodopa/carbidopa (D9628/C1335, Sigma), 0.15 mg/kg ropinirole (R2530, Sigma) with 7.5/1.875 mg/kg levodopa/carbidopa, or 10% sucrose (w/v) solution only (VH). Based on a person weighing 80 kg, the dosages are equivalent to 600/150 mg levodopa/carbidopa, 5 mg/day pramipexole, 12 mg/day ropinirole or 120 mg/day dopamine based on 10% from a high levodopa dose (1200 mg/day). On the last treatment day, all rats received their dose supplemented with 1.2% (w/v) carmine red to determine their small-intestinal motility, and rats for the D and VH groups received instead of their original dose on average 7.5/1.875 mg/kg levodopa/carbidopa in order to determine the potential levodopa uptake differences between treated groups. After an average of 18.5±0.68 minutes (time of heart-puncture), after the rats started drinking continuously (2-3 min for drinking), the rats were anesthetized with isoflurane and were killed. No differences in time of heart puncture were observed between groups (D, 18.55±0.69; P, 18.68±0.80; R, 18.4±0.67; VH, 18.28±0.47; One-way-ANOVA statistics, F=0.4977, P-value= 0.6865). Blood was withdrawn by heart puncture and placed in tubes pre-coated with 5 mM EDTA and stored on ice during the experiment. The collected blood samples were centrifuged at 1500× g for 10 min at 4 °C and the plasma was stored at −80 °C prior to catecholamine extraction. The small-intestine from stomach to cecum was dissected and the first 5 cm was considered as duodenum, the remaining part (jejunum and ileum) were dissected in 6 equal pieces and their luminal contents were

collected from every section by gentle pressing and were stored on ice during the experiment. Directly after, the samples were used for carmine red determination and colony forming unit (CFU) counting, as described below. After the samples were processed they were snap frozen in liquid N_2 and stored at −80 °C.

Carmine red assay

Part of the luminal content per small intestinal section was suspended in DMSO 20% (w/v) were vortexed vigorously and 80µl was distributed in a 96 well plate. Spectrum from 450-800 (10 nm/step) was measured (carmine red has 2 peaks at 530/570). Because of high background differences, the spectrum was linearized between 510 and 590 nm using a fitted line (y= a * x + b). The slope (a) and the intercept (b) were calculated using the data points from 510 and 590 nm, and the calculated value (x) for 570 nm (y) was subtracted from the measured value. Next, because the animals were not fasting before the treatment, the linearized values were scored binary, a score of 1 was given when the value was larger than the threshold of 0.003. Finally the geometric center, concluded to be the most sensitive and reliable measure of intestinal transit [51], was calculated by multiplying the binary score by the segment number (1 to 7, from end of stomach to beginning cecum).

Colony Forming Unit assay

Contents from the jejunal segments and ileal segments were mixed and suspended in GM17/17% glycerol media to preserve the bacterial viability after storing at −80 °C. The suspended jejunal and ileal contents were 10-fold serial diluted in PBS and 10 µl was spotted in triplicates on chopped meat media plates (CMM; beef extract, 10 g/L; casitone, 30 g/L; yeast extract, 5 g/L; K_2HPO_4, 5 g/L, menadione, 1 µg/mL, cysteine, 0.5 g/L; hemin 5 µg/mL, 15 g/L agar), which were incubated for 48 hours aerobically and anaerobically (1.5% H_2, 5% CO_2, balance with N_2) in a Coy Laboratory Anaerobic Chamber (neo-Lab Migge GmbH, Heidelberg, Germany) at 37 °C before colony forming units were counted.

Catecholamine extraction

Plasma samples were thawed on ice and a spatula-tip (~5mg) of activated alumina powder (199966, Sigma) was added to each well of a 96-well AcroPrep filter plate with 0.2 µM wwPTFE membrane (514-1096, VWR). A100 µL of plasma sample, 1 µM DHBA (3,4-dihydroxybenzylamine hydrobromide, 858781, Sigma) as an internal standard, and 800 µL of TE buffer (2.5% EDTA; 1.5 M Tris/HCl pH 8.6) were added sequentially to the wells. Liquid was removed using a 96-well plate vacuum manifold and the alumina were washed twice with 800 µl of H_2O. Catechols were eluted using 0.7% $HClO_4$, which was incubated for 30 min at RT. Samples were injected in a HPLC-ED system (Ultimate 3000 SD HPLC system coupled to Ultimate 3000 ECD-3000RS electrochemical detector with a glassy carbon working electrode (DC amperometry at 800 mV), Thermo Scientific). Samples were analyzed on a C18 column (Kinetex 5 µM, C18 100 Å, 250 × 4.6 mm, Phenomenex, Utrecht, The Netherlands) using a gradient of water/methanol with 0.1% formic acid (0–3 min, 99% H_2O; 3–7 min, 99–30% H_2O;

7–10 min 30–5% H_2O; 10–11 min 5% H_2O; 11–18 min, 99% H_2O). Data recording and analysis were performed using Chromeleon software (version 6.8 SR13). Potential intake differences of levodopa were corrected by using carbidopa as an internal standard.

Levodopa decarboxylation activity test

Samples stored at −80 °C in GM17/17% glycerol were thawed ice and 300 µL of 10% (w/v) jejunal or ileal suspensions were washed once with 1 mL of ice-cold PBS to remove levodopa (given during the treatment) and glycerol from the storage medium. Pellets were resuspended in 600 µL EBB (as described before [55]) supplemented with 20µg/mL kanamycin (EBB/K) resulting in a 5% (w/v) suspension. A100 µM of levodopa was added to the suspensions and samples were incubated anaerobically (1.5% H_2, 5% CO_2, balance with N2) in a Coy Laboratory Anaerobic Chamber (neo-Lab Migge GmbH, Heidelberg, Germany) at 37 °C. Samples of 100 µl were taken at 0 and 24 h and 400 µL of methanol was added. Cells and protein precipitates were removed by centrifugation at 20,000 × g for 10 min at 4 °C. Supernatant was transferred to a new tube and the methanol fraction was evaporated in a Savant speed-vacuum dryer (SPD131, Fisher Scientific, Landsmeer, The Netherlands) at 60 °C for 90 min. The aqueous fraction was reconstituted to 0.5 mL with 0.7% $HClO_4$. Samples were filtered and injected into the HPLC system described above. Dopamine and levodopa concentrations were quantified from the 24 h samples and the ratio between dopamine and levodopa was calculated to determine levodopa decarboxylation activity.

DNA isolation and Sequencing

DNA isolation was performed based on repeated beat beating (RBB) protocol described in [61,62]. Approximately 150-200 mg of jejunal or ileal content was weighted in screw-cap tubes containing ~0.5 g 0.1 mm glass/silica beads and 3 large 3 mm glass beads. Bacterial cells were lysed by adding 750 µL lysis buffer (NaCl, 500 mM; Tris-HCL at pH 8, 50 mM; EDTA, 50 mM; SDS, 4 % (w/v)) with sequential bead-beating 3 × 1 min with 1 min intervals on ice in a mini bead-beater (Biospec, Bartlesville, USA). Samples were incubated for 15 min, with regular mixing, at 95 °C, placed for 5 min on ice, and centrifuged at 20,000 × *g* for 30 min at 4 °C. Approximately 600 µL of the samples was recovered, centrifuged again for 5 min, before 550 µl was transferred to a new tube containing 200 µL, 10 M ammonium acetate and mixed. Samples were incubated for 5 min at ice before centrifugation at 20,000 × *g* for 30 min at 4 °C. Approximately 700 µl was transferred to a new tube, centrifuged again for 5 min before 650 µL of supernatant was transferred to a new tube containing 650 µL 2-propanol and mixed. Samples were incubated for 30 min at ice and centrifuged at 20,000 × *g* for 15 min at 4 °C. Pellets containing the DNA were washed twice with 800 and 500 µL 70% (v/v) ethanol by centrifugation at 20,000 × *g* for 10 min at 4 °C. The supernatant was discarded and the pellet was dried to air in a 37 °C heat block for 30 min. After drying, the pellets were dissolved in 200 µL TE buffer (1 mM, EDTA; 10 mM Tris-HCl at pH 8) by vortexing and incubating at 65 °C for 10 min. DNA extracted samples were stored at -80 before further clean up with the Genomic

DNA Clean & Concentrator (gDCC) kit (D4011, Zymo Research, BaseClear Lab Products, The Netherlands). Samples were thawed at RT and to 0.1 mg/ml RNAse A (EN0531, Thermo Scientific) was added and incubated for 15 min at 37 °C before the clean-up with the gDCC kit. Added ChiP Binding Buffer to the RNAse A treated samples (2:1), mixed, and transferred the mixture to the gDDC column, which was centrifuged at 14,000 × *g* for 30 sec at RT. DNA bound the column was washed twice at 14,000 × *g* for 60 sec at RT with wash buffer before eluted in pre-heated (65 °C) elution buffer which was incubated for 3 min on the column. DNA integrity was checked on agarose gel before samples were outsourced for 16s (region V3-V4) amplicon metagenomic sequencing by Novogene Co., Ltd..

16S rRNA gene regions V3-V4 were amplified with primers 314F (5'-CCTAYGGGRBGCASCAG-'3) and 806R (5'-GGACTACNNGGGTATCTAAT-3') with Phusion High-Fidelity PCR Master mix (New England Biolabs) and amplified products were verified using Agilent 5400 Fragment analyzer, which all passed the quality control. PCR products were equally mixed and purified with Qiagen Gel Extraction kit before libraries for paired-end 250bp Illumina sequencing were prepared with NEBNext Ultra DNA Library Prep Kit (New England Biolabs).

Data analysis

Paired-end reads were assigned to their samples and the barcodes and primer-sequence were truncated before merging using FLASH (V1.2.7) [63]. Quality filtering was performed as described here [64] using QIIME (V1.7.0) [65]. Chimera sequences were removed using the UCHIME algorithm (with "Gold" database) [66]. Finally OTU calling was performed using UPARSE (v7.0.1001) [67] and sequences with ≥97% similarity were assigned to the same OTUs. Mothur software [68] was used for species annotation at each taxonomic rank (threshold: 0.8-1) against the SILVA Database [69] and the phylogenetic tree was constructed using MUSCLE (Version 3.8.31) [70].

The OTU table and phylogenetic tree were imported in the R package *phyloseq* (v1.32.0) [71]. Richness and diversity were estimated on the raw OTU-counts table using *phyloseq*. For further data analysis the OTU-counts were normalized using the cumulative-sum scaling normalization (CSS) method using the R package *metagenomeSeq* (v 1.30.0) [54] and taxa were agglomerated on genus level using *phyloseq*. Unweighted UniFrac [72] distances were calculated in *phyloseq* using the phylogenic tree rooted on the longest branch using the *root* function from R package *ape* (v5.4-1) [73].

Statistical analyses

Data and statistical analyses were performed in GraphPad Prism (v7.0), IBM SPSS Statistics (v 26) or R (v4.0.4) in Rstudio (v 1.2.5042). The One-way ANOVAs followed by Fisher's LSD test with FDR correction in **Figure 1 and 2** were performed in GraphPad Prism. For the CFU data outliers were determined with the ROUT method (Q=0.1%) and removed using GraphPad Prism. The One-way ANOVA followed by Dunnet's test in **Figure 5AB** was performed in

SPSS. Principal Coordinate Analysis (PCoA), Principal Component Analysis (PCA) and Correspondence Analysis (CA) were performed in *phyloseq*. PERMANOVA (Permutational Multivariate Analysis of Variance) was performed using the *adonis2* function from the R package *vegan* (v2.5-6) [74] and environmental vector fitting was performed using the function *envfit* from *vegan*. For differential abundance analysis the R package *metagenomeSeq* was used for the zero-inflated log-normal model [54] and LDA Effect Size (LEfSe) [53] analysis was performed in the Galaxy web application (http://huttenhower.sph.harvard.edu/galaxy/). Specific tests and significance are indicated in the figure legends.

REFERENCES

1. Aho, V. T. E. *et al.* Gut microbiota in Parkinson's disease: Temporal stability and relations to disease progression. *EBioMedicine* **44**, 691–707 (2019).
2. Barichella, M. *et al.* Unraveling gut microbiota in Parkinson's disease and atypical parkinsonism. *Mov. Disord.* **34**, 396–405 (2019).
3. Scheperjans, F. *et al.* Gut microbiota are related to Parkinson's disease and clinical phenotype. *Mov. Disord.* **30**, 350–358 (2015).
4. Qian, Y. *et al.* Alteration of the fecal microbiota in Chinese patients with Parkinson's disease. *Brain. Behav. Immun.* **70**, 194–202 (2018).
5. Unger, M. M. *et al.* Short chain fatty acids and gut microbiota differ between patients with Parkinson's disease and age-matched controls. *Parkinsonism Relat. Disord.* **32**, 66–72 (2016).
6. Bedarf, J. R. *et al.* Functional implications of microbial and viral gut metagenome changes in early stage L-DOPA-naïve Parkinson's disease patients. *Genome Med.* **9**, 1–13 (2017).
7. Hasegawa, S. *et al.* Intestinal dysbiosis and lowered serum lipopolysaccharide-binding protein in Parkinson's disease. *PLoS One* **10**, 1–15 (2015).
8. Hill-Burns, E. M. *et al.* Parkinson's disease and Parkinson's disease medications have distinct signatures of the gut microbiome. *Mov. Disord.* **32**, 739–749 (2017).
9. Hopfner, F. *et al.* Gut microbiota in Parkinson disease in a northern German cohort. *Brain Res.* **1667**, 41–45 (2017).
10. Keshavarzian, A. *et al.* Colonic bacterial composition in Parkinson's disease. *Mov. Disord.* **30**, 1351–1360 (2015).
11. Li, W. *et al.* Structural changes of gut microbiota in Parkinson's disease and its correlation with clinical features. *Sci. China Life Sci.* **60**, 1223–1233 (2017).
12. Lin, A. *et al.* Gut microbiota in patients with Parkinson's disease in southern China. *Park. Relat. Disord.* **53**, 82–88 (2018).
13. Petrov, V. A. *et al.* Analysis of gut microbiota in patients with parkinson's disease. *Bull. Exp. Biol. Med.* **162**, 734–737 (2017).
14. Weis, S. *et al.* Effect of Parkinson's disease and related medications on the composition of the fecal bacterial microbiota. *npj Park. Dis.* **5**, 1–9 (2019).

15. Pietrucci, D. *et al.* Dysbiosis of gut microbiota in a selected population of Parkinson's patients. *Park. Relat. Disord.* **65**, 124–130 (2019).
16. Heintz-Buschart, A. *et al.* The nasal and gut microbiome in Parkinson's disease and idiopathic rapid eye movement sleep behavior disorder. *Mov. Disord.* **33**, 88–98 (2018).
17. Romano, S. *et al.* Meta-analysis of the Parkinson's disease gut microbiome suggests alterations linked to intestinal inflammation. *npj Park. Dis.* **7**, 27 (2021).
18. Li, Z. S., Schmauss, C., Cuenca, A., Ratcliffe, E. & Gershon, M. D. Physiological modulation of intestinal motility by enteric dopaminergic neurons and the D2 receptor: analysis of dopamine receptor expression, location, development, and function in wild-type and knock-out mice. *J. Neurosci.* **26**, 2798–807 (2006).
19. Singaram, C. *et al.* Dopaminergic defect of enteric system in Parkinson ' s disease patients with chronic constipation. *Lancet* **346**, 861–864 (1995).
20. Pinoli, M., Marino, F. & Cosentino, M. Dopaminergic Regulation of Innate Immunity: a Review. *J. Neuroimmune Pharmacol.* **12**, 602–623 (2017).
21. Sarkar, C., Basu, B., Chakroborty, D., Dasgupta, P. S. & Basu, S. The immunoregulatory role of dopamine: An update. *Brain. Behav. Immun.* **24**, 525–528 (2010).
22. van Kessel, S. P. & El Aidy, S. Contributions of gut bacteria and diet to drug pharmacokinetics in the treatment of Parkinson's disease. *Front. Neurol.* **10**, (2019).
23. Zar, M. A., Ebong, O. & Bateman, D. N. Effect of metoclopramide in guinea-pig ileum longitudinal muscle: evidence against dopamine-mediation. *Gut* **23**, 66–70 (1982).
24. Görich, R., Weihrauch, T. R. & Kilbinger, H. The inhibition by dopamine of cholinergic transmission in the isolated guinea-pig ileum. Mediation through alpha-adrenoceptors. *Naunyn. Schmiedebergs. Arch. Pharmacol.* **318**, 308–12 (1982).
25. Lucchelli, A., Boselli, C. & Grana, E. Dopamine-induced relaxation of the guinea-pig isolated jejunum is not mediated through dopamine receptors. *Pharmacol. Res.* **22**, 433–44 (1990).
26. Kirschstein, T. *et al.* Dopamine induces contraction in the proximal, but relaxation in the distal rat isolated small intestine. *Neurosci. Lett.* **465**, 21–26 (2009).
27. Zhang, X. *et al.* Dopamine receptor D1 mediates the inhibition of dopamine on the distal colonic motility. *Transl. Res.* **159**, 407–414 (2012).
28. Zizzo, M. G., Mulè, F., Mastropaolo, M. & Serio, R. D1 receptors play a major role in the dopamine modulation of mouse ileum contractility. *Pharmacol. Res.* **61**, 371–378 (2010).
29. Auteri, M., Zizzo, M. G., Amato, A. & Serio, R. Dopamine induces inhibitory effects on the circular muscle contractility of mouse distal colon via D1- and D2-like receptors. *J. Physiol. Biochem.* **73**, 395–404 (2016).
30. Walker, J. K., Gainetdinov, R. R., Mangel, A. W., Caron, M. G. & Shetzline, M. A. Mice lacking the dopamine transporter display altered regulation of distal colonic motility. *Am. J. Physiol. Gastrointest. Liver Physiol.* **279**, G311-8 (2000).

31. Fioramonti, J., Fargeas, M. J., Honde, C. & Bueno, L. Effects of central and peripheral administration of dopamine on pattern of intestinal motility in dogs. *Dig. Dis. Sci.* **29**, 1023–1027 (1984).
32. Bueno, L., Fargeas, M. J., Fioramonti, J. & Honde, C. Effects of dopamine and bromocriptine on colonic motility in dog. *Br. J. Pharmacol.* **82**, 35–42 (1984).
33. Marzio, L., Neri, M., Di Giammarco, A. M., Cuccurullo, F. & Lanfranchi, G. A. Dopamine-induced migrating myoelectrical complex-like activity in human duodenum. *Dig. Dis. Sci.* **31**, 349–354 (1986).
34. Marzio, L. *et al.* Dopamine interrupts gastrointestinal fed motility pattern in humans. *Dig. Dis. Sci.* **35**, 327–332 (1990).
35. Levein, N. G., Thörn, S. E. & Wattwil, M. Dopamine delays gastric emptying and prolongs orocaecal transit time in volunteers. *Eur. J. Anaesthesiol.* **16**, 246–50 (1999).
36. Dive, A., Foret, F., Jamart, J., Bulpa, P. & Installé, E. Effect of dopamine on gastrointestinal motility during critical illness. *Intensive Care Med.* **26**, 901–907 (2000).
37. Falony, G. *et al.* Population-level analysis of gut microbiome variation. *Science* **352**, 560–4 (2016).
38. Fasano, A., Visanji, N. P., Liu, L. W. C., Lang, A. E. & Pfeiffer, R. F. Gastrointestinal dysfunction in Parkinson's disease. *Lancet Neurol.* **14**, 625–639 (2015).
39. Dutkiewicz, J. *et al.* Small intestine dysfunction in Parkinson's disease. *J. Neural Transm.* **122**, 1659–1661 (2015).
40. Knudsen, K. *et al.* Gastrointestinal Transit Time in Parkinson's Disease Using a Magnetic Tracking System. *J. Parkinsons. Dis.* **7**, 471–479 (2017).
41. Quigley, E. M. M. & Quera, R. Small intestinal bacterial overgrowth: Roles of antibiotics, prebiotics, and probiotics. *Gastroenterology* **130**, 78–90 (2006).
42. Gabrielli, M. *et al.* Prevalence of Small Intestinal Bacterial Overgrowth in Parkinson's Disease. *Mov. Disord.* **26**, 889–892 (2011).
43. Fasano, A. *et al.* The role of small intestinal bacterial overgrowth in Parkinson's disease. *Mov. Disord.* **28**, 1241–1249 (2013).
44. Tan, A. H. *et al.* Small intestinal bacterial overgrowth in Parkinson's disease. *Park. Relat. Disord.* **20**, 535–540 (2014).
45. Kenna, J. E. *et al.* Characterization of Gastrointestinal Symptom Type and Severity in Parkinson's Disease: A Case–Control Study in an Australian Cohort. *Mov. Disord. Clin. Pract.* **8**, 245–253 (2021).
46. Khoshbin, K., Hassan, A. & Camilleri, M. Cohort Study in Parkinsonism: Delayed Transit, Accelerated Gastric Emptying, and Prodromal Dysmotility. *Neurol. Clin. Pract.* (2020).
47. van Kessel, S. P. *et al.* Gut bacterial deamination of residual levodopa medication for Parkinson's disease. *BMC Biol.* **18**, 137 (2020).

48. Okuzumi, A. *et al.* Metabolomics-based identification of metabolic alterations in PARK2. *Ann. Clin. Transl. Neurol.* **6**, 525–536 (2019).
49. Kustrimovic, N. *et al.* Dopaminergic Receptors on CD4+ T Naive and Memory Lymphocytes Correlate with Motor Impairment in Patients with Parkinson's Disease. *Sci. Rep.* **6**, 1–17 (2016).
50. van Kessel, S. P. & El Aidy, S. Bacterial Metabolites Mirror Altered Gut Microbiota Composition in Patients with Parkinson's Disease. *J. Parkinsons. Dis.* **9**, S359–S370 (2019).
51. Miller, M. S., Galligan, J. J. & Burks, T. F. Accurate measurement of intestinal transit in the rat. *J. Pharmacol. Methods* **6**, 211–217 (1981).
52. Lagkouvardos, I. *et al.* Sequence and cultivation study of Muribaculaceae reveals novel species, host preference, and functional potential of this yet undescribed family. *Microbiome* **7**, 1–15 (2019).
53. Segata, N. *et al.* Metagenomic biomarker discovery and explanation. *Genome Biol.* **12**, R60 (2011).
54. Paulson, J. N., Colin Stine, O., Bravo, H. C. & Pop, M. Differential abundance analysis for microbial marker-gene surveys. *Nat. Methods* **10**, 1200–1202 (2013).
55. van Kessel, S. P. *et al.* Gut bacterial tyrosine decarboxylases restrict levels of levodopa in the treatment of Parkinson's disease. *Nat. Commun.* **10**, 310 (2019).
56. Murata, K., Noda, K., Kohno, K. & Samejima, M. Bioavailability and pharmacokinetics of oral dopamine in dogs. *J. Pharm. Sci.* **77**, 565–8 (1988).
57. Dooley, M. & Markham, A. Pramipexole. *Drugs Aging* **12**, 495–514 (1998).
58. Kaye, C. M. & Nicholls, B. Clinical Pharmacokinetics of Ropinirole. *Clin. Pharmacokinet.* **39**, 243–254 (2000).
59. Diao, L., Shu, Y. & Polli, J. E. Uptake of pramipexole by human organic cation transporters. *Mol. Pharm.* **7**, 1342–1347 (2010).
60. Li, D. *et al.* Microbial Biogeography and Core Microbiota of the Rat Digestive Tract. *Sci. Rep.* **8**, 1–16 (2017).
61. Yu, Z. & Morrison, M. Improved extraction of PCR-quality community DNA from digesta and fecal samples. *Biotechniques* **36**, 808–812 (2004).
62. Salonen, A. *et al.* Comparative analysis of fecal DNA extraction methods with phylogenetic microarray: Effective recovery of bacterial and archaeal DNA using mechanical cell lysis. *J. Microbiol. Methods* **81**, 127–134 (2010).
63. Magoč, T. & Salzberg, S. L. FLASH: Fast length adjustment of short reads to improve genome assemblies. *Bioinformatics* **27**, 2957–2963 (2011).
64. Bokulich, N. A. *et al.* Quality-filtering vastly improves diversity estimates from Illumina amplicon sequencing. *Nat. Methods* **10**, 57–59 (2013).
65. Caporaso, J. G. *et al.* QIIME allows analysis of high-throughput community sequencing data. *Nat. Methods* **7**, 335–336 (2010).

66. Edgar, R. C., Haas, B. J., Clemente, J. C., Quince, C. & Knight, R. UCHIME improves sensitivity and speed of chimera detection. *Bioinformatics* **27**, 2194–2200 (2011).
67. Edgar, R. C. UPARSE: Highly accurate OTU sequences from microbial amplicon reads. *Nat. Methods* **10**, 996–998 (2013).
68. Schloss, P. D. *et al.* Introducing mothur: Open-source, platform-independent, community-supported software for describing and comparing microbial communities. *Appl. Environ. Microbiol.* **75**, 7537–7541 (2009).
69. Quast, C. *et al.* The SILVA ribosomal RNA gene database project: Improved data processing and web-based tools. *Nucleic Acids Res.* **41**, 590–596 (2013).
70. Edgar, R. C. MUSCLE: Multiple sequence alignment with high accuracy and high throughput. *Nucleic Acids Res.* **32**, 1792–1797 (2004).
71. McMurdie, P. J. & Holmes, S. Phyloseq: An R Package for Reproducible Interactive Analysis and Graphics of Microbiome Census Data. *PLoS One* **8**, (2013).
72. Lozupone, C. & Knight, R. UniFrac: A new phylogenetic method for comparing microbial communities. *Appl. Environ. Microbiol.* **71**, 8228–8235 (2005).
73. Paradis, E. & Schliep, K. Ape 5.0: An environment for modern phylogenetics and evolutionary analyses in R. *Bioinformatics* **35**, 526–528 (2019).
74. Dixon, P. Computer program review VEGAN , a package of R functions for community ecology. *J. Veg. Sci.* **14**, 927–930 (2003).

SUPPLEMENTARY INFORMATION

Availability of data and materials

The 16s rDNA metagenomic sequence data were deposited under BioProject number PRJNA725395.

Authors' Contributions

S.P.K. and S.E.A conceived and designed the study. S.P.K., A.B., G.D. S.E.A performed the experiments and S.P.K. and S.E.A. analyzed the data. S.P.K. wrote the original manuscript that was reviewed by S.E.A. Funding was acquired by S.E.A. All authors read and approved the final manuscript.

SUPPLEMENTARY FIGURES

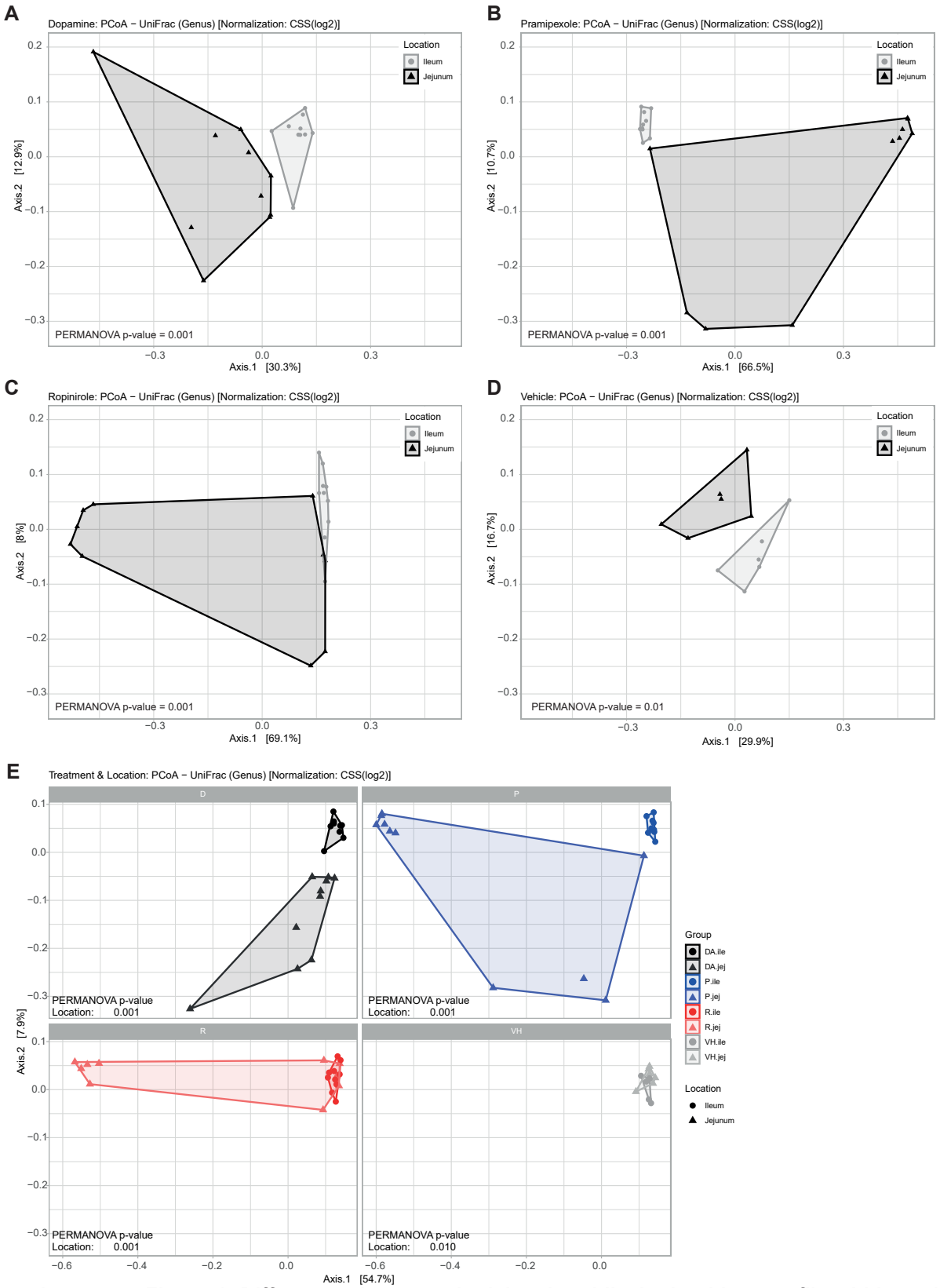

Supplementary Figure 1. Differences between the jejunal and ileal microbiota profile within and among the treatment groups (See legend on next page.)

(See figure on previous page.)

Supplementary Figure 1. Differences between the jejunal and ileal microbiota profile within and among the treatment groups. (**A-D**) represent a PCoA using unweighted UniFrac distances at genus level using CSS scaled data of dopamine (**A**), pramipexole (**B**), ropinirole (**C**), and vehicle (**D**) treated groups in jejunum (depicted by black triangles) and ileum (depicted by gray circles). (**E**) depicts a PCoA using unweighted UniFrac distances at genus level using CSS scaled data of jejunum and ileum (faceted by treatment). D, dopamine; P, pramipexole; R, ropinirole; VH, vehicle (10% sucrose). Significant contribution of the variables to the variance of the PCoA was tested with Permutational Multivariate ANOVA (PERMANOVA).

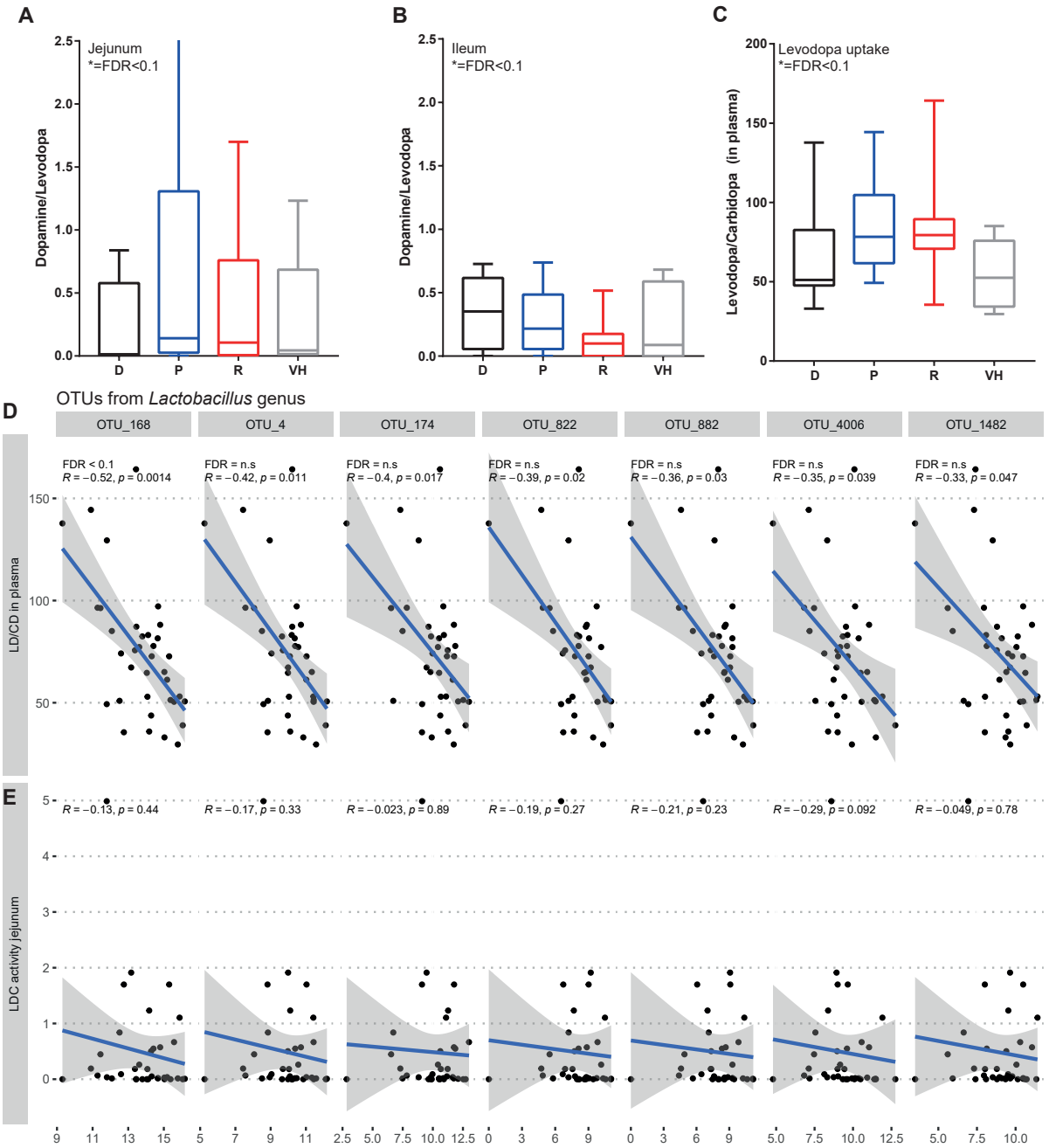

Supplementary Figure 2. LDC activity and levodopa uptake. (**A,B**) depict the levodopa decarboxylase activity (LDC) in the jejunal (**A**) and ileal content (**B**). (**C**) represents the levodopa/carbidopa ratio in plasma at Cmax. D, dopamine; P, pramipexole; R; VH, vehicle (10% sucrose). Boxes represent the median with interquartile range, and whiskers represent the maxima and minima. Significance compared to VH (asterisks) was tested with One-way-ANOVA followed by Fisher's LSD test with FDR correction (**E**) illustrates graphs with linear models and spearman correlations of the significant OTUs of the top 50 abundant OTUs with the levodopa uptake. Only *Lactobacillus* OTU_168 remained significant after FDR correction. (**D**) shows graphs with linear models and spearman correlations of the significant OTUs with LDC activity is depicted.

Back to table of contents

CHAPTER 5

Gut Bacterial Tyrosine Decarboxylase Gene Abundance Associates with Medication Exposure and Gastrointestinal Symptoms in a Longitudinal Cohort of Parkinson's Disease Patients.

Sebastiaan P. van Kessel[1], Filip Scheperjans[2,†*] and Sahar El Aidy[1,†*]

Unpublished
medRxiv 2021
DOI: 10.1101/2021.07.13.21259300

[1]Host-Microbe Interactions, Groningen Biomolecular Sciences and Biotechnology Institute (GBB), University of Groningen, Nijenborgh 7, 9747 AG Groningen, The Netherlands.
[2]Department of Neurology, Helsinki University Hospital, and Clinicum, University of Helsinki, Haartmaninkatu 4, 00290 Helsinki, Finland

[†]shared last author

*Correspondence: Filip Scheperjans (filip.scheperjans@hus.fi) and Sahar El Aidy, (sahar.elaidy@rug.nl)

Gut Bacterial Tyrosine Decarboxylase Gene Abundance Associates with Medication Exposure and Gastrointestinal Symptoms in a Longitudinal Cohort of Parkinson's Disease Patients

Sebastiaan P. van Kessel, Filip Scheperjans, and Sahar El Aidy

ABSTRACT Gut microbiota influences the clinical response of a wide variety of orally administered drugs. However, the underlying mechanisms by which drug-microbiota interactions occur are still obscure. Previously, we reported that tyrosine decarboxylating (TDC) bacteria may restrict the levels of levodopa reaching the circulation in patients with Parkinson's disease (PD). We observed a significant positive association between disease duration and the abundance of the bacterial TDC gene. The question arises whether increased exposure to anti-PD medication could affect the abundance of bacterial TDC, to ultimately impact drug efficacy. To this end, we investigated the potential association between anti-PD drug exposure and bacterial *tdc*-gene abundance over a time period of two years in a longitudinal cohort of PD patients and healthy controls. Our data reveal significant associations between *tdc*-gene abundance, anti-PD medication, and gastrointestinal symptoms and warrants further research on the effect of anti-PD medication on microbial changes and gastrointestinal-function.

Unpublished
medRxiv 2021
DOI: 10.1101/2021.07.13.21259300

INTRODUCTION

In recent years, many studies focused on the changes in the microbiota composition in individuals with Parkinson's disease (PD) compared to healthy subjects (extensively covered in several (systemic) reviews [1,2] among others). While certain differential abundance alterations were reproduced across multiple studies, variation of results across studies was considerable [1,2].

One of the reasons that may explain the inconsistency among these studies, are confounding factors such as anti-PD medications, disease duration, and GI symptoms. Indeed, studies took these factors into account with variable effort. Catechol-O-methyltransferase (COMT) inhibitors, anticholinergic and potentially levodopa/carbidopa were found to have a significant effect on the changes in the microbiota profile [3–6].

Besides medication, GI-dysfunction should be considered when analyzing the altered microbiota in PD patients. Indeed, PD patients usually experience more GI-dysfunction symptoms compared to healthy controls (HC) [7,8] and intestinal transit time can impact microbiota composition [9].

Moreover, it has been shown that there is an association between anti-PD medications and GI symptoms. For example, anti-PD medications were shown to have associations (corrected for disease duration) with the total GI Symptoms Rating Score, upper GI symptoms and hypoactive GI functions [8]. Furthermore, the proportion of the COMT inhibitors dosage prescription was significantly higher in patients with an abnormal transit compared to those with normal transit [10]. However, the statistical analysis in that study could not distinguish whether the levodopa equivalent daily dose (LEDD) or disease duration was the more contributing factor to the slow colon transit [10]. In addition, *ex vivo* rodent studies and *in vivo* dog and human studies showed an effect of dopamine agonists and/or dopamine (which can originate from levodopa in PD patients) on the gut motility, recently reviewed (van Kessel and El Aidy [11], and citations in there). Gut microbial metabolization of unabsorbed residues of levodopa were also shown to influence ileal-motility *ex vivo* [12].

Recent studies have shown that tyrosine decarboxylating (TDC) bacteria can decarboxylate levodopa into dopamine in the periphery, thereby may restrict the levels of levodopa available for the brain [13,14]. Potentially, TDC-harboring bacteria could create a vicious-circle, where peripheral dopamine production affects the gut motility, favoring the colonization of (TDC)-bacteria [13]. Additionally, non-levodopa anti-PD medications (Monoaminoxidase inhibitors, COMT inhibitors, and dopamine agonists), which affect the peripheral dopaminergic-balance, may lead to an altered GI-function, potentially leading to an overgrowth of (TDC)-bacteria, ultimately affecting the bioavailability of levodopa. However, levels of TDC-bacteria have not been measured nor were previously correlated with GI symptoms in longitudinal PD cohorts.

In this study we focused on measuring fecal *tdc*-gene abundance and its association with anti-PD medication exposure in a 2 year longitudinal cohort consisting of 67 PD and 65 healthy matched subjects, that was used previously for investigating microbiota and PD [4,5].

METHODS

Cohort

The original gender, age and sex matched cohort was recruited for a pilot study in 2015 investigating PD and gut microbiota [5]. All subjects were invited to a follow-up on average 2.25±0.20 years later to investigate temporal stability in the PD microbiota [4]. The study was approved by the ethics committee of the Hospital District of Helsinki and Uusimaa. All participants gave informed consent and the study was registered at clinicaltrials.gov (NCT01536769).

From the total 165 subjects (77 PD, 88 HC) recruited in the baseline and follow-up studies [4,5], 13 subjects (6 PD, 7 HC) were excluded because they did not return for the follow-up study, and 20 subjects (4 PD, 16 HC) were excluded because of various other reasons at baseline or follow up. In the control group, 1 subject was excluded for a sibling with PD, 3 subjects for having a common cold, 8 subjects for hyposmia (pre-motor PD symptom), 2 subjects had a recent surgery, 1 subject had no matching sample, and 1 sample was missing. In the PD group, 1 subject was excluded because of recent surgery, 1 subject had a change in diagnosis, 1 subject because of a sampling handling issue, 1 subject because of medical history. In total 33 subjects (10 PD, 23 HC) were excluded, resulting in 132 subjects (67 PD, 65 HC) used in this study.

The following parameters were assessed as described in the previous studies (Scheperjans *et al*.[5], Aho *et al.* [4]): Non-motor symptoms (Wexner constipation score [15], Rome III IBS questionnaire [16]), the severity of the disease (Unified Parkinson's Disease Rating Scale (UPDRS) [17]), medication exposure, and stool consistency at follow-up (Victoria Bowel Performance Scale (BPS) [18]).

DNA extraction

Stool sample collection and DNA isolation was performed in a previous study Aho *et al*. [4]. Briefly, stool samples were collected by the study subjects into collection tubes with pre-filled DNA stabilizer (PSP Spin Stool DNA Plus Kit, STRATEC Molecular), and stored in the refrigerator until transport (for up to 3 days). After receival of the samples, they were transferred to −80 °C. DNA from both baseline and follow-up samples were extracted with the PSP Spin Stool DNA Plus Kit (STRATEC Molecular). Each extraction batch included one blank sample to assess potential contamination. (Of note, to prevent potential technical differences DNA form the baseline samples were extracted at the baseline [5] and at follow-up study [4], thus the baseline samples were thawed twice.)

Determination of *tdc*-gene abundance

The DNA concentration of the samples was directly estimated from the 96-well plates by measuring the (pathlength corrected) absorbance at 260 nm and 320 nm in a multimode reader, the DNA concentration was calculated as followed: $50 \times (\text{sample}^{260\text{-}320} - \text{blank}^{260\text{-}320})$. Samples that were negative, very low, or very high in concentration were measured with the nanodrop to confirm. All DNA samples were diluted 20× so that the concentration range would fall in a range of 2-25 ng/µl (median, 13.7 ng/µL, interquartile range, 6.9 - 21.8 ng/

µl) and 2 µl was used for quantitative PCR (qPCR). qPCR of *tdc* genes was performed using primers Dec5f (5'-CGTTGTTGGTGTTGTTGGCACNACNGARGARG-3') and Dec3r (5'-CCGCCAGCAGAATATGGAAYRTANCCCAT-3') targeting a 350 bp region of the *tdc* gene [19]. Primers targeting 16S rRNA gene for all bacteria [20], Eub338 (5'-ACTCCTACGGGAGGCAGCAG-3') and Eub518 (5'-ATTACCGCGGCTGCTGG-3') were used as an internal control. All qPCR experiments were performed in a Bio-Rad CFX96 RT-PCR system (Bio-Rad Laboratories, Veenendaal, The Netherlands) with iQ SYBR Green Supermix (170-8882, Bio-Rad) in 10 µL reactions using the manufacturer's protocol. qPCR was performed using the following parameters: 3 min at 95 °C; 15 sec at 95 °C, 1 min at 58 °C, 40 cycles. A melting curve was determined at the end of each run to verify the specificity of the PCR amplicons. Data analysis was performed using Bio-Rad CFX Manager 3.1 software. Ct[DEC] values were corrected with the internal control (Ct[16s]) and linearized using $2^{-(Ct^{[DEC]}-Ct^{[16s]})}$ based on the $2^{-\Delta\Delta Ct}$ method [21].

Statistics

All statistical tests were performed in IBM SPSS Statistics version 26. The p-value adjustments were performed in R version 4.0.0 using p.adjust(p-values, "fdr"). The qPCR data were tested for outliers per group and timepoint using the ROUT method (Q=0.1%) in GraphPad Prism v7 and the identified outliers were removed. All variables were tested for normality using Kolmogorov-Smirnov and Shapiro-Wilk tests using the Explore function in SPSS. Based on the distribution of the data, the differences were tested using the appropriate statistical tests. The general linear models (GLMs) were performed using the Generalized Linear Models function in SPSS and the main effects were tested using the Wald Chi Square test. Additionally, the variance inflation factor (VIF) was computed to check for potential collinearity between variables.

RESULTS

Clinical variables

Comparing the clinical variables between the longitudinal cohort of PD and HC did not reveal any significant differences in sex, age (at stool collection) and BMI, no antibiotics were used within the last month (**Supplementary Table 1**). The duration of motor and non-motor symptom onset in the PD cohort at baseline was ~8 years (**Supplementary Table 1**). Over time (between baseline and follow-up), the levodopa equivalent daily dose (LEDD) significantly increased by an average of 116 mg (**Table 1**). On average, the UPDRS I and II scores significantly increased while UPDRS III (at ON-state) significantly decreased over time, respectively (**Supplementary Table 2**). The latter may be explained by the significant LEDD increase over time. The Hoehn & Yahr (at ON-state) score slightly increased over time (**Supplementary Table 2**).

The gut bacterial *tdc*-gene abundance, GI-symptoms, and medication exposure significantly increased over time in PD patients

Recently, it has be shown that TDC-bacteria in the GI-tract interfere with the availability of levodopa medication in animal models and that longer disease duration and exposure to levodopa may further increase the abundance of TDC-bacteria in the gut [13]. Thus, we sought to investigate the changes in the levels of gut bacterial *tdc*-gene abundance over time in the longitudinal PD cohort including the differences between PD patients and matching HC.

When comparing PD patients and HC, PD patients tended to have a higher *tdc*-gene abundance levels (p=0.057) at follow-up (**Figure 1 and Table 2**). Correspondingly, the increase in *tdc*-gene abundance, over time, was significantly higher in PD patients compared to HC subjects (Wilcoxon-test, p=9.7E-07) with a mean difference increase of 2.6-fold (**Table 1 and Figure 1**). The results indicate that, over time, *tdc*-gene abundance increases more rapidly in PD patients compared to HC subjects.

Because the GI transit time also impacts the microbial composition [9], including the TDC bacteria, differences in GI-symptoms were assessed at baseline and follow-up. At both time points, the GI symptoms were significantly more severe in PD patients compared to HC subjects (**Table 2**). At follow up, the Victoria Bowel Performance Scale was also assessed. The defecations per week, the stool characteristics, and the bowel control had significantly lower scores compared to control subjects. Only the Wexner scores, but not the Rome III scores, increased significantly over time in PD patients (**Table 1**). In HC subjects, the Wexner scores decreased significantly over time (**Table 1**).

Although the LEDD increased significantly over time (**Table 1**), no significant increase was observed for any individual drug in PD patients after correction for FDR, possibly due to the changes of the type of medication (**Table 1**). Nonetheless, at baseline, anticholinergic medication use was significantly higher in PD patients compared to HC subjects (**Table 2**). Only in the HC group, a significant decrease in anacidic medication use was observed over time (**Table 1**).

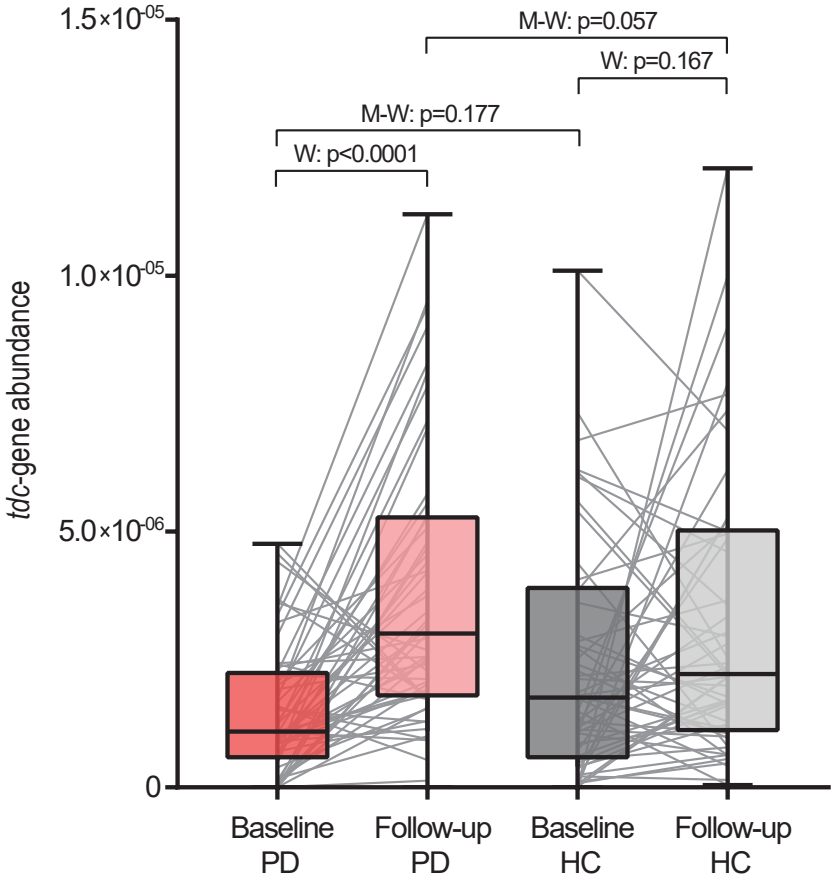

Figure 1 | *tdc*-gene abundance in Parkinson's disease and healthy control subjects. The *tdc*-gene abundance is depicted for Parkinson's disease patients (PD, red boxes; dark, baseline; light, follow-up) and healthy control subjects (HC, grey boxes; dark, baseline; light, follow-up) for both time points. Nonparametric paired Wilcoxon tests (W) were performed to test for significant increase overtime between paired samples (grey lines). Significant outliers were removed using the ROUT method (Q=0.1%). Nonparametric unpaired Mann-Whitney tests (M-W) were performed to test for significant differences between PD and HC at baseline and follow-up. Boxes represent the median with the interquartile range and whiskers the maxima and minima.

Table 1 | Paired tests between follow-up and baseline samples in PD and HC of tdc-gene abundance, gastrointestinal symptoms and medication. Significant test-results are printed in bold.

	Paired tests (Follow-up - Baseline)														PD on medication	
	PD							Control								
	Paired mean difference	Baseline Mean ± SD (n)	Follow up Mean ± SD (n)	T- test	Wilcoxon	McNemar	FDR	Paired mean difference	Baseline Mean ± SD (n)	Follow up Mean ± SD (n)	T- test	Wilcoxon	McNemar	FDR	Baseline (%)	Follow up (%)
***tdc*-gene abundance**																
tdc-gene abundance (outliers removed)	**2.2E-06**	1.5E-6 ± 1.3E-6 (55)	3.7E-6 ± 2.6E-6 (55)		**9.7E-07**		**na**	8.61E-07	2.2E-6 ± 2.2E-6 (54)	3.1E-6 ± 2.7E-6 (54)		0.167		na		
Gastrointestinal symptoms																
Wexner total score	**0.72**	5.66 ± 4.01 (67)	6.37 ± 4.63 (67)		**0.033**		**0.059**	**-0.54**	2.92 ± 2.61 (65)	2.38 ± 2.58 (65)		**0.010**		**0.030**		
Rome III (constipation and defecation)	-0.01	7.37 ± 5.96 (67)	7.36 ± 5.17 (67)		0.685		0.685	-0.22	2.97 ± 3.60 (65)	2.75 ± 3.60 (65)		0.651		0.977		

(Continued)

Table 1 | Continued

	Paried tests (Follow-up - Baseline)															
	PD							Control							PD on medication	
	Paired mean difference	Baseline Mean ± SD (n)	Follow up Mean ± SD (n)	T- test	Wilcoxon	McNemar	FDR	Paired mean difference	Baseline Mean ± SD (n)	Follow up Mean ± SD (n)	T- test	Wilcoxon	McNemar	FDR	Baseline (%)	Follow up (%)
Anti-PD medication exposure																
LEDD (mg)	116.40	444.2 ± 315.6 (66)	560.6±294.0 (66)		1.8E-06		**3.06E-05**									
Levodopa																
levodopa IR (mg)	54.10	99.63 ± 159.46 (67)	153.73 ± 204.92 (67)		**0.028**		0.221								35.8	41.8
duodopa (mg)	19.33	0.00 ± 0.00 (66)	19.33 ± 157.06 (66)		0.317		0.708								0.0	1.5
levodopa CR (mg)	-8.96	47.76 ± 157.98 (67)	38.81 ± 115.41 (67)		1.000		1.000								11.9	14.9
levodopa (with entacapone) (mg)	19.03	88.06 ± 220.17 (67)	107.09 ± 226.33 (67)		0.513		0.872								14.9	22.4

(Continued)

Table 1 | Continued

	Paired tests (Follow-up - Baseline)															
	PD							Control							PD on medication	
	Paired mean difference	Baseline Mean ± SD (n)	Follow up Mean ± SD (n)	T- test	Wilcoxon	McNemar	FDR	Paired mean difference	Baseline Mean ± SD (n)	Follow up Mean ± SD (n)	T- test	Wilcoxon	McNemar	FDR	Baseline (%)	Follow up (%)
COMT inhibitors																
entacapone (mg)	49.25	146.27 ± 357.74 (67)	195.52 ± 385.51 (67)		0.319		0.708								14.9	22.4
MAO inhibitors															0.0	0.0
selegeline (mg)	-0.51	4.10 ± 4.84 (67)	3.59 ± 4.74 (67)		0.348		0.708								43.3	38.8
rasagiline (mg)	0.06	0.25±0.44 (67)	0.31±0.47 (67)		0.102		0.434								25.4	31.3
Dopamine agonists																
rotigotine (mg)	0.42	0.00 ± 0.00 (67)	0.42 ± 1.62 (67)		**0.039**		0.221								0.0	7.5
pramipexole (mg)	-0.06	0.62 ± 0.82 (67)	0.56 ± 0.88 (67)		0.613		0.885								43.3	38.8

(Continued)

Table 1 | Continued

	Paried tests (Follow-up - Baseline)															
	PD							Control							PD on medication	
	Paired mean difference	Baseline Mean ± SD (n)	Follow up Mean ± SD (n)	T- test	Wilcoxon	McNemar	FDR	Paired mean difference	Baseline Mean ± SD (n)	Follow up Mean ± SD (n)	T- test	Wilcoxon	McNemar	FDR	Baseline (%)	Follow up (%)
ropinirole (mg)	0.04	3.15 ± 5.18 (67)	3.19 ± 6.02 (67)		0.951		1.000								34.3	29.9
bromocriptine (mg)	n.a.	0.15 ± 1.22 (67)	0.15 ± 1.22 (67)		1.000		1.000								1.5	1.5
Other medication																
amantadine (mg)	1.49	6.72 ± 40.73 (67)	8.21 ± 38.53 (67)		1.000		1.000								3.0	4.5
biperiden (mg)	-0.11	0.21 ± 0.94 (67)	0.10 ± 0.55 (67)		0.345		0.708								6.0	4.5
exelon (mg)	n.a.	0.00 ± 0.00 (67)	0.00±0.00 (67)		1.000		1.000								0.0	0.0
Use of anacidic (Yes/No)	-3%	6/61 (67)	4/63(67)		0.317	0.625	0.885	**-11%**	7/58 (65)	0/65 (65)			**0.016**	**0.032**	9.0	6.0
Use of anti-cholinergic (Yes/No)	-4%	6/61 (67)	3/64(67)		0.180	0.375	0.708	2%	0/65 (65)	1/65 (65)			1.000	1.000	9.0	4.5

Table 2 | Independent tests between PD and HC of *tdc*-gene abundance, gastrointestinal symptoms and medication. Significant test-results are printed in bold

	Independent-tests (PD - Control)													
	Baseline							Follow up						
	Mean Difference	PD Mean±SD (n)	Control Mean±SD (n)	T- test	Mann-Whitney	Fisher's test	FDR	Mean Difference	PD Mean±SD (n)	Control Mean±SD (n)	T- test	Mann-Whitney	Fisher's test	FDR
***tdc*-gene abundance**														
tdc-gene abundance (outliers removed)	-7.4E-07	1.5E-6 ± 1.3E-6 (55)	2.2E-6 ± 2.2E-6 (54)		0.177		na	6.47E-07	3.8E-6 ± 2.6E-6 (57)	3.1E-6 ± 2.7E-6 (55)		0.057		na
Gastrointestinal symptoms														
Wexner total score	**2.73**	5.66 ± 4.01 (67)	2.92 ± 2.61 (65)		**2.4E-05**		**3.6E-05**	**3.99**	6.37 ± 4.63 (67)	2.38 ± 2.58 (65)		**5.9E-09**		**4.1E-08**
Rome III (constipation and defecation)	**4.40**	7.37 ± 5.96 (67)	2.97 ± 3.60 (65)		**1.2E-06**		**3.6E-06**	**4.60**	7.36 ± 5.17 (67)	2.75 ± 3.60 (65)		**1.3E-08**		**4.6E-08**

(Continued)

Table 2 | Continued

	Independent-tests (PD - Control)													
	Baseline							Follow up						
	Mean Difference	PD Mean±SD (n)	Control Mean±SD (n)	T- test	Mann-Whitney	Fisher's test	FDR	Mean Difference	PD Mean±SD (n)	Control Mean±SD (n)	T- test	Mann-Whitney	Fisher's test	FDR
Victoria Bowel Perfromance Scale														
Average defecations per week								**-1.92**	7.49 ± 4.38 (67)	9.42 ± 4.59 (65)		**0.003**		**0.004**
Average characteristic								**-0.46**	-0.42 ± 1.34 (67)	0.04 ± 0.90 (65)	**0.022**			**0.026**
Average frequency								-0.31	-0.15 ± 1.11 (67)	0.16 ± 0.84 (65)		0.119		0.119
Average control								**-0.51**	-1.13 ± 1.14 (67)	-0.61 ± 0.80 (65)		**0.001**		**0.002**
Medication														
Use of anacidic (Yes/No)	-2%	6/61 (67)	7/58(65)			0.777	0.777	6%	4/63 (67)	0/65 (65)			0.119	0.238
Use of anticholinergic (Yes/No)	**9%**	6/61 (67)	0/65 (65)			**0.028**	0.056	3%	3/64 (67)	1/64 (65)			0.619	0.619

Anti-PD medications and GI symptoms associate with the gut bacterial *tdc*-gene abundance over time

Using general linear models (GLM), the contribution of the difference in anti-PD medication exposure to the difference in *tdc*-gene abundance over time (follow-up − baseline) was assessed (**Table 3**). The model showed that dose changes of entacapone, rasagiline, pramipexole, and ropinirole significantly contributed to the difference in *tdc*-gene abundance over time. Entacapone and the dopamine agonists contributed positively to the difference in *tdc*-gene abundance, while MAOi contributed negatively to the *tdc*-gene abundance over time, respectively.

Because the Wexner scores, but not Rome III, significantly increased over time in the PD group (**Table 1**), this factor was included in the model to correct for its potential contribution to the *tdc*-gene abundance. Remarkably, Wexner total scores significantly contributed negatively to the *tdc*-gene abundance (**Table 3**), suggesting that subjects with less constipation have an increased *tdc*-gene abundance. Correction for Wexner scores showed that the difference in exposure to anti-PD medication, stated above, still contributed to the model except for ropinirole (p=0.107). The results indicate that prolonged exposure of these specific anti-PD medications, excluding levodopa, contributed to *tdc*-gene abundance independent of the changes in GI symptoms measured by Wexner scores.

PD patients usually require change in the anti-PD dosage regimen during the disease progression, compared to patients in a steady state of the disease. Thus, we sought to investigate whether the differences in anti-PD dosage regimen between the two groups was the factor contributing to the changes in *tdc*-gene abundance observed above (**Table 3**). To this end, the PD-group was sub-divided into steady (n=35) and progressing (n=12) PD patients as described and performed in Aho *et al*. [4]. Comparing the mean differences of the medications of the stable and progressing PD patients over time showed that exposure to levodopa and entacapone significantly increased, while pramipexole exposure significantly decreased in the progressing group compared to the steady group (**Table 4**).

When comparing the steady PD patients group with the progressed PD patients group (**Table 5**) only entacapone was not associated with *tdc*-gene abundance and rotigotine now significantly contributed to the model (which was not observed in all the PD patients, **Table 3**), however the significance was lost when correcting for Wexner-score.

In the progressing PD group, only entacapone contributed significantly to the change in *tdc*-abundance (**Table 5**). Because the variation inflation factor (VIF, which tests if the variance of a variable increases with another) suggested collinearity between the factors in the progressing PD group, DA-agonists and MAO-inhibitors were combined using LED calculation [22]. Using the combined variables in the GLM, no collinearity was observed anymore, while entacapone still contributed significantly to the *tdc*-gene abundance (**Supplementary Table 3**). These results indicate that the difference in drug exposure over time between stable and progressed

Table 3 | General linear model of the difference *tdc*-gene abundance overtime with anti-PD medication and Wexner-score as variables. Significant variable contributions to the model are printed in bold. VIF; Variance Inflation Factor

All PD patients (n=55)	Difference *tdc*-gene abundance 2y-0y (no outliers)					
	Not corrected for Wexner score			Corrected for Wexner score		
	β	p-value	VIF	β	p-value	VIF
(Intercept)	**2.1E-06**	**0.000**		**2.5E-06**	**0.000**	
Difference levodopa sum (mg)	1.0E-09	0.671	1.375	-3.2E-10	0.895	1.466
Difference entacapone (mg)	**2.1E-09**	**0.032**	1.163	**2.4E-09**	**0.011**	1.189
Difference selegeline (mg)	-9.4E-08	0.258	1.215	-1.0E-07	0.191	1.218
Difference rasagiline (mg)	**-2.7E-06**	**0.035**	1.366	**-3.0E-06**	**0.013**	1.388
Difference rotigotine (mg)	2.3E-07	0.245	1.161	1.7E-07	0.374	1.184
Difference pramipexole (mg)	**2.0E-06**	**0.001**	1.415	**1.7E-06**	**0.005**	1.515
Difference ropinirole (mg)	**2.2E-07**	**0.028**	1.367	1.6E-07	0.107	1.472
Difference in Wexner total score	Not included			**-3.0E-07**	**0.024**	1.265

Table 4 | Independent tests between progressed and stable PD patients of exposure of anti-PD medications overtime. Significant test-results are printed in bold.

	Independent-tests (Progressed-Stable)						
	Mean Difference	**Progressed Mean ± SD (n)**	**Stable Mean±SD (n)**	**T-test**	**Mann-Whitney**	**Fishers's test**	**FDR**
Difference levodopa sum (mg)	**103.5**	208.33 ± 156.43 (12)	104.86 ± 116.32 (36)		**0.022**		**0.051**
Difference entacapone (mg)	**361.1**	366.67 ± 510.50 (12)	5.56 ± 255.17 (36)		**0.009**		**0.051**
Difference selegeline (mg)	1.5	0.83 ± 5.15 (12)	-0.68 ± 4.46 (36)		0.737		0.983
Difference rasagiline (mg)	0.0	0.08 ± 0.29 (12)	0.08 ± 0.28 (36)		0.934		0.983
Difference rotigotine (mg)	0.4	0.83 ± 2.89 (12)	0.39 ± 1.34 (36)		0.983		0.983
Difference pramipexole (mg)	**-0.4**	-0.31 ± 0.65 (12)	0.10 ± 0.58 (36)		**0.019**		**0.051**
Difference ropinirole (mg)	-0.3	-0.58 ± 5.53 (12)	-0.28±3.18 (36)		0.785		0.983

Table 5. General linear model of the difference of *tdc*-gene abundance overtime with anti-PD medication and Wexner-score as variable in steady and progressing PD patients. Significant variable contributions to the model are printed in bold. VIF; Variance Inflation Factor

	Stable PD patients (n=36)						**Progressed PD patients (n=12)**					
	Difference *tdc*-gene abundance 2y-0y (no outliers)						Difference *tdc*-gene abundance 2y-0y (no outliers)					
	Not corrected for Wexner score			Corrected for Wexner score			Not corrected for Wexner score			Corrected for Wexner score		
	β	pvalue	VIF	β	p-value	VIF	β	p-value	VIF	β	p-value	VIF
(Intercept)	**2.1E-06**	**0.001**		**2.4E-06**	**0.000**		6.5E-07	0.589		1.3E-06	0.511	
Difference levodopa sum (mg)	3.4E-09	0.436	2.120	2.7E-09	0.506	2.133	7.1E-10	0.868	1.879	-1.2E-09	0.848	4.149
Difference entacapone (mg)	-4.1E-10	0.777	1.164	-2.0E-10	0.884	1.171	**5.2E-09**	**0.000**	1.780	**4.8E-09**	**0.002**	2.665
Difference selegeline (mg)	-1.8E-07	0.053	1.442	**-1.9E-07**	**0.033**	1.445	-2.4E-07	0.163	3.392	-2.6E-07	0.145	3.538
Difference rasagiline (mg)	**-3.5E-06**	**0.006**	1.100	**-3.8E-06**	**0.002**	1.114	-4.0E-06	0.173	2.998	-3.8E-06	0.190	3.045
Difference rotigotine (mg)	**6.1E-07**	**0.038**	1.287	4.5E-07	0.117	1.388	4.8E-07	0.072	2.494	4.3E-07	0.141	3.033
Difference pramipexole (mg)	**2.3E-06**	**0.002**	1.496	**2.4E-06**	**0.001**	1.502	1.8E-06	0.092	2.152	7.6E-07	0.789	14.750
Difference ropinirole (mg)	**5.4E-07**	**0.000**	1.937	**4.5E-07**	**0.003**	2.126	1.3E-07	0.296	1.930	4.3E-08	0.857	7.454
Difference in Wexner total score	Not included			**-2.8E-07**	**0.048**	1.217	Not included			-2.7E-07	0.680	8.843

PD patients (**Table 4**), reflect their contribution to the *tdc*-gene abundance in the GLMs (**Table 5 and Supplementary Table 3**). In summary these observations show that, likely due to the change in exposure to these specific anti-PD medications, entacapone is the significant factor contributing to the increase in the *tdc*-gene abundance in progressing PD patients, while the other anti-PD medications contribute to the *tdc*-gene abundance in stable PD patients.

DISCUSSION

In this study, we have established that gut bacterial *tdc*-gene abundance is significantly increasing over time in PD patients (**Table 1**), in line with previous results, where a significant correlation between the disease duration and the *tdc*-gene abundance was observed [13]. The levels of gut bacterial *tdc*-gene abundance were not significantly different compared to HC at baseline, but close to significant at follow-up (**Table 2**). Accordingly, the increase in *tdc*-gene abundance was 2.6-fold higher in PD than HC, suggesting that that the increased gene abundance occurs more rapidly in PD patients. In this study we did not find a significant correlation between the levodopa dosages and the *tdc*-gene abundance. This discrepancy could be explained by the relative lower proportion of high levodopa dosages in this study. At baseline and follow-up 19.4% (max 900 mg) and 26.9% (max 875 mg) of the PD patients had a dose higher than 400 mg/day respectively, while in the previous study [13] 60% of the PD patients received a dosage higher than 400 mg/day (max 1100 mg).

Using GLMs, we showed that other anti-PD medications than levodopa contributed significantly to the *tdc*-gene abundance. Importantly, all the tested medications (**Table 3**) affect the (peripheral) dopaminergic-system; COMT inhibitors prevent methylation of levodopa, dopamine, and norepinephrine; MAO inhibitors prevent dopamine, and norepinephrine oxidation; and DA-agonists act on dopamine receptors expressed in the gut. Collectively, these medications were recently shown to elicit an effect on the GI symptoms [8]. Although GI-dysfunction might be caused by the degeneration of enteric neurons, as observed in PD patients with chronic constipation [23] and reported in a MPTP mouse model for PD [24], additional dopaminergic medication may impact the GI-function even further. Indeed, the Wexner-score, which significantly increased over time in PD patients, did not change the associations between anti-PD medication and *tdc*-gene abundance (except for ropinirole exposure) when considered as a confounder. This potential link between changes in GI symptoms, as measured by Wexner score, and anti PD medications is in agreement with the outcome of a comprehensive meta-analysis showing that PD patients on ropinirole did not have higher risk of constipation compared to placebo, while those on pramipexole had a higher risk of constipation [25]. Unlike the Wexner score, The Rome III (constipation and defecation) score did not change over time in PD patients which may be explained by the fact that Rome III assesses symptoms retrospectively over a 3-month period which may reduce sensitivity to change. The difference observed between the two questionnaires, conforms the need of the development for more sophisticated protocols to detect and investigate GI symptoms in PD patients [8].

Notably, only entacapone exposure in progressing PD patients contributed to the fecal *tdc*-abundance. In fact, *Enterococcus* (genus consisting of species harboring TDCs), among others were found to be significantly increased only in PD patients treated with entacapone [6]. However, in their study, Weis et al. did not report whether the tested PD patients were on medications, such as MAOi or DA-agonists, other than levodopa and/or entacapone [6]. Here we show that, next to entacapone, other anti-PD medications may affect gut bacterial *tdc*-gene abundance as well (**Table 3**).

The major limitation of this study is that we determined the bacterial *tdc*-gene abundance in fecal samples, which might not reflect the *tdc*-gene levels in the small-intestine, the main absorption site of levodopa and other medication. Besides, the presence of these genes do not necessarily reflect the TDC activity.

In summary, the present study implies important associations between anti-PD medication and gut bacterial *tdc*-gene abundance. These associations point towards a complex interactions between anti-PD medication, GI symptoms and gut bacterial *tdc*-gene abundance, which warrants for further research.

REFERENCES

1. Boertien, J. M., Pereira, P. A. B., Aho, V. T. E. & Scheperjans, F. Increasing Comparability and Utility of Gut Microbiome Studies in Parkinson's Disease: A Systematic Review. *J. Parkinsons. Dis.* **9**, S297–S312 (2019).
2. van Kessel, S. P. & El Aidy, S. Bacterial Metabolites Mirror Altered Gut Microbiota Composition in Patients with Parkinson's Disease. *J. Parkinsons. Dis.* **9**, S359–S370 (2019).
3. Hill-Burns, E. M. *et al.* Parkinson's disease and Parkinson's disease medications have distinct signatures of the gut microbiome. *Mov. Disord.* **32**, 739–749 (2017).
4. Aho, V. T. E. *et al.* Gut microbiota in Parkinson's disease: Temporal stability and relations to disease progression. *EBioMedicine* **44**, 691–707 (2019).
5. Scheperjans, F. *et al.* Gut microbiota are related to Parkinson's disease and clinical phenotype. *Mov. Disord.* **30**, 350–358 (2015).
6. Weis, S. *et al.* Effect of Parkinson's disease and related medications on the composition of the fecal bacterial microbiota. *npj Park. Dis.* **5**, 1–9 (2019).
7. Fasano, A., Visanji, N. P., Liu, L. W. C., Lang, A. E. & Pfeiffer, R. F. Gastrointestinal dysfunction in Parkinson's disease. *Lancet Neurol.* **14**, 625–639 (2015).
8. Kenna, J. E. *et al.* Characterization of Gastrointestinal Symptom Type and Severity in Parkinson's Disease: A Case–Control Study in an Australian Cohort. *Mov. Disord. Clin. Pract.* **8**, 245–253 (2021).

9. Falony, G. *et al.* Population-level analysis of gut microbiome variation. *Science* **352**, 560–4 (2016).
10. Khoshbin, K., Hassan, A. & Camilleri, M. Cohort Study in Parkinsonism: Delayed Transit, Accelerated Gastric Emptying, and Prodromal Dysmotility. *Neurol. Clin. Pract.* (2020)
11. van Kessel, S. P. & El Aidy, S. Contributions of gut bacteria and diet to drug pharmacokinetics in the treatment of Parkinson's disease. *Front. Neurol.* **10**, (2019).
12. van Kessel, S. P. *et al.* Gut bacterial deamination of residual levodopa medication for Parkinson's disease. *BMC Biol.* **18**, 137 (2020).
13. van Kessel, S. P. *et al.* Gut bacterial tyrosine decarboxylases restrict levels of levodopa in the treatment of Parkinson's disease. *Nat. Commun.* **10**, 310 (2019).
14. Maini Rekdal, V., Bess, E. N., Bisanz, J. E., Turnbaugh, P. J. & Balskus, E. P. Discovery and inhibition of an interspecies gut bacterial pathway for Levodopa metabolism. *Science* **364**, eaau6323 (2019).
15. Agachan, F., Chen, T., Pfeifer, J., Reissman, P. & Wexner, S. D. A constipation scoring system to simplify evaluation and management of constipated patients. *Dis. Colon Rectum* **39**, 681–685 (1996).
16. Longstreth, G. F. *et al.* Functional Bowel Disorders. *Gastroenterology* **130**, 1480–1491 (2006).
17. Fahn, S., Elton, R., and Members of the UPDRS Development Committee, The Unified Parkinson's Disease Rating Scale. in *Recent Developments in Parkinson's Disease* (ed. Fahn, S., Marsden, C.D., Calne, D.B. and Goldstein, M.) 153–163 (McMellam Health Care Information, 1987).
18. Hawley, P., Barwich, D. & Kirk, L. Implementation of the Victoria bowel performance scale. *J. Pain Symptom Manage.* **42**, 946–953 (2011).
19. Torriani, S. *et al.* Rapid detection and quantification of tyrosine decarboxylase gene (*tdc*) and its expression in gram-positive bacteria associated with fermented foods using PCR-based methods. *J. Food Prot.* **71**, 93–101 (2008).
20. Fierer, N., Jackson, J. A., Vilgalys, R. & Jackson, R. B. Assessment of Soil Microbial Community Structure by Use of Taxon-Specific Quantitative PCR Assays. *Appl. Environ. Microbiol.* **71**, 4117–4120 (2005).
21. Livak, K. J. & Schmittgen, T. D. Analysis of relative gene expression data using real-time quantitative PCR and the 2-ΔΔCT method. *Methods* **25**, 402–408 (2001).
22. Tomlinson, C. L. *et al.* Systematic review of levodopa dose equivalency reporting in Parkinson's disease. *Mov. Disord.* **25**, 2649–2653 (2010).
23. Singaram, C. *et al.* Dopaminergic defect of enteric system in Parkinson ' s disease patients with chronic constipation. *Lancet* **346**, 861–864 (1995).

24. Anderson, G. *et al.* Loss of enteric dopaminergic neurons and associated changes in colon motility in an MPTP mouse model of Parkinson's disease. *Exp. Neurol.* **207**, 4–12 (2007).
25. Kulisevsky, J. & Pagonabarraga, J. Tolerability and Safety of Ropinirole versus Other Dopamine Agonists and Levodopa in the Treatment of Parkinsons Disease: Meta-Analysis of Randomized Controlled Trials. *Drug Saf.* **33**, 147–161 (2010).

SUPPLEMENTARY INFORMATION

Author Contributions

S.P.K. performed the qPCR, the statistical analysis, and wrote the original manuscript which was reviewed and modified by F.S. and S.E.A. S.P.K., F.S. and S.E.A. contributed to interpreting the results and the conceptualization of the study. F.S. performed the clinical evaluations of subjects and was responsible for the original cohort-data.

Supplementary Table 1 | Independent test of the basic variables Sex, Age, and BMI. Significant test-results are printed in bold.

	Independent-tests (PD - Control)						
	Mean Difference	PD Mean±SD (n)	Control Mean±SD (n)	T-test	Mann-Whitney	Fishers's test	FDR
Sex (Female/Male)	0.02%	33/34 (67)	32/33 (65)			1.000	
BMI at baseline (kg/m^2)	0.95	27.2±4.3 (62)	26.2±3.5 (61)	0.181			
BMI at follow up (kg/m^2)	0.71	27.3±4.6 (67)	26.6±3.7 (65)	0.330			
Age at stool collection baseline (years)	0.76	65.4±5.5 (67)	64.6±7.0 (65)	0.486			
Age at stool collection follow up (years)	0.92	67.6±5.5 (66)	66.7±6.9 (64)	0.399			
Antibiotic last month at baseline (yes/no)	0%	0/67 (67)	0/65 (65)			na	
Antibiotic last month at follow-up (yes/no)	-3%	1/66 (67)	3/62 (65)			0.362	
Age symptom onset							
Age at motor symptoms onset (years)		59.5±5.3 (66)					
Age at non-motor symptoms onset (years)		57.7±7.8 (53)					
Duration of motor symptoms (years)		8.2±4.1 (66)					
Duration of non-motor symptoms (years)		10.0±6.9 (52)					

Supplementary Table 2 | Paired tests between follow-up and baseline of LEDD, and UPDRS scores. Significant test-results are printed in bold.

	Paired-tests (Follow-up - Baseline)						
	Mean Difference	Baseline Mean±SD (n)	Follow up Mean±SD (n)	T-test	Wilcoxon	McNemar	FDR
UPDRS I (total)	0.63	1.8±1.8 (67)	2.5±1.8 (67)		**0.002**		**0.003**
UPDRS II (total)	1.78	11.6±5.5 (67)	11.6±5.5 (67)		**0.001**		**0.003**
UPDRS III (total; ON-state)	-3.11	31.9±8.9 (64)	28.8±8.7 (64)	**0.001**			**0.003**
UPDRS III (total; OFF-state)		na	33.7+10.6 (65)				
UPDRS IV (total)	0.84	2.2±2.2 (67)	3.1±3.2 (67)		**0.008**		**0.010**
UPDRS V [H&Y] (total; ON-state)	0.13	2.4±.5 (64)	2.5±0.7 (64)		0.054		0.054
UPDRS V [H&Y] (total; OFF-state)		na	2.5±0.8 (64)				

Supplementary Table 3. General linear model of the difference *tdc*-gene abundance overtime with anti-PD medication LEDD combined and Wexner-score as variables in progressing PD patients.

Progressed PD patients (n=12)	Difference *tdc*-gene abundance 2y-0y (no outliers)					
	Not corrected for Wexner score			Corrected for Wexner score		
	β	p-value	VIF	β	p-value	VIF
(Intercept)	6.8E-07	0.550		1.5E-06	0.273	
Difference levodopa sum (mg)	-4.8E-10	0.913	1.500	-2.3E-09	0.619	1.783
Difference entacapone (mg)	**4.5E-09**	**0.001**	1.414	**4.6E-09**	**0.000**	1.421
Difference MAOi LED (mg)	-1.0E-08	0.534	1.315	-9.6E-09	0.547	1.317
Difference in DA agonist LED (mg)	7.1E-09	0.219	2.383	3.2E-09	0.641	3.601
Difference in Wexner total score	Not included			-3.4E-07	0.323	1.874

Back to table of contents

CHAPTER 6

Summary and Discussion

INTRODUCTION

The absorption of an orally administered drug from the bowel into the blood circulation is dependent on a highly complex and dynamic process involving the gastrointestinal (GI) tract, the dosage form, and the active pharmaceutical ingredient [1]. Physiochemical properties such as the solubility at different pH and difference in permeability are important factors for the clinical applicability of a drug [1,2]. Intraluminal pH is an important factor for the pH-dependent solubility of a multitude of drugs. In the GI tract the pH varies considerably dependent on the orally administered substances and location within the gut, and thus can impact drug delivery [2–4] (**Figure 1A**). The first part of the GI tract (from mouth to and including stomach) does not have a direct function in the process of nutrient absorption, but rather helps in preprocessing ingested substances and forms a barrier against the passage of unwanted substances such as harmful microbes or ingested compounds, due to the very low intraluminal pH (median 1.5-1.9, however with a wide range from 1.4 to 7.5) of the stomach.

Unlike the low pH in the stomach, the small intestine is characterized by a higher pH gradient (pH ~6 in the proximal jejunum) in order to facilitate further digestion and absorption of nutrients and other ingested substances such as drugs [1].

In the small intestine polar compounds such as amino-acids and monosaccharides have to be actively transported in order to facilitate absorption, thus providing the need for a large surface area to effectively absorb nutrients from food. To establish this extensive surface, the epithelial cells lining the small intestine constitute finger-like projections called villi and microvilli (the brush border) on the epithelial apical surface. The absorptive surface area of the adult small intestine is estimated to be 30-40 m^2, compared to only ~1.9 m^2 in the large intestine, in humans [5]. This large surface area results in oral drug delivery to be completed for the majority of ingested drugs in the proximal small intestine [1,4].

Furthermore, several medications are absorbed and recirculated via enterohepatic circulation (**Figure 1B**). After their uptake in the intestine, the drugs pass through the hepatic portal vein, which directs the blood from the GI tract to the liver before entering the systemic circulation. Consequently, some drugs are reabsorbed in the small intestine via the bile duct, resulting in drug recirculation. It is unknown which physiochemical properties a drug should have to be recirculated in the small intestine. However, this drug recirculation occurs predominantly for small, and less-polar molecules [6], again highlighting the significance of the small intestine in the process of oral drug absorption.

Thousand to 10 thousand (10^3-10^4, upper bound 10^7), 100 million (10^8, upper bound 10^{11}), and one hundred billion (10^{11}, upper bound 10^{14}) bacteria per milliliter have been estimated to reside in the human upper-small intestine, ileum and colon, respectively [7]. In disease situations like small intestinal bacterial overgrowth (SIBO), the bacterial load in the small intestine can be significantly higher, at least >10^5 CFU/mL [8]. The number and metabolic activity of these small

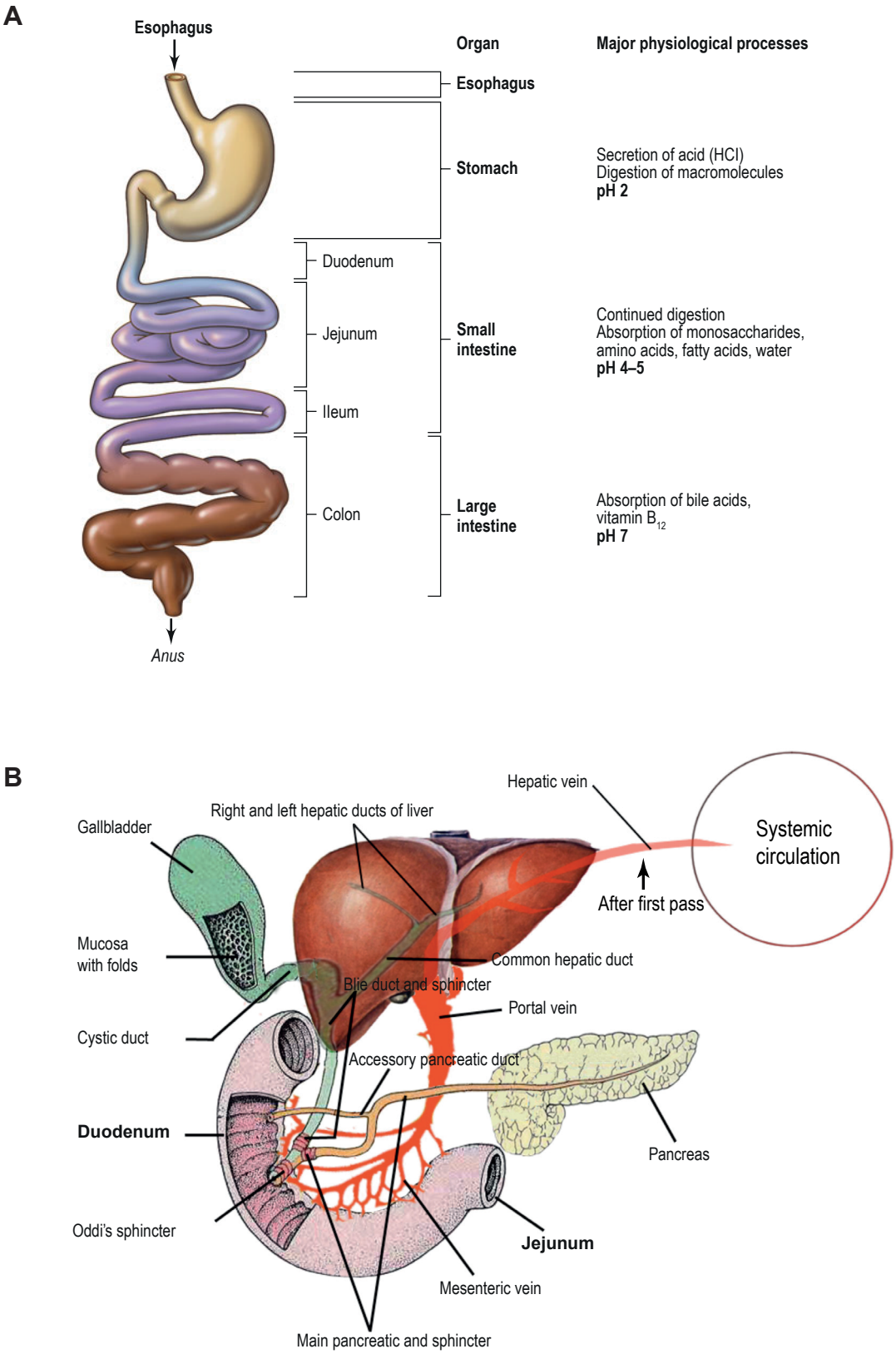

Figure 1. Regional functionality of the gastrointestinal tract and enterohepatic circulation. A) the gastrointestinal tract is depicted from esophagus to anus with specific regions and major functions described on the right-hand side. Figure adapted from Madigan *et al.* [32]. **B**) the gallbladder, liver, pancreas connected to the upper part of the small intestine, the duodenum, are depicted. Upon the uptake of nutrients or drugs from the small intestine, the content will pass through the portal vein to the liver and ultimately to the systemic circulation, or will be recirculated into the duodenum via the bile duct at Oddi's sphincter. Figure adapted from Gao *et al.* [6].

intestinal bacteria are likely to affect absorption, and subsequently, the bioavailability of orally administered drugs.

Recently, the European Network on Understanding Gastrointestinal Absorption related Processes (UNGAP) stated that the mechanistic understanding of the role of the gut microbiota on the absorption of orally administered drugs remain relatively understudied, and that the microbiota contribution to drug absorption *in vivo* is warranted [9]. Over half a century, several studies have described gut microbial conversions of orally prescribed medications [10–18]. However, the majority of the available studies have focused on the colonic bacteria. For example, Sousa *et al.* concluded that many medications are substrates for colonic bacteria and stated that the colon is the main site for gut microbiota-attributed conversions because the bacterial counts are highest in the colon, compared to the small intestine [10]. Zimmerman *et al.* found that 65 % of the medications studied are reduced by at least one of the 76 gut bacteria included (mainly anaerobic, residing in the lower parts of the intestines) and anticipated that these microbiota-attributed conversions could influence intestinal and systemic drug and drug-metabolite exposure [13]. However, in the context of drug bioavailability, bacterial conversions of medications are only clinically relevant at the main (re)absorption site of orally administered drugs, the small intestine. Maier *et al*. estimated the drug concentrations in the large intestine based on drug excretion in feces. Out of the 1111 drugs examined, 17% were excreted in feces with fractions ranging from 0.001-0.98 (median 0.37, interquartile range: 0.15-0.65) [18]. These findings indicate that only 17 % of the tested medications could be exposed to and metabolized by colonic microbiota, while the remaining 83% are likely to be absorbed in the small intestine and plausibly affected by the residing microbiota in that region of the GI tract. Nonetheless, in the context of drug side-effects (e.g. toxicity), investigation of the microbial conversions throughout the whole GI tract are important if unabsorbed residues of medications reach in fact these parts of the GI tract.

SUMMARY

This thesis focused on the interplay between gut bacteria and Parkinson's disease (PD) medication. **Chapters 2-3** focused mainly on levodopa, which remains the gold standard in the treatment of PD [19]. Besides levodopa, other anti-PD medications, such as specific dopamine agonists, are commonly prescribed. **Chapters 4-5** described the potential impact of these agonists on the gut motility, a comorbidity of PD, and GI-microbiota profiles.

In **Chapter 2,** we uncovered how bacteria in proximal jejunal content could convert levodopa to dopamine coinciding with the conversion of tyrosine to tyramine. This observation led to the hypothesis that bacteria harboring tyrosine decarboxylase (TDC) enzymes could be responsible for the observed decarboxylation. Indeed, we identified small-intestinal bacteria able to convert levodopa to dopamine via TDC enzymes. Although the affinity for tyrosine was significantly higher than that for levodopa, it did not prevent the decarboxylation of levodopa. Furthermore, the co-prescribed DDC-inhibitors did not exert a significant effect on the levodopa

decarboxylation by these bacteria. *tdc*-gene abundance significantly correlated with the levodopa dosage requirements and disease duration, suggesting that the increased levodopa dosage and the duration of the disease may result in increased TDC bacterial levels.

Investigating, whether TDC bacteria could interfere with the levels of levodopa reaching the circulation, at the site of absorption, the upper small-intestine, showed a negative correlation between the *tdc*-gene abundance and the levels in the blood circulation in healthy rats. Furthermore, replacing the small-intestinal microbiota with an *Enterococcus faecalis* strain devoid of TDC resulted in higher levodopa levels in the blood circulation compared to when the small-intestinal microbiota was replaced with the wild-type strain. These findings suggested that increased bacterial TDC levels may result in higher luminal dopamine levels, which could, in turn, affect (together with potentially prescribed dopamine agonists) the gut motility favoring the colonization of these TDC-harboring bacteria, creating a vicious circle, ultimately restricting the levels of levodopa available to reach the brain (**Chapter 2: Figure 7**).

Part of the levodopa dose could reach the lower parts of the (small) intestine, where more anaerobic bacteria reside and are different in composition compared to the proximal small intestine. These bacteria could perform similar or other metabolic conversions of levodopa as described in **Chapter 1 (Figure 1).** Thus, **Chapter 3** identified a bacterial metabolic-reaction for levodopa by *Clostridium sporogenes*. *C. sporogenes* was able to reductively deaminate aromatic amino acids and we showed that next to tryptophan, tyrosine, and phenylalanine, *C. sporogenes* was also able to deaminate levodopa. Levodopa was deaminated through a multi-step enzymatic pathway, as confirmed by NMR, MS and genetic knock-outs, to 3-(3,4-dihydroxyphenyl)propionic acid (DHPPA), a phenolic acid. This reductive deamination pathway for levodopa was active in 70% of the PD samples (**Chapter 3, Figure 4**). Phenolic acids have been associated with gut motility alterations [20,21]. In agreement, using an *ex vivo* organ bath system, DHPPA reduced the acetylcholine induced contractility in mouse ileum (**Chapter 3, Figure 3)**. Moreover, the DHPPA levels were significantly higher in PD patients than their age-matched healthy controls. These findings are important as PD patients experience GI-dysfunction, especially constipation. Overall, these results highlighted the urgency for the investigation of bacterial mediated drug conversions potentially leading to unwanted side-effects of prescribed medications.

Besides levodopa/carbidopa prescription, other medications are co-prescribed to cope with the loss of dopamine in the brain. These are commonly a combination of dopamine agonists and levodopa/carbidopa. Moreover, PD patients are exposed to high dopamine levels as a result of levodopa decarboxylation. These higher dopamine levels, as well as exposure to dopamine agonists, not only exert effects on the immune homeostasis [22,23], which affects the progression of the disease and microbial composition, but also gut motility [24] an important factor in microbiota composition [25] and small intestinal bacterial overgrowth [8,26]. Therefore, **Chapter 4** followed up

on the potential effect of these anti-PD medication on gut motility and the consequence on small intestinal bacterial composition, bacterial load, and ultimately SIBO.

Dopamine agonists, pramipexole and ropinirole in combination with levodopa/carbidopa, significantly decreased the small intestinal motility after a treatment of 14 days. Both treatments showed that the bacterial counts were increased in the ileum, but only significantly for ropinirole. Further investigation of the microbiota profile revealed that only species richness in the jejunum was significantly higher for both agonists but the diversity did not differ compared to the vehicle group. Especially in the jejunum, and to lesser extent, in the ileum, both the treatment and gut-motility contributed significantly to the variation observed. Looking further for the detailed changes revealed *Lactobacillus spp* increased in all treatments and *Lachnospiraceae spp.* decreased. Remarkably, alterations in these species are often observed in PD microbiota studies based on fecal samples. The results suggest that fecal microbiota analysis could, to some extent, be a reflection of the small intestinal microbial alterations. Overall, **Chapter 4** highlights the importance of the confounding medications in the PD microbiota studies which could alter the microbiota profiles through their effect on gut motility. Moreover, the data showed that the desirable effect of dopamine agonists on restoring the loss of dopamine levels in the brain of PD patients may elicit unwarranted side-effects in the periphery.

To confirm the interplay between the gut microbiota and anti-PD medications, mainly studied in animal models or tested on a small cohort of PD patients **(Chapters 2-4**), **Chapter 5** investigated the association of anti-PD medications (including the above-mentioned) with the *tdc*-gene abundance levels in a human longitudinal cohort consisting of PD and age and sex-matched healthy controls. *tdc*-gene abundances significantly increased overtime, only in PD patients and not in the matched healthy controls. Furthermore, the difference in the exposure of anti-PD medications that those patients received over the period of two years were significantly associated with the difference in *tdc*-gene abundance overtime, independent of constipation symptoms (except for ropinirole), which was significantly contributing to the *tdc*-gene abundance. Furthermore, the difference in type of medication reflected the difference in the associations with the *tdc*-gene abundance when looking into subgroups of patients which were either stable or progressing in their disease. Collectively, **Chapter 5** revealed important parameters that link dopamine agonists and GI-function to the levels of the bacterial *tdc*-gene abundance, which may ultimately affect the levels of levodopa available to reach the brain (**Chapter 2**).

FUTURE PERSPECTIVES

The effect of dopamine and dopamine agonists on the decrease of (small) intestinal motility, which is a comorbidity in PD patients, urges to further investigate the effect of these compounds on the gut motility in PD patients. Similarly, it is crucial to accurately measure levels of SIBO in PD patients, especially in those who administer proton pump inhibitors which affect the gut microbiota [27]. These precautions will help reduce the factors contributing to compromised

levodopa bioavailability and the unwarranted side effects that result potentially in and from increased frequency of dosage treatment regimen.

Further research on the metabolites produced by the gut microbiota, including the metabolism of anti-PD medication is necessary to unravel the impact of the complex interaction of multiple facets of metabolites originating from altered microbial composition and pharmacological treatment on the immune system, microbiota profiles, GI-function, and drug availability in PD patients.

Insights in the mechanistic molecular processes in bacterial uptake and metabolization of levodopa (and other microbiota affected drugs) are important to determine potential candidate proteins for targeted inhibition, aimed to prevent, in contrast to antibiotics, potential disturbance of the microbiota composition. Levodopa is processed through the same pathway as tyrosine and importantly the tyrosine decarboxylase operon in *Enterococcus faecalis* is regulated both by tyrosine levels (thus potentially also levodopa) and pH which increased the fitness of *E. faecalis* [28]. This example illustrates that high levels of medication analogues to natural prevalent nutrients (e.g. tyrosine) could impact the fitness and thus colonization of certain microbiota members that can metabolize these compounds, potentially creating a vicious circle.

Finally, the clinical contribution of the inter-individual variation in drug-microbe interactions, pharmacomicrobiomcis [29], in PD patients should be investigated in a longitudinal cohort study including newly diagnosed drug naïve PD patients in order to follow their pharmacological treatment, microbiota composition, and microbial levodopa decarboxylase activity over time.

CONCLUDING REMARKS

A reduction in striatal dopamine levels leads to an "off"-episode (i.e. when PD symptoms reoccur), especially in patients with advanced stage of PD, who have a reduced capacity to store dopamine in the brain [30,31]. Gut bacteria could be a contributing factor to the reduced efficacy of levodopa treatment in PD patients, especially in the advanced state of the disease with narrow treatment windows. Additionally, anti-PD medication contribute to the alteration of gut motility and microbiota composition, which should be considered in the (poly)pharmacological treatment of PD.

REFERENCES

1. Vertzoni, M. *et al.* Impact of regional differences along the gastrointestinal tract of healthy adults on oral drug absorption: An UNGAP review. *Eur. J. Pharm. Sci.* **134**, 153–175 (2019).
2. Koziolek, M. *et al.* Investigation of pH and Temperature Profiles in the GI Tract of Fasted Human Subjects Using the Intellicap®System. *J. Pharm. Sci.* **104**, 2855–2863 (2015).

3. Ovesen, L. *et al.* Intraluminal pH in the stomach, duodenum, and proximal jejunum in normal subjects and patients with exocrine pancreatic insufficiency. *Gastroenterology* **90**, 958–962 (1986).
4. Kararli, T. T. Comparison of the gastrointestinal anatomy, physiology, and biochemistry of humans and commonly used laboratory animals. *Biopharm. Drug Dispos.* **16**, 351–380 (1995).
5. Helander, H. F. & Fändriks, L. Surface area of the digestive tract-revisited. *Scand. J. Gastroenterol.* **49**, 681–689 (2014).
6. Gao, Y. *et al.* Drug enterohepatic circulation and disposition: Constituents of systems pharmacokinetics. *Drug Discov. Today* **19**, 326–340 (2014).
7. Sender, R., Fuchs, S. & Milo, R. Revised Estimates for the Number of Human and Bacteria Cells in the Body. *PLoS Biol.* **14**, 1–14 (2016).
8. Quigley, E. M. M. & Quera, R. Small intestinal bacterial overgrowth: Roles of antibiotics, prebiotics, and probiotics. *Gastroenterology* **130**, 78–90 (2006).
9. Vinarov, Z. *et al.* Current challenges and future perspectives in oral absorption research: An opinion of the UNGAP network. *Adv. Drug Deliv. Rev.* **171**, 289–331 (2021).
10. Sousa, T. *et al.* The gastrointestinal microbiota as a site for the biotransformation of drugs. *Int. J. Pharm.* **363**, 1–25 (2008).
11. Zimmermann, M., Zimmermann-Kogadeeva, M., Wegmann, R. & Goodman, A. L. Separating host and microbiome contributions to drug pharmacokinetics and toxicity. *Science* **363**, eaat9931 (2019).
12. Haiser, H. J. *et al.* Predicting and manipulating cardiac drug inactivation by the human gut bacterium *Eggerthella lenta*. *Science* **341**, 295–8 (2013).
13. Zimmermann, M., Zimmermann-Kogadeeva, M., Wegmann, R. & Goodman, A. L. Mapping human microbiome drug metabolism by gut bacteria and their genes. *Nature* (2019)
14. van Kessel, S. P. *et al.* Gut bacterial tyrosine decarboxylases restrict levels of levodopa in the treatment of Parkinson's disease. *Nat. Commun.* **10**, 310 (2019).
15. van Kessel, S. P. *et al.* Gut bacterial deamination of residual levodopa medication for Parkinson's disease. *BMC Biol.* **18**, 137 (2020).
16. Waclawiková, B. *et al.* Gut bacteria-derived 5-hydroxyindole is a potent stimulant of intestinal motility via its action on L-type calcium channels. *PLoS Biol.* **19**, 1–27 (2021).
17. Maini Rekdal, V., Bess, E. N., Bisanz, J. E., Turnbaugh, P. J. & Balskus, E. P. Discovery and inhibition of an interspecies gut bacterial pathway for Levodopa metabolism. *Science* **364**, eaau6323 (2019).
18. Maier, L. *et al.* Extensive impact of non-antibiotic drugs on human gut bacteria. *Nature* **555**, 623–628 (2018).
19. Mercuri, N. B. & Bernardi, G. The 'magic' of L-dopa: Why is it the gold standard Parkinson's disease therapy? *Trends Pharmacol. Sci.* **26**, 341–344 (2005).

20. Aviello, G. *et al.* Inhibitory effect of caffeic acid phenethyl ester, a plant-derived polyphenolic compound, on rat intestinal contractility. *Eur. J. Pharmacol.* **640**, 163–167 (2010).
21. Roager, H. M. *et al.* Colonic transit time is related to bacterial metabolism and mucosal turnover in the gut. *Nat. Microbiol.* **1**, 16093 (2016).
22. Pinoli, M., Marino, F. & Cosentino, M. Dopaminergic Regulation of Innate Immunity: a Review. *J. Neuroimmune Pharmacol.* **12**, 602–623 (2017).
23. Sarkar, C., Basu, B., Chakroborty, D., Dasgupta, P. S. & Basu, S. The immunoregulatory role of dopamine: An update. *Brain. Behav. Immun.* **24**, 525–528 (2010).
24. Li, Z. S., Schmauss, C., Cuenca, A., Ratcliffe, E. & Gershon, M. D. Physiological modulation of intestinal motility by enteric dopaminergic neurons and the D2 receptor: analysis of dopamine receptor expression, location, development, and function in wild-type and knock-out mice. *J. Neurosci.* **26**, 2798–807 (2006).
25. Falony, G. *et al.* Population-level analysis of gut microbiome variation. *Science* **352**, 560–4 (2016).
26. Quigley, E. M. M. Small intestinal bacterial overgrowth. *Curr. Opin. Gastroenterol.* **30**, 141–146 (2014).
27. Imhann, F. *et al.* Proton pump inhibitors affect the gut microbiome. *Gut* **65**, 740–748 (2016).
28. Perez, M. *et al.* Tyramine biosynthesis is transcriptionally induced at low pH and improves the fitness of *Enterococcus faecalis* in acidic environments. 3547–3558 (2015)
29. Rizkallah, M., Saad, R. & Aziz, R. The Human Microbiome Project, Personalized Medicine and the Birth of Pharmacomicrobiomics. *Curr. Pharmacogenomics Person. Med.* **8**, 182–193 (2012).
30. Olanow, C. W. & Koller, W. C. An algorithm (decision tree) for the management of Parkinson's disease: treatment guidelines. American Academy of Neurology. *Neurology* **50**, S1-57 (1998).
31. Olanow, C. W., Watts, R. L. & Koller, W. C. An algorithm (decision tree) for the management of Parkinson's disease (2001): treatment guidelines. *Neurology* **56**, S1–S88 (2001).
32. Madigan, M. T., Clark, D. P., Stahl, D. & Martinko, J. M. *Brock biology of microorganisms*. (Pearson Education, Inc., publishing as Benjamin Cummings, 2012).

Nederlandse Wetenschappelijke Samenvatting

Vertaling van Chapter 6

INTRODUCTIE

De opname van een oraal toegediend geneesmiddel vanuit de darm in de bloedcirculatie is afhankelijk van een zeer complex en dynamisch proces waarbij het maagdarmkanaal, de doseringsvorm en het actieve farmaceutische ingrediënt betrokken zijn [1]. Fysiochemische eigenschappen zoals de oplosbaarheid bij verschillende pH-waarden en verschil in permeabiliteit zijn belangrijke factoren voor de klinische toepasbaarheid van een geneesmiddel [1,2]. Intraluminale pH is een belangrijke factor voor de pH-afhankelijke oplosbaarheid van een groot aantal geneesmiddelen. In het maagdarmkanaal varieert de pH aanzienlijk, afhankelijk van de oraal toegediende stoffen en de locatie in de darm, en kan dus de medicijnafgifte beïnvloeden [2–4] (**Figuur 1A**). Het eerste deel van het maagdarmkanaal (van mond tot en met de maag) heeft geen directe functie in de opname van voedingsstoffen, maar helpt eerder bij het voorbewerken van ingenomen stoffen en vormt een barrière tegen de doorgang van ongewenste stoffen zoals schadelijke microben of ingenomen chemische-bestandsdelen, vanwege de zeer lage intraluminale pH (mediaan 1,5-1,9, maar met een breed bereik van 1,4 tot 7,5) van de maag.

In tegenstelling tot de lage pH in de maag, wordt de dunne darm gekenmerkt door een hogere pH-gradiënt (pH ~6 in het proximale jejunum) om verdere vertering en opname van voedingsstoffen en andere ingenomen stoffen zoals medicijnen te bevorderlijken [1].

In de dunne darm moeten polaire verbindingen zoals aminozuren en monosachariden actief worden getransporteerd om de opname te faciliteren, waardoor er een groot oppervlak nodig is om voedingsstoffen uit voedsel effectief te absorberen. Om dit enorme oppervlak te bewerkstelligen, vormen de epitheelcellen, die de dunne darm bekleden, vingerachtige uitsteeksels op het apicale epitheliale oppervlak die villi en microvilli (de borstelrand) worden genoemd. Het absorberend oppervlak van de volwassen dunne darm bij mensen wordt geschat op 30-40 m^2, vergeleken met slechts ~1,9 m^2 in de dikke darm [5]. Dit grote oppervlak zorgt ervoor dat voor de meeste oraal toegediende geneesmiddelen al volledig zijn opgenomen in de proximale dunne darm [1,4].

Bovendien worden verschillende medicijnen geabsorbeerd en gerecirculeerd via enterohepatische circulatie (**Figuur 1B**). Na hun opname in de darm passeren de medicijnen de hepatische poortader, die het bloed van het maagdarmkanaal naar de lever leidt voordat het de systemische circulatie binnengaat. Als bijgevolg worden sommige geneesmiddelen via de galwegen in de dunne darm geresorbeerd, wat resulteert in recirculatie van het geneesmiddel. Het is niet bekend welke fysisch-chemische eigenschappen een medicijn moet hebben om in de dunne darm gerecirculeerd te worden. Echter, vinden deze medicijnrecirculaties voornamelijk plaats voor kleine en minder polaire moleculen [6], wat opnieuw het belang van de dunne darm in het proces van orale medicijnabsorptie benadrukt.

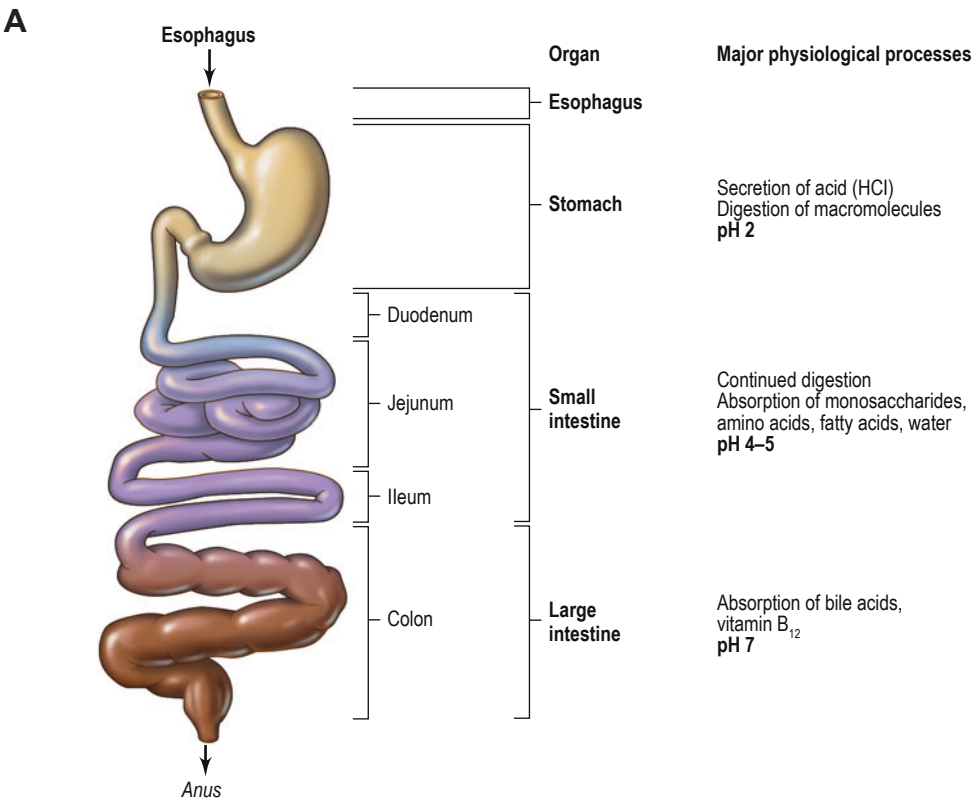

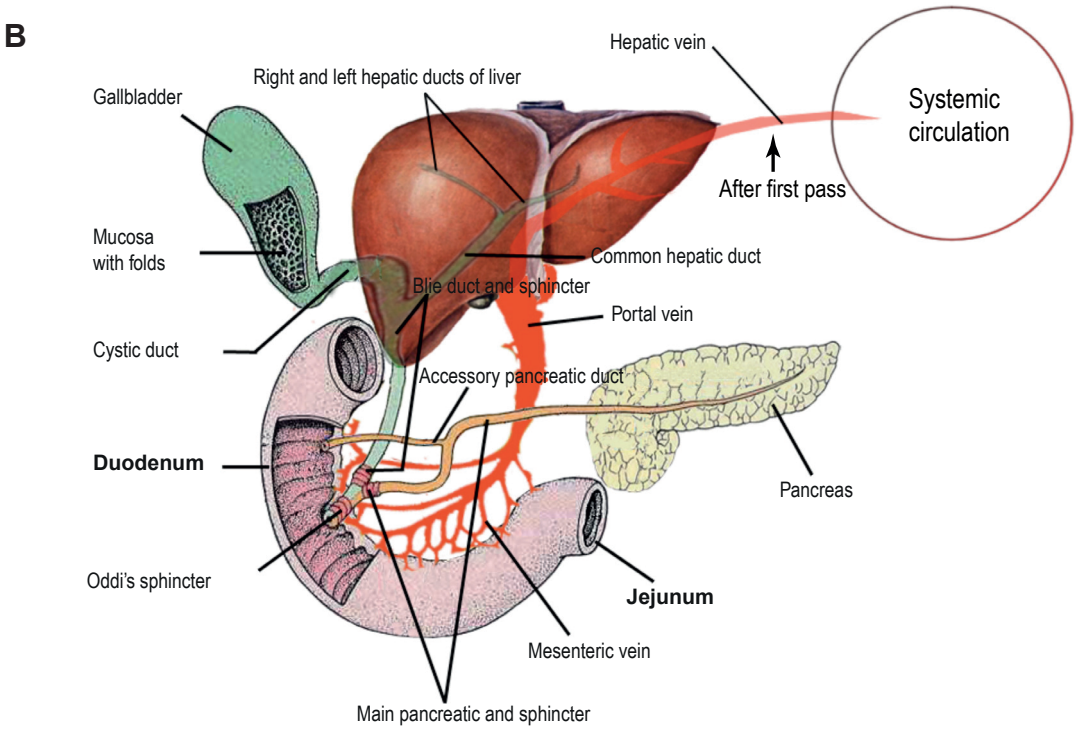

Figuur 1. Regionale functionaliteit van het maagdarmkanaal en enterohepatische circulatie. A) het maagdarmkanaal is afgebeeld van slokdarm tot anus met specifieke regio's en belangrijke functies aan de rechterkant. Figuur aangepast van Madigan *et al.* [32]. **B**) de galblaas, lever, pancreas verbonden met het bovenste deel van de dunne darm, de twaalfvingerige darm, zijn afgebeeld. Na opname van voedingsstoffen of medicijnen uit de dunne darm, gaat de inhoud door de poortader naar de lever en uiteindelijk naar de systemische circulatie, of wordt via het galkanaal bij Oddi's sluitspier in de twaalfvingerige darm gerecirculeerd. Figuur aangepast van Gao *et al.* [6].

Naar schatting zijn er duizend tot 10 duizend (10^3-10^4, bovengrens 10^7), 100 miljoen (10^8, bovengrens 10^{11}) en honderd miljard (10^{11}, bovengrens 10^{14}) bacteriën per milliliter respectievelijk aanwezig in de menselijke proximale dunne darm, ileum en colon [7]. In ziektesituaties zoals bacteriële overgroei in de dunne darm (SIBO), kan het aantal bacteriën in de dunne darm significant hoger zijn (ten minste >10^5 CFU/ml) [8]. De hoeveelheid en de metabolische activiteit van deze bacteriën in de dunne darm hebben waarschijnlijk invloed op de absorptie en de biologische beschikbaarheid van oraal toegediende geneesmiddelen.

Onlangs stelde het European Network on Understanding Gastrointestinal Absorption Related Processes (UNGAP) dat het mechanisme van de darmmicrobiota op de absorptie van oraal toegediende geneesmiddelen relatief onderbelicht blijft en dat onderzoek naar de *in vivo* bijdrage van de microbiota aan de absorptie van geneesmiddelen noodzakelijk is [9]. Sinds meer dan een halve eeuw geleden hebben verschillende onderzoeken de darmmicrobiële omzettingen van oraal voorgeschreven medicijnen beschreven [10–18]. Echter, het merendeel van de beschikbare onderzoeken was gericht op de darmbacteriën die zich in de colon bevinden. Zo hebben Sousa *et al.* geconcludeerd dat veel medicijnen substraten zijn voor darmbacteriën en stelden dat de dikke darm de belangrijkste plaats is voor deze darmmicrobiota toegeschreven conversies, omdat het aantal bacteriën in de dikke darm het hoogst is in vergelijking met de dunne darm [10]. Zimmermann *et al.* ontdekte dat 65% van de bestudeerde medicijnen wordt verminderd door ten minste één van de 76 onderzochte darmbacteriën (voornamelijk anaerobe darmbacteriën, die zich in de lagere delen van de darmen bevinden) en verwachtte dat door deze microbiota toegeschreven conversies de intestinale en systemische blootstelling van geneesmiddelen en geneesmiddelmetabolieten zouden kunnen beïnvloeden [13]. Echter, in de context van de biologische beschikbaarheid van geneesmiddelen zijn bacteriële omzettingen van medicijnen alleen klinisch relevant op de belangrijkste (re)absorptieplaats van oraal toegediende geneesmiddelen, de dunne darm. Maier *et al.* maakte een schatting van de geneesmiddelconcentraties in de dikke darm op basis van de uitscheiding van geneesmiddelen in de ontlasting. Van de 1111 onderzochte geneesmiddelen werd 17% uitgescheiden in de feces met fracties variërend van 0,001-0,98 (mediaan 0,37, interkwartielbereik: 0,15-0,65) [18]. Deze bevindingen geven aan dat slechts 17% van de geteste medicijnen kan worden blootgesteld aan en gemetaboliseerd door de darmmicrobiota in the colon, terwijl de resterende 83% wordt geabsorbeerd in de dunne darm en waarschijnlijk wordt beïnvloed door de aanwezige microbiota in dat gebied van het maagdarmkanaal. Desalniettemin, in de context van bijwerkingen van geneesmiddelen (bijv. toxiciteit), is onderzoek van de microbiële omzettingen in het gehele maagdarmkanaal belangrijk wanneer niet-geabsorbeerde residuen van medicijnen daadwerkelijk deze delen van het maagdarmkanaal bereiken.

SAMENVATTING

Dit proefschrift richtte zich op het samenspel tussen darmbacteriën en medicatie voor de ziekte van Parkinson (ZvP). **Hoofdstukken 2-3** waren voornamelijk gericht op levodopa, dat nog

steeds de gouden standaard is in de behandeling van ZvP [19]. Naast levodopa worden vaak andere anti-ZvP medicijnen, zoals specifieke dopamine-agonisten, voorgeschreven. **Hoofdstukken 4-5** beschrijven de mogelijke impact van deze agonisten op de darmmotiliteit, een comorbiditeit van ZvP, en maagdarmkanaal microbiota-profielen.

In **Hoofdstuk 2** hebben we ontdekt hoe bacteriën in de proximale jejunum levodopa kunnen omzetten in dopamine, gelijktijdig met de omzetting van tyrosine in tyramine. Deze observatie leidde tot de hypothese dat bacteriën die beschikken over tyrosine decarboxylase (TDC) enzymen verantwoordelijk zouden kunnen zijn voor de waargenomen decarboxylering. Inderdaad hebben we bacteriën in de dunne darm geïdentificeerd die levodopa via TDC-enzymen in dopamine kunnen omzetten. Hoewel de affiniteit voor tyrosine significant hoger was dan die voor levodopa, verhinderde dat de decarboxylering van levodopa niet. Bovendien hadden de gelijktijdig voorgeschreven DDC-remmers geen significant effect op de levodopa-decarboxylering door deze bacteriën. De *tdc*-gen abundantie correleerde significant met de dosering van levodopa en de duur van de ziekte, wat suggereert dat de verhoogde levodopadosering en de duur van de ziekte kunnen leiden tot verhoogde bacteriële TDC-niveaus.

Een negatieve correlatie tussen de *tdc*-gen abundantie en de niveaus in de bloedcirculatie bij gezonde ratten toonde aan dat TDC-bacteriën in de proximale dunne darm, de plaats van levodopa absorptie, kunnen interfereren met de niveaus van levodopa in de bloedsomloop. Bovendien resulteerde het vervangen van de microbiota van de dunne darm door een *Enterococcus faecalis*-stam zonder TDC in hogere levodopa-niveaus in de bloedcirculatie in vergelijking met wanneer de microbiota van de dunne darm werd vervangen door de wildtype stam. Deze bevindingen suggereerden dat verhoogde bacteriële TDC-niveaus kunnen resulteren in hogere luminale dopamine-niveaus, wat op zijn beurt (samen met mogelijk voorgeschreven dopamine-agonisten) de darmmotiliteit zou kunnen beïnvloeden die vervolgens de kolonisatie van deze TDC-dragende bacteriën bevordert, waardoor een vicieuze cirkel ontstaat die uiteindelijk kan leiden tot het beperken van de niveaus van levodopa die beschikbaar zijn om de hersenen te bereiken (**Hoofdstuk 2: Figuur 7**).

Een deel van de levodopa dosis zou de lagere delen van de (dunne) darm kunnen bereiken, waar meer anaerobe bacteriën verblijven en die een andere samenstelling hebben dan in de proximale dunne arm. Deze bacteriën zouden vergelijkbare of andere metabole omzettingen van levodopa kunnen uitvoeren zoals beschreven in **Hoofdstuk 1** (**Figuur 1**). Aldus, in **Hoofdstuk 3** identificeerden we een bacteriële metabolische reactie van levodopa door *Clostridium sporogenes*. *C. sporogenes* was in staat aromatische aminozuren reductief te deamineren en we toonden aan dat naast tryptofaan, tyrosine en fenylalanine, *C. sporogenes* ook in staat was levodopa te deamineren. Levodopa werd gedeamineerd via een meerstaps enzymatische route, die werd bevestigd door NMR, MS en genetische knock-outs, tot 3-(3,4-dihydroxyfenyl) propionzuur (DHPPA), een fenolzuur. Deze reductieve deamineringsroute voor levodopa was actief in 70% van de ZvP-monsters (**Hoofdstuk 3, Figuur 4**). Fenolzuren zijn in verband

gebracht met veranderingen in de darmmotiliteit [20,21]. Overeenstemmend, met behulp van een *ex vivo* orgaanbadsysteem, verminderde DHPPA de door acetylcholine geïnduceerde contractiliteit in het ileum van de muis (**Hoofdstuk 3, Figuur 3**). Bovendien waren de DHPPA-niveaus significant hoger bij ZvP-patiënten dan bij hun op leeftijd gematchte gezonde controles. Deze bevindingen zijn belangrijk omdat ZvP-patiënten maagdarmkanaal disfunctie ervaren, met name constipatie. Kortom, deze resultaten benadrukten de urgentie voor het onderzoek naar door bacteriën gemedieerde geneesmiddelconversies die mogelijk kunnen leiden tot ongewenste bijwerkingen van voorgeschreven medicijnen.

Naast het voorschrijven van levodopa/carbidopa worden ook andere medicijnen voorgeschreven om het verlies van dopamine in de hersenen op te vangen. Deze zijn gewoonlijk een combinatie van dopamine-agonisten en levodopa/carbidopa. Bovendien worden ZvP-patiënten blootgesteld aan hoge dopaminegehalten als gevolg van levodopa-decarboxylering. Deze hogere dopaminegehalten, evenals blootstelling aan dopamine-agonisten, hebben niet alleen effecten op de immuunhomeostase [22,23], die de progressie van de ziekte en de microbiële samenstelling beïnvloedt, maar ook op de darmmotiliteit [24], een belangrijke factor in de samenstelling van de microbiota [25] en bacteriële overgroei in de dunne darm [8,26]. Daarom werd in **Hoofdstuk 4** het mogelijke effect van deze anti-ZvP medicatie op de darmmotiliteit en het gevolg op de bacteriële samenstelling van de dunne darm en de bacteriële overgroei dat uiteindelijk tot SIBO zou kunnen leiden, onderzocht.

Dopamine-agonisten, pramipexole en ropinirole in combinatie met levodopa/carbidopa, verminderden de motiliteit van de dunne darm significant na een behandeling van 14 dagen. Beide behandelingen toonden aan dat het aantal bacteriën in het ileum was verhoogd, maar alleen significant voor ropinirole. Nader onderzoek van het microbiota-profiel onthulde dat alleen de soortenrijkdom in het jejunum significant hoger was voor beide agonisten, maar dat de diversiteit niet verschilde in vergelijking met de controlegroep. Vooral in het jejunum, en in mindere mate in het ileum, droegen zowel de behandeling als de darmmotiliteit significant bij aan de waargenomen variatie. Verder kijkend naar de gedetailleerde veranderingen bleek dat *Lactobacillus spp.* toenam en *Lachnospiraceae spp.* afnam in alle behandelingen. Opmerkelijk is dat veranderingen in deze soorten vaak worden waargenomen in ZvP-microbiota-onderzoeken op basis van fecale monsters. De resultaten suggereren dat fecale microbiota-analyse tot op zekere hoogte een weerspiegeling zou kunnen zijn van de microbiële veranderingen in de dunne darm. Over het algemeen benadrukt **Hoofdstuk 4** het belang van de verstorende werking van medicijnen in de ZvP-microbiota-onderzoeken die de microbiota-profielen zouden kunnen veranderen door hun effect op de darmmotiliteit. Bovendien toonden de gegevens aan dat het gewenste effect van dopamine-agonisten op het herstel van het verlies van dopaminegehalten in de hersenen van ZvP-patiënten ongewenste bijwerkingen in de periferie kan veroorzaken.

Om het samenspel tussen de darmmicrobiota en anti-ZvP medicijnen te bevestigen, voornamelijk bestudeerd in diermodellen of getest op een klein cohort van ZvP patiënten (**Hoofdstukken 2-4**),

onderzocht **Hoofdstuk 5** de associatie van anti-ZvP medicijnen (inclusief het bovengenoemde) met de *tdc*-gen abundantieniveaus in een menselijk longitudinaal cohort bestaande uit ZvP en leeftijd en geslacht-gematchte gezonde controles. De *tdc*-gen abundantie nam in de loop van de tijd significant toe, alleen bij ZvP-patiënten en niet bij de gematchte gezonde controles. Bovendien was het verschil in blootstelling aan anti-ZvP medicatie die deze patiënten ontvingen gedurende de periode van twee jaar significant geassocieerd met het verschil in *tdc*-gen abundantie over tijd, onafhankelijk van constipatiesymptomen (behalve voor ropinirole), wat significant bijdroeg aan de *tdc*-gen abundantie. Bovendien weerspiegelde het verschil in type medicatie het verschil in de associaties met de *tdc*-gen abundantie bij het kijken naar subgroepen van patiënten die ofwel stabiel waren of progressief waren in hun ziekte. Gezamenlijk onthulde **Hoofdstuk 5** belangrijke parameters die dopamine-agonisten en maagdarmkanaalfunctie koppelen aan de niveaus van de bacteriële *tdc*-gen abundantie, die uiteindelijk de niveaus van levodopa die beschikbaar zijn om de hersenen te bereiken kunnen beïnvloeden (**Hoofdstuk 2**).

TOEKOMSTPERSPECTIEVEN

Het effect van dopamine en dopamine-agonisten op de afname van de (dunne) darmmotiliteit, wat een comorbiditeit is bij ZvP-patiënten, dringt aan tot verder onderzoek van het effect van deze verbindingen op de darmmotiliteit bij ZvP-patiënten. Evenzo is het van cruciaal belang om de niveaus van SIBO nauwkeurig te meten bij ZvP-patiënten, vooral bij degenen die protonpompremmers nemen, die invloed hebben op de darmmicrobiota [27]. Deze voorzorgsmaatregelen zullen de factoren helpen verminderen die bijdragen aan een verminderede biologische beschikbaarheid van levodopa en de ongewenste bijwerkingen die mogelijk het gevolg zijn van of kunnen zorgen voor een verhoogde frequentie van het doseringsbehandelingsregime.

Verder onderzoek naar de metabolieten geproduceerd door de darmmicrobiota, inclusief het metabolisme van anti-ZvP-medicatie, is nodig om de impact van de complexe interactie van meerdere facetten van metabolieten afkomstig van veranderde microbiële samenstelling en farmacologische behandeling op het immuunsysteem, microbiota-profielen, maagdarmkanaalfunctie en beschikbaarheid van geneesmiddelen bij ZvP-patiënten te ontrafelen.

Inzichten in de mechanistische moleculaire processen in bacteriële opname en metabolisatie van levodopa (en andere door microbiota aangetaste geneesmiddelen) zijn belangrijk om potentiële kandidaat-eiwitten te bepalen voor gerichte inhibitie, rekening houdend met het voorkomen, in tegenstelling tot antibiotica, van een mogelijke verstoring van de microbiotasamenstelling. Levodopa wordt via dezelfde decarboxylatie route verwerkt als tyrosine en, belangrijker nog, het tyrosinedecarboxylase-operon in *Enterococcus faecalis* wordt gereguleerd door zowel de tyrosineniveaus (dus mogelijk ook levodopa) als de pH, wat de overlevingskansen van *E. faecalis* verhoogde [28]. Dit voorbeeld illustreert dat hoge medicatieniveaus die analoog zijn aan natuurlijk voorkomende voedingsstoffen (bijv. tyrosine) de overlevingskansen en dus de

kolonisatie van bepaalde microbiota-soorten die deze verbindingen kunnen metaboliseren, kunnen beïnvloeden, waardoor mogelijk een vicieuze cirkel ontstaat.

Ten slotte moet de klinische bijdrage van de interindividuele variatie in geneesmiddel-microbe-interacties, farmacomicrobiomcis [29], bij ZvP-patiënten worden onderzocht in een longitudinaal cohortonderzoek met nieuw gediagnosticeerde medicijn-naïeve ZvP-patiënten om hun farmacologische behandeling, microbiota-samenstelling en microbiële levodopa-decarboxylase-activiteit in de loop der jaren te volgen.

SLOTOPMERKINGEN

Een verlaging van de striatale dopaminegehalten leidt tot een "off"-episode (d.w.z. wanneer de ZvP-symptomen terugkeren), vooral bij patiënten met een gevorderd stadium van ZvP, die een verminderd vermogen hebben om dopamine in de hersenen op te slaan [30,31]. Darmbacteriën kunnen een factor zijn die bijdraagt aan de verminderde werkzaamheid van levodopa-behandeling bij ZvP-patiënten, vooral in de gevorderde staat van de ziekte met smalle behandelvensters. Bovendien draagt anti-ZvP-medicatie bij aan de verandering van darmmotiliteit en microbiota-samenstelling, waarmee rekening moet worden gehouden bij de (poly)farmacologische behandeling van ZvP.

REFERENTIES

1. Vertzoni, M. *et al.* Impact of regional differences along the gastrointestinal tract of healthy adults on oral drug absorption: An UNGAP review. *Eur. J. Pharm. Sci.* **134**, 153–175 (2019).
2. Koziolek, M. *et al.* Investigation of pH and Temperature Profiles in the GI Tract of Fasted Human Subjects Using the Intellicap®System. *J. Pharm. Sci.* **104**, 2855–2863 (2015).
3. Ovesen, L. *et al.* Intraluminal pH in the stomach, duodenum, and proximal jejunum in normal subjects and patients with exocrine pancreatic insufficiency. *Gastroenterology* **90**, 958–962 (1986).
4. Kararli, T. T. Comparison of the gastrointestinal anatomy, physiology, and biochemistry of humans and commonly used laboratory animals. *Biopharm. Drug Dispos.* **16**, 351–380 (1995).
5. Helander, H. F. & Fändriks, L. Surface area of the digestive tract-revisited. *Scand. J. Gastroenterol.* **49**, 681–689 (2014).
6. Gao, Y. *et al.* Drug enterohepatic circulation and disposition: Constituents of systems pharmacokinetics. *Drug Discov. Today* **19**, 326–340 (2014).
7. Sender, R., Fuchs, S. & Milo, R. Revised Estimates for the Number of Human and Bacteria Cells in the Body. *PLoS Biol.* **14**, 1–14 (2016).

8. Quigley, E. M. M. & Quera, R. Small intestinal bacterial overgrowth: Roles of antibiotics, prebiotics, and probiotics. *Gastroenterology* **130**, 78–90 (2006).
9. Vinarov, Z. *et al.* Current challenges and future perspectives in oral absorption research: An opinion of the UNGAP network. *Adv. Drug Deliv. Rev.* **171**, 289–331 (2021).
10. Sousa, T. *et al.* The gastrointestinal microbiota as a site for the biotransformation of drugs. *Int. J. Pharm.* **363**, 1–25 (2008).
11. Zimmermann, M., Zimmermann-Kogadeeva, M., Wegmann, R. & Goodman, A. L. Separating host and microbiome contributions to drug pharmacokinetics and toxicity. *Science* **363**, eaat9931 (2019).
12. Haiser, H. J. *et al.* Predicting and manipulating cardiac drug inactivation by the human gut bacterium Eggerthella lenta. *Science* **341**, 295–8 (2013).
13. Zimmermann, M., Zimmermann-Kogadeeva, M., Wegmann, R. & Goodman, A. L. Mapping human microbiome drug metabolism by gut bacteria and their genes. *Nature* (2019) doi:10.1038/s41586-019-1291-3.
14. van Kessel, S. P. *et al.* Gut bacterial tyrosine decarboxylases restrict levels of levodopa in the treatment of Parkinson's disease. *Nat. Commun.* **10**, 310 (2019).
15. van Kessel, S. P. *et al.* Gut bacterial deamination of residual levodopa medication for Parkinson's disease. *BMC Biol.* **18**, 137 (2020).
16. Waclawiková, B. *et al.* Gut bacteria-derived 5-hydroxyindole is a potent stimulant of intestinal motility via its action on L-type calcium channels. *PLoS Biol.* **19**, 1–27 (2021).
17. Maini Rekdal, V., Bess, E. N., Bisanz, J. E., Turnbaugh, P. J. & Balskus, E. P. Discovery and inhibition of an interspecies gut bacterial pathway for Levodopa metabolism. *Science* **364**, eaau6323 (2019).
18. Maier, L. *et al.* Extensive impact of non-antibiotic drugs on human gut bacteria. *Nature* **555**, 623–628 (2018).
19. Mercuri, N. B. & Bernardi, G. The 'magic' of L-dopa: Why is it the gold standard Parkinson's disease therapy? *Trends Pharmacol. Sci.* **26**, 341–344 (2005).
20. Aviello, G. *et al.* Inhibitory effect of caffeic acid phenethyl ester, a plant-derived polyphenolic compound, on rat intestinal contractility. *Eur. J. Pharmacol.* **640**, 163–167 (2010).
21. Roager, H. M. *et al.* Colonic transit time is related to bacterial metabolism and mucosal turnover in the gut. *Nat. Microbiol.* **1**, 16093 (2016).
22. Pinoli, M., Marino, F. & Cosentino, M. Dopaminergic Regulation of Innate Immunity: a Review. *J. Neuroimmune Pharmacol.* **12**, 602–623 (2017).
23. Sarkar, C., Basu, B., Chakroborty, D., Dasgupta, P. S. & Basu, S. The immunoregulatory role of dopamine: An update. *Brain. Behav. Immun.* **24**, 525–528 (2010).

24. Li, Z. S., Schmauss, C., Cuenca, A., Ratcliffe, E. & Gershon, M. D. Physiological modulation of intestinal motility by enteric dopaminergic neurons and the D2 receptor: analysis of dopamine receptor expression, location, development, and function in wild-type and knock-out mice. *J. Neurosci.* **26**, 2798–807 (2006).
25. Falony, G. *et al.* Population-level analysis of gut microbiome variation. *Science* **352**, 560–4 (2016).
26. Quigley, E. M. M. Small intestinal bacterial overgrowth. *Curr. Opin. Gastroenterol.* **30**, 141–146 (2014).
27. Imhann, F. *et al.* Proton pump inhibitors affect the gut microbiome. *Gut* **65**, 740–748 (2016).
28. Perez, M. *et al.* Tyramine biosynthesis is transcriptionally induced at low pH and improves the fitness of Enterococcus faecalis in acidic environments. 3547–3558 (2015).
29. Rizkallah, M., Saad, R. & Aziz, R. The Human Microbiome Project, Personalized Medicine and the Birth of Pharmacomicrobiomics. *Curr. Pharmacogenomics Person. Med.* **8**, 182–193 (2012).
30. Olanow, C. W. & Koller, W. C. An algorithm (decision tree) for the management of Parkinson's disease: treatment guidelines. American Academy of Neurology. *Neurology* **50**, S1-57 (1998).
31. Olanow, C. W., Watts, R. L. & Koller, W. C. An algorithm (decision tree) for the management of Parkinson's disease (2001): treatment guidelines. *Neurology* **56**, S1–S88 (2001).
32. Madigan, M. T., Clark, D. P., Stahl, D. & Martinko, J. M. *Brock biology of microorganisms*. (Pearson Education, Inc., publishing as Benjamin Cummings, 2012).

Back to table of contents

APPENDICES

Acknowledgements

Although I spent already three years following my HBO bachelor's "Biology and Medical Laboratory Research" I only realized in my last year, doing my final research internship, how much I liked being on the lab doing research. A major role in realizing this was the enthusiasm, optimism and excellent guidance I received during my project from **Dirk-Jan Scheffers**. That really initiated a great motivation to pursue with further education. During my two master's projects I learned that this enthusiasm and optimism also existed in other professors, **Jan-Willem Veening** and **Matthias Heinemann**. Being part of the research-groups felt great, where I learned, besides the long working hours, there were regular social activities. All these good experiences made me start a PhD, thank you all for that!

After I graduated Jan-Willem offered me a short 3 month project working on CRISPRi in *S. pneumoniae*, which I really enjoyed doing. Looking for a PhD position afterwards, Jan-Willem pointed me out to **Sahar El Aidy**. Sahar, being appointed in September 2015 would study the "Microbiota-Gut-Brain Axis". This sounded very interesting! Could gut bacteria actually make neurotransmitters?

I wrote Sahar an email, we exchanged our ideas, and we had a relatively brief phone-call (no video!), concluding that I could join Sahar's group. However first, I had to pass by **Lubbert Dijkhuizen**, who thoroughly checked my résumé and luckily confirmed I could start in October 2015.

- **Sahar El Aidy.** Sahar, one thing is clear, this thesis could not have existed without you! When I started my PhD you just started your group a month ago, meaning that we could still go many directions, which was very exciting. This also meant we had to setup the lab and techniques dedicated for host-microbiota work, which wasn't always straightforward. I was always and am impressed by your perseverance and fighting spirit and I like your combination of directness and heartiness at the same time.
  Another consequence of just starting a research-group is finding the best way of group-management. Which we have tried in different ways and forms, no form fits all, thus requiring a personalized approach. The approach with me was successful and maybe very natural, at least that is how it felt. During our almost daily interactions, you made me get to know myself better, a good thing.
  Sahar, thank you for guiding me through the process of my PhD-trajectory, I learned a lot and I think we form(ed) a good team!

- **Lubbert Dijkhuizen.** Lubbert, thank you for guiding us in the beginning and making sure everything was going in the right direction. Thank you for letting us free in what we did but also for the willingness to help out if it would be required.

During my PhD I guided many bachelor's and master's students. They taught me many things and showed me that guiding people (in the lab) is something I like to do. I enjoyed working with all of you!

- **Marten Chaillet.** Marten, you were the first student doing a project with me. Luckily you were an excellent student and I have great memories exploring new techniques in the lab and conversing with you. Thank you!
- **Dildar Baz.** Dildar, it is strange how life unfolds while making different plans. Thank you for helping in the first steps of my PhD.
- **Alexandra Frye.** Alex, I really enjoyed working with you in the lab and I liked your enthusiasm and excitement. Thank you for your contribution to the Chapter 2. By the way, I still have your "macaron card" hanging on our fridge which you gave me when you left, reminding me of the great time, thank you.
- **María Castejón.** María, I remember you started your project very independently and you were very happy working in the lab. Thank you for your contribution to Chapter 2. It was always fun with you on the lab.
- **Julie Brouillet.** Julie, in your project you helped me out with a cell-culture project doing a lot of qPCRs and initiation the alumina extraction, thank you! I remember the food you brought back from France, especially the macarons, explaining the macaron card, described above.
- **Hiltje de Jong.** Hiltje, your project included cloning 9 transaminase proteins and testing their activity (as described in Chapter 3). I remember when you just started the rest of the pathway was "scooped", but luckily not the first transaminase step. Thank you for your contribution to my PhD-thesis!
- **Thom Weitenberg.** Thom, I remember you really enjoyed doing experiments on the lab, especially with the right music. Sometimes you needed some "pressure" but you could commit yourself really to something. When your report deadline was approaching we might have been a bit worried. But after you told us what you had found we were impressed and you said: "*Yeah, diamonds are shaped under pressure!"*. Resulting in a lot of laughter! Thank you for your contribution to my PhD.
- **Simon Winkel.** Simon, the stories you told during lunch kept everybody silent and listening to you. You were an open book and I will never forget you love for Joy Radio. Thank you for your contribution to Chapter 3!

- **Rogier van Essen.** Rogier, you were the first student that actually already had experience with cloning! This made me very excited because cloning, although sometimes very frustrating, is so much fun to do, especially when your construct is working. Thank you for your contribution to my PhD!

- **Amber Bullock.** Amber, you started as a master's student with us before COVID-lockdown and came back afterwards to finish your project. You did not hesitate to work at any hour whatsoever during the week. You were a great help for Chapter 4, thank you!

I want to thank my former Microbial Physiology-colleagues that helped somewhere along the way:

- **Ahmed Soliman.** Ahmed, although our paths diverged, I really enjoyed starting together with you in the lab and helping you when you just moved here in Groningen.

- **Hien Pham and Huifang Yin.** Huifang and Hien, you were my first office mates and I really enjoyed sharing my office with you and remember your warm welcome when I first joined the group!

- **Hans-Jörg Frasch.** Hajö, in the beginning I remember I was always asking you where to find stuff and could always ask you for advice. I was always amazed how you found the right chemical in a second, while I was looking for an hour to find it (later I learned this is a skill one learns over time being on the lab).

- **Sander van Leeuwen and Geralt ten Kate.** Geralt and Sander, basically you both taught me the basics of a HPLC (using old machines, which really helps) and helped me setting up the detection of catecholamines. Thank you for helping with the NMR experiments. I could always go up to the 9th floor for your help on chemistry questions and I was always happy to join your punctual coffee breaks.

- **Mirjan Petrusma and Laura Fernández De Las Heras.** Mirjan and Laura, we could always ask you for HPLC-troubleshooting and advice, also you helped us out enormously with the HPLC-MS! Laura, fun-fact, we still have an HPLC-column named after you: "The Laura-column".

- **Joana Gangoiti Muñecas.** Joana, you were always happy to help us out with understanding and interpreting enzyme-kinetics.

- **Evelien te Poele.** Evelien, while sitting across my lab-bench I could always ask you about your opinion or advice on any experiment. The best advice you gave me was on determination of CFUs. Instead of plating one technical replicate per dilution on a single plate just spot 3 technical replicates from 6 dilutions on a single plate (saving 17 plates and time). Very useful!

- **Willem Dijkman.** Willem, I really enjoyed the time we were sharing our lab-bench and you were always happy to help out!
- **Chrysovalantou Chatziioannou.** Valantou, you were enormously helpful to everyone. I remember the things we fixed with superglue. And I was always impressed with your dedication for your work.
- **Pieter Grijpstra**, Pieter, you helped out with everything in the lab fixing, ordering and moving stuff while talking about all sorts of things you learned or experienced.
- **Rivca Valk-Weeber.** Rivca, we started our PhD's around the same time on completely different topics. I was always impressed by your organized and precise way of working. I enjoyed our talks and you helped out on all the (analytical) questions.
- **Markus Böger.** Markus, when I just started your contract was more than halfway and you told me that time really flies, and you were absolutely right! I really enjoyed our conversations.
- **Xiangfeng Meng, Lara Martín-Sánchez, Yuxiang Bai, Vincent Valk, Cecile Deelman-Driessen, Ana Ceniceros, and Alicia Brandt.**

During the phasing out of the Microbial Physiology department, the Host-Microbe Interactions (HMI) group expanded with my "Host-Microbe" colleagues. I could not have wished a better group of close colleagues and friends. I enjoyed all our get-togethers and all the things we shared and talked about.

- **Carmen Aranzamendi.** Carmen, you were the first new member in the group that would take care of the cell-culture and other lab organizing-stuff. You learned me how to culture eukaryotic cells. If something needed to be done, you made sure it will be arranged. Besides the lab you learned me how to stay 30-years young forever! I really enjoy(ed) working with you and all the things we talk(ed) about. Thank you!
- **Bára Waclawiková.** Bára, you were the first PhD-student to join HMI and I was very excited when you joined. Thank you for all your conversations, discussions, and your help till the very end (even with writing these acknowledgements). Your catchy laugh always brings a substantial amount of extra laughter! It is really fun working with you and thank you for being my paranymph!
- **Ahmed Osama El-Gendy.** Osama, during your short stay in our group you did a lot of work, contributing to Chapter 2. Thank you for teaching me the valuable plating techniques (to screen for decarboxylation) you performed in the lab. I really enjoyed working with you!
- **Pamela González Dávila.** Pamela, your great skill of bringing people together always

amazes me. Also you have a great ability to bring plants to places where there were no plants before (the office)! I really enjoy you being my office-mate, and supplying me with the right water-bottles! Thank you!

- **Julia Aresti Sanz.** Julia, what always amazed me is the pace you can work in, music on, and go! I always enjoyed your critical attitude towards proper preparation of food and enjoying the perfect dish. Thank you!
- **Jack Jansma.** Jack, I really enjoyed all the (philosophical) discussions we had about work, but also at lunch about a wide variety of subjects! Also I learned to appreciate "local-music" as you regularly played this in the lab. Thank you, and thank you for being my paranymph!
- **Panagiotis Kelefiotis Stratidakis.** Panagiotis, Panos, I was really excited when I heard you would join our lab, because you would kind of follow-up my PhD-project. You fitted-in perfectly among us and I enjoyed all of our (non-)work related conversations. Thank you!
- **Markus Schwalbe**. Markus, thank you for your advice and helpful discussions on how to approach bioinformatic questions.

I want to thank all colleagues from the Molecular Immunology group with whom we shared the lab for some while and brought a great atmosphere with regular "borrels"!

- **Sjors Maassen.** Sjors, I enjoyed the time we shared our office together and I always appreciated your effort to collaborate on anything interesting.
- **Geert van den Bogaart, Femmy Stempels, Frans Bianchi, Maxim Baranov, Harry Warner, Deepti Dabral, Alexine de Wit, and Myrthe Frans.**

I want to thank the collaborators that contributed to this thesis,

- **Gertjan van Dijk.** Gertjan, thank for your expertise and great help with the animal experiments, your optimism and enthusiasm.
- **Ad Nelemans**. Ad, thank you for your great help with setting up the *ex vivo* organ-bath system and teaching us how to use it and interpret the data.
- **Ali Keshavarzian.** Ali, thank you for helping us with obtaining PD and HC samples. I enjoyed your enthusiasm and your ability to know more about the status of the Dutch football team in the European Championship than us!
- **Hjalmar Permentier.** Hjalmar, thank you for initial trials with the HPLC-ECD-MS and for the analysis of the samples.
- **Filip Scheperjans.** Filip, thank you for giving the possibility to investigate the *tdc*-gene

abundance in a longitudinal cohort of PD and HC subjects.

I want to thank,

- **Jan Kok** and **Harma Karens** for providing many strains to us, advice and help.
- **Anmara Kuitert** and **Bea Zand-Scholten** for helping out with the secretarial duties and anything else I asked for.
- **Marten Exterkate** and **Niels de Kok** for their help with running samples on the HPLC-MS.
- **Steffen van Heijningen** and **Warner Hoornenborg** for helping with collecting the gastrointestinal tissues and helping out with anything when needed.
- **Anne de Jong** for helping me performing a microarray experiment and with any bioinformatic question.
- **Tjaard Pijning** for exploring the possibilities of protein crystallography.
- **Gea Schuurman-Wolters** helping and teaching me how to perform radioisotope uptake experiments.
- **Jonas Cremer, Arjo Bunskoeke, Erica Zuidersma, Katrin Beilharz, Morten Kjos, Rieza Aprianto, Robin Sorg, Jelle Slager, Patrice Garnier, Xavier Manière, Nicole McKnight, Ignacio Faustino, Jan Bruggink, Wendy Kaspers, Wanda Douwenga, Memoona Arshad, Maira Jiménez Sánchez, Fleur Brinkman, Akke Visser, Maartje Wolf, Hussam Abbas, Gwen Ruitenbeek, Stephanie Roethig**, **Lard de Jong, Semih Toptas, Pinar Onat, Marta Cardoso, Willemijn Brouwer, Bindert Algra, and Maja Stevanoska.**

Finally I want to thank,

- **My parents, Joke and Peter, my brother Maarten and my Family. Mam en pap**, ik kan mij herinneren, nadat ik vroeg of ik wel aan een promotie moest beginnen, dat jullie zeiden dat ik dit vooral moest doen als het me maar leuk genoeg leek, wat doorslaggevend was. Bedankt voor jullie constante belangstelling en interesse!
- **My life partner. Virginia**, zonder jou en zonder al jouw geduld en begrip, hulp en interesse, het tolereren en bedaren van de verontrusting en beroering die soms met mij mee naar huis kwamen, was dit nooit gelukt. De komst van onze dochter is het mooiste wat ons is overkomen en heeft zij onbewust het schrijven van dit proefschrift bespoedigd. Bedankt. *I'll be loving you always.*

About the Author

ENGLISH

Sebastiaan Pieter van Kessel was born on December 9, 1990 in Groningen. In 2008 he obtained his HAVO diploma at the H. N. Werkman college in Groningen and started with his bachelor's program Biology and Medical Laboratory Research at the Hanze University of Applied Sciences in Groningen. In September 2012, he completed his bachelor's with a research internship at the department of Molecular Microbiology at the University of Groningen. After finishing his pre-master's program, he started in February 2013 with the master's program Molecular Biology and Biotechnology at the University of Groningen, where he did two research internships at the Molecular Genetics and Molecular Systems Biology departments. In February 2015, he obtained his master's degree (*cum laude*) and then worked for 3 months as a research assistant at the Molecular Genetics department. In October 2015 he started his PhD research in the department of Microbial Physiology (later subdivided into the department of Host-Microbe Interactions), as described in this thesis. Currently he is employed as postdoc researcher at the department of Host-Microbe Interactions at the University of Groningen.

NEDERLANDS

Sebastiaan Pieter van Kessel werd op 9 december 1990 geboren te Groningen. In 2008 behaalde hij zijn HAVO diploma aan het H. N. Werkman college te Groningen en startte zijn bachelor Biologie en Medisch Laboratoriumonderzoek aan de Hanzehoogeschool Groningen. In september 2012 heeft hij de opleiding afgerond met een onderzoekstage bij de afdeling Moleculaire Microbiologie van de Universiteit Groningen. Na een pre-master is hij begonnen in februari 2013 met de master opleiding Moleculaire Biologie en Biotechnologie aan de Universiteit van Groningen waar hij twee onderzoekstages heeft gelopen bij de afdelingen Moleculaire Genetica en Moleculaire Systeembiologie. In februari 2015 heeft hij deze master-opleiding afgerond (*cum laude*) en heeft vervolgens 3 maanden gewerkt als onderzoekmedewerker bij de afdeling Moleculaire Genetica. In oktober 2015 is hij begonnen aan zijn promotieonderzoek bij de afdeling Microbiële Fysiologie (later afgesplitst in de afdeling Host-Microbe Interactions), zoals beschreven in dit proefschrift. Momenteel is hij werkzaam als postdoc onderzoeker bij de afdeling Host-Microbe Interactions aan de Universiteit van Groningen.

List of Publications

Publications in this thesis:

van Kessel, S.P., Frye, A.K., El-Gendy, A.O., Castejon, M., Keshavarzian, A., van Dijk, G., and El Aidy, S. (**2019**). Gut Bacterial Tyrosine Decarboxylases Restrict Levels of Levodopa in the Treatment of Parkinson's Disease. *Nat. Commun. 10*, 310.

van Kessel, S.P., and El Aidy, S. (**2019**). Contributions of Gut Bacteria and Diet to Drug Pharmacokinetics in the Treatment of Parkinson's Disease. *Front. Neurol. 10*, 1087.

van Kessel, S.P., and El Aidy, S. (**2019**). Bacterial Metabolites Mirror Altered Gut Microbiota Composition in Patients with Parkinson's Disease. *J. Parkinsons. Dis. 9*, S359–S370.

van Kessel, S.P., de Jong, H.R., Winkel, S.L., van Leeuwen, S.S., Nelemans, S.A., Permentier, H., Keshavarzian, A., and El Aidy, S. (**2020**). Gut Bacterial Deamination of Residual Levodopa Medication for Parkinson's Disease. *BMC Biol. 18*, 137.

Other publications:

Król, E.*, **van Kessel, S.P.***, van Bezouwen, L.S., Kumar, N., Boekema, E.J., and Scheffers, D.J. (**2012**). *Bacillus subtilis* SepF Binds to the C-Terminus of FtsZ. *PLoS One 7*, e43293. *shared first authorship

Liu, X., Gallay, C., Kjos, M., Domenech, A., Slager, J., **Kessel, S.P.**, Knoops, K., Sorg, R.A., Zhang, J., and Veening, J.W. (**2017**). High-Throughput CRISPRi Phenotyping Identifies New Essential Genes in *Streptococcus pneumoniae*. *Mol. Syst. Biol. 13*, 931.